

**Unraveling the mechanisms of *Sr35*-based resistance in the wheat-*Puccinia graminis* f.sp.
tritici pathosystem**

by

Andrés Felipe Salcedo

B.Sc., Universidad del Valle, Colombia, 2003

M.Sc., University of Puerto Rico, 2011

AN ABSTRACT OF A DISSERTATION

Submitted in partial fulfillment of the requirements for the degree

DOCTOR OF PHILOSOPHY

Department of Plant Pathology
College of Agriculture

KANSAS STATE UNIVERSITY
Manhattan, Kansas

2018

Abstract

The fungus *Puccinia graminis* f. sp. *tritici* (*Pgt*) is the causal agent of the wheat stem rust disease. Wheat stem rust has attracted a lot of attention after the emergence of the *Ug99* race group, which at the time of its origin was virulent on most of the wheat varieties cultivated around the world. The evolution and spread of the *Pgt* isolates from the *Ug99* race group posed a serious threat to worldwide wheat production. To mitigate the potential impact of new rust epidemics in major wheat production areas, it remains critical to identify new strategies for breeding durable resistance traits. A detailed understanding of the plant-pathogen interaction mechanisms in the wheat-*Pgt* pathosystem should be the foundation of these strategies. The interaction between the matching pair of resistance (*R*) and avirulence (*Avr*) genes, an important element of the plant-pathogen interactions, is described by the broadly documented gene-for-gene model. The cloning of the *Sr35* gene, which confers near immunity against all isolates from the *Ug99* race group provided a unique opportunity to investigate the molecular mechanisms of resistance to stem rust in wheat. The goals of the present study were: (1) to determine whether the *Sr35* gene alone is sufficient for conferring resistance against *Ug99*, (2) to assess the *Sr35* transcript levels during the time course of infection, and (3) to identify and validate the corresponding *Avr* gene interacting with *Sr35*. The cloning of *Avr* genes from the biotrophic fungi represents a substantial challenge due to the variability, redundant nature, the lack of similarity to known proteins, and lack of adequate functional tools to validate them. To overcome these limitations, we performed a comparative genomic analysis using multiple *Sr35*-avirulent and *Sr35*-virulent races, including 15 chemically mutagenized *Pgt* strains that acquired virulence on the *Sr35* gene. Whole genome shotgun sequencing of the *Pgt* mutants identified a single candidate gene, which carried strong effect mutations in each mutant strain. The *Avr* gene candidate (*AvrSr35*) was expressed at early stages of infection and had a signal peptide indicating that the gene product is secreted. Comparative microscopic analysis of the infected tissues at different time points after infection indicated that *AvrSr35* secretion occurs before haustoria formation. The re-sequencing of the *AvrSr35* candidate gene in a panel of *Sr35*-virulent and *Sr35*-avirulent isolates including isolates from the *Ug99* race group, revealed the presence of a mobile DNA element inserted into the coding sequence of virulent isolates. This insertion resulted in a premature termination codon and explains the origin of *Pgt* field isolates virulent in

the presence of the *Sr35* gene. Co-expression of *AvrSr35* with the *Sr35* in *N. benthamiana* leaves induced a specific hypersensitive response confirming the avirulence function of the candidate effector gene. Subcellular localization, bi-molecular fluorescence complementation, and co-immunoprecipitation assays in *N. benthamiana* leaves revealed that the *AvrSr35* and *Sr35* proteins interact and are likely associated with the endoplasmic reticulum and plasma membrane. Thus, this study identified and functionally characterized the first matching pair of *Avr/R* genes for cereal rusts.

**Unraveling the mechanisms of *Sr35*-based resistance in the wheat-*Puccinia graminis* f.sp.
tritici pathosystem**

by

Andrés Felipe Salcedo

B.S., Universidad del Valle, Colombia 2003
M.S., University of Puerto Rico, 2011

A DISSERTATION

Submitted in partial fulfillment of the requirements for the degree

DOCTOR OF PHILOSOPHY

Department of Plant Pathology
College of Agriculture

KANSAS STATE UNIVERSITY
Manhattan, Kansas

2018

Approved by:

Major Professor
Eduard Akhunov

Copyright

© Andrés Felipe Salcedo 2018.

Abstract

The fungus *Puccinia graminis* f. sp. *tritici* (*Pgt*) is the causal agent of the wheat stem rust disease. Wheat stem rust has attracted a lot of attention after the emergence of the *Ug99* race group, which at the time of its origin was virulent on most of the wheat varieties cultivated around the world. The evolution and spread of the *Pgt* isolates from the *Ug99* race group posed a serious threat to worldwide wheat production. To mitigate the potential impact of new rust epidemics in major wheat production areas, it remains critical to identify new strategies for breeding durable resistance traits. A detailed understanding of the plant-pathogen interaction mechanisms in the wheat-*Pgt* pathosystem should be the foundation of these strategies. The interaction between the matching pair of resistance (*R*) and avirulence (*Avr*) genes, an important element of the plant-pathogen interactions, is described by the broadly documented gene-for-gene model. The cloning of the *Sr35* gene, which confers near immunity against all isolates from the *Ug99* race group provided a unique opportunity to investigate the molecular mechanisms of resistance to stem rust in wheat. The goals of the present study were: (1) to determine whether the *Sr35* gene alone is sufficient for conferring resistance against *Ug99*, (2) to assess the *Sr35* transcript levels during the time course of infection, and (3) to identify and validate the corresponding *Avr* gene interacting with *Sr35*. The cloning of *Avr* genes from the biotrophic fungi represents a substantial challenge due to the variability, redundant nature, the lack of similarity to known proteins, and lack of adequate functional tools to validate them. To overcome these limitations, we performed a comparative genomic analysis using multiple *Sr35*-avirulent and *Sr35*-virulent races, including 15 chemically mutagenized *Pgt* strains that acquired virulence on the *Sr35* gene. Whole genome shotgun sequencing of the *Pgt* mutants identified a single candidate gene, which carried strong effect mutations in each mutant strain. The *Avr* gene candidate (*AvrSr35*) was expressed at early stages of infection and had a signal peptide indicating that the gene product is secreted. Comparative microscopic analysis of the infected tissues at different time points after infection indicated that *AvrSr35* secretion occurs before haustoria formation. The re-sequencing of the *AvrSr35* candidate gene in a panel of *Sr35*-virulent and *Sr35*-avirulent isolates including isolates from the *Ug99* race group, revealed the presence of a mobile DNA element inserted into the coding sequence of virulent isolates. This insertion resulted in a premature termination codon and explains the origin of *Pgt* field isolates virulent in

the presence of the *Sr35* gene. Co-expression of *AvrSr35* with the *Sr35* in *N. benthamiana* leaves induced a specific hypersensitive response confirming the avirulence function of the candidate effector gene. Subcellular localization, bi-molecular fluorescence complementation, and co-immunoprecipitation assays in *N. benthamiana* leaves revealed that the *AvrSr35* and *Sr35* proteins interact and are likely associated with the endoplasmic reticulum and plasma membrane. Thus, this study identified and functionally characterized the first matching pair of *Avr/R* genes for cereal rusts.

Table of Contents

List of Figures	xiii
List of Tables	xv
Acknowledgements	xvi
Dedication	xvii
Introduction	1
Chapter 1 - Literature review	3
1.1 Wheat rusts are a global threat to food security	3
1.2 The cereal rusts	5
1.2.1 Stem rust life cycle	7
1.3 Emergence of the <i>Ug99</i> race	10
1.4 The Borlaug global rust initiative (BGRI)	14
1.5 Strategies to control stem rust	15
1.5.1 Integrated management practices	15
1.5.1.1 Agronomical management and cultural practices	15
1.5.1.2 Use of mixtures or multilines and regional deployment of resistance under evolutionary principles	16
1.5.1.3 Chemical control	17
1.5.1.4 Barberry eradication	18
1.5.2 Genetic control of stem rust epidemics	19
1.5.2.1 Horizontal resistance	20
1.5.2.2 Vertical resistance	21
1.5.3 Plant breeding for stem rust resistance	23
1.5.4 Gene pyramiding and biotechnological approaches	24
1.6 Resistance genes used to control stem rust	26
1.6.1 Mapped genes effective against <i>Ug99</i> race of stem rust	26
1.6.2 Cloned genes effective against cereal rusts	29
1.7 Plant immunity	30
1.7.1 The gene-for-gene concept	30
1.7.2 Nonhost resistance	31

1.7.3 PAMP-triggered immunity (PTI)	32
1.7.4 Effector triggered immunity (ETI)	33
1.7.5 Co-evolution of plant-pathogen interaction	34
1.8 Molecular mechanisms of <i>R</i> gene resistance	35
1.8.1 <i>R</i> gene categories	35
1.8.2 NBS-LRR genes	37
1.8.3 <i>R</i> gene evolution	38
1.9 Effectors vs Avr proteins	39
1.10 Mechanisms of <i>R-Avr</i> recognition.....	40
1.10.1 Direct interaction	40
1.10.2 Indirect interaction	41
1.10.2.1 Guard model	41
1.10.2.2 Simple decoy model.....	42
1.10.2.3 Switch-bait model.....	44
1.10.2.4 Integrated decoy/sensor model	44
1.11 Effector delivery and translocation	46
1.11.1 Fungi with extracellular effectors.....	46
1.11.2. Fungi with host-cell translocated (cytoplasmatic) effectors.....	47
1.12 Cloning of fungal effectors	47
Chapter 2 - Time course gene expression analysis of the resistance gene <i>Sr35</i> and validation of wheat lines with the <i>Sr35</i> -transgene.....	50
2.1 Introduction.....	50
2.2 Objectives	52
2.3. Materials and methods.....	52
2.3.1 Plant material and BAC clones.....	52
2.3.2 <i>Pgt</i> inoculation and growth conditions	52
2.3.3 Validation of specific primers for two alternative splicing variants of <i>Sr35</i>	53
2.3.4 DNA isolation.....	55
2.3.5 RNA isolation.....	56
2.3.6 <i>Sr35</i> transgene screening.....	57
2.3.7 Relative expression of <i>Sr35</i> isoforms during the course of infection.....	57

2.4 Results	58
2.4.1 Specific primer design for <i>Sr35</i> -isoforms	58
2.4.2 Relative expression of <i>Sr35</i> -isoforms during the time course of infection.....	58
2.4.3 PCR-based screening and gene expression analysis of <i>Sr35</i> transgenic plants	59
2.5 Discussion.....	62
2.5.1 Gene expression of <i>Sr35</i> -alternative isoforms during time course infection with <i>Pgt</i>	62
2.5.2 <i>Sr35</i> -transgene screening and progeny analysis.....	65
2.6 Conclusions.....	66
Chapter 3 - Identification of the <i>AvrSr35</i> gene in <i>Puccinia graminis</i> f.sp. <i>tritici</i>	67
3.1 Introduction.....	67
3.2 Objectives	70
3.3 Materials and methods.....	71
3.3.1 Plant bacterial and pathogenic materials.....	71
3.3.2 <i>Pgt</i> inoculation.....	71
3.3.3 EMS mutagenesis of <i>Pgt</i>	72
3.3.4 DNA isolation from <i>Pgt</i> urediniospores	73
3.3.5 RNA isolation.....	73
3.3.6 NGS libraries preparation and sequencing.....	74
3.3.7 Bioinformatic analysis	75
3.3.7.1 Assembly of the RKQQC reference genome	75
3.3.7.2 Annotation of RKQQC genome assembly	76
3.3.7.3 Mutation discovery on RKQQC EMS mutants and identification of candidates for the <i>AvrSr35</i> gene.....	76
3.3.8 PCR-based cloning of the <i>AvrSr35</i>	77
3.3.9 Confirmation by Sanger sequencing of predicted mutations on <i>Sr35</i> - virulent <i>Pgt</i> EMS-mutant strains.....	78
3.3.10 Diversity analysis of <i>AvrSr35</i>	79
3.3.11 Confocal laser scanning microscopy (CLSM)	79
3.4 Results	82
3.4.1 Histological characterization of early time course infection of <i>Pgt</i> on susceptible and resistant <i>Sr35</i> genotypes.....	82

3.4.2 Chemical mutagenesis of <i>Pgt</i> race RKQQC	85
3.4.3 Bioinformatic analysis for the identification of the <i>AvrSr35</i> candidate	86
3.4.3.1 Assembling of RKQQC race genome	86
3.4.3.2 Mutation discovery on <i>Pgt</i> mutants and identification of candidate gene for <i>AvrSr35</i>	88
3.4.4 Sequence analysis of <i>AvrSr35</i> gene on <i>Sr35</i> -virulent mutant strains	88
3.4.5 Diversity analyses of <i>Sr35</i> -virulent and <i>Sr35</i> -avirulent field isolates of <i>Pgt</i>	90
3.4.6 PCR-based cloning of the <i>AvrSr35</i> candidate	93
3.4.7 Sequence analysis and characterization of <i>AvrSr35</i> candidate	94
3.5 Discussion	97
3.5.1 Developing of <i>Pgt</i> EMS-mutants with virulence for the <i>Sr35</i> gene	98
3.5.2 Diversity analysis of <i>AvrSr35</i> locus	101
3.5.3 Microscopy analysis of <i>Pgt</i> time course of infection	103
3.6 Conclusions and perspectives	106
Chapter 4 - Functional characterization of the <i>AvrSr35</i> gene	109
4.1 Introduction	109
4.2 Objectives	112
4.3 Materials and methods	112
4.3.1 Plant material	112
4.3.2 Bacterial strains	113
4.3.3 Time course expression analysis of <i>AvrSr35</i>	113
4.3.4 Tobacco agroinfiltration	114
4.3.4.1 Binary vector construction for <i>N. benthamiana</i> agroinfiltration	114
4.3.4.2 <i>Agrobacterium</i> transformation	119
4.3.4.3 <i>Agrobacterium</i> mediated transient assay in <i>N. benthamiana</i>	119
4.3.4.4 Hypersensitive response evaluation using 3'3-DAB uptake method	120
4.3.5 Infiltration of <i>AvrSr35</i> heterologous protein on wheat	121
4.3.5.1 Construction of recombinant expression vectors	121
4.3.5.2 Expression, detection, purification and cleavage of (-SP) <i>AvrSr35</i> recombinant protein	121
4.3.6 Subcellular localization in <i>N. benthamiana</i> leaves	123

4.3.7 Bimolecular fluorescent complementation (BiFC) assay in <i>N. benthamiana</i> leaves	124
4.3.8 Co-immunoprecipitation assay	124
4.4 Results	125
4.4.1 Time course gene expression of <i>AvrSr35</i> during the infection	125
4.4.2 Agroinfiltration of <i>N. benthamiana</i> leaves	126
4.4.3 <i>AvrSr35</i> heterologous protein infiltration on wheat leaves	129
4.4.4 Subcellular localization of <i>AvrSr35</i> and <i>Sr35</i>	132
4.4.5 Bimolecular fluorescent complementation (BiFC) assay	133
4.4.6 Co-immunoprecipitation of <i>AvrSr35</i> and <i>Sr35</i> on tobacco leaves	134
4.5 Discussion	136
4.5.4 Relative expression <i>Avrsr35</i> during time course infection	136
4.5.6 <i>AvrSr35</i> induces HR in presence of <i>Sr35</i>	137
4.5.7 <i>AvrSr35</i> and <i>Sr35</i> proteins co-localizes in the same sub-cellular compartment and interacts	139
4.6 Conclusions and Perspectives	143
Chapter 5 - Final conclusions	145
References	148
Appendix B	192
Appendix C	193
Appendix D	204
Appendix E	206

List of Figures

Figure 1.1 Uredinial stage of leaf, stem and stripe rust.....	5
Figure 1.2. <i>Puccinia graminis</i> f.sp. <i>tritici</i> life cycle	8
Figure 1.3 The Guard and Decoy models for indirect interaction between <i>R</i> and <i>Avr</i> genes..	43
Figure 2.1. Alternative splicing isoforms of <i>Sr35</i> and specific primer validation.	55
Figure 2.2. Relative transcript levels of the <i>Sr35</i> isoforms during time course of infection with the <i>Pgt</i> race RKQQC..	59
Figure 2.3. PCR-base screening of selected T ₀ transgenic events to identify the presence of the <i>Sr35</i> transgene..	60
Figure 2.4. PCR-base screening of selected T ₀ transgenic events to identify the presence of the <i>bar</i> gene.	60
Figure 2.5. Relative transcript levels of the <i>Sr35</i> main isoform in four positive transgenic lines assessed using qRT-PCR.	61
Figure 2.6. PCR-base progeny segregation screening of the T ₁ generation of the transgenic line #1123	62
Figure 3.1. Confocal microscopy at the early stages of <i>Pgt</i> infection to detect fungal infection structures.....	83
Figure 3.2. Confocal microscopy at early stages of <i>Pgt</i> infection to detect cell death on the wheat host..	84
Figure 3.3. Phenotypic response at seedling stage of wheat infected with <i>Pgt</i>	85
Figure 3.4. Laser-scanning confocal microscopy of <i>Pgt Sr35</i> -virulent mutant strains growth in leaves of susceptible wheat cultivar <i>Morocco</i> (<i>Sr35</i> -).....	86
Figure 3.5. Ethidium Bromide-stained agarose gel (1.8%) showing PCR-product length polymorphism for the <i>AvrSr35</i> gene among several <i>Pgt</i> isolates.	91
Figure 3.6. <i>AvrSr35</i> gene model and gene based phylogenetic relationship among <i>Sr35</i> -virulent and avirulent isolates	92
Figure 3.7. Sequence of the miniature inverted transposable element (MITE) inserted into the exon six of the <i>AvrSr35</i> gene of the group V of haplotypes.	93
Figure 3.8. Ethidium Bromide-stained agarose gel (1.8%) showing the RT-PCR amplification of the <i>AvrSr35</i> gene.	94

Figure 3.9. Search of similarity on NCBI database (Blastx) for <i>AvrSr35</i>	95
Figure 3.10. Prediction of secretion signal peptide (SP) for the <i>AvrSr35</i> using SignalP software	96
Figure 3.11. Secondary structure prediction based on amino acid sequence of the candidate gene <i>AvrSr35</i>	97
Figure 4.1. Binary vectors used in <i>N. benthamiana</i> agroinfiltration.....	118
Figure 4.2. Relative expression of the <i>AvrSr35</i> gene during time course of infection with <i>Pgt</i> race RKQQC.	126
Figure 4.3. <i>AvrSr35</i> with and without deduced signal peptide (SP) induces HR in the presence of <i>Sr35</i>	127
Figure 4.4. <i>AvrSr35</i> induces specific HR in the presence of <i>Sr35</i>	128
Figure 4.5. Evaluation of the <i>Sr35</i> and <i>AvrSr35</i> expression on tobacco leaves after agroinfiltration.	129
Figure 4.6. Expression and purification of the fusion protein SUMO- Δ SP- <i>AvrSr35</i>	130
Figure 4.7. Cleavage of the SUMO portion of fusion recombinant protein SUMO- Δ SP- <i>AvrSr35</i>	130
Figure 4.8. Infiltration of Δ SP- <i>AvrSr35</i> protein into leaves of Marquis- <i>Sr35</i> (<i>Sr35</i> +) and Marquis (<i>Sr35</i> -) cultivars.....	132
Figure 4.9. Subcellular localization of the <i>Sr35</i> and <i>AvrSr35</i> gene products.....	133
Figure 4.10. Bimolecular fluorescent complementation (BiFC) assay confirming interaction between <i>Sr35</i> and <i>AvrSr35</i> proteins.	135
Figure 4.11. Co-immunoprecipitation assays confirming interaction between <i>Sr35</i> and <i>AvrSr35</i> proteins.....	136

List of Tables

Table 1.1. Main features of cereal rusts	4
Table 1.2. Summary of the <i>Ug99</i> race group variants.	13
Table 1.3. Chromosomal location, description and source of stem rust resistance genes effective and moderate effective against <i>Puccinia graminis</i> f. sp. <i>tritici</i> race of <i>Ug99</i> and its variants	277
Table 1.4. Gene category and strategy used to clone resistance genes for cereal rust.....	299
Table 2.1. Primers used for <i>Sr35</i> -transgene PCR screening and gene expression.	54
Table 2.2. Co-segregation of the <i>Sr35</i> -transgene with the infection type on T ₁ plants from transgenic line #1123.	63
Table 3.1. Primers used for the cloning and the diversity analysis of <i>AvSr35</i> candidate.	78
Table 3.2. <i>Pgt</i> isolates used for <i>AvrSr35</i> allele diversity analysis.	80
Table 3.3. Summary assembling metrics and completeness of the genome of <i>Pgt</i> wild-type RKQQC isolate 99KS76A-1.	87
Table 3.4. Predicted single point mutations of the <i>AvrSr35</i> gene on 15 <i>Sr35</i> -virulent RKQQC mutant strains.....	89
Table 4.1. Primer list used for binary vector construction	115
Table 4.2. Summary of vectors used in planta assay experiments.....	117
Table 4.3. Evaluation of HR 24 hours after the infiltration with the heterologous protein Δ SP- <i>AvrSr35</i> into leaves of resistant Marquis <i>Sr35</i> (<i>Sr35</i> +) and susceptible Marquis (<i>Sr35</i> -) wheat cultivars.....	131

Acknowledgements

A very special gratitude to my advisor Dr. Eduard Akhunov for providing me the opportunity to grow professionally and for his guidance and encouragement throughout the research project. Special thanks to the distinguished faculty members who served on my committee: for their support, patience, encouragement, and useful suggestions. Professor Robert Bowden, who I am always be grateful for the training, wise advice, and open office every time I needed. Professor Frank White, by his continuous support and insightful comments during my graduate study. Profesor Susan Brown for her helpful and independent comments and her willingness to support me from the first day.

My thanks go to labmates and former/current Postdocs from the Akhunov lab Dr. Shichen Wang (A=0), Dr. William Rutter, Dr. Cyrille Santeniach, Dr. Wei Wang and Dr. Katherine Jordan for their friendship, expertise, warm encouragement and support during my PhD.

I would also like thank Dr. Alina Akhunova and the staff the Integrated Genomics Facility Yanni Lun and Huanquan Liang for the excellent guidance, training and expertise.

Thanks to my wife Mónica for her continuous support and encouragment, being a patient teacher, help in performing experiments and tremendous contribution to this research.

Thanks to Plant Pathology Department Faculty for contributing to my professional improvement and opening doors to the wonderful world of the living things.

Thanks to my fellow Graduated students for their help in hard times and offering me friendship: Miguel Arango, Andres Reyes, Ismael Badillo, Mónica Navia, Elina Adhikari, Christian Cruz, Rodrigo Pedrozo and many more.

Finally, I would like to thank my mentees Beth Lowry, Victor Ryu, Bliss Blitzen for their contribution to research and teaching me how to teach. Also, I would like to thank Sheena Deuny and Duane L. Wilson for supporting me during my Ph.D. work.

Dedication

I dedicate my dissertation work to my wife and travel partner Monica without whose love, permanent caring and support it would be impossible to accomplish my goals. A special feeling of gratitude to my loving parents, Yolanda and Manuel and my brother John whose words of love, encouragement and push for tenacity always will ring in my ears.

Preface

This thesis submitted for Ph.D. degree is based on experimental work carried out at Department of Plant Pathology at Kansas State University. The experimental work was conducted under supervision of professor Eduard Akhunov. The thesis is based on studies reported in two published papers:

Saintenac, C.¹, Zhang, W.¹, **Salcedo, A.**, Rouse, M., Trick, H., Akhunov, E.², & Dubcovsky, J.². (2013). Identification of Wheat Gene *Sr35* That Confers Resistance to *Ug99* Stem Rust Race Group. *Science*, 341, 783–786.

Salcedo, A.¹, Rutter, W.¹, Wang, S., Akhunova, A., Bolus, S., Chao, S., Anderson, N., Fernandez De Soto, M., Rouse, M., Szabo, L., Bowden, R. L., Dubcovsky, J., Akhunov, E.² (2017). Variation in the *AvrSr35* gene determines *Sr35* resistance against wheat stem rust race *Ug99*. *Science* 358, 1604-1606

¹ these authors contributed equally to the work.

² corresponding author(s).

Introduction

The basidiomycete *Puccinia graminis* f. sp. *tritici* (*Pgt*) is an obligate biotrophic pathogen that causes the wheat stem rust, one of the most devastating diseases in the history of the agriculture (Leornad & Szabo, 2005). The widespread adoption of wheat cultivars with stem rust resistance genes (*Sr*) during the *Green Revolution* and improved crop management have limited the epidemics of stem rust during many years (Khush, 2001; Singh et al., 2008b). However, the discovery of a new *Pgt* pathotype called *Ug99* (TTKSK, for North American nomenclature) (Pretorius et al., 2000), that was able to overcome the resistance present in most of the cultivated wheat varieties clearly demonstrated that single gene-based resistance will not last forever, and *Pgt* can develop virulence to the existing *Sr* genes used for decades (Singh et al., 2015). The recent origin and spread of new *Ug99*-derived isolates with a broader virulence spectrum in several countries in Africa and the Middle East (Jin et al., 2008, 2009; Singh et al., 2011, 2015) indicated that *Ug99* represents a substantial threat to the global wheat production. Enhancing crop protection strategies by developing wheat varieties with durable resistance continue is the most cost-efficient and environmentally friendly approach to mitigate the pathogen epidemics (Hogenboom, 1993). In this context, *Sr* genes present in wheat relatives are invaluable sources of resistance against *Ug99* (Jin et al., 2007). The *Sr35* resistance gene mapped in the wheat relative *Triticum monoccocum* (Zhang et al., 2010) confer near-immunity (null or low disease severity) against *Ug99* and several relatives (Singh et al., 2011; Singh et al., 2015). The *Sr35* gene was cloned (Saintenac et al., 2013), but it was necessary to characterize it and evaluate if this gene by itself is sufficient to confer protection against *Ug99*. To answer these questions, this project assessed the transcriptional activity of the *Sr35* gene during time course of infection with a *Sr35*-avirulent *Pgt* race, and also it evaluated the presence and expression of the *Sr35*-transgene in transgenic hexaploid wheat.

Pgt, like many other plant pathogens, interacts with its wheat host according to the gene-for-gene model (Flor, 1947; Flor, 1971; Williams et al., 1966). This model predicts that successful plant defense against disease is triggered only if a resistance gene (*R*) product, present in the plant, can recognize directly or indirectly a specific avirulence (*Avr*) protein from the pathogen (van der Biezen & Jones, 1998; Jones & Dangl, 2006; Ellis et al., 2009). Identification of interacting *R*-

Avr gene pairs opens doors to understanding host pathways targeted by a pathogen, and can provide information important for developing novel strategies based, for example, on engineering the host protein targets or resistance genes. However, the major obstacle to devising these strategies for stem rust resistance is the lack of mechanistic understanding of the interactions among the *Pgt* proteins, their targets, and the *Sr* genes. Unfortunately, only a handful of *Avr* proteins has been validated in rust fungi and despite the abundance of candidates, no functional characterization of a *Avr* gene associated with race-specific resistance gene in the cereal rust have been done.

Besides the functional characterization of the *Sr35* gene, this study was also aimed at identifying *AvrSr35*, the avirulence gene product that is recognized by *Sr35* gene product. This research used a forward genetic approach where a population of chemically mutagenized *Pgt* spores was screened for *Sr35*-virulent mutant strains. The genomes of the mutants strains were sequenced, and bioinformatic analysis was performed to identify a candidate for the *AvrSr35* gene. The sequence diversity of *AvrSr35* candidate gene was analyzed in several *Pgt* isolates, and showed association between the presence of the *AvrSr35* candidate gene and avirulence on *Sr35*. Finally, the *AvrSr35* candidate was functionally validated using *in planta* assays that confirmed its avirulence function and interaction with the *Sr35* gene product. The results of the study lead to the conclusion that this fungal gene is an *Avr* gene recognized by the *Sr35* gene product constituting one of the first *Avr* genes characterized in cereal rusts.

Aims of the project

- To evaluate the expression of the stem rust resistance gene *Sr35* during infection.
- To evaluate the presence and the expression of the *Sr35*-transgen in hexaploid transgenic lines.
- To investigate the *Pgt* development on wheat lines with and without the *Sr35* resistance gene.
- To identify, characterize and functionally validate the *Avr* gene recognized by the *Sr35* gene.

Chapter 1 - Literature review

1.1 Wheat rusts are a global threat to food security

Wheat is a staple food for over one billion people in developing countries (FAO, 2014), constituting the main source of proteins in their diets (Shewry, 2009; Bhardwaj et al., 2014). Since the Green Revolution, wheat has reduced human malnutrition due to the constant increase in production (Khan et al., 2013). According to the FAO the world wheat production in 2016 was estimated at more than 760 million metric tons. FAO (2017) *World food situation*. Retrieved from <http://www.fao.org/worldfoodsituation/csdb/en/>, and by the year 2050 the demand is expected to rise by 60% over the current production (Singh et al., 2011). The impact of climate change is predicted to make the crop more vulnerable by the emergence of new pests and diseases, changes in its geographical ranges and loss of resistance, reducing the global production by more than 29% (Rosegrant, et al., 1995; Oerke, 2006; Manoharachary & Kunwar, 2014). Nearly 37% of global wheat production is concentrated in north and east Africa, Middle East and central and south Asia (Singh et al., 2011b). It is in these regions where wheat is particularly important for human dietary needs contributing essential amino acids, minerals, and vitamins as well as livelihoods. These regions are also very vulnerable to wheat rusts (Shewry, 2009; FAO, 2014), which is becoming the major limitation to sustainable wheat cultivation (Afzal et al., 2016).

There are three main wheat rust diseases: stem (eponym: black) rust caused by *Puccinia graminis* Pers f. sp. *tritici*, Erikss and E. Henning (henceforth *Pgt*); stripe (yellow) rust caused by *P. striiformis* Westend f. sp. *tritici* (*Pst*); and leaf (brown) rust caused by *P. triticina* Erikss (*Pt*) (formerly known as *P. recondita* f. sp. *tritici*.) (McIntosh et al., 1995; Dean et al., 2012). In addition, other fungal species cause rust in other cereal crops. For example, *Puccinia hordei* G.H. Otth (*Ph*) causes leaf rust on barley; and *Puccinia coronata* Corda (*Pc*) causes crown rust on oat (Zhao et al., 2016). Cereal rusts reduce grain yields annually by an estimated 10%. However, during epidemics, they have caused severe food shortages and even ruined the economy of some countries (Agrios, 2005). Despite the differences in the optimal environmental conditions for their development, the three wheat cereal rusts are some of the most widespread pathogens. They can be present in the field at different plant developmental stages and may show different levels of severity (Table 1.1) (Afzal et al., 2016; Agrios, 2005). The adaptation of the

rust fungi to different environments determines the rust distribution and the frequency of epidemics (Zhao et al., 2016). Historically stripe rust had major impacts in west Asia, southern Africa, China, South America and northern Europe. The incidence of leaf rust is more frequent and widely distributed; the disease had caused serious losses in south Asia, north Africa, southeast Asia and South America. Traditionally stem rust has been an important disease in North America, Australia, northern Africa, south Africa and to some extent in Europe (Roelfs et al., 1992).

The most notorious phenotypes of rust disease can easily be observed by the naked eye during the developmental stages and are the basis for their common names (Figure 1.1). For example, the name of stem rust or black rust comes from the black color of the telial stage. Rust infections may occur on any plant tissue above ground, but generally, the pathogen attack leaves and stems. The uredinial stage appears as spots, stripes or pustules called *uredia* or *uredinia* containing millions of windborne spores called urediniospores. These spores can spread thousands of miles away and re-infect wheat crops. Cereal rusts debilitate or even kill seedlings, but typically the most important effects are the reduction of foliage and root systems as well as grain yield. These symptoms are metabolic effects associated with a reduction in photosynthesis rate, an increase in the respiration rate, and a decreasing in translocation of carbohydrates (Agrios, 2005; Leornad & Szabo, 2005).

Table 1.1. Main features of cereal rusts based on Roelfs et al. (1992) and Chen et al. (2014b).

Disease	Causal agent	Cereal host	Main alternate host	Main symptoms
Leaf rust	<i>Puccinia triticina</i> f. sp. <i>tritici</i>	Bread & durum, wheat and triticale	<i>Thalictrum</i> , <i>Anchusa</i> , <i>Isopyrum</i> and <i>Clematis</i>	Isolated uredinia on upper leaf surface rarely on leaf sheaths
Stem rust	<i>Puccinia</i> <i>graminis</i> f. sp. <i>tritici</i>	Bread & durum, wheat barley and triticale	<i>Berberis</i> <i>vulgaris</i>	Isolated uredinia on upper and low leaf surfaces stem and spikes
Stripe rust	<i>Puccinia</i> <i>striiformis</i> f. sp. <i>tritici</i>	Bread & durum, wheat barley and triticale	<i>Berberis spp.</i> , <i>Mahonia</i> <i>aquifolium</i>	Systemic uredinia in leaves and spikes and rarely on leaf sheaths



Leaf rust

Stem Rust

Stripe rust

Figure 1.1. Uredinial stage of leaf, stem and stripe rust. Source: Cereal Disease Lab Minnesota U.S. Department of Agriculture, Agricultural Research Service.

Historically, the stem rusts is one of the most feared crop diseases ever, causing up to 100% yield losses in susceptible varieties and influencing the development of humankind since the invention of agriculture (Park, 2007; Dean et al., 2012). Archeological evidence in Israeli excavations dates the presence of stem rust to about 3300 BCE (Kislev, 1982). The disease was mentioned in the classical literature of ancient Greece and Rome (Chester, 1946), whose inhabitants offered sacrifices to the god Robigus to protect their crops against rust (McIntosh et al., 1995).

Despite the fact that stem rust is not the most widespread and common of cereal rust, it has been considered as the most destructive one because, in addition to the stem, it can infect leaves and heads of developing plants, and because severely damage plants are prone to lodging, thus complicating harvesting (De Wolf et al., 2011). The disease has been difficult to control due to the high evolutionary potential of the pathogen and the extensive wheat cultivation in favorable infection conditions (Dean et al., 2012). Unfortunately, today the main losses due to stem rust occur in developing countries where food security is most vulnerable (Dubin & Brennan, 2009).

1.2 The cereal rusts

Rust fungi are highly specialized obligated plant biotrophs with more than 7000 species described and with a long evolutionary history that can be traced back to the Carboniferous age

when they infected ferns (Kolmer et al., 2009a, b; Anikster & Wahl, 1979). Rust fungi belong to the phylum Basidiomycota which also include mushrooms, smuts and puffballs. Most of the known rust species are grouped into the Pucciniomycetes (formerly known as Urediniomycetes class) where the cereal rust order or *Puccinales* order (formerly known as Uredinales) is considered a monophyletic group (Kolmer et al., 2009a; Aime, 2006; Bauer et al., 2006). The *Puccinales* order is divided in 13 families based on the morphology of their teliospores (Aime, 2006). The *Pucciniaceae* family contains 20 genera; about half of the species belong to the genus *Puccinia*, which contains all species that cause rust disease in the major cereal crops (Kirk et al., 2008; Zhao et al., 2016) except for rice (Webb & Fellers, 2006).

In 1767 Fontana and Targioni Tozzetti associated the cereal rust with a fungal parasite, and some years later Persoon (1797) named *Puccinia graminis* as the causal agent of stem rust. *Puccinia graminis* has been divided into two subspecies: *graminicola* and *graminis* based on spore morphology, host range and fertility observed after crosses [Urban (1967) cited by (Leonard & Szabo, 2005)]. The subspecies *graminicola* contained stem rusts found on non-cereal grasses and is considered the ancestral form. The subspecies *graminis* contains the stem rusts found on cereal crops. *P. graminis* ssp. *graminis* was further subdivided into var. *graminis* and var. *Stakmanii*. The wheat stem rust fungus is included in *P. graminis* ssp. *graminis* var. *graminis*, whereas the oat stem rust and rye stem rust fungi are included in *P. graminis* ssp. *graminis* var. *stakmanii* (Leonard & Szabo, 2005). In 1894 the Swedish pathologist Eriksson defined an infraspecific taxonomic category called the *formae specialis* (f. sp.) to describe a particular form of the pathogen based on the host specialization or preference, i.e., the most common genus that the pathogen attacks or alternatively the host in which the pathogen was initially identified (McIntosh et al., 1995; Roelfs et al., 1992; Voegelé et al., 2009). Despite the appropriate taxonomic divisions the rust fungi are directly named avoiding the subspecies designation but instead using *formae speciales* (f. sp.): for example, *P. graminis* f.sp. *tritici*, *P. graminis* f.sp. *avenae*, etc. CABI (Septemeber, 2016) *Invasive species compendium*. Retrieved from <http://www.cabi.org/isc/datasheet/45797>.

The study of cereal rusts has addressed the discovery of various foundational principles of plant pathology (Afzal et al., 2016). In the early 20th century, Elvin Stakman and his colleagues at the

University of Minnesota demonstrated that the infraspecific category *forma specialis* of *Pgt* contains stable and identifiable variants. They called this taxon *physiological races* or simply *races*. Races can be represented by one or several populations of individuals with a uniform genotype called biotypes [Schafer et al (1984) cited by McIntosh et al., (1995)]. Two biotypes can have the same avirulence/virulence profile. However, the phenotype can be either the result of homozygous or heterozygous state. Therefore, the progeny of a urediniospore theoretically, would constitute a pathogen biotype. Races are determined by a particular profile of avirulence/virulence over a selected group of host plants called *differential host lines* or *differentials* that usually carry a single race-specific resistance gene. This set of differentials determines the race of a particular test isolate, which in in US and Canada is composed of 20 near-isogenic lines grouped into sets of four resistance genes. The specific avirulence/virulence pattern in each set, codes for a consonant ranging from B (avirulent on all four differentials) to T (virulent on all four differentials) (McIntosh et al., 1995).

Pgt can infect at least 74 species in 34 genera, but only 28 of those species in eight genera were known to be natural hosts of the pathogen including economically important crops like wheat (*Triticum aestivum* L. and *Triticum turgidum* L. var. *durum*), barley (*Hordeum vulgare* L.) and triticale. The first symptoms of *Pgt* consist of small chlorotic flecks followed by small elongated millimetric brownish-red pustules. Pustules are the result of epidermal rupture by the mass of asexual urediniospores which take on a ragged appearance. Every one can produce up to 10,000 urediniospores per day (Figure 1.1). These pustules are frequently located on the leaf sheaths, stem, leaves, glumes, and awns. As the disease progresses, the urediniospore production ceases and is replaced by a layer of black teliospores, which causes the stems of heavily infected plants to appear blackened. Under severe infection the stems are weakened and the flow of nutrients is reduced causing grain shriveling and lodging (falling over) of the plant (Leonard & Szabo, 2005; Singh et al., 2008a, Kolmer et al., 2009a,b).

1.2.1 Stem rust life cycle

Cereal rusts are heteroecious, completing their life cycle on two taxonomically unrelated hosts. They are macrocyclics and have five distinct spore stages in their life cycle: teliospores, basidiospores and urediniospores on the cereal or primary hosts, and pycniospores and

aeciospores on the alternate hosts. Those spores can contain three different nuclear types (haploid, diploid and dikaryotic) (Alexopoulos et al., 1996; Leonard & Szabo, 2005; Kolmer, 2013). The life cycle of *Puccinia graminis* is shown in figure 2.2. The germination of the diploid teliospores which in *Pgt* has a long dormancy (produced in the previous season on cereal host and stored in pustules called telia), starts in the spring producing by meiosis four or more haploid spores called basidiospores (n) in a structure called promycelium (or basidium). Mature basidiospores possess two mating types (+/-) that are ejected into the air and travel by the wind to what is considered the alternate dicot host. The dicot hosts are a large number of species of shrubs, which belong to the genera *Berberis* and *Mahonia*. The most common dicot host species is *Berberis vulgaris* (Anikster & Wahl, 1979; Alexopoulos et al., 1996; Singh et al., 2008b).

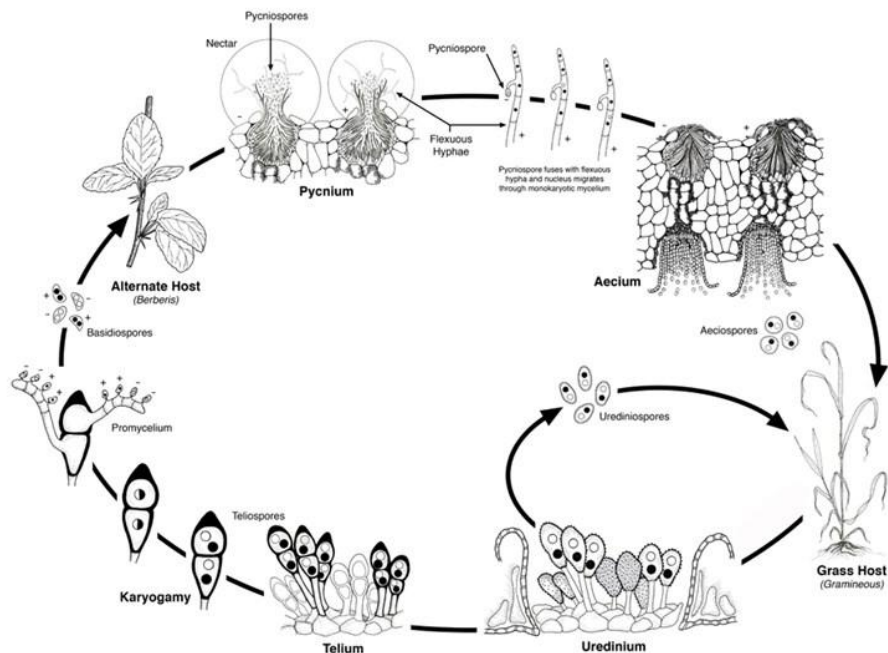


Figure 1.2. *Puccinia graminis* f.sp. *tritici* life cycle. In the asexual stage urediniospores infect cereals and grasses, the sexual stage is completed on the dicot alternate host (*Berberis*) (From Leonard & Szabo, 2005, line drawing by J. Morison).

Basidiospores infect through direct penetration of the alternated host epidermal cells producing haploid colonies that appear as a dense yellowish mat of hyphae beneath the host epidermis with a flask shaped structures called pycnium (spermogonium). Pycnia produce receptive hyphae and pycniospores with two mating types that are exuded and embedded in a nectar attractive to insects. This nectar, as well as moisture on the plant surface distributes the pycniospores over the

host or neighboring plants resulting in fertilization (plasmogamy) when receptive hyphae in the pycnium are fertilized by pycniospores from a pycnium of a different mating type. Plasmogamia forms a dikaryotic cell (a single cell with two haploid nuclei or n+n), where new virulence combinations result from sexual re-assortment of *Avr*-genes. The dikaryotic hyphae proliferate to form aecial colonies that produce Aeciospores in large quantities on the lower epidermis. Aeciospores can travel long distances to reach the gramineous host.(Schumann & Leonard, 2000 Leonard & Szabo, 2005; Kolmer et al., 2009a, b).

Once the aeciospores colonize the gramineous host, they germinate rapidly and invade cells via stomata. The resulting infection and colony formation results in another pustule called the *uredinium* which contains urediniospores. The uredinium stage is the most economically relevant stage of the *Pgt* life cycle. Urediniospores are capable of perpetuating by cycling infection on gramineous hosts such as wheat and barley. The urediniospore cycles can every 14-20 days, and under favorable conditions, a rapid increase of millions of wind-borne urediniospores is capable of causing explosive epidemics (Leornad & Szabo, 2005; Kolmer, et al., 2009b; Bhardwaj et al., 2014). Urediniospore germination usually occurs at night on the plant surface when dew is present, making the urediniospores swell when they contact with the water. The optimal temperature for infection on wheat ranges from 15°C to 25°C (59°F to 75°F) and for disease development 24°C to 30°C (75°F to 86°F) (Murray et al., 2010). After 4-6 hours a germ tube is produced and its development is controlled by a thigmotropic response according to the topography of the host surface (Wynn & Staples, 1981 cited by Kolmer et al., 2009a; Singh, et al., 2008). The germ tube continues to elongate until it come into contact with a stomate. Once the stomate is located the germ tube stops the elongation, and its tip differentiates into a structure called the *appressorium* (Leornad & Szabo, 2005).

At dawn, the fungal growth resumes followed by the formation of a *penetration peg* from the appressorium that pushes through the stomate to enter the intercellular space under the epidermis and thus forming a *substomal vesicle*. *Infection hyphae* grow from each end of the substomal vesicle towards the mesophyll cells. As the tips of the infection hyphae become in close proximity with a mesophyll host cell wall, they differentiate in a cellular type called *haustorial mother cell* which is delimited from the infection hypha by a septum. A penetration peg is

formed from the haustorial mother cell apparently mediated by enzymatic dissolution and pressure that allows the expansion of a specialized fungal hypha called dikaryotic *haustorium* (Kolmer et al., 2009a).

The haustorium (plural haustoria) is not truly an intracellular structure, it remains outside of the physiological barrier of the host cells. The haustorium is formed in the mesophyll cells of the host, as an invagination in the periplasmic space of the host cell that involves the host cell wall and the extrahaustorial membrane which is derived from the host cell plasma membrane remaining. Fungal nutrient uptake and secretome interchange with the host take place on the extrahaustorial membrane in order to support fungal colonization. It is believed fungus use signals from the haustorium to manipulate host cell metabolism in order to suppress the host defense responses and reprogram the host metabolism, but maintaining the biotrophism: (the transport of vital nutrients like sugars and amino acids to the pathogen while the host cell viability is maintained) (Voegelé et al., 2003; Leornad & Szabo 2005; Kolmer et al., 2009a,b) While the first haustorium is forming, the infection hypha resume growth and branches to form additional haustorial mother cells and new haustoria are formed to extract nutrients after contact with new mesophyll cell walls. After 7-10 days in the host tissue the fungal mycelia forms sporogenous cells in the intercellular space under the epidermis. Then spore buds break the epidermis and the urediniospores accumulate in form of *uredinia* after they are formed on the emergent spore buds. Eventually, the host stops supplying nutrients and uredinia are converted to telia that produce teliospores. This conversion takes place in late summer or autumn coinciding with the end of the growing season of the gramineous host. Teliospores serve as overwintering spores thanks to their thick walls that make them resistant to cold or dry conditions. Inside teliospores the dikaryotic nuclei merge to form a diploid nucleus before the teliospore enters into dormancy a process called karyogamy, and the cycle starts over (Leornad & Szabo, 2005; Kolmer et al., 2009a).

1.3 Emergence of the *Ug99* race

Stem rust epidemics became a rare event in developed countries after the adoption of resistant and early maturity wheat varieties combined with the near eradication of the *Pgt* alternate dicot host, the common barberry. As a result of these strategies, the wheat world production was barely affected by stem rust for decades, and research interest against the disease declined

(Singh, et al., 2006; Singh et al., 2008b; Murray et al., 2010; Afzal et al., 2016). Nevertheless, some geographic regions such as the highlands of eastern Africa historically have been considered a “hot spot” for rust epidemics and the evolution of new highly virulent races (Saari & Prescott, 1985). Several ecological, environmental and agronomy factors contribute to creating ideal conditions for new epidemics in that region of the world. Climate conditions in the region support facilitate the constant presence of stem rust populations, and the continuous cultivation of susceptible wheat genotypes provide a green-bridge for the survival of inoculum (Afzal et al., 2016; Bhardwaj et al., 2014).

In 1998, William Wagoire reported a new *Pgt* isolate in an experimental field in Uganda that was highly virulent on several wheat accessions carrying the resistance gene *Sr31*. Since the 1970’s, wheat breeding programs around the world started to use extensively the *Sr31* gene derived from the rye chromosomal translocation 1BL.1RS. The frequency of the *Sr31* gene in breeding materials reached approximately 70% in CIMMYT’s spring wheat germplasm and up to 45% in commercial cultivars in more than 17 countries (Purnhauser et al., 2006; Germán et al., 2007). This new *Pgt* isolate with virulence against *Sr31* was confirmed as a new race of *Pgt* in 1999 by Zacharias Pretorius from the University of the Free State in Bloemfontein, South Africa, and was coined with acronym *Pgt-Ug99* or *Ug99* (Pretorius et al., 2000; Bhardwaj et al., 2014). However, some authors suggest that *Ug99* was already present in Kenya by 1993 (Singh et al., 2008b). Jin et al. (2008), later denominated *Ug99* as the race TTKSK according to the North American Nomenclature system.

After its emergence, new breakdowns of resistance against *Ug99* were initially detected in 2006 and 2007 in Kenya due to the daughter *Ug99* races TTKST and TTTSK, which were found to be virulent on *Sr24* and *Sr36*, respectively (Jin et al. 2008, 2009). By 2007, screening in 22 countries showed that varieties with adequate resistance against *Ug99* represented only between 5-10% (Singh et al., 2011). Resistance genes *Sr9h*, *Sr13*, *SrTmp*, and *Sr1RS*^{Amigo} effective against the original *Ug99* isolate, were recently defeated by the race TTKSF+ and other pathogen races such as TKTTF and TRTTF (Olivera et al., 2012; Bajgain et al., 2015; Olivera et al., 2015). The rapid emergence and diversification of *Ug99* revealed the vulnerability of wheat cultivated germplasm to the pathogen, and the threat of *Ug99* to the food security was recognized. Also, the

consensus was that the best option to reduce *Ug99* impact was to identify more resistance genes in wheat germplasm or develop resistant varieties carrying available genes adapted to environments that are under risk and release them (Singh et al., 2008a; Murray et al., 2010). In 2005, the Borlaug Global Rust Initiative (BGRI) consortium was created, coordinating several research and development projects to reduce wheat's vulnerability to cereal rust and also increasing its productivity. BGRI seeks to monitor the spreading of *Ug99* by screening and delivering resistant wheat germplasm to breeding programs (Singh et al., 2008a; Bhardwaj et al., 2014) *Borlaug Global Rust Initiative* (September, 2016). Retrieved from <http://www.globalrust.org>.

A series of reviews by Singh et al. (2008ab, 2011 and 2015) have documented the spread of *Ug99*. After *Ug99* was identified in Uganda, it was subsequently detected in Kenya and Ethiopia in 2005 and by the end of 2006 was already found in Sudan and Yemen. This pattern implied that the *Ug99* was migrating towards important wheat growing areas of the Middle East and Asia, which are considered the breadbasket zone of the world. The presence of *Ug99* in Iran in 2008 confirmed this suggestion. By 2016, thirteen countries had already detected *Ug99* including Egypt. This situation increases the potential for *Ug99* spreading in the Mediterranean basin and becoming a problem in Europe (West et al., 2012); CIMMYT (September, 2016) *A Global Wheat Rust Monitoring*. Retrieved from <http://rusttracker.cimmyt.org/>. An epidemic of *Ug99* would affect a large number of wheat-farming families and impact the economic growth of several developing countries with global estimated losses over USD 3 billion, and affecting 25% of worldwide cultivated wheat area (Singh et al., 2008b; Singh et al., 2011; Khan et al., 2013).

The *Ug99* populations have undergone mutations, and to date, 13 variants have been detected (Table 1.2), allowing it to expand its geographical impact CIMMYT (September 2016) *A Global Wheat Rust Monitoring*. Retrieved from <http://rusttracker.cimmyt.org/>. DNA fingerprinting of *Ug99* variants suggests that this group is a monophyletic lineage that evolved recently as the result of asexual mutations and sexual recombination in the dicot host *B. holstii* present in the Ethiopian highlands. The race TTKSF or its theoretical ancestor the race PTKSF (avirulent for *Sr31*) is considered as the most probable predecessor of *Ug99* race group (Visser et al., 2009; Singh et al., 2011, 2015).

Table 1.2. Summary of the *Ug99* race group variants. The virulence (+) and avirulence (-) for the stem rust resistance genes (*Sr*) are indicated.

Race ¹	Alias	Key virulence (+) or avirulence (-)	Year of identification	Confirmed countries (year)
TTKSK	<i>Ug99</i>	0	1999	Uganda (1998/9), Kenya (2001), Ethiopia (2003), Sudan (2006), Yemen (2006), Iran (2007), Tanzania (2009), Eritrea (2012), Rwanda (2014), Egypt (2014)
TTKSF		0	2000	South Africa (2000), Zimbabwe (2009), Uganda (2012)
TTKST	<i>Ug99</i> + <i>Sr24</i>	+ <i>Sr31</i> , + <i>Sr24</i>	2006	Kenya (2006), Tanzania (2009), Eritrea (2010), Uganda (2012), Egypt (2014), Rwanda (2014)
TTTSK	<i>Ug99</i> + <i>Sr36</i>	+ <i>Sr31</i> , + <i>Sr36</i>	2007	Kenya (2007), Tanzania (2009), Ethiopia (2010), Uganda (2012), Rwanda (2014)
TTKSP		- <i>Sr31</i> , + <i>Sr24</i>	2007	South Africa (2007)
PTKSK		+ <i>Sr31</i> , - <i>Sr21</i>	2007	[Uganda (1998/9)?], Kenya (2009), Ethiopia (2007), Yemen (2009)
PTKST		+ <i>Sr31</i> , + <i>Sr24</i> , - <i>Sr21</i>	2008	Ethiopia (2007), Kenya (2008), South Africa (2009), Eritrea (2010), Mozambique (2010), Zimbabwe (2010)
TTKSF+		- <i>Sr31</i> , + <i>Sr9h</i>	2012	South Africa (2010), Zimbabwe (2010)
TTKTT		+ <i>Sr31</i> , + <i>Sr24</i> , + <i>SrTmp</i>	2015	Kenya (2014)
TTKTK		+ <i>Sr31</i> , + <i>SrTmp</i>	2015	Kenya (2014), Egypt (2014), Eritrea (2014), Rwanda (2014), Uganda (2014)
TTHSK		+ <i>Sr31</i> , - <i>Sr30</i>	2015	Kenya (2014)
PTKTK		+ <i>Sr31</i> , - <i>Sr21</i> , + <i>SrTmp</i>	2015	Kenya (2014)
TTHST		+ <i>Sr31</i> , - <i>Sr30</i> , + <i>Sr24</i>	2015	Kenya (2013)

Source: <http://rusttracker.cimmyt.org/>. Last accessed October 10 2016. ¹According with North American Nomenclature.

This diversification in the *Ug99* populations, with the ability to defeat several additional resistance genes lead to its designation as a race group (hereafter *Ug99 race group*) (Murray et al., 2010; Pretorius et al., 2012). The *Ug99* race group carries a particular combination of virulence against most of the resistance genes traditionally used in wheat breeding (Singh et al., 2008a,b, 2011, 2015). Those genes include at least 39 resistance genes, among them the widely used *Sr31*, the *Sr36*, *Sr24*, and *Sr38*, which have been used extensively in US wheat breeding

and also in Europe and Australia. Therefore a considerable number of wheat varieties are susceptible to Ug99 race group variants independent of the place they were deployed (Jin et al., 2007; Murray et al., 2010; Zhang, et al., 2014a; Singh et al., 2015).

The emergence of new stem rust races complicates even more the breeding for *Ug99* race group, producing virulence against the available sources of resistance (Afzal et al., 2016). Some of the resistance genes effective against *Ug99* race group are susceptible to other *Pgt* races reducing their utility as source of resistance. Examples include the *Sr35* gene (Saintenac et al., 2013) and the *Sr25* gene, which provides resistance gene against TTKSK that was defeated by the race PKTSC in India, (Jain et al., 2009). Recently, a variant of the race TKTTF as well as the races TKTTP and TTTTF virulent to *Sr24*, *SrTmp* *Sr1RS^{Amigo}* *Sr9h* and *Sr13* were found in Germany. The presence of these non *Ug99* races makes susceptible the 55% of breeding lines resistant to TTKSK (*Ug99*) in Europe (Olivera et al., 2017). This loss of resistance has sounded the alarms of a possible global wheat production threat as the wheat resistance gene pool is declining, and some of the defeated genes are used in breeding programs in the US, Australia, Europe and South America (Singh et al., 2008a).

1.4 The Borlaug global rust initiative (BGRI)

With the emergence of *Ug99*, plant pathologist Norman Borlaug warned about the threat that this new race represents. The importance of *Ug99* was recognized worldwide inspiring several research and development projects under the coordination of an international consortium of hundreds of institutions called The Borlaug Global Rust Initiative (BGRI) (www.globalrust.org), launched in 2005. BGRI seeks to reduce the vulnerability to cereal rust, to facilitate the international wheat breeding partnerships and to increase the wheat productivity by using the following approaches: (1) monitoring the spread of *Ug99* race group beyond eastern Africa for early warning and potential chemical interventions, (2) screening of released varieties and germplasm for resistance, (3) distributing sources of resistance worldwide for either direct use as varieties or for breeding, and (4) breeding to incorporate diverse resistance genes and adult plant resistance into wheat germplasm. The initiative considers reducing susceptible cultivars in “primary risk areas” of east Africa, Arabian Peninsula, north Africa, Middle East, and west-south

Asia and replacing them by resistant high yielding adapted varieties (Singh et al., 2008a). Since the launching of the BGRI much has been done to develop a monitoring system and to introduce *Ug99* resistant cultivars. However, there are still challenges since there is a necessity to deploy additional resistant cultivars as new stem rust races would overcome the resistance available. This makes it imperative to understand the nature of the resistance available to grant the protection of the crops against new variants of *Pgt* (Sharma et al., 2013; FAO, 2014).

1.5 Strategies to control stem rust

1.5.1 Integrated management practices

1.5.1.1 Agronomical management and cultural practices

There are several alternatives to controlling stem rust. Some of them have been very successful in reducing both the variability of the pathogen and the amount of inoculum for long periods, relieving the disease pressure over the crop. Farmers have used several strategies to control stem rust, including cultural practices and the use of chemical agents such as fungicides (Murray et al., 2010). Cultural practices have been used to reduce the intensity of epidemics. These cultural controls include the reduction of self-sown over-summering plants and overlapping crops (wheat and barley) that serve as a green bridge, thus reducing the carryover of rust spores and the risk of early infection (Grain Research and Development Corporation, 2011). Retrieved from <https://www.agric.wa.gov.au>. This strategy generates local bottlenecks in pathogen populations and led to the extinction of locally adapted races (Burdon et al., 2014). A second strategy consists of crop rotations with non-cereal crops or planting early maturing varieties, which avoid the time of exposure to possible epidemics late in the growing season. This strategy allows farmers to destroy any volunteer plant around farms that may host the rust spores and infect the crop next season. CABI (October 2016) *Invasive species compendium*. Retrieved from <http://www.cabi.org/isc/datasheet/45797>.

1.5.1.2 Use of mixtures or multilines and regional deployment of resistance under evolutionary principles

Cereal cropping systems tend to be predominantly a monocultures of a few purified varieties in large areas of land, increasing the potential for host susceptibility after the selection of fungal isolates that are capable of overcoming the crop resistance (Wolfe, 1988; Lo Presti et al., 2015). Breeders can control the disease by recycling defeated resistance genes and by using the knowledge about the pathogen population. (Wolfe, 1988; Mundt, 2002; Reddy, 2013; Mikaberidze et al., 2015). Mixtures also called cultivar blends (cultivars that vary for many characters including disease resistance but have sufficient similarity to be grown together), or multilines (mixtures of genetically uniform lines of a crop species or near-isogenic lines that differ only in a specific disease or pest resistance) can be used for this purpose. Obtaining mixtures and multilines combining varieties with resistance to different diseases is less demanding compared to the development of a single variety with resistance to several diseases (Reddy, 2013). Therefore the increase of the crop's genetic diversity would reduce the severity of the disease since viable pathotypes would require multiple mutations to counteract several *R* genes present in the mixtures or multilines but with a possible fitness deficit compared to pathotypes without such mutations (Crute & Pink, 1996).

Mixtures are not only being used in small-scale agriculture, but also in large-scale systems of small grains in Europe (Wolfe, 2001). Currently, 6-15% of the wheat production area in Washington, Oregon, and Kansas in the US is planted with mixtures every year (Faraji, 2011). Very often, growers mix a high-yielding but disease-susceptible variety with one that has good disease resistance, though less yield potential (Cowger, 2007). Advantages in the yield stabilization, compensation effect and dilution of pest pressure among varieties are most significant benefits from mixture deployment (Bowden et al., 2001).

Market limitations and quality are considered the major limitations of using of mixtures (Faraji, 2011). Some additional disadvantages in the use of mixtures are the time and cost associated in developing them and the investment in equipment for seed mixing. Also, the mixture can be incompatible with desired agronomic traits such as plant height and maturity, and require standardized management practices specific for each variety (e.g., plant density, fertilization,

planting date, etc.) (Bowden et al., 2001; Reddy, 2013). Mixtures reduce the severity of disease in most cases studied, although there is a wide variation in the results. Multilines have the advantage of a uniform genetic background which is useful for mechanized industrial farming and food processing but, require years of backcrossing and field testing (Mikaberidze et al., 2015). Finally, a potential disadvantage of mixtures is that they would contribute to the evolution of complex pathogen races that can overcome many resistance genes reducing the mixture efficacy. However, several factors such as the fitness cost associated with virulence or the diversity of the pathogen could prevent the prevalence of such super races (Mundt, 2002).

Resistant cultivars can be deployed in a spatial and temporal way. Under this strategy, resistant genes can be allocated in different wheat producing regions or on a farm using variable deployment methods such as intercropping, inter-field diversification, etc. The idea is that the spores (races) adapted (matched with resistant genes) in a region will not be adapted in other regions, thus limiting the spread of the disease. Also, temporal rotations that introduce different resistance genes in a regulated sequence can contribute to the reduction of epidemics increasing the longevity of resistance and constant changes in the structure of the pathogen population (Marcroft et al., 2012; Burdon et al., 2014; Murray et al., 2010).

1.5.1.3 Chemical control

Fungicides can be applied at early stages of rust infection; many of the available fungicides would provide acceptable control to stem rust and can be allies in the integrated management of the disease before new varieties with resistance become available (De Wolf et al., 2011). However, Wanyera et al. (2010) and Kinyoro et al. (2013) suggest that, unlike leaf and stripe rust, the number of fungicides recommended to control stem rust are limited, and their effects on the prevention of yield loss are barely understood. In general, the efficacy of fungicide applications is determined by the overall level of disease in the field at the time of application and the critical growth stage of the wheat. The most significant reductions in disease severity take place when fungicides are applied between the full extension of the flag leaves and anthesis. In the case of stem rust, preventive applications provide better results compared to applications when first symptoms of disease appear.

Most fungicides provide from 14-21 days of protection against the disease, even though a gradual increase in disease severity is expected without compromising the yield (Wanyera et al., 2010; De Wolf et al., 2011). Field experiments in Africa show differences among fungicides in their ability to suppress disease development. However, several authors suggest that more research needs to be done to identify the precise timing of fungicide application, dosage, and economic benefits associated with fungicide use (Wanyera et al., 2009). This is critical due to their cost a disadvantage that limits their use by farmers in developing countries. Therefore, during heavy epidemics repeated applications of fungicides are necessary and since epidemics are difficult to predict, is not feasible to keep large inventories of chemical with limited shelf-lives. CABI *Invasive species compendium*. Retrieved from <http://www.cabi.org/isc/datasheet/45797>. Besides the economic cost, fungicides have harmful effects on the environment, and run the risk of losing their effectiveness and can spur the development of resistant pathogens under intense selection (Wolfe, 1988; Singh et al., 2011; Mikaberidze et al., 2015; Oliver, 2014).

There is limited information published on the use of fungicides in controlling *Ug99* despite several experiments that have been conducted under natural infection environments to determine their efficacy. Available data indicates that the most effective fungicides in reducing stem rust infections belongs to the triazole type (Tebuconazole) used at growth stages between heading and flowering (Wanyera et al., 2009; Kinyoro et al., 2013). However, Murray et al., (2010) have pointed out that there are differences in efficacy to control stem rust among the member of this fungicide family.

1.5.1.4 Barberry eradication

Pgt is a heteroecious fungus which needs alternate dicot hosts to complete its sexual life cycle. Alternate hosts have played a significant role in epidemics by letting the pathogen survive during winter, generating the initial inoculums for the cereal host and creating new genetic combinations of the pathogen (Zhao et al., 2016). The most notable alternate host for *Pgt* is the common barberry (*Berberis vulgaris*) introduced in North America by early European settlers who used the plant as food, wood, and as barrier for livestock, poultry, and crops. *Pgt* genetic

recombination during the sexual stage on the plant surface of Barberry is considered as the main source of new stem rust races (Schumann & Leonard, 2000). The USDA funded an eradication program to remove more than 500 million of barberry plants from 1919 to 1981. As a result of the eradication program, the number of new stem rust races was reduced significantly making possible the durable protection of wheat in the United States. From 1919 to the 1950s, 10 to 38 stem rust races were detected annually in the US, by contrast since 1960 the surveys are detecting less than ten races (Groth & Roelfs, 1987).

1.5.2 Genetic control of stem rust epidemics

In 1898, the wheat breeder William Farrer discovered that resistance to wheat stem rust had a genetic basis after he identified *off type* plants with a resistant phenotype (Biffen, 1905). Later at Cambridge University, R.H. Biffen working with *Puccinia striiformis*, found that the high level of resistance or immunity phenotype was inherited as a simple Mendelian character, starting the extensive use of resistance genes in wheat breeding (Keane, 2012). Resistance against pathogens is an evolutionary temporal mechanism, usually of biochemical nature, used by the host to interfere with growth or development of a parasite which differs from avoidance and tolerance (Ribeiro Do Vale et al., 2001; Parlevliet, 2002; Agrios, 2005). Van der Plank (1963,1968) using potato-late blight pathosystem presented evidence for the existence of two types of plant resistance coined as horizontal and vertical resistance. Hayes et al., (1925) cited by Keane (2012) apparently described both types of resistance years before, but used the terms morphological (horizontal) and protoplasmic (vertical) resistance for the stem rust-wheat pathosystem. Currently, horizontal resistance is also called incomplete, partial, quantitative, field, polygenic, non-specific, general, adult, durable, minor gene, and broad spectrum resistance. Several terms also have been used to describe vertical resistance including: complete, qualitative, *R*-gene, specific, monogenic, major gene, narrow-spectrum resistance. This variety of terms reflects several interests and assumptions of plant breeders, geneticists and plant pathologists including the type of crop, disease phenotype, distribution, the genetic basis of the resistance, etc. However, although these types of resistance can be considered different, they might be only two ends of a continuum (Poland et al., 2009; St.Clair, 2010; Keane, 2012). Moreover, variation that has a

practical use for the breeder is categorized merely as race specific and race nonspecific (Burdon et al., 2014).

1.5.2.1 Horizontal resistance

The term horizontal is derived from the observation of uniform levels of disease in the host when the amount of disease (Y-axis) is plotted against a series of pathogen races (X-axis) (Van der Plank, 1963). This type of resistance appears more or less horizontal or with a continuous distribution (quantitative), showing some ups and downs from almost imperceptible to quite strong resistance (partial resistance) depending on the relative ‘aggressiveness’ of the races and the environment. The horizontal resistance of a given host cultivar is not an absolute measure; it needs to be compared with a well-known highly susceptible standard cultivar under similar environmental conditions (Ribeiro Do Vale et al., 2001; Keane, 2012). Observations of the crop’s performance have led to the conclusion that horizontal resistance tends to be more durable than the vertical resistance. When the breakdown of horizontal resistance occurs; it is expressed as a slow ‘erosion’ of resistance rather than total loss of resistance (Poland et al., 2009; Keane, 2012). However, horizontal resistance has not been as widely utilized as major gene-based resistance (Parlevliet, 2002; Keane, 2012; St.Clair, 2010).

Traditionally it has been accepted that horizontal resistance is controlled by multiple genes (very often less than four or five genes) with small additive effects. Each gene could have a lower selection pressure on the pathogen population and as a result pathogen variants with slight fitness will gain only a marginal selective advantage (Knott, 1988; Agrios, 2005; Burdon et al., 2014). Horizontal resistance has been identified in most of plant pathosystems studied to date but without a full understanding of the nature of the genes involved (Poland et al., 2009; Keane, 2012). This can be a problem when the concept of horizontal resistance is applied in all pathosystems, since the resistance may appear to be nonspecific or effective against all races until a virulent race of the pathogen is discovered (Ribeiro Do Vale et al., 2001). Also, race-specific effects of quantitative loci have been reported in multiple pathosystems (Ribeiro Do Vale et al., 2001; Parlevliet, 2002; Poland et al., 2009), including rice-*Xanthomonas oryzae* pv. (Li et al., 2006), *Puccinia hordei*-barley (Parlevliet, 1978), *Puccinia graminis*-wheat (Dunckel et

al., 2015), *Puccinia graminis-durum* wheat (Haile et al., 2012), *Fusarium oxysporum*- melon (Perchepped et al., 2005) and others.

Horizontal resistance and its durability in wheat has been known for years, particularly the phenomena of slow rusting, or *adult plant resistance* (APR) characterized by the development of slow rust. This type of non-specific resistance is a complex trait controlled by quantitative trait loci (QTL), and is considered key for the protection of all grain crops around the world. (Knott, 1988; Lowe et al., 2011). The main drawback of APR is the evaluation of the resistance because it can only be screened in adult plants under specific environmental conditions (Sharma et al., 2013). Both APR and *R* genes for wheat rust resistance genes are designated as *Lr*, *Sr* and *Yr* for leaf, stem, and stripe rust respectively (Ellis et al., 2014). Only three APR genes have been cloned in wheat: *Lr34* (Krattinger et al., 2009), *Yr36* (Fu et al., 2009) and *Lr67* (Moore et al., 2015), from which the *Lr34* and *Lr67* has been associated with complex resistance to stem rust (Singh et al., 2011). Currently, a total of five genes (*Sr2*, *Sr55*, *Sr56*, *Sr57*, and *Sr58*) conferring quantitative APR against stem rust have been characterized (Yu et al., 2014). *Sr2* has provided a durable and broad-spectrum resistance against all *Pgt* races for decades including the *Ug99* race group when it is combined with other uncharacterized APR genes. This APR combination has been called the *Sr2* complex, and it has been the foundation for durable resistance against stem rust in several parts of the world (Singh et al., 2011) However, *Sr2* displays recessive heritance, partial resistance, varying levels of protection during heavy epidemics, and undesirable associated phenotypes that limits the selection process for breeding and farmer acceptance (Roelfs, 1988; McIntosh et al., 1995;. Kota et al., 2006; Singh et al., 2011).

1.5.2.2 Vertical resistance

The term vertical resistance came from the extreme vertical differences evident in the graphic plot of the degree of resistance (Y-axis) against a series of races of the pathogen (X-axis) (Van der Plank, 1963). The wide contrast between varieties with high levels of disease and those with low levels of immunity, allowed the identification of resistance genes with strong effects, those genes are often referred to as ‘major resistance genes’, ‘resistance genes’ or just *R genes* (Ellis et al., 2000; Keane, 2012). These resistance genes are analyzed using segregating populations and

are often inherited dominantly with Mendelian segregation ratios (Ribeiro Do Vale et al., 2001; St. Clair, 2010). For these reasons, they are relatively easy to manipulate for breeders and basic researchers (Poland et al., 2009).

In biotrophic pathogens, *R* genes mediated an effective immune response; frequently this response is a race-specific *hypersensitive response (HR)*, or a specialized hypersensitive necrosis response (cell death) of cells surrounding the area of pathogen invasion (Poland et al., 2009). However, HR in the host is not a general feature of vertical resistance. Even with host-pathogen specificity, HR can be absent, and resistance does not necessarily require cell death (Keane, 2012; Burdon et al., 2014). In the case of cereal rust, resistance can be manifested as small uredinia growing in type “1” and “2” on the Stakman scale (Stakman et al., 1962) surrounded by chlorosis. The Stakman scale for stem rust has been used to indicate of vertical resistance for years (Van der Plank, 1978). In this way, the resistance provides for major genes for cereal rust may permit some sporulation (i.e., race-specific partial resistance) that would result in an epidemic only under very favorable conditions for the pathogen (Burdon et al., 2014).

Resistance to necrotrophic pathogens in contrast with biotrophic pathogens is characterized by a limited number of resistance genes that encode for detoxification enzymes (Johal & Briggs, 1992; Brandwagt et al., 2002). No *R* gene has been associated with resistance against necrotrophs (Mengiste, 2012), except *Arabidopsis* RML3 protein which is involved in broad immunity to several necrotrophs (Staal et al., 2008). Necrotrophic fungal pathogens produce host-specific toxins that can be considered necrotrophic effectors (NE), but in contrast with biotrophic fungi, the recognition of NE by the plant immune system results in host susceptibility (Liu et al., 2012).

Vertical resistance tends to be complete or reduces reproduction of the pathogen to a tiny amount (Keane, 2012). However, there are examples of *R* genes with incomplete resistance in other pathosystems. Such examples include a mutant version of the *Xa21* gene that confers partial resistance against rice blast (Andaya & Ronald, 2003), the *L6* gene in flax rust (Lawrence et al., 1995), *R₁*, *R₁₀*, and *R₁₁* genes for potato late blight (Stewart et al., 2003), and *Cf 4-9* tomato leaf mold (Parniske et al., 1997). *R* genes also can show interaction with the environment,

particularly the interactions between host genetic background and temperature (McIntosh et al., 1995), like the *Sr21* gene which confers temperature-sensitive resistance to *Ug99* race group isolates (Chen et al., 2015). The durability of vertical resistance eventually is overcome for virulent races; this process can be particularly fast in some pathosystems such as cereal rust. For decades this limitation has been a constant challenge for plant breeders, pathologists and farmers since *R* genes tend to prevent epidemics only temporarily due to the strong selection for virulent pathogen variants in the agrosystems (McDonald & Linde, 2002; Keane, 2012; Mengiste, 2012).

1.5.3 Plant breeding for stem rust resistance

Plant breeding for resistance is a relatively straightforward process based on keep two components: guaranteeing the durability of the resistance of a cultivar in a particular area, and maintaining resistance diversity as insurance against lack of durability (McIntosh, 1988). The conventional view among wheat pathologists and breeders is that horizontal resistance to stem rust is rare in hexaploid wheat (*Triticum aestivum* L.) (Van der Plank, 1968; Knott, 1988). In fact, horizontal resistance against stem rust in wheat is very narrow, and available resistance traditionally has depended mainly on two tetraploid wheat relatives, *T. turgidum* var. *dicoccum* (cv Yaroslav Emmer) and *T. turgidum* var. *durum* (cv Iumillo) (McIntosh et al., 1995).

In the early 20 century, the most common spring wheat in the USA was the cultivar Marquis, which was released in 1907, but it was very susceptible to stem rust. The stem rust epidemics of the following years activated the efforts to produce resistant wheat cultivars. The first red spring wheat for stem rust resistance in North America was Ceres. It was released in 1926 by the North Dakota Agricultural Experiment Station but, this variety succumbed to the stem rust race 56, which was responsible for the great epidemics from 1935-1947. Ceres was replaced by Thatcher (1935) which was produced from crosses with wheat tetraploid “Iumillo” durum and “Yaroslav” emmer, respectively carrying the genes *Sr5*, *Sr9g*, *Sr12*, and *Sr16* and *APR* genes highly effective against race 56. Plant breeders also started to use other sources of resistance such as the *APR* gene *Sr2* derived from Yaroslav emmer (McIntosh et al., 1995). These combinations gave origin to the cultivars Hope and H-44, which were developed by selecting progeny derived from a cross between Marquis and Yaroslav emmer (Kolmer et al., 1991; Kolmer et al., 2009a).

In the epidemics that took place in North America from 1950 to 1954, the resistance provided by Thatcher and *Sr2* was insufficient to control the race 15B (or TPMKC according to the North American nomenclature). In response to 15B the cultivars Selkirk in Canada (1954) and Chris in USA (1966) carrying the highly effective gene *Sr6* gene were released. The descendants of Hope and Chris contributed to the high-yielding, semi-dwarf wheat varieties that were used during the “Green Revolution” in the 1970s. From 1970 to 1980 breeding programs started using alien resistance genes from *Agropyron elongatum* (*Sr24* and *Sr26*), *T. timopheevi* (*Sr36*) used in the soft red winter wheat in the US and to some extent in Australia; *T. ventricosum* (*Sr38*) used also in Europe, and *Sr31* obtained from the 1BL.1RS translocation from “Pektus” rye secale (Singh et al., 2008b, 2011; Kolmer et al., 2009a). The *Sr31* translocation has been extensively used in worldwide agriculture since 1980 except in Australia. In the U.S the *Sr31* gene is present in some hard and soft red winter wheat as well as CIMMYT-derived wheat cultivars (McIntosh et al., 1995). These CIMMYT cultivars were responsible for the breakthrough in wheat production in several developing countries and carried additional resistance genes including (*Sr24* and *Sr36*) that are not able to control *Ug99* variants (Khan et al., 2013). The extensive use of *Sr31* is explained because in addition to stem rust resistance the translocation carries the genes *Lr26*, *Yr9*, and *Pm8* which confer resistance to leaf and stripe rust and powdery mildew, respectively. Also, the translocation carries genes that increase the grain yield. The *Sr31* protection lasted for almost 30 years reducing the incidence of stem rust to a minimum but, creating a resistance monoculture in Africa, Asia and other parts of the world (Singh et al., 2008a; Kolmer et al., 2009a; Khan et al., 2013).

1.5.4 Gene pyramiding and biotechnological approaches

Several authors have pointed out that one effective strategy to avoid the fast breakdown of resistance genes is to use gene combinations by backcrossing or gene pyramiding. Under this strategy, it is expected that a significant reduction in the probability of infection can be achieved by the combination of 4- 5 genes that would include multiple *R* genes or few *APR* genes in a single wheat cultivar (Nagori, 2009; Bajgain et al., 2015). Those genes need to be effective against most, if not all, of the local races of the pathogen forcing it towards a rare event that involves multiple and independent mutations in the pathogen’s genome to overcome the resistance provided by gene pyramiding. (Ellis et al., 2014; Burdon et al., 2014). The use of

conventional breeding methods makes gene pyramiding difficult and time-consuming, requiring simultaneous disease evaluation using several races on the same breeding material, which is usually expensive for conventional breeding programs (Khan et al., 2013). Marker Assisted Selection (MAS) using the gene itself or closely linked markers is a convenient alternative to facilitate gene pyramiding, as well as contributing to the dissection of quantitative trait loci (QTLs). This is possible because the presence of a specific resistance gene can be predicted by linked molecular markers without the need for disease evaluation in a large number of progeny thereby reducing the time investment in breeding programs and the screening using multiple races. MAS has been used for QTL mapping to identify regions in the wheat genome that contain genes that confer resistance to *Ug99* and other *Pgt* races. (Singh et al., 2008b; Leornad & Szabo, 2005; St.Clair, 2010; Yu et al., 2010; Haile & Röder 2013; Ellis et al., 2014).

Genetic Modified Organisms (GMOs) are an alternative to control rust disease and overcome the problems associated with conventional breeding (sexual incompatibility, genetic drag, genetic background, recombination suppression on the introgressed region, negative pleiotropic effects and genes linked in repulsion phase in a non-recombining region, etc.). The increasing number of cloned wheat rust resistance genes makes it possible to combine several major resistance genes and *APR* genes in a single cassette (cisgenesis) avoiding segregation problems allowing the breeder to focus on other agronomic traits of interest. Alternatively, genes can be introduced by the insertion of multi-cassettes or by using plant genome editing technology that is under development (Nagori, 2009; Ellis et al., 2014; Singh et al., 2015).

The main technical limitation of GMO approach for cereal rust resistance is the size of the genes. The combination of the coding sequence and native promoters makes the size of *R* genes between 7-9 Kb and for the known *APR* genes, like *Lr34*, the size increases up to 16 Kb. These lengths reduce *Agrobacterium* transformation efficiency. In addition, it is possible to find epistatic effects among cassette's components, for example *R* genes can be suppressed particularly when alleles are combined together, and some components of the cassette could induce susceptibility to necrotrophs. Finally, there are concerns about the acceptance by consumers and the cost associated with GMO management in developing countries (Nagori, 2009; Wulff & Moscou, 2014; Kumar et al., 2014).

1.6 Resistance genes used to control stem rust

Most of the resistance genes discovered and broadly used against cereal rusts are *R*-genes that provide vertical resistance against the disease (McIntosh et al., 1995). Their cloning has provided valuable information at multiple levels: they can be used as perfect functional markers for MAS, they can contribute to the identification of functional alleles (allele mining), and be incorporated as components of gene cassette stacking multiple resistance genes. Also, the cloning of *R* genes allows their functional characterization and identification of its molecular interactions (Lowe et al., 2011).

1.6.1 Mapped genes effective against *Ug99* race of stem rust

Plant pathologist and breeders are constantly trying to clone resistance genes or produce closely-linked molecular markers that can be used to accelerate the breeding in commercial varieties (Nagori, 2009). Unfortunately, several genes are derived from wild wheat relatives and are stored as large alien introgressions associated with agronomically undesirable linkage drag which makes them difficult to use commercialization (Singh et al., 2015). Stem rust resistance genes have been identified in different genetic stocks. Approximately 73 *Sr* genes effective against *Pgt* races have been cataloged, including those that show resistance to the *Ug99* race group. (Singh et al., 2015; Rahmatov et al., 2016; Kumar & Pratap, 2014). Monogenic clones with those resistance genes are available in several wheat backgrounds, but only 39 genes confer moderate to effective resistance against the *Ug99* race group (Jin et al., 2007; Singh et al., 2015) (Table 1.3). Resistance genes *Sr22*, *Sr25*, *Sr26*, *Sr33*, *Sr35*, *Sr45*, and *Sr50* are considered to be the most useful race-specific genes against *Ug99* race group. The genetic source of stem rust resistance genes has been expanded from the A, B, and D wheat genomes (*Triticum aestivum* L.) to its wild relatives due to the wheat genomes have a limited genetic diversity in disease resistance (Feuillet et al., 2008). From the primary gene pool represented by *Triticum monococum* a closely related species to *Triticum urartu* (related to the A genome on wheat), three genes have been introgressed *Sr21*, *Sr22*, and *Sr35* (Rouse & Jin, 2011).

Table 1.3. Chromosomal location, description and source of stem rust resistance genes effective and moderate effective against *Puccinia graminis* f. sp. *tritici* race of *Ug99* and its variants. Based on Haile & Röder, (2013) and Singh et al., (2015).

Gene	Location	General description	Source
Vertical resistance			
<i>Sr15^{abc}</i>	7A	Satisfactory protection at lower temperatures (18°C)	<i>Triticum aestivum</i>
<i>Sr28^b</i>	1D	Present in a very high proportion of common wheat lines	<i>Triticum aestivum</i>
<i>Sr29^{cd}</i>	6DL		<i>Triticum aestivum</i>
<i>Sr42^{bc}</i>	6DS	Confers resistance to TTKSK and variants TTKST and TTTSK	<i>Triticum aestivum</i>
<i>Sr48</i>	2AL	Linked to <i>Yr1</i>	<i>Triticum aestivum</i>
<i>Tpm (Sha7)^{bc}</i>	6DS	Exists in several hard red winter wheat cultivars Low infection type to race <i>Ug99</i> , faile individual <i>Ug99</i> races	<i>Triticum aestivum</i>
<i>Huw234^{bc}</i>	2BL	Temporally designed	<i>Triticum aestivum</i>
<i>ND643^c</i>	4AL	Temporally designed	<i>Triticum aestivum</i>
<i>Yaye^c</i>	6DL	Temporally designed	<i>Triticum aestivum</i>
<i>Sr13^{bc}</i>	6AL	Virulent <i>Pgt</i> race on durum wheat in Ethiopia was reported	<i>Triticum turgidum</i>
<i>Sr14^{bc}</i>	5BL	Resistant for <i>Ug99</i>	<i>Triticum turgidum</i>
<i>Sr22</i>	7AL	Confers resistance to <i>Ug99</i> and other important races Limited use due to chromosome translocations harboring a yield penalty and a delay in heading date.	<i>Triticum monococcum</i>
<i>Sr35^b</i>	3AL	Near immunity against race TTKSK (<i>Ug99</i>) and its variants	<i>Triticum monococcum</i>
<i>Sr37^d</i>	4BL	Because of linkage drag, it has not been used in wheat breeding	<i>Triticum timopheevi</i>
<i>Sr32^d</i>	2A	Presence of deleterious gene(s) derived from the donor species	<i>Aegilops speltoides</i>
<i>Sr39^d</i>	2BL	Moderately to highly resistance to <i>Ug99</i> in seedling	<i>Aegilops speltoides</i>
<i>Sr47^f</i>	2BL	High level of resistance to <i>Ug99</i> in tetraploid wheat	<i>Aegilops speltoides</i>
<i>Sr33</i>	1DS	Confers only moderate levels of resistance on field	<i>Aegilops tauschii</i>
<i>Sr45</i>	1DS	locus proximal to <i>Sr33</i> , confers only moderate levels of resistance on field	<i>Aegilops tauschii</i>
<i>Sr46</i>	2DS	Confers only moderate levels of resistance on field	<i>Aegilops tauschii</i>

<i>TA10171</i>	7DS	No tested in field trials	<i>Aegilops tauschii</i>
<i>TA10187</i>	6DS	No tested in field trials	<i>Aegilops tauschii</i>
<i>TA1662</i>	1DS	No tested in field trials	<i>Aegilops searsii</i>
<i>Sr51</i>	3A,3B,3D	Resistance for <i>Ug99</i>	<i>Aegilops searsii</i>
<i>Sr53</i>	5DL	Effective against <i>Ug99</i>	<i>Aegilops geniculata</i>
<i>Sr52</i>	6AL	Shows a temperature-sensitive resistance pattern to race <i>Ug99</i>	<i>Dasypyrum villosum</i>
<i>Sr40^d</i>	2BS	Moderately to highly resistance to <i>Ug99</i> in seedling tests	<i>Triticum araraticum</i>
<i>Sr25^b</i>	7AL, 7DL	Conferred a high level of resistance only in some genetic backgrounds Linked with another <i>Th. ponticum</i> derived gene causing undesirable yellow flour	<i>Thinopyrum elongatum</i>
<i>Sr26</i>	6AL	Confers resistance to <i>Ug99</i> and other races. Not widely deployed in commercial varieties due to yield penalty	<i>Thinopyrum elongatum</i>
<i>Sr43^{b,d}</i>	7DL	Resistant to TTKSK, TTKST and TTTSK	<i>Thinopyrum elongatum</i>
<i>Sr44^{b,d}</i>	7DS	Moderately to highly resistance to <i>Ug99</i> in seedling tests	<i>Thinopyrum intermedium</i>
<i>Sr27^b</i>	3A	Effective against <i>Ug99</i> Has not been used in wheat improvement	<i>Secale cereale</i>
<i>Sr50^b</i>	1DL.1RS	Effective against <i>Ug99</i>	<i>Secale cereale</i>
<i>Sr1RS(Amigo)^{b,c}</i>	1A.1R	Confers moderate resistance to <i>Ug99</i> Present in several hard red winter wheat cultivars	<i>Secale cereale</i>
Horizontal resistance			
<i>Sr55^{ce}</i>	4D	Breeding option available pleiotropic effect	<i>Triticum aestivum</i>
<i>Sr55^{ce}</i>	5BL	Breeding option available	
<i>Sr57^{ce}</i>	7DS	Breeding option available	<i>Triticum aestivum</i>
<i>Sr58^{ce}</i>	1BL	Breeding option available	<i>Triticum aestivum</i>
<i>Sr2^{ce}</i>	3BL	Durable resistance (combined with other genes) Pseudo-black chaff (morphological marker)	<i>Triticum turgidum</i>

^a Data from multiple research groups are not consistent. ^b Virulence for the gene is known to occur in other races. ^c Level of resistance conferred in the field usually inadequate under high disease pressure. ^d Unsuitable for utilization due to linkage with undesirable traits in the translocation. ^e Confers slow rusting adult plant resistance. ^f Not tested for resistance to *Ug99* in field trials to determine effectiveness.

From the secondary gene pool which include several species of the genera *Aegilops* (related to the B genome in wheat), the *Sr39* was introgressed into hexaploid wheat from *Aegilops speltoides* (Niu et al., 2011). The genes *Sr33*, *Sr45* and *Sr46* have been introgressed from *Aegilops tauschii* (related to the D genome in wheat) (Rouse, et al., 2011b). The tertiary gene pool (no-homologous genome) also has been useful in providing additional *Ug99* resistance genes (Rahmatov et al., 2016). Additional *Ug99* resistance genes such as *Sr29*, *Sr32*, *Sr37*, *Sr40*, and *Sr44* have not been extensively evaluated using other *Pgt* races and thus are not massively incorporated in breeding programs (Rouse & Jin, 2011; Singh et al., 2015).

1.6.2 Cloned genes effective against cereal rusts

Most of the cloned *R* genes for cereal rust encode proteins belonging to the NBS-LRR family. The first cloned resistance gene for rust was *Rpd-1* in maize (Collins et al., 1998). In recent years, several resistance genes between *R* and *APR* genes for cereal rust have been cloned (Table 1.4). For leaf rust *Lr10*, *Lr1*, *Lr21*, *Lr34* and *Lr67*, for stripe rust two *APR* genes *Lr34/Yr18* and *Yr36* and the major gene *Yr10*, and for stem rust *Rpg1* and *Rpg5* in Barley and *Sr33*, *Sr35*, *Sr22* *Sr45*, *Sr50* and *Sr13* in wheat wild relatives.

Table 1.4. Gene category and strategy used to clone resistance genes for cereal rust.

Specie	Gene	Product	Disease	Cloning approach	Reference
Wheat relatives and Rye	<i>Lr1</i>	CC_NBS_LRR	Leaf rust	Positional cloning	Cloutier et al., 2007
	<i>Lr10</i>	CC_NBS_LRR	Leaf rust	Positional cloning	Feuillet et al., 2003
	<i>Lr21</i>	NBS_LRR	Leaf rust	Positional cloning	Huang et al., 2003
	<i>Lr67</i>	Hexose transporter	Leaf rust	Comparative genomics	Moore et al., 2015
	<i>Lr34</i>	ABC transporter	Leaf rust	Positional cloning	Krattinger et al., 2009
	<i>Sr35</i>	CC_NBS_LRR	Stem rust	Positional cloning	Saintenac et al., 2013
	<i>Sr33</i>	CC_NBS_LRR	Stem rust	Positional cloning	Periyannan et al., 2013
	<i>Sr22</i>	CC_NBS_LRR	Stem rust	MutRenSeq	Steuernagel et al., 2016
	<i>Sr45</i>	CC_NBS_LRR	Stem rust	MutRenSeq	Steuernagel et al., 2016
	<i>Sr50</i>	CC_NBS_LRR	Stem rust	Positional cloning	Mago et al., 2015
<i>Sr13</i>	CC_NBS_LRR	Stem rust	Positional cloning	Zhang et al., 2017	
	<i>Yr36</i>	Kinase-start	Stripe rust	Positional cloning	Fu et al., 2009
	<i>Yr10</i>	CC_NBS_LRR	Stripe rust	Positional cloning	Liu et al., 2014
Maize	<i>Rp1_D</i>	NBS_LRR	Common rust	Transposon tagging	Collins et al., 1998
	<i>Rp3</i>	NBS_LRR	Common rust	RGA	Webb et al., 2002
Barley	<i>Rpg1</i>	Kinase-Kinase	Stem rust	Positional cloning	Brueggeman et al., 2002
	<i>Rpg5</i>	NB_LRR	Stem rust	Positional cloning	Brueggeman et al., 2008

1.7 Plant immunity

1.7.1 The gene-for-gene concept

In the early 20th century, it was already known that resistance to plant pathogens could be inherited as a monogenic trait following the laws of Mendelian segregation. However, inconsistent results after artificial infections with cereal rust collected in fields across different locations and years were not understood until the characterization of differential reaction between pathogen races and monogenic resistant genes. This information was the basis for the *gene by gene concept* developed in the 1940s. The gene by gene concept was developed independently by Harold. H. Flor in the USA working with flax rust (*Melampsora lini*) and flax (*Linum usitatissimum*), and Arend Oort in Netherlands working with the loose smut of wheat (*Ustilago tritici*) (Oort 1944 cited by Ali et al., 2014). Flor and Oort used genetic experiments based on crossing susceptible and resistant host genotypes and fungal isolates that differed in their virulent capacity over a particular host genotype, to demonstrate the genetic interdependence of both host and pathogen in the host-pathogen interaction (Strange, 2003; de Wit, 1992).

Harold Flor infected flax lines carrying different resistant genes with the progeny of crosses between various races of flax rust, and he concluded that genetic factors of both plant and pathogen are complementary and required to explain the observed resistance. The observed resistance is based on the specific recognition between two components: a monogenic dominant resistance gene (*R-gene*) in the plant and a corresponding dominant avirulent gene (*Avr gene*) present in the pathogen. This interaction is called *gene-for-gene interaction* and is typical in biotrophic pathogens such as mildews and rusts, in contrast to the necrotrophic pathogens, which usually do not show a race-specific interaction. (Flor, 1942; Flor, 1971; Keller et al., 2000; Wang et al., 2014). The gene-by-gene relationship is not limited to plant-fungus interactions, but also can be found in any other plant host-parasite system (Person, 1959; Ribeiro Do Vale et al., 2001). Although there is empirical support for the gene-for-gene concept in animal host-parasite systems, these interactions are generally described based on another model called the *matching allele model* (Thrall et al., 2015).

The gene-for-gene relationship is a fundamental principle in plant pathology, and it has been used as a model for both classical and molecular genetics analyses in cereal rusts and other pathogens. As a complement to the gene-for-gene relationship, studies of resistance in rust fungi have led to the formulation of the *compatibility model of specificity* (Heath, 1991). Under the compatibility model, the disease response is analyzed based on the interaction between host and pathogen. The response is defined as *compatible*, or *high response*, if the host is susceptible and the pathogen is virulent, whereas the interaction is defined as *incompatible*, or *low response* type if the host shows resistance (Kolmer et al., 2009a).

1.7.2 Nonhost resistance

Plants are sessile organisms challenged by biotic and abiotic stresses. Unlike animals they do not have differentiated circulating immune cells to detect pathogens; they rely on the autonomous innate immune system where every cell needs to recognize and respond to microbial challenges (Jones & Dangl, 2006; Cesari et al., 2014; Mukhtar et al., 2016). Bacteria, fungi, oomycetes, viruses, nematodes, etc. can be pathogens that constitute a threat to plant homeostasis. Initially, plants try to safeguard their physiological integrity against harmful microorganisms by a robust passive or pre-invasive defense also called *non-host resistance*. This defense is represented by physical barriers like wax coating the plant surface, pre-formed plant cell walls, cytoskeleton, etc. Non-host resistance also by chemical barriers which include antimicrobial enzymes such as phytoanticipins and secondary metabolites, such as phytoalexins. Microorganisms that are able to overcome this passive defense face an active defense mechanism that has evolved in plants as a rapid and efficient response once pathogens are recognized. This active mechanism represents the immune system in plants (Thordal-Christensen, 2003; Anderson et al., 2010; Surico, 2013). Unlike the adaptive immune response in animals, plant immunity relies on systemic signals produced at the infection site, or a cellular innate immune system represented for an extensive repertoire of immune receptors developed during millions of years of co-evolution with pathogens. In this context, disease is the result of the avoidance of recognition or suppression of the host defense mechanism or both (Jones & Dangl, 2006; Dodds & Rathjen, 2010).

1.7.3 PAMP-triggered immunity (PTI)

All the conceptual models that explain plant immune system propose that plant immunity depends on immune receptors that identify microbial invasion (Flor, 1971; van der Biezen & Jones, 1998; Jones & Dangl, 2006). Among these conceptual models, the *zig-zag model* proposed by Jones & Dangl, (2006) has gained acceptance in the plant pathology community. This model includes both general elicitors and *Avr* genes and represents the plant immune system by two layers of active defense. The first layer is the basal defense or PAMP-triggered immunity (PTI), is considered as the most ancient one. Basal defense uses a repertoire of membrane-associated proteins called *pattern recognition receptors* (PRRs) that contain an extracellular domain. This type of proteins, represented by transmembrane receptor kinases and transmembrane receptor-like proteins (Dodds & Rathjen, 2010), activate the immune response in plants after the recognition with some degree of redundancy conserved and generic microbial molecules called pathogen-associated molecular patterns (PAMPs). Those molecules were once known as general *elicitors* and are exposed in the apoplastic space. Since these molecules, are also present in the non-pathogenic microorganism, these microbial signals are also called *microbial-associated molecular patterns* (MAMPs). PAMPs include proteins, carbohydrates, lipids and small molecules. As examples of MAMPs we have the 22 amino acid epitope called Flg22 from bacterial flagellin, chitin (a fundamental building block of fungal cell walls), peptidoglycans, lipopolysaccharides, the bacterial elongation factor TU (EF-TU), etc. In addition to PAMPs, PTI can be also induced by endogenous molecules released after pathogen invasion called *danger-associated molecular patterns* (DAMPs), these endogenous elicitors included cell wall fragments, cutin monomers or systemins. The recognition of MAMPs or DAMPs by PRRs activates a general defense response called *PAMP-triggered immunity* (PTI) that involves morphological and physiological changes including callose deposition and stomata closure to blocking the pathogen's infection progression within the host (Jones & Dangl, 2006; Bent & Mackey, 2007; Boller & Felix, 2009; Anderson et al., 2010; Dodds & Rathjen, 2010; Chaudhari et al., 2014; Surico, 2013; Gururani et al., 2012; Lo Presti et al., 2015).

1.7.4 Effector triggered immunity (ETI)

Pathogens can overcome the first active layer of defense or PTI by deploying an arsenal of molecules called *effectors* encoded by specific *Avr* genes, which are delivered into the plant cells during the initial stage of infection to benefit pathogen proliferation (Gururani et al., 2012). Effectors can alter several cellular processes, including the recognition of PRRs and PTI response. According to Jones & Dangl, (2006) because of the effector's activity, the PTI is altered and the host undergoes a condition called *Effector Trigger Susceptibility* (ETS). To reverse the ETS plants have evolved a second layer of defense known as *Effector Trigger Immunity* (ETI). ETI is based on direct or indirect recognition by host immune receptors of pathogen effectors proteins. This recognition is transduced to downstream components through a phosphorylation cascade which typically results in a strain or race-specific *Hypersensitive Response* (HR). HR is a local immune response that suppresses the advancement of the pathogen infection. This reaction includes localized cell death, faster influx of calcium ions, burst of reactive oxygen species (ROS) activation of mitogen-activated protein kinase (MAPKs), increase of salicylic acid, re-programming of gene expression including defense or pathogenic associated genes, propagation of immunity to neighboring cells, etc. PTI can produce a similar response to ETI including cell death, although ETI is qualitatively stronger and faster compare with PTI. Recognition of *Avr* genes or effectors by immune receptors was interpreted as the basis for the Flor's gene-for-gene interaction and the basic compatibility model of specificity in a oversimplified way. In this interpretation, the *R* gene (receptor) triggers an immune response after recognizing the pathogen that has an avirulent gene or effector (Jones & Dangl, 2006; Thordal-Christensen, 2003). However, molecular biology experiments to confirm this direct interaction often produce negative results leading to alternative explanations for the R-Avr interaction (Bent & Mackey, 2007; de Wit et al., 2009; Surico, 2013; Wirthmueller et al., 2013; Chaudhari et al., 2014).

Any mutation in the *Avr* gene can lead to non-recognition by the corresponding *R*-gene, restoring the pathogenicity or resistance breakdown and the HR is overcome. The mutation can be the product of a single nucleotide change which can affect the secondary and tertiary structure, leading to an amino acid change or a premature stop codon (Joosten., 1994), or complete deletion

of the *Avr* gene (Joosten & de Wit, 1999; Parlevliet, 2002). Also, virulence can be the product of epistatic effectors that suppress the immune reaction product of other *Avr* gene (Chen & Halterman, 2012; Bourras et al., 2015) or changes in gene expression by a mutation in promoter sequences (Shan et al., 2004; Ali et al., 2014).

Despite the broadly accepted conceptual model that suggests a difference between PAMPs and effectors, PRRs and R proteins, and consequently a separation between PTI and ETI, the study of several pathosystems indicates that this dichotomy between PTI and ETI cannot be maintained (Thomma et al., 2011). Some *R* genes encode proteins similar to PRRs but interact with extracellular effectors secreted by apoplastic fungal pathogens (no haustoria builders) (Win et al., 2012). PRRs display a variation similar to the internal receptors, PAMPs could play a role in virulence, *R* genes that code for internal receptors are not necessarily limited to a specific pathosystem. Also, the occurrence of HR is not restricted to ETI but can also occur in PTI, and this response can be fast or slow depending on the specific interaction, making the PTI and ETI a continuum more than separate layers. Because the limitations of the current paradigm in the interpretation of the plant immune system, some authors have proposed alternative models such as *Effector trigger defense* or ETD model (Stotz et al., 2014) and the *invasion model* (Cook et al., 2015).

1.7.5 Co-evolution of plant-pathogen interaction

Jones & Dangl, (2006) proposed a single model of innate immunity in plants and the co-evolution of plant-pathogen interaction called the “zig-zag” model which encompasses PTI, ETI, and ETS. The zig-zag model describes four immunity stages: in stage 1 PAMPs or DAMPs are detected by the PRRs producing PTI, which is followed by stage 2 in which pathogens deliver effectors to interfere with PTI inducing ETS. During stage 3, the effector is recognized by an R-gene inducing ETI. Finally, at stage 4, the pathogen population evolves by either losing or altering the effector that is being recognized or by gaining novel effectors that suppress the ETI response. In turn, the plant populations evolve new receptors that recognize the altered or the newly acquired effectors, resulting again in ETI. This co-evolutive play becomes an *arms race*,

with continuous selection for new effector variants that overcome ETI and new plant genotypes that restore ETI.

Pritchard & Birch (2014) have proposed modifying the zig-zag model with a more predictive quantitative model. These authors postulate that the plant pathogen interaction is better described as a stochastic process where the action and detection of effectors, PAMPs and DAMPs are combined, creating doubts about the conceptual division between PTI and ETI (Zipfel et al., 2006; Thomma et al., 2011) . Therefore, the zig-zag model does not account for necrotrophic pathogens and other symbiotic processes as well as environmental conditions and physical and temporal scales (Pritchard & Birch, 2014). Finally, the zig-zag model is challenged by the evidence that not all effectors target PTI; there are effectors with enzymatic functions or proteins that mimic transcriptional activators such as transcription activator-like (TAL) effectors of *Xanthomonas* spp. which induces the expression of host-specific genes that contribute to infection development (Kay & Bonas, 2009).

1.8 Molecular mechanisms of *R* gene resistance

1.8.1 *R* gene categories

In the last decades, sequence analysis of cloned genes associated with disease resistance has revealed a structural similarity across the plant kingdom. Furthermore, the considerable structural homology of *R* genes and genes involved in mammalian immunity suggests that plant *R* genes may have a common evolutionary origin (Hammond-Kosack & Jones, 1997). The number of cloned and functionally characterized *R*-genes has been increasing in recent years (Bouktila et al., 2014) reaching about 113 genes Plant Resistance Gene database (December, 2016). Retrieved from <http://prgdb.org.eu/>. Since the cloning of the first resistance gene, the *Hm1* from maize (Johal & Briggs, 1992), the characterization of *R* genes has provided valuable information about their structure, function, evolution and also has generated useful genetic materials to engineer novel resistant plants (Liu et al., 2007).

In plant genomes, resistance genes are found in four types according to their genomic organization giving clues about their evolution and diversity (Hammond-Kosack & Jones, 1997; Keller et al., 2000; Strange, 2003):

1. Single genes with an array of distinct alleles each providing different recognition specificity (e.g. Flax *L* locus with thirteen specificities).
2. Single copy genes, like *RPM1* gene from *Arabidopsis*.
3. Tandem arrays of closely linked resistance genes homologs with differing specificities (e.g. Flax *M* locus).
4. Loose clusters (1-2 cM) of genes in an *R* gene-rich area of the chromosome. (*Cf-2*, *Cf-5* and *Mi* in *Lycopersicon esculentum*).

R genes can interact directly or indirectly with the *Avr* genes, detect the presence of PAMPs or encode enzymes that degrade toxins produced by the pathogen. Sequence analysis of *R*-genes indicates that most of them contain at least seven different conserved protein domains: NBS (nucleotide-binding site), LRR (leucine-rich repeat), TIR (Toll/Interleukin-1 receptor), CC (coiled-coil), LZ (leucine zipper), TM (transmembrane) and STK (serine-threonine kinase). Based on domain organization several authors have defined structural classes of *R* genes (Ellis et al., 2000; Sharma et al., 2009; Bouktila et al., 2014; Gururani et al., 2012). Sanseverino & Ercolano, (2012) defined at least five categories based on the presence of specific domains. **1) CNL (CC-NBS-LRR)**, **2) TNL (TIR-NBS-LRR)**, **3) RLP (Receptor-Like Proteins)** which consist of proteins with extracellular LRR, a TM (transmembrane) domain and small cytoplasmatic region with no kinase domain, as an example the gene *Cf2* that recognizes *Avr2* of *Cladosporium fulvum*. **4) RLK (Receptor-Like Kinases)** which consist of extracellular LRR and an intracellular kinase domain for downstream activation. This category is represented by the gene *Xa21* that confers resistance in rice against *Xanthomonas oryzae* pv. *Oryzae*. **5) KIN** this class of proteins containing only a kinase domain-like such as the *Pto* gene that confers resistance against *Pseudomonas syringae* pv tomato. Other types of *R* genes have been discovered, but they are structurally and functionally divergent; for example, the gene *Bs3* encodes a flavin monooxygenase (FMO) activated by the binding of *AvrBs3* in the promoter region of the *R* gene (Römer et al., 2007), the recessive gene *Mlo* in *Hordeum vulgare* which

confers resistance against the powdery mildew caused by *Blumeria graminis* (Büschges et al., 1997), the gene *Asc1* in tomato which confers resistance to *Alternaria alternata* f sp *lycopersici* (Brandwagt et al., 2000), the gene *xa5* for resistance to *Xanthomonas oryzae* pv. *oryzae* (Xoo) in rice that encodes a transcription factor (TFIIA) (Jiang et al., 2006), and the gene *xa27* for resistance to *Xanthomonas oryzae* pv. *oryzae* (Xoo) in rice that encodes a protein without any hits in the protein databases (Gu et al., 2005).

1.8.2 NBS-LRR genes

The *R* genes that encode for proteins with a nucleotide binding site (NBS) and leucine rich-repeat (LRRs) domains represent the largest and one of the most ancient protein families among plant genomes (Marone et al., 2013). The size of these proteins ranges from about 860 to 1,900 amino acids, and a large number have been predicted in different species of monocotyledons and dicotyledons. There are approximately 150 NBS-LRR encoding genes in *Arabidopsis thaliana*, over 400 in *Oryza sativa* (McHale et al., 2006) and for the hexaploid wheat genome, about 1700 potential NBS-LRRs encoding sequences have been predicted (Bouktila et al., 2014; Gu et al., 2015). Comparative genomic analyses suggest that NBS-LRR genes are frequently clustered as the result of segmental and tandem duplications. They also exhibit intraspecific sequence variation and diverse copy number among plant species (McHale et al., 2006; Gu et al., 2015). NBS-LRRs tend to be co-localized with their cognate effectors and interacting proteins in multiple sub-cellular compartments for the induction of defense responses (Takken & Govere, 2012).

Every single domain on NBS-LRR proteins seems to have a distinct function depending on the activation state of the protein and the class of protein they belong to (Takken & Govere, 2012; Hammond-Kosack & Jones, 1997). The central domain of NBS-LRR proteins is called NBS (Nucleotide Binding Site domain) or NB-ARC (Nucleotide-Binding adaptor shared by Apaf1, certain R genes and CED4) domain. This domain is found in numerous ATP and GTP-binding proteins and is characterized by three motifs critical for nucleotide binding: a consensus kinase 1a (P-loop), a kinase 2 and a kinase 3a. The remaining sub-domains are known as ARC1 and ARC2 and together form a closed nucleotide-binding pocket when the protein is in its resting

state. NB-ARC proteins belong to even bigger protein families known as the STAND superfamily (Signal Transduction ATPases with Numerous Domains). This is a class of proteins with a modular structure that functions simultaneously as a stimuli sensor and as a switch and response factor in several cellular processes such as immunity, apoptosis and transcriptional regulation (McHale et al., 2006; Hammond-Kosack & Jones, 1997; Takken & Govere, 2012). The second component of an NBS-LRR is the highly irregular C-terminal Leucine-Rich Repeat domain (LRR), which is composed of repeats of a motif with variable serial leucine and other hydrophobic residues (McHale et al., 2006). LRRs motifs are proposed to play a role in intramolecular signal transduction and pathogen recognition specificity (Takken & Govere, 2012).

The N-terminal region of NBS-LRRs can present a domain extension called TIR (Toll/interleukin 1-like receptor) or a CC (coiled-coil) which distinguishes the two major NBS-LRR protein classes (TNLS and CNLs). TNLS constitute about 75% of all NBS-LRR. However, CNLs are the unique class in all monocot genomes analyzed to date (Marone et al., 2013; Gu et al., 2015). Given the diversity of CC and TIR domains, it is thought that they are involved in protein-protein interactions with other proteins or with downstream signaling components (McHale et al., 2006; Liu et al., 2007). Takken & Govere (2012) proposed that the NB-ARC domain interacts with the N-terminal part of the LRR domain, and in the case of CNLs class, the CC domain interacts simultaneously with the NB-ARC and the LRR domains to keep the protein in compact globular closed conformation in the absence of pathogen effectors. This conformation makes the C-terminal end of the LRR domain to be exposed like an antenna to sense changes in the environment, but in auto-inhibited state although it remains signaling-competent. The establishment and maintenance of this closed conformational state is possible thanks to chaperone-assisted protein maturation and control of protein levels by proteasome degradation.

1.8.3 *R* gene evolution

Hammond-Kosack & Jones (1997) proposed two possible scenarios to explain the origin of *R* genes; one scenario points out that *R* genes descend from proteins involved in endogenous

recognition/signaling systems required for plant normal growth or development. The alternative scenario is less likely and suggests that *R* genes evolved from ancient *R* genes involved in pathogen recognition by unicellular ancestors. Michelmore & Meyers(1998) developed a model to explain the *R* gene evolution called *birth and death* model in which new *R* genes are generated by duplication and unequal crossing-over followed by purifying selection. Genetic variation on NBS-LRR would be the result of basic genetic mechanisms including gene duplication, unequal crossing over, sequence exchange and gene conversion at variable rate of occurrence. Among those mechanisms, recombination and gene conversion can play a role in reasserting variation in alleles and paralogues, and also by reducing and expanding of the number of LRR domains, changing the spatial distribution of the ligand contact points and adjusting both identity and affinity. The diversification also is influenced by point mutations which alter the identity of potential contact points for the ligand (Ellis et al., 2000; Wulff et al., 2001; McHale et al., 2006; Liu et al., 2007).

1.9 Effectors vs Avr proteins

Pathogens deploy in a spatiotemporal way an arsenal of proteins and other molecules to facilitate colonization, survival, and reproduction in the host. These proteins target multiple subcellular compartments interfering with the host immune response and other metabolic processes. These molecules are called effectors or Avr proteins, and their presence can be recognized by the host plasma membrane or cytoplasmic immune receptors called resistance (R) proteins. This recognition causes an immune condition called *avirulence* that is associated with a defense response that includes a localized kind of programmed cell death called the hypersensitive response (HR) (Ellis et al., 2009; Yin & Hulbert, 2010; Giraldo & Valent, 2013; Grant et al., 2013; Dong et al, 2015).

The term *effector* is a central jargon in plant-microbe interactions and increased its popularity in the last decades because the teleological concept of *avirulent gene* or *Avr* gene, used in the gene-for-gene concept eventually became conceptually restrictive (Hogenhout et al., 2009; Win et al., 2012). Over the years, it was assumed that the default pathogenicity displayed by the pathogen favored a compatible reaction with a susceptible host lacking of a matching *R* gene, making the *virulent gene* an empty concept (Ribeiro Do Vale et al., 2001). However, molecular pathologists

discovered that some pathogenic bacteria deliver proteins into the host using the type III secretion system (TTSS) triggering a HR in the presence of R proteins (avirulence activity). But later, it was found that the presence of TTSS also called *hrp* genes (for *hypersensitive reaction and pathogenicity*) (Lindgren, 1997) would contribute to virulence on susceptible plants (virulence or pathogenic activity), Eventually, it was concluded that the same molecule could display avirulence activity in incompatible interactions or virulence activity on compatible interactions (Hogenhout et al., 2009). It becomes evident that the terms avirulence and virulence depend on the specific host in which the phenotype is being observed, this makes the term effector more neutral, inclusive and extended to other symbiotic relationships (Plett et al., 2011; Chaudhari et al., 2014). It has been accepting, that most of the avirulence genes in fact code for effectors to stress their presumed inherent virulence function and the *effect* that they have over one or more genotypes. However, when an effector is recognized, the immune response or avirulence function overlaps the pathogenic or virulence function. (van der Hoorn & Kamoun, 2008; Yin & Hulbert, 2010; Vleeshouwers & Oliver, 2014). This made that some authors called them also as *Avr-effectors* (Na & Gijzen, 2016).

Hogenhout et al., (2009) suggested a broad definition of the term effectors defining them as proteins and small molecules that alter host cell structure and physiology facilitating infection (virulence factors and toxins) or triggering defense responses (avirulence factors and elicitors) or both. This definition is extended from "Avr protein = effector protein" to PAMPs, toxins, degrading enzymes, molecules that can mimic phytohormones, small RNAs (Weiberg et al., 2013), etc. However, Alfano, (2009) pointed out that even as the broad definition of effector is appropriated, a narrow definition considering only pathogen-derived proteins allows a focused research.

1.10 Mechanisms of *R-Avr* recognition

1.10.1 Direct interaction

The gene-for-gene model has been interpreted as a recognition phenomenon at the molecular level. The R protein is proposed to act as an immune receptor that is able to recognize a corresponding pathogen Avr protein and form an R-Avr complex that activates an immune

response (Liu et al., 2007). Despite the increasing number of R proteins and matching *Avr* gene/effector pairs characterized in the last years, we ignore much about the mechanism of effector perception by R proteins and the downstream plant defense response (Stergiopoulos & de Wit, 2009). Traditionally, two alternatives have been considered to explain the gene-for-gene model the “direct” and “indirect” interaction. The molecular basis of direct interaction has been explained mainly by two models: the *elicitor-suppressor* model proposed by Bushnell & Rowell (1981) and the *elicitor-receptor* model proposed by Albersheim & Prouty (1975). The *elicitor-suppressor* model suggests that pathogens produce a general set of non-specific elicitors that induce an immune reaction after being recognized by receptors in plants. However certain pathogen races produce specific suppressors that block the action of non-specific elicitors (suppression of general defense) making the plant susceptible. This model has not proved experimentally. The simplest and oversimplified interpretation of direct interaction is the *elicitor-receptor* model. Under this model, proteins or metabolites are recognized by host receptor proteins. The *Avr*-gene encodes a ligand that binds directly to the *R* gene product which then activates downstream signaling events to induce various defense responses (Hammond-Kosack & Jones, 1997). This model was later expanded and refined by including endogenous elicitors and receptors (cytoplasmatic) and intracellular signaling mechanisms. The model has been supported by the fact that of most of *Avr* genes code for small proteins and that are co-localized into the cell with the *R* gene product (van der Hoorn & Kamoun, 2008). Experimental evidence for direct physical interaction between effectors and NBS-LRR proteins has been found in the flax rust R proteins M and L6 and their cognate effectors proteins AvrL567 and AvrM, respectively (Dodds et al., 2006). Also, direct interaction has been demonstrated between the *R* protein Pi-ta in rice and Avr-Pita from the pathogen *Magnaporthe grisea* (Jia et al., 2000), and the gene products of the resistance gene *RRS1-R* and the *Avr* gene *popP2* in *Arabidopsis* (Deslandes et al., 2003).

1.10.2 Indirect interaction

1.10.2.1 Guard model

Indirect effector perception may explain how multiple effectors could be perceived by a single R protein reducing the number of *R* genes required to confer resistance against a broad diversity of

pathogens that attack plants (Dangl & Jones, 2001; Stergiopoulos & de Wit, 2009). Researchers noted that several NB-LRRs require unique accessory proteins for detection of pathogen effectors. For example, the protein serine threonine kinase Pto is necessary for the recognition function of *R* gene *Prf* in tomato (Mucyn et al., 2006). The protein RIN4 is required for the resistance genes *RPM1/RPS2* in *Arabidopsis* to protect against the action of effectors AvrRpm1/AvrB and AvrRpt2 delivered by *Pseudomonas syringae* (Mackey et al., 2002; Mackey et al., 2003). In *Arabidopsis*, the resistance gene *RPS5* has been shown to guard the protein PBS1, a serine/ threonine kinase protein that is a target of the AvrRphB of *Pseudomonas syringae* (Jones & Dangl, 2006). These examples led to the proposal of alternative models to the direct interaction model in which NBS-LRR proteins do not directly detect an effector (Figure 1.3), but monitor its effect on a host protein. Depending on the function of the effector's targets NB-LRRs are referred to as a 'guards' for virulence targets, or 'decoys' for proteins mimicking virulence targets (Takken & Govere, 2012).

The *guard model* was proposed by van der Biezen & Jones (1998) and implies the involvement of more than two proteins in plant-pathogen recognition. The guard model requires a third, intermediate plant protein (called guardee) that interacts directly with pathogen effector(s), being modified and facilitating pathogen's infection. The resistance response is initiated when the *R* protein detects a physiological change or an attack over its guardee product or when the *R* gene can recognize the residual product of pathogen attack with no direct interaction (van der Hoorn & Kamoun, 2008; Gururani et al., 2012).

1.10.2.2 Simple decoy model

Accumulated evidence of effectors indirectly recognized shows inconsistently with the predictions of the guard model, since many pathogen effectors have multiple targets in the host cells, suggesting that the guardee proteins are not essential as effector's target in the absence of *R* proteins. Also, one prediction of the model is that the guardee protein is in an unstable evolutionary situation since it is subject to two antagonistic natural selection forces that depend on the absence/presence of *R* protein. In the absence of *R* protein, natural selection is expected to select a decreasing in the binding affinity between the guardee and the pathogen effector evading the modification. However, in presence of *R* protein, the natural selection is expected to increase

the affinity of the guardee with the effector to enhance the indirect perception of the R protein. (Gupta et al., 2010).

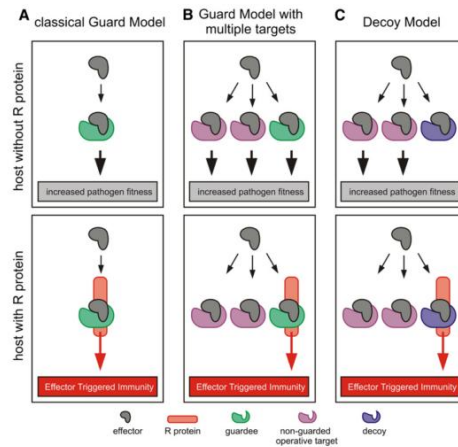


Figure 1.3 The Guard and Decoy models for indirect interaction between *R* and *Avr* genes (effector). The classical Guard Model (A) Guard Model in which the effector targets multiple plant proteins (B) and the Decoy Model (C). From Figure 2 (van der Hoorn & Kamoun, 2008).

An alternative model to the guard model was proposed by Van der Hoorn & Kamoun (2008) called *the decoy model*. This model provides an evolutive justification to the weakness of the guard model. The ‘decoy’ proteins are mimics of actual pathogen effector’s targets or ‘guardees’ that evolved to enhance the binding with the Avr protein and the perception by R protein, trapping the pathogen in a recognition event (Gupta et al., 2010). The decoy does not have any function either in the development of disease or resistance, but it competes with the real host guardee or effector’s target without affecting the pathogen fitness independent of the presence or absence of R protein. A few cases support this model: a case involves the interaction of Avr2 of *C. fulvum* and the protein Rcr3, which acts as a distractor (decoy) for the Avr2 from its real target the plant protease PIP1. The interaction with Rcr3 activates *Cf-2* a resistant gene against *C. fulvum* (Shabab et al., 2008). The AvrBs3 of *Xanthomonas campestris* pv *vesicatoria* activates in resistant plants the promoter of the gene *pBs3* (decoy) that also is an unusual *R* gene coding for a flavin monooxygenase (Römer et al., 2007). Typically, the *AvrBs3* gene product binds to the promoter of the gene *upa20* (effector operative target), a master regulator of cell size. Finally, the *AvrPto* of *P. syringae* blocks the function of FLS2 and EFR two receptor kinases involved in PTI. The Pto protein confers resistance mediated by the *R* gene *Prf*. The effector *AvrPto* contributes to virulence in both tomato and *Arabidopsis*, but not in *Arabidopsis* lacking FLS2

which makes it an effector operative target. In contrast, the absence of *Pto* does not reduce the virulence mediated by *P. syringae* strains carrying *AvrPto* making *Pto* itself a decoy protein. The decoy proteins would be the result of duplication of actual host targets, with selective evolution of those duplicated genes to the ‘decoy’ version of proteins mimicking the effector’s target (van der Hoorn & Kamoun, 2008; Gupta et al., 2010; Stergiopoulos & de Wit, 2009; de Wit et al., 2009).

1.10.2.3 Switch-bait model

Since there is no convincing proof to prefer the guard model or decoy model, “switch” models like “refine switch” and “bait-and-switch” models were proposed (Collier & Moffett, 2009). Under this model, the effector is recognized in a two-step event. First, the effector interacts with the effector’s target, but in this model, it is just a cofactor (a bait with no specific function). This effector-target interaction leads to a second event of recognition between the effector and an NBS-LRR protein activating a molecular switch that results in the induction of the resistance response. The “bait” or effector target protein is a facilitator of the direct recognition of the pathogen effector by the NBS-LRR protein, which shows diversifying selection of the LRR domain to different recognition specificities. The “bait” proteins identified so far interact with the N-terminal domain of their respective NB-LRR. For example, the proteins RIN4 and PBS1 interact with the CC domain of RPM1 and RPS2. The protein *Pto* interacts with the SD (Solanaceae domain) domain of *Prf* (Collier & Moffett, 2009; Eitas & Dangl, 2010; Hann & Boller, 2011). The conformation of the NBS-LRR in the inactive state makes that the bait be in close proximity of C-terminal half of the LRR domain. Moreover, the NBS-LRR in inactive conformation allows the LRR region to monitor effector-induced alterations on the bait, such as its cleavage, phosphorylation or any other modification. The recognition of the effector can occur either via direct interaction with the NB-LRR protein or indirectly via alterations on the “bait” protein bound to NBS-LRR N-terminal domain (Ma et al., 2012a).

1.10.2.4 Integrated decoy/sensor model

Researchers have observed that resistance to pathogens can be mediated by complementary pairs of NBS-LRRs involving both TIR-NBS-LRR and CC-NBS-LRR proteins (Eitas & Dangl, 2010). In *Arabidopsis*, the R proteins RPP2A and RPP2B are necessary for resistance against

Hyaloperonospora arabidopsidis (Sinapidou et al., 2004), and RPS4 and RRS1 are required for the recognition of AvrRps4 of *Colletotrichum higginsianum* (Narusaka et al., 2009). In cereals, the pair Lr10 and RGA2 confer resistance to leaf rust *Puccinia triticina* (Loutre et al., 2009), the pair RPG5 and RGA1 confer resistance to *Puccinia graminis* (Wang et al., 2013) and in rice the pair RGA4/RGA5 are required for the direct recognition of the *Magnaporthe oryzae* effector AVR1-CO39 (Cesari et al., 2013).

All known examples of resistance mediated by the complementary pairs of NBS-LRRs show a direct binding between Avr proteins and at least one NBS-LRR member of the pair acting as an Avr protein receptor. This receptor carries an additional, not conserved domain or non-canonical domains frequently occurring on the C or N-terminal portion of the protein. In the case of RRS1, it carries an additional WRKY domain; in the case of RGA5, it is fused to a heavy metal-associated domain called RATX. The N-terminal domain (TIR or CC) of the signal inducer partner translates the recognition into activation of resistance responses. Plant NBS-LRRs with these integrated domains were recently called NBS-LRR-IDs or NBS-LRRS with integrated domain and would constitute 10% of all NBS-LRR proteins. There is evidence that IDs also are present in proteins related with susceptibility or families of proteins involved in defense signaling. These observations suggest that IDs have been integrated into the NBS-LRR protein acting as a decoy receptor to recognize and physically bind Avr proteins/effectors. These decoy domains are not conserved in NBS-LRRs, suggesting that they are not playing a critical role in signaling or regulation. IDs would originate by duplication of paired NLR genes followed by the acquisition of new domains through random genome re-arrangements, and selection favoring NBS-LRR-ID-decoy proteins for resistance. This model called the *integrated decoy/sensor model* is an extension of the decoy model (Cesari et al., 2014; Sarris et al., 2016; Ellis, 2016).

To summarize, according to the integrated decoy/sensor model, the pair of NBS-LRR proteins form a homo or heterocomplex with a specialized task (i.e., Avr protein-receptor or signal inducer), recognizing multiple Avr proteins through direct binding of the Avr protein to a chimeric domain located on the receptor partner. This model implies that the dichotomy of direct and indirect recognition is replaced by an intermediary between both recognition models (Cesari et al., 2014).

1.11 Effector delivery and translocation

The fungal effectors can be categorized in two main groups according to their delivery strategy: (1) extracellular effectors or effectors secreted into apoplast or xylem where they interact with cellular targets or immune receptors, and (2) cytoplasmic effectors which are translocated into the host. The second strategy has been associated with the development of specialized structures such as haustorium, (e.g. cereal rust), biotrophic interfacial complex (BIC) (e.g. *Magnaporthe oryzae*) (Stergiopoulos & de Wit, 2009; Giraldo et al., 2013; Selin et al., 2016), or a total invagination of intracellular hyphae with an extensive area of contact (e.g. *Ustilago Maydis*) (Djamei & Kahmann, 2012).

1.11.1 Fungi with extracellular effectors

Among the fungi that deliver extracellular effectors and have served as model organisms for research, we have *Cladosporium fulvum*, *Fusarium oxysporum* f. sp., *lycopersici*, *Leptosphaeria maculans*, *Magnaporthe oryzae*, and *Rhynchosporium secalis* (Stergiopoulos & de Wit, 2009; Bent & Mackey, 2007). In the case of *C. fulvum*, five effectors *Avr2*, *Avr4*, *Avr4E*, *Avr5*, and *Avr9* have been cloned and are recognized by the cognate R proteins Cf-2, Cf4, Cf4E and Cf9, therefore five extracellular proteins (Ecps) that induce HR in the presence of the *Cf-Epc* gene have been characterized. Those effectors serve as chitinase protector (*Avr4*), or target host molecules like proteases (*Avr2*), carboxypeptidase inhibitor (*Avr9*) and scavenger of chitin fragments (Sánchez-Vallet et al., 2013; Mesarich et al., 2014) or they have unknown function (EcPs). Five effectors have been cloned from *Fusarium oxysporum* designated as *Six1*, 3, 4, 5 and 6 (because they are secreted in the plant xylem). They produced HR in the presence of the series of R genes designated as *II-I4* (Stergiopoulos & de Wit, 2009), more recently the *AvrFom2* was cloned from *Fusarium oxysporum* using comparative genome analysis (Schmidt et al., 2016). Eleven effectors (*AvrIm1*, 2, 3, 4, 5, 6, 7, 9, 11, *AvrLep1* and *AvrLmJ1*) have been cloned in *Leptosphaeria maculans* the causal agent of stem canker in oilseed rape. However; their cognate R genes have not been cloned. In *Magnaporthe oryzae* 16 *Avr* genes have been cloned including *Bas4*, *Avr1-CO39*, and *Slp1*. In *Rhynchosporium secalis*, the causal agent of leaf scald on barley three effectors designated as *Nip1* to *Nip3* have been cloned (Stergiopoulos & de Wit, 2009; Zhang et al., 2014b; Selin et al., 2016).

1.11.2. Fungi with host-cell translocated (cytoplasmatic) effectors

Effectors can be translocated into the host cell and target different subcellular compartments including the nucleus, organelles and membrane compartments (Win et al., 2012). In the case of fungal biotrophs, with effectors delivered in the cytoplasm, four *Avr* genes and their variants have been cloned from *Melampsora lini* loci: *AvrL567*, *AvrM*, *AvrP123*, and *AvrP4* (Dodds et al., 2004; Catanzariti et al., 2006). The ascomycete *Blumeria graminis* f. sp. *hordei* (*Bgh*) the causal agent of powdery mildews on cereals, probably contains the highest number of *Avr* genes studied, with over 500 candidate effectors that have been predicted in the last years. However only two *Avr* genes have been cloned (*Avrk1* and *Avra10 AvrPm3²*), both genes belong a large multigene family with more than 30 paralogs (Ridout et al., 2006; Bourras et al., 2015; Ahmed et al., 2016). Nirmala et al., (2011) presented evidence for the pre-haustorial concerted dual action of effectors proteins RGD-binding and VPS9 in spores of *Pgt* that trigger HR in the presence of the resistance gene *RPG1*. In a preliminary screening, Upadhyaya et al., (2014) identified a candidate effector called PGTAUSPE-10-1 that induced cell death in a host line carrying the resistance gene *Sr22*. PGTAUSPE-10-1 was considered as a candidate gene for *AvrSr22*. However, no further functional characterization has been reported for this candidate (Selin et al., 2016).

1.12 Cloning of fungal effectors

After Harold Flor formulated the gene-for-gene concept, it took almost 50 years until the first *Avr* gene in fungi was cloned in 1991 (van Kan et al., 1991). Over the past two decades, numerous novel *Avr* genes and their cognate *R* genes have been discovered and cloned in several pathosystems increasing our understanding of the molecular basis of the gene for gene relationship. (Stergiopoulos & de Wit, 2009; Kamoun, 2007; Bent & Mackey, 2007; Wirthmueller et al., 2013).

Most of the cloned effectors or *Avr* genes in fungi encode small secreted proteins (SSPs) between 63 and 300 amino acids in length (Selin et al., 2016). Many effectors could work simultaneously as a team making their individual contribution minor, undetectable, redundant or overlapping (Stergiopoulos & de Wit, 2009; De Wit et al., 2009). Individual effectors could be

contributing to the global virulence, but they would be not essential to guarantee pathogen viability (Bent & Mackey, 2007). Unlike many bacterial counterparts, it has been difficult to assign a precise function to the effectors cloned in fungi based merely on deduced orthology with proteins stored in databases. Exemptions have been found in effectors of *Magnaporthe oryzae* *Avr-Pita* (a putative metalloprotease) (Jia et al., 2000) and *Ace1* (a hybrid polyketide synthase/nonribosomal peptide synthetase) (Bohnert et al., 2004). Usually, protein effectors in eukaryotes are secreted using the route of endoplasmic reticulum-Golgi apparatus and exocytosis which requires the presence of an N-terminal secretion signal in order to translocate the protein (Dodds et al., 2004; O'Connell & Panstruga, 2006; Tang et al., 2015). However, among the fungal effectors cloned so far, there is not a clear consensus signature that suggests any association with translocation and an uptake mechanism (Stergiopoulos & de Wit, 2009; de Wit et al., 2009). In fact some cytoplasmic effectors (*Avr10* and *Avrk1* of *B. graminis* f. sp. *hordei*) lack of a signal peptide sequence for secretion (Ridout et al., 2006). This unique feature found in fungal effectors contrasts with the motif RXLR-dEER near to N-terminus of several oomycetes effectors, which has been associated with translocation into the host cell (Ellis et al., 2009; Bozkurt et al., 2012).

By 2016, 83 effectors from economically relevant fungi and oomycetes had been cloned. In particular, the cloning of fungal effectors has been restricted to only eight species (Selin et al., 2016). Historically, fungal effectors have been cloned by reverse genetic approaches, including the isolation of peptides from apoplastic fluids that induce necrosis, followed by the screening of cDNA libraries with derived probes based on amino acid sequence (de Wit et al., 1985, van Kan et al., 1991). They have also been identified by genetic map-based cloning combined with complementation tests after transformation of a virulent fungal strain (Orbach et al., 2000; Fudal et al., 2007). Alternative methods of cloning are based on functional validation of candidate *Avr* genes depending on technical developments (Ellis et al., 2009).

The approaches to cloning and functional validation of fungal candidate effectors have included:

1. Avirulence functional screening of candidate effectors for hypersensitive response including cDNAs in heterologous system using *A. tumefaciens* infiltration or particle bombardment (Houterman et al., 2009).

2. Avirulence functional screening using Potato X virus-mediated cDNA expression (Takken et al., 2000; Houterman et al., 2009; van Esse, 2012).
3. Avirulence functional screening using of heterologous proteins that can be delivered via the Type III secretion pathway from genetically engineered non-pathogenic bacteria (Thomas et al., 2009; Yin & Hulbert, 2010; Upadhyaya et al., 2014).
4. Site-specific integration of linear DNA using restriction enzymes (Mutagenesis using restriction enzyme-mediated integration or REMI) (Thon et al., 2000).
5. Comparative genomic analysis and comparative transcriptomic analysis during infection (Cantu et al., 2013; Duplessis et al., 2011a; Nemri et al., 2014; Liu et al., 2015).
6. Host induced gene silencing (HIGS) for characterizing gene function (Panwar et al., 2013; Pliego et al., 2013; Yin et al., 2015).

Since some of these methods are labor intensive and show a low rate of success, the integration of sequencing of the whole genome, transcriptome, secretome, proteome, metabolome and the development of bioinformatics approaches for comparative genomics of fungal pathogens have been recently used to identify candidate effectors. Those candidate effectors are later validated experimentally by different approaches including some methods described above as well as gene disruption or silencing in fungal isolates (if it is possible), and subsequent avirulence assays on host plants (Garnica et al., 2013; Upadhyaya et al., 2015; Cuomo et al., 2016; Thatcher et al., 2016; Mogga et al., 2016; Dong et al., 2016; Plissonneau et al., 2017). Unless complementary genetic evidence exists, the main challenge in use genomic data is the identification of candidate effectors *ab initio* using only genomic and gene expression data since most of the effectors have unique sequences or low levels of homology with other potential orthologs (Stergiopoulos & de Wit, 2009; Ellis et al., 2009).

There is lack of information about the wheat-*Pgt* pathosystem in particularly the characterization *R/Avr* gene pairs, this information is crucial to develop new breeding strategies to control Ug99. In the following chapters, we show the molecular characterization of the *Sr35* gene and its use as entry point to clone and functional characterization of its corresponding *Avr* gene, the *AvrSr35*.

Chapter 2 - Time course gene expression analysis of the resistance gene *Sr35* and validation of wheat lines with the *Sr35*-transgene

2.1 Introduction

The stem rust resistance gene *Sr35* is derived from the diploid wheat *Triticum monococcum* L. ($2n = 14 = AA$) (genome A^m), which is a close relative of *Triticum urartu* (genome A^u), the diploid donor of the A genome in both the tetraploid (*T. turgidum*, pasta wheat) and hexaploid wheat (*T. aestivum*, bread wheat) (McIntosh et al., 1995; Rouse & Jin, 2011). The *Sr35* gene is localized on chromosome 3AL, and unlike other wheat relatives, it recombines relatively easily with the hexaploid wheat chromatin (McIntosh et al., 1995; Zhang et al., 2010; Rouse & Jin, 2011). Although several *Pgt* races are virulent against *Sr35*, its cloning was considered a priority because it confers near immunity against several members of the *Pgt Ug99* race group including TTKSK, TTKSK, TTKST and TTTSK (Jin et al., 2007; Zhang et al., 2010). The *Sr35* also confers resistance against the race TRTTF, which is virulent for other major resistance genes available against *Ug99* (Olivera et al., 2012; Singh et al., 2015).

Saintenac et al., (2013) cloned the *Sr35* gene using a positional cloning approach. The *Sr35* gene encodes for a CC-NBS-LRR and it is located in a cluster of resistance genes with both intact R-gene analogs and pseudogenes. The genes in the cluster were designed as *CNL1*, *CNL2*, *CNL4*, *CNL6*, and *CNL9*, which was eventually identified as the *Sr35* gene. Rapid amplification of cDNA ends (RACE) found that the *Sr35* has two *alternative splicing* (AS) isoforms. The most abundant transcript (main isoform) has a 196-bp 5'-untranslated region (UTR) and a 1526 bp 3'-UTR that includes three introns. The second isoform of *Sr35* (isoform-2) is a splicing variant that contains the third intron (2nd intron of the 3'-UTR) (Saintenac et al., 2013).

The alternative splicing (AS) isoforms of the messenger RNA use differential splice sites to create diversity in the transcriptome and are involved in the modulation of the gene function affecting both protein activity and stability (Graveley, 2001; Black, 2003; Soergel et al., 2013). AS isoforms are the result of four basic molecular processes: alternative 5' or 3' splice-site, exon

inclusion, exon skipping, and intron retention (Nilsen & Graveley, 2010). The regulation of AS isoforms is poorly understood, but their role in plant immunity and pathogen defense has been recognized (Staiger et al., 2013). AS isoforms can be induced by environmental stresses and can be expressed in different tissues and developmental stages (Yang et al., 2014). Many plant disease resistance gene including CC-NBS-LRR (CNL) and TIR-NBS-LRR (TNL) classes undergo alternative splicing. For CNLs, several alternative splicing isoforms have been identified, including *Lr10* in wheat (Sela et al., 2012), *Mla* in barley (Halterman et al., 2003), *JAltr* in common bean (Ferrier-Cana et al., 2005), *RGA5* (Cesari et al., 2013) and *Pi-ta* (Costanzo & Jia, 2009) in rice. However, the events of alternative splicing in CNLs have not been associated with disease resistance to date (Yang et al., 2014). In contrast, some events of alternative splicing-related resistance have been functionally characterized in TNL genes including the *Arabidopsis* genes *RPS4* (Zhang & Gassmann, 2007), *RPS6* (Kim et al., 2009), *RAC1* (Borhan et al., 2004), *RPP5* (Parker et al., 1997), Flax *L6* (Ayliffe et al., 1999), tobacco *N* gene (Dinesh-Kumar & Baker, 2000), and *M. truncatula RCT1* (Tang et al., 2013).

Data accumulated in the last years, indicate that the expression of *R* genes can be variable, but most of the *R* genes analyzed are constitutively expressed at basal levels and induced after the pathogen is recognized (Brown & Rant, 2013). Other *R* genes, such as Flax *L6*, remain constitutively expressed even after inoculation with a pathogen containing the corresponding avirulent gene (Ayliffe et al., 1999). By contrast, in some pathosystems, the *R* genes are induced only after pathogen challenge. Examples of these genes include *Xa1* (Yoshimura et al., 1998), *SSI4* (Shirano et al., 2002), *Mla13* (Halterman et al., 2003), *RPW8.1* and *RPW8.2* (Xiao et al., 2003), *HTR* (Chandra-Shekara et al., 2004); *N* gene for tobacco mosaic virus (Levy et al., 2004), *Xa27* (Gu et al., 2005), and *RPS4* (Zhang & Gassmann, 2007). Regulation of *R* gene expression levels is common phenomenon since its constitutive overexpression would have negative effects on plant growth and fitness (Li et al., 2010; Brown & Rant, 2013). It was shown that the reallocation of resources from growth to defense has a grain yield penalty in wheat (Smedegaard-Petersen & Stolen, 1981).

This chapter describes my contribution to the characterization of the *Sr35* gene. Here, I investigated the expression of two alternative splicing isoforms of the *Sr35* gene during *Pgt*

infection. I also studied the relationship between the presence of the *Sr35*-transgene and resistance against the *Pgt* race TTKSK (*Ug99*).

2.2 Objectives

- To evaluate the expression of the *Sr35*-alternative splicing (AS) isoforms during the infection with the *Sr35*-avirulent *Pgt* race RKQQC.
- To evaluate the presence of *Sr35*-transgene by PCR.
- To evaluate the gene expression of *Sr35* in the transgenic wheat lines.
- To evaluate if the presence and expression of the *Sr35*-transgene is associated with the resistance to the *Ug99* (TTKSK) race of stem rust.

2.3. Materials and methods

2.3.1 Plant material and BAC clones

T. monococcum accession G2919 (= PI428170, *Sr35*-resistant) was used to evaluate the expression of *Sr35*-alternative splicing (AS) isoforms using qRT-PCR method. T₀ and T₁ generations of selected transgenic lines of Fielder and Bobwhite wheat cultivars (susceptible to *Pgt* races RKQQC and TTKSK) were co-transformed with the plasmid pCR-II-TOPO-Sr35 and the plasmid pAHC20 carrying *bar* gene reporter (Saintenac et al., 2013). These lines were screened by PCR for transgenic events; the *Sr35* gene expression was evaluated by qRT-PCR. BAC clones 64A22 (containing *CNL4*) and 245M16 (containing *CLN9*), which cover the region surrounding the *Sr35* gene (Saintenac et al., 2013, supplementary materials Figure S1), were obtained from a BAC library for the *T. monococcum* accession DV92 (resistant to *Pgt* races RKQQC and TTKSK) (Cyrille Saintenac et al., 2013). These BAC clones were used to validate primer specificity for the *Sr35* alternative splicing isoforms.

2.3.2 *Pgt* inoculation and growth conditions

T. monococcum G2919 seeds were grown in a growth chamber. Seeds were germinated in Metro-Mix 360 soil (Sun-Gro Horticulture, Vancouver, Canada) at 22°C, photoperiod of 16 hours, 40-50% relative humidity, and 1000 lux light level until they reached two-leaf stage for

inoculation (12 days old). Urediniospores of the *Pgt* race RKQQC (*Sr35*-avirulent) were activated by immersing the vial with spores in a water bath at 42°C for 6 min. Activated urediniospores were resuspended in Soltrol[®] 170 isoparaffin solvent (Philips 66, Bartlesville, OK). The urediniospores suspension (1% w/v) was sprayed over a seedling set of *T. monococcum* G2919, using an atomizer and air compressor (Craftsman). Soltrol[®] 170 isoparaffin solvent was used for mock inoculation. Inoculated seedlings were left at room temperature (28°C ±2) for 20 min until the oil suspension was dried out, then the seedlings were incubated in a Percival I-36D dew chamber for 12 hours (Percival Scientific Inc., Perry, IA) (18-22°C, 100% relative humidity under dark conditions). After dew chamber treatment, inoculated seedlings were transferred immediately back to the growth chamber under the conditions described above. Plant tissue samples (six biological reps) for each treatment (RKQQC and mock) were collected before entering the dew chamber treatment and at 24, 48, 96 and 144 hours after removal from the dew chamber.

2.3.3 Validation of specific primers for two alternative splicing variants of *Sr35*

Amplification of the two *Sr35* AS isoforms was performed using primers NL9_F22 and CNL9Main_rv_2 for the main isoform, and primers NL9_F22 and CNL9_iso_intron_rv_2 for the isoform-2 (Table 2.1) (Saintenac et al., 2013, supplementary materials Table S5). Primers were designed based on the exon-exon boundaries or the intronic sequence of the 3' UTR region (Figure 2.1A). Specificity of PCR amplification for each isoform was determined using genomic DNA and cDNA from *T. monococcum* G2919 and the BAC clones carrying a single gene: BAC 245M16 (containing *Sr35* also called CNL9) and BAC 64A22 (containing CNL4) (Saintenac et al., 2013, supplementary materials Figure S1).

PCRs were performed using 1X GeneAmp PCR buffer II (Life technologies, Carlsbad, CA) containing 2.5 mM MgCl₂, 0.2 mM dNTP's, 0.2 μM of forward and reverse primer and 0.2 μl Amplitaq Gold[®] DNA polymerase (5U/μl) (Life technologies, Carlsbad, CA).

Table 2.1. Primers used for *Sr35*-transgene PCR screening and gene expression (Saintenac et al., 2013, supplementary materials Table S4 and S5)

Forward	Sequence	Reverse	Sequence	PCR profile	Purpose
BARabF	CCTGCCTTCATACGCTATTTATTTGC	BARabR	CTTCAGCAGGTGGGTGTAGAGCGT	94°C 5 min, (58°C, 30 sec 72°C 30 sec)	Transgene screening
CNL9_F1	GGACAACGAGAGAACACACCA	CNL9_R1	GAGAGATTCGATGCCCTTTCTC	X10 cycles , (52°C 30 sec 72°C 30 sec) X35 cycles, 72°C 7 min	
CNL9_F4	AGAGAGCAAGGTTTCGCAGG	CNL9_R4	ATACCCAACATCGGAGACATG	94°C 5 min, (62°C 30 sec 72°C 30 sec) X10 cycles , (55°C 30 sec 72°C 30 sec) X10 cycles, 72°C 7 min	Transgene screening
M13_F	CACACAGGAAACAGCTATGAC	CNL9_R2	CGTCTCTCTGCCATTCCTCCT		
CNL9_F19	GCGGGTCGTCTATGCGTGTC	T7	AATACGACTCACTATAGGG		
CNL9_F22	GGCTTAAACGCCTTTGGTTCA	CNL9Main_rv_2*	CGGCTGCCTGAAACTCAATC	95 °C for 5 min; 40 cycles of 95 °C for 30 sec, 58 °C for 30 sec, 72 °C for 40 sec	<i>Sr35</i> gene expression
CNL9_F22	GGCTTAAACGCCTTTGGTTCA	CNL9_iso_intron_rv_2**	GAAAACACTTTGTACAAAATCGTGG		
Phych_F1	GTATGTCCTCCTACCTCACGAAGT	Phych_R1	CGCTGCTGCGATAATCTGCT		

* Specific primer to the main isoform of *Sr35*. ** Specific primer for the isoform-2 of *Sr35* that retained the third intron (=2nd intron of the 3' UTR). Phych: Phytochelatin gene.

PCR was performed under the following conditions: 98°C for 5 min; 10 cycles at 98°C for 15 sec, 60°C for 30 sec and 72°C for 2 min; 35 cycles of 98°C for 15 sec, 55°C for 30 sec and 72°C for 2 min; a final extension at 72°C for 7 min. All PCR products were run on 1.8% agarose gels (w/v) prepared in 1X TAE buffer (40 mM Tris pH 7.6, 20 mM Acetic Acid, and 1 mM EDTA pH 8.0) and stained with ethidium bromide. Electrophoresis was carried out at 4-8 V/cm, and nucleic acid bands were visualized and documented under UV light (GeneFlash gel documentation system, Syngene, Frederick, USA).

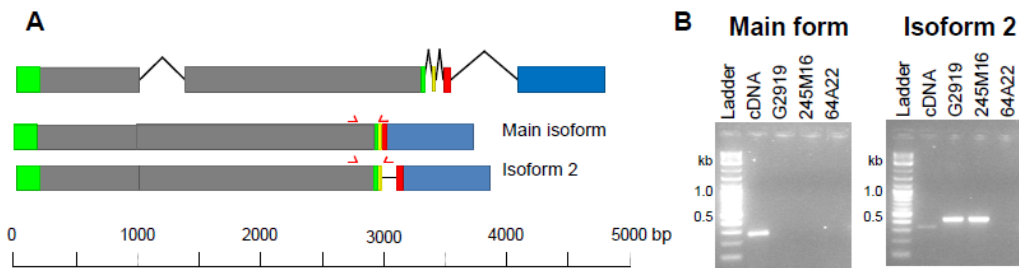


Figure 2.1. Alternative splicing isoforms of *Sr35* and specific primer validation (Saintenac et al., 2013, supplementary materials Figure S6). (A) *Sr35* gene has two transcribed exons (gray boxes), 5' and 3'-UTR regions (green boxes) and intronic sequence (black line). The 3'-UTR region has three exons (yellow red and blue boxes) and three introns. *Sr35* encodes two isoforms that differ by the absence (main form) or presence (isoform-2) of the 2nd intron in the 3'-UTR region. The positions of the isoform-specific primers are indicated with red arrows. (B) Validation of isoform-specific primers. PCR was performed using cDNA from *T. monococcum* G2919 seedlings (cDNA), G2919 genomic DNA (G2919), and DNA from BAC clones 245M16 (*Sr35*) and 64A22 (*CNL4*). Left panel: Primers NL9_F22 and NL9Main_rv_2 are specific for the main *Sr35* isoform and amplify 273 bp product from cDNA samples. Right panel: Isoform 2 specific primers NL9_F22 and NL9_iso_intron_rv_2 amplify products of 302 bp from cDNA and 390 bp from genomic DNA due to the presence of an additional intron.

2.3.4 DNA isolation

T₀ plants from Fielder and Bobwhite cultivars were tested for the expression of the selectable *bar* resistance gene using a 0.2% (v/v) solution of herbicide Liberty® (Bayer, Leverkusen, Germany). Positive transgenic lines were selected for further PCR screening. Genomic DNA from selected T₀ and T₁ transgenic lines was obtained using a high-throughput sodium bisulfate DNA isolation protocol. Briefly, leaf tissue (about 100 mg) was harvested on 1.5 ml microcentrifuge tubes containing two 4.5 mm steel beads. Samples were immersed in liquid nitrogen immediately and

stored at -80°C. Three rounds of 30 sec tissue grinding was performed using a TissueLyser II (Quiagen, Hilden, Germany) set at 25 Hz. After each round tubes were chilled in liquid nitrogen to avoid defrosting. The samples were spun down, and after adding 700 µl of 65°C warmed DNA lysis buffer vortexed until no tissue clumps were visible. Samples were incubated at 65°C one hour in a water bath and centrifuged at 10,000 x g, 10 min at room temperature in a tabletop microcentrifuge. The supernatant (~450 µl) was transferred to a new 1.5 ml microcentrifuge tube. DNA was precipitated by adding 50 µl of 10 M ammonium acetate and 450 µl of isopropanol followed by centrifugation at 10,000 x for 10 min at room temperature. The supernatant was removed, the DNA pellet was washed with 450 µl of 70% ethanol and centrifuged at 10,000 x g, 5 min at room temperature. Ethanol was removed by pipetting and DNA pellets were dried at room temperature for 30 min. Finally, the DNA pellet was resuspended in 1X TE buffer (10 mM tris pH 7.6, 1 mM EDTA pH 8.0) and stored at -20°C.

DNA Lysis buffer

Buffer A (1L)

NaCl 5 M 100 ml

Tris HCl 1 M 100 ml

EDTA 0.5 M 100 ml

pH to 7.2 and fill to 1000 ml

Lysis Buffer (30 samples)

Components:

Buffer A	25 ml	
Sodium bisulfate	0.125 g	Sigma S9000
Sodium diethyldithio carbamate	0.038 g	Sigma D3506
Ascorbic Acid	0.25 g	Sigma A5960
Polyvinylpyrrolidone (PVP10)	0.5 g	Sigma PVP40

2.3.5 RNA isolation

For total RNA isolation, 120 mg of leaf tissues were frozen in liquid nitrogen and ground three times using a TissueLyser II (Quiagen, Hilden, Germany) set at 25 Hz, for 30 sec as described above. Ground tissue was used for RNA extraction by using Trizol reagent (Invitrogen, Carlsbad, CA, USA) following the manufacturer's instructions. RNA pellet was resuspended in 50 µl of RNase-free water. RNA was quantified using Nanodrop-1000 (Agilent; Palo Alto, CA, USA) and RNA integrity was evaluated using Bioanalyzer (Agilent, Palo Alto, CA).

2.3.6 *Sr35* transgene screening

T₀ plants positives for the *bar* gene expression according to Liberty[®] herbicide staining were screened by PCR to detect the reporter *bar* gene using the primers BARabF and BARabR (Table 2.1). The the presence of the *Sr35*-transgene was determined using the primer combinations M13/CNL9_R2, CNL9_F1/R1, CNL9_F4/R4, and CNL_F19 and T7 (Table 2.1). All PCRs were performed using 1X PCR buffer (10 mM Tris HCl pH 8.3, 50 mM KCl, 0.1% Triton X-100), 1.8 mM MgCl₂, 0.2 mM dNTP's, 0.25 μM each primer, 150 ng DNA and 0.5 μl Taq DNA polymerase 5 U/μl. PCR conditions for each primer combination are shown in Table 2.1. PCR products were run on 1.8 % agarose gels (w/v) prepared in 1X TAE buffer and stained with ethidium bromide. Electrophoresis was carried out at 4-8 V/cm, and nucleic acid bands were visualized and documented under UV light (GeneFlash gel documentation system, Syngene, Frederick, USA).

2.3.7 Relative expression of *Sr35* isoforms during the course of infection

Once total RNA quantity and quality was assessed, 1 μg of total RNA was treated with 1 μl of amplification grade DNase I (1 U/μl) (Invitrogen Inc, Carlsbad, CA) in a final volume of 10 μl according to the manufacturer's instructions. cDNA was obtained from each sample using ~0.8 μg of DNase treated RNA, which were reverse transcribed with 1 mM of Oligo (dT)₂₀, 0.5 mM dNTP mix and 1 μL Superscript III reverse transcriptase (200 U/μl) (Invitrogen, Carlsbad, CA) in a final volume of 20 μL following the manufacturer's instructions. The qRT-PCRs were performed in a CFX96 Touch[™] Real-time PCR detection system (BioRad, Hercules, CA) using SYBR[®] Green to monitor dsDNA synthesis. Reactions were prepared containing 5 μL of 2X IQ[™] SYBR[®] Green Super Mix reagent (BioRad, Hercules, CA), 4 μL of cDNA diluted 1:4 and 0.25 μM of each gene-specific primer (Table 2.1) in a final volume of 10 μl. The following thermal profile was used for all qRT-PCRs: 95°C for 5 min; 40 cycles of 95°C for 30 sec, 58°C for 30 sec, 72°C for 40 sec. At the end of this profile, the PCR samples were subjected to an automatic dissociation analysis to confirm the specificity of the amplification. *Phytochelatinsynthase* gene (GeneBank BJ274652) was used as the reference gene (Saintenac et al., 2013). Primer efficiency test for qRT-PCR was performed using serial dilutions of cDNA (1/5, 1/25, 1/125, 1/625) (Saintenac et al., 2013). Ct values were exported into Microsoft Excel file and

transcript levels were expressed as the ratio between target and the internal control (fold-*Phytochelatase synthase* levels) using the $2^{-\Delta CT}$ method (Livak & Schmittgen, 2001). All experiments were conducted in a complete randomized block design, where each treatment consisted of six biological replicates and two independent technical replications. One-way analysis of variances (ANOVAs) and T-test were performed using InfoStat[®] statistical software (Infostat group, Córdoba, Argentina) to determine significant differences in the gene expression of *Sr35* gene among the treatments.

2.4 Results

2.4.1 Specific primer design for *Sr35*-isoforms

Specific primers to quantify the expression level of the alternative splice (AS) main isoform and isoform-2 were validated using *T. monococcum* G2919 cDNA and BAC clones 64A22 (containing the *CNL4*) and 245M16 (containing the *Sr35* gene) (Figure 2.1). Based on the specific amplification of each isoform using cDNA, genomic DNA and BAC clones, we concluded that the designed primer combinations can discriminate between main isoform and isoform-2.

2.4.2 Relative expression of *Sr35*-isoforms during the time course of infection

The changes in gene expression of the *Sr35* isoforms during the course of infection of the *Sr35*-avirulent race RKQQC in leaves of *T. monococcum* accession G2919 were measured using qRT-PCR (Figure 2.2). ANOVAs were carried out to determine significant differences among the selected time points (Appendix A). While no significant differences were detected between the expression of the main isoform on RKQQC- and mock-inoculated plants at all time points using ANOVA (at $p < 0.05$), we detected significant differences in gene expression at 24 hours after growth chamber transfer using *t*-test ($p < 0.05$). The pattern of the gene expression of isoform-2 did not change compared to the main isoform during the course of infection and also no significant differences were detected; but its overall expression represented about 20% of the main isoform.

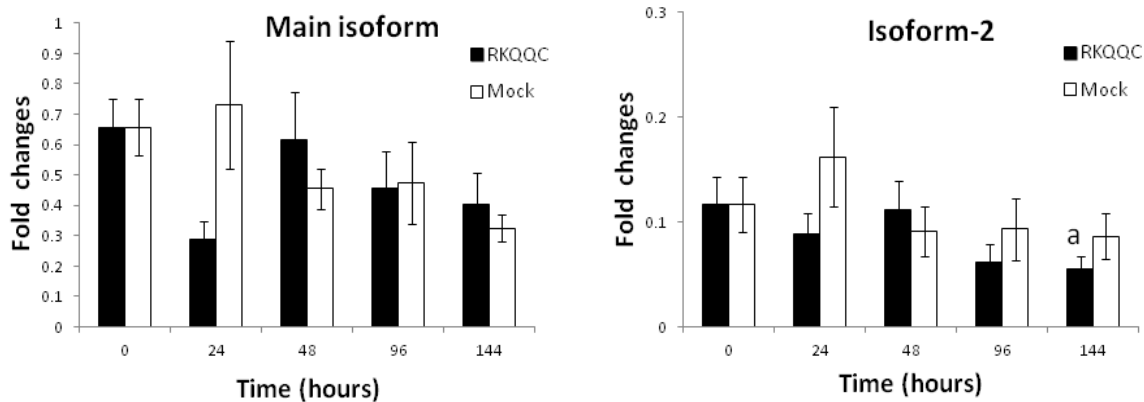


Figure 2.2. Relative transcript levels of the *Sr35*-isoforms during time course infection with the *Pgt* race RKQQC. Leaves of *T. monococcum* genotype G2919 were inoculated with the *Sr35*-avirulent race RKQQC and paraffin oil (mock). Leaves were collected after inoculation (0 hours), and 24, 48, 96, and 144 hours after transfer the seedlings from the dew chamber to the growth chamber. Transcript levels are expressed relative to the Phytochelatin synthase internal control using the $2^{-\Delta C_t}$ method (Livak & Schmittgen, 2001). Values represent \pm standard error of the mean (SEM). Data analysis were based on six biological and two technical replicates. Significant differences in RKQQC-inoculated and mock-inoculated plants at each time point are shown in lower case letter (ANOVA, t-test $p \leq 0.05$).

2.4.3 PCR-based screening and gene expression analysis of *Sr35* transgenic plants

To determine if the *Sr35* gene is sufficient to confer resistance against *Ug99* (race TTKSK), transgenic hexaploid wheat lines were generated using Fielder and Bobwhite cultivars. The construct used for transformation contained the genomic sequence of the *Sr35* gene driven by its native promoter. The construct used for transformation included 2,462 bp upstream of the start codon, the complete coding region, and the 2,615 bp-long 3'UTR. The genomic DNA fragment was amplified by PCR and subcloned into the pCR[®] II-TOPO[®] vector (Invitrogen, Carlsbad, CA) to create the vector pCR-II-TOPO XL-*Sr35*, which was biolistically co-transformed with plasmid pAHC20 containing the *bar* gene under the control of the maize ubiquitin promoter (Saintenac et al., 2013).

Four primer combinations that spanned the *Sr35* gene, and primers that anneal to the M13 and T7 promoter sequences present in the pCR-II-TOPO XL-*Sr35* plasmid, were used to confirm the presence of the *Sr35*-transgene in the transformed plants (Table 2.1). Based on the presence of consistent single strong bands in PCR reactions with the primer combinations M13/CNL9_R2

and CNL9_F4/R4, among 84 T₀ plants, we detected four transformation events (701, 967, 1007 and 1123). Also, these plants were positive for the presence of reporter gene *bar* (Figure 2.3, Figure 2.4).

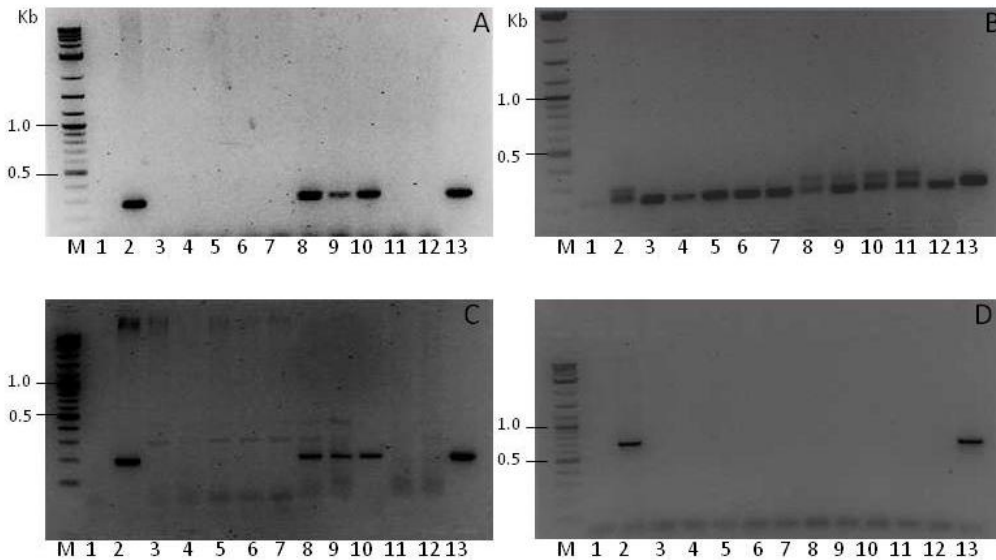


Figure 2.3. PCR-based screening of selected T₀ transgenic events to identify the presence of the *Sr35* transgene (inverted gel pictures). Primer combinations: A) M13/CNL9_R2, B) CNL9_F1/R1, C) CNL9_F4/R4, D) CNL_F19_T7. M: molecular marker (Kb). Transgenic lines 1) 658, 2) 701, 3) 708, 4) 713, 5) 758, 6) 856, 7) 962, 8) 967, 9) 1007, 10) 1123, 11) 1143, 12) 1163, 13) control PCR II TOPO XL-*Sr35*.

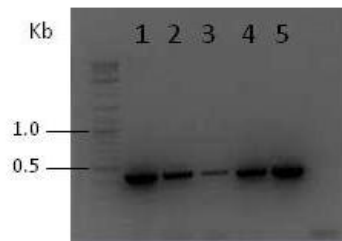


Figure 2.4. PCR-based screening of selected T₀ transgenic plants to identify the presence of the *bar* gene (inverted gel picture). Transgenic lines: 1) 701, 2) 967, 3) 1007, 4) 1123, 5) control pAHC20 (*bar* gene).

Among four transgenic plants showing the presence of the *Sr35*-transgene, the expression of *Sr35* was confirmed only in transgenic line #1123 (Figure 2.5). Even though, the relative expression of *Sr35* in the line #1123 was roughly nine-fold lower than the average transcript

levels observed in *T. monococcum* G2919 during time course experiments, this transgenic line displayed resistance against TTKSK (*Ug99*), and showed no evidence of negative pleiotropic effect on the plant morphology.

The primer combinations M13/CNL9_R2 and CNL9_F4/R4 were used to evaluate the co-segregation of the *Sr35* transgene and the resistance to TTKSK (*Ug99*) in the progeny of transgenic line #1123. The analysis of the T₂ progeny of line #1123 showed a relationship between the presence of the transgene and resistance against TTKSK (*Ug99*) (Figure 2.6, Table 2.2). Moreover, all T₁ and T₂ plants of #1123 were susceptible to *Sr35*-virulent race QTHJC, regardless of the presence or absence of the transgene (Saintenac et al., 2013).

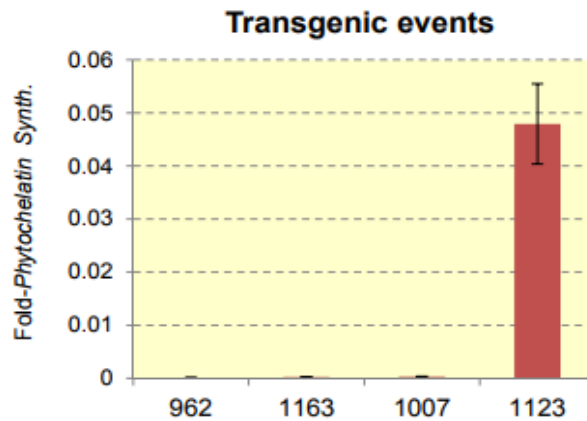


Figure 2.5. Relative transcript levels of the *Sr35* main isoform in four positive transgenic lines assessed using qRT-PCR (Saintenac et al., 2013, supplementary materials Figure S4). qRT-PCR reactions were performed using primers NL9_F22 and CNL9Main_rv_2. *Sr35* expression was observed only in the line #1123. Transcript levels are expressed relative to the phytochelatin synthase internal control using the $2^{-\Delta C_t}$ method (Livak & Schmittgen, 2001). Error bars denote the standard error of the mean (SEM). Data is based on six biological and two technical replicates.

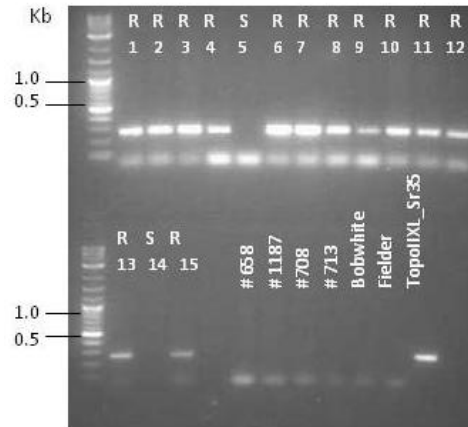


Figure 2.6. PCR-based progeny segregation screening of the T₁ generation of the transgenic line #1123. PCRs were carried out using primer combinations M13/CNL9_R2. The phenotype obtained after the infection with TTKSK (*Ug99*) (R= resistant, S susceptible) and the plant number are indicated on top of the gel lanes. Negative controls: transgenic lines #658, #1187, #708 and 713, and non-transgenic lines Bobwhite and Fielder cultivars. Positive control: PCR II TOPO XL-Sr35.

2.5 Discussion

2.5.1 Gene expression of *Sr35*-alternative isoforms during time course infection with *Pgt*

We identified the presence of two alternative splicing isoforms for the *Sr35* gene (Saintenac et al., 2013). Specific primers for both isoforms were designed and validated for qRT-PCR, and the mRNA levels of each isoform were quantitated in seedlings inoculated with the *Sr35*-avirulent race RKQQC as well as paraffin oil (mock control inoculation). Gene expression analysis did not show any evidence of gene induction due to *Pgt*-infection at any time point during the infection. This finding differs from what is usually observed in *R* genes, which are basally expressed and induced after pathogen recognition (Brown & Rant, 2013). We speculate that it is likely that *Sr35* is not regulated as a product of the incompatible interaction with the pathogen. However, this needs to be explored further, as well as the fitness cost associated with the *Sr35* gene basal expression.

Table 2.2. Co-segregation of the *Sr35*-transgene with the infection type on T₁ plants from transgenic line #1123 based in Saintenac et al., 2013, supplementary materials Table S8.

Plant	<i>Sr35</i> presence (PCR)	Infection type (TTKSK)
1	(+)	3c_LIF
2	(+)	3c_LIF
3	(+)	0. ;
4	(+)	0. ;
5	(-)	3+
6	(+)	0, ; 1
7	(+)	0, ; 1
8	(+)	1, 3-
9	(+)	1, 3-
10	(+)	1, 3-
11	(+)	0
12	(+)	0
13	(+)	1, 3c_LIF
14	(-)	3+
15	(+)	1, 3c_LIF

Only the IT (infection type¹) scores ≥ 3 after TTKSK (*Ug99*) infection were considered as susceptible (all others are resistant). (Saintenac et al., 2013 supplementary table S8) The ", " separating scores indicates separate infection types on a single plant. Plant number corresponds with the well's number on the gel image on Figure 2.6.

Infection types (ITs) scale (0 to 4) according to (Stakman et al., 1962)

IT="0" indicates immune reaction: no uredia or other visible symptoms.

IT= ';' indicates a nearly complete immune reaction: no uredia, but visible hypersensitive flecks.

IT= '1' indicates a very resistant reaction: small, round uredia by necrotic or chlorotic plant tissue.

IT= '3' indicates a moderately susceptible reaction: medium, elongated uredia observed and often associated with limited chlorotic plant tissue.

When multiple infection types were observed on the same leaf, all infection types were recorded in order, starting with the most common IT. Signs '+' or '-' indicate larger or smaller size uredia within each infection type. 'c' indicates substantial plant chlorosis. 'LIF' indicates low infection frequency.

We detected a some reduction of the relative expression of the main isoform at 24 hours after infection comparing RKQQC-infected vs. mock-inoculate G2919 seedlings. This reduction in the *Sr35* gene expression could be explained by the circadian clock regulation which has been observed in the resistance *Tsn1* gene on wheat (Faris et al., 2010). Alternatively, this reduction of expression could be a snapshot of the progressive increase in gene expression as a preparatory

response due to a change in environmental conditions associated with a risk of microbial invasion. Experiments measuring the changes in gene expression of resistance genes in *Arabidopsis* across diverse environments, support the idea that changes in the environment can promote an increase of *R* gene expression to defend the plants against pathogens (Macqueen & Bergelson, 2016). In particular, the conditions of high humidity and temperature that artificially were set up for *Pgt* infection, have been shown to be the environmental conditions required for severe fungal outbreaks (Holub et al., 1995). Furthermore, the *Sr35* gene is located in a cluster of resistance gene analogs. Some clusters of resistance genes such as the *Arabidopsis RPP5* show a pattern of complex coordinated regulation through both transcriptional activation and negative feedback mechanisms contributing to the optimization of the defense response (Yi & Richards, 2007). These mechanisms would reduce the fitness cost associated with the expression of *R* gene and defense response pathways when the pathogen is not present, but at the same time, they would contribute to enhancing the capacity and diversity in the response to pathogen attack (Eckardt, 2007). We speculate that such mechanism could be present on in the *Sr35* resistance gene cluster maximizing the response of *Sr35* against *Pgt*.

We observed a similar pattern of expression for isoform-2 as the main *Sr35* isoform in terms of increasing and decreasing expression, but at a much smaller scale, suggesting a coordinated co-expression of both isoforms. The reduction of the expression of isoform-2 could be mediated by nonsense-mediated decay (NMD) pathway, a quality control mechanism that degrades mRNA products detrimental or energy costly for the cell (Shyu et al., 2008). Such detrimental mRNA products are frequently associated with premature termination codon or mRNAs with long 3'-UTRs (>350 bp) and are under strong regulation in *Arabidopsis* (Kalyna et al., 2012). These 3'-UTR intronic sequences are a well-conserved feature in the *Sr35* disease resistance gene cluster (Saintenac et al., 2013) and more research will be needed to confirm a possible functional role of this 3'-UTR intron retention. Studies have shown that AS isoforms could work as accessory proteins involved in pathogen effector detection or signal transduction during the defense response (Nandety et al., 2013), or as suppressors of the negative regulators of immunity activation (Belkhadir et al., 2004). More research should be conducted to confirm if there is a possible functional role of isoform-2 of *Sr35* and if the NMD pathway is responsible for the reduced expression of isoform-2.

2.5.2 *Sr35*-transgene screening and progeny analysis

We detected a single transgenic line (#1123) out of T₀ 84 plants that carried the expressed full-length *Sr35* transgene, suggesting that the remaining three positive T₀ events for PCR screening (#962, #1163, #1007) were false positives or the transgenes were silenced. The expression of the *Sr35*-transgene in the transgenic line #1123 was lower compared with the expression of the gene in the G2919 genotype, but it conferred enough resistance against TTKSK. This is a favourable feature since overexpression of resistance gene can produce pleiotropic effects that reduce the agronomic value of transgenic lines (Brunner et al., 2011).

Although comparing and calculating transformation efficiency in wheat is a difficult task (Janakiraman et al., 2002), comparable results in transformation efficiency obtained for *Sr35* (about 5%) using co-bombarding into embryogenic calli have been reported by Ayella et al., (2007). The progeny analysis of line #1123 confirmed an association between the presence of the *Sr35*-transgen and the resistance against *Ug99* (TTKSK). Given that the *Sr35* gene is required to confer resistance against several members of the *Ug99* race group (Zhang et al., 2010), these results support the hypothesis that *Sr35* is also sufficient to confer full resistance to the disease. The *Sr35* gene constitutes a conventional case where a unique *R* gene confers resistance against several races of pathogens. Only for some cases it was shown that resistance against pathogens requires the cooperation of more than one *R*-gene (Loutre et al., 2009; Cesari et al., 2013). Also, the results of inoculation experiment with *Sr35*-virulent race QTHJC carried out on T₀ and T₁ plants of 1123 progeny confirmed the specificity of *Sr35* response (Saintenac et al., 2013).

Despite the plasticity of the wheat genome, the introgression of resistance genes is still a slow process that faces the problem of linkage drag of deleterious genes as well as the rapid breakdown of the resistance conferred by individuals genes (Wulff & Moscou, 2014). Genetic transformation emerges as an alternative tool to create new resistant varieties, and the methods based on biolistic or *Agrobacterium* mediated transformation have been improving in efficiency (Ishida et al., 2015; Hamada et al., 2017). In the last years, wheat transgenesis has produced plants with improved resistance to pathogens, including thaumatin-like protein gene against wheat scab Chen et al., (1999), trichothecene acetyltransferase against *Fusarium* Okubara et al.,

(2002), *Lr34* against leaf rust Risk et al., (2012), *NPR1* gene against *Fusarium* head blight. Makandar et al., (2006) and *Pm3b* against powdery mildew (Brunner et al., 2011). The cloning of resistance genes and their use to generate transgenic resistant plants reduce the cost and time required for resistant variety production. It allows the expression of alien genes from unrelated species or species whose genes are difficult to introgress (Li et al., 2012; Christelle et al., 2015), and could facilitate the deployment of *R* gene cassettes that can confer durable resistance. The cloning of *Sr35* together with other major dominant *Sr* genes, *Sr33* (Periyannan et al., 2013), *Sr50*, *Sr22*, *Sr45* (Steuernagel et al., 2016) and *Sr13* (Zhang et al., 2017) could be combined into a single transgene locus (genetically modified cassette) ensuring co-segregation and avoiding single gene deployment (Wulff & Moscou, 2014), thereby extending the durability against *Ug99* and avoiding the fast breakdown of resistance (Nagori, 2009; Bajgain et al., 2015). The *Sr35* transgenic lines could be part of an iterative strategy for gene stacking where two or more transgenes can be sequentially introduced into a plant using different strategies. For example, a transgenic line containing one *R* gene can be crossed with individuals harboring other *R* genes or, alternatively, they can be transformed sequentially (Halpin, 2005).

2.6 Conclusions

Wheat production is constantly threatened by the emergence of new pathogen races. The cloning of resistance genes against the *Pgt Ug99* race group opens the possibility to control the disease using different approaches from conventional plant breeding to biotechnologically oriented options, including plant transformation. We concluded that the *Sr35* gene product is specific, necessary and sufficient to confer resistance against *Ug99* (TTKSK). Gene expression studies during the course of infection showed that *Sr35* isoforms are not induced under pathogen attack, but probably are subjected to environmental regulation. More research needs to be done to understand the role of *Sr35* alternative splicing in gene regulation and defense.

Chapter 3 - Identification of the *AvrSr35* gene in *Puccinia graminis* f.sp. *tritici*

3.1 Introduction

Genomic science has revolutionized the plant pathology studies, allowing the full sequencing of plant pathogen genomes and the discovery and characterization of candidate effectors. This is possible by using predictive computational methods combined with gene expression data collected from infected tissues (Yin & Hulbert, 2010; Spanu & Kämper, 2010; Rutter et al., 2017). In the last century, the cereal rusts have been extensively used for genetic and host-pathogen-interaction studies (Staples, 2000), and a *Pgt* reference genome sequence became recently available (Duplessis et al., 2011a,b). Likewise, other genomes of rust species are completely or partially sequenced. These fungal rust genomes include wheat leaf rust *Puccinia triticina*, (Kiran et al., 2016), *Melampsora lini* (Nemri et al., 2014), *Melampsora larici-populina* (Duplessis et al., 2011b), *Cronartium quercuum* f. sp. *fusiforme* (<http://genome.jgi.doe.gov/Croqu1/Croqu1.home.html>) and the Asian soybean rust *Phakopsora pachyrhizi* (Loehrer et al., 2014).

Genome data has revealed the presence of numerous genes encoding putative effectors showing evidence of lineage-specific diversification among fungal genomes. In fact, effectors are one of the fastest-evolving groups of genes in the pathogen genomes. Fungal effectors display a high sequence divergence even within the same species and a lack of conserved signal motifs associated with translocation into the host. The rapid evolution and the lack of homology with known proteins make the use the database searches for effector identification difficult (Duplessis et al., 2011b.; Yin et al., 2015; Win et al., 2012). Effectors are delivered either into the apoplastic space or intercellularly having functions on the cytoplasm or nucleus, or both. In the case of cereal rust, effectors are predicted to be secreted during the infection and recognized in the host cytoplasm. This assumption is based on the fact that most of the R proteins characterized in the rust pathosystems are located in cytoplasm (Yin & Hulbert, 2010; Duplessis et al., 2011b; Chaudhari et al., 2014).

Genetic mapping had been a classical approach for the identification of *Avr* genes (Zambino et al., 2000). Map-based cloning of effectors was successful in the model rust species *Melampsora lini* leading to the cloning of effectors *AvrM14* and *AvrL2* (Anderson et al., 2016). However, due to the heteroecious nature of *Pgt* to obtain the mapping populations the dicot host (barberry) is used to perform fungal crosses. These crosses are difficult to perform under greenhouse conditions (Anikster, 1984; Gates & Loegering, 1991). Besides genetic mapping, association genetics is another tool to identify and validate effectors in field populations of rust species. GWAS based on natural variation in virulence, has the potential to be a powerful complement to *in silico* effector prediction (Plissonneau et al., 2017). This approach has been used to detect candidate effector in *Pst* (Xia et al., 2016) and *Pt* (Wu et al., 2017).

Most of our understanding of the rust effector biology comes from studies in flax rust fungus (*Melampsora lini*) and its flax host (*Linum usitatissimum*). Dodds et al., (2004) cloned the first rust *Avr* gene (*AvrL567*) from flax rust combining subtractive hybridization with a map-based strategy. This first rust *Avr* protein had 127 residues and was expressed in haustorial cells. For this reason, these types of proteins were called *haustorial expressed secreted proteins* (HESPs). The features of *AvrL567* were used to identify and clone three more *Avr* genes in *Melampsora lini*: *AvrM*, *AvrPI23*, and *AvrP4* by using cDNA libraries made from RNA isolated from haustoria (Catanzariti et al., 2006). In addition to flax rust, another rust effector called RPT1p from the bean rust fungus *Uromyces fabae* has been isolated and characterized analyzing HESPs (Kemen et al., 2005; Kemen et al., 2013). All cloned flax rust *Avr* genes encode small secreted proteins (65-347 amino acids). These proteins are expressed in haustoria cells, translocated to host cell, and induced HR after transient expression in flax. Some of the *Avr* proteins contain cysteine-rich sequences and all of them harbor high levels of polymorphism as result of diversifying selection associated with differences in recognition specificity (Catanzariti et al., 2006; Rafiqi et al., 2010; Duplessis et al., 2011b).

To identify protein effectors on cereal rusts, much of the effort has been focused on characterize HEPs in the secretome (the repertoire of proteins predicted by the presence of hydrophobic N-terminal signal peptide, expressed during infection in haustoria) (Saunders et al., 2012). In the case of the causal agent of stripe rust *Puccinia striiformis* f. sp. *tritici* (*Pst*), RNA isolated from

haustoria was used by Yin et al., (2009) to generate cDNAs libraries resulting in the discovery of 15 candidate effector sequences that encode for HESPs. Recently Dagvadorj et al., (2017) found that one of them activates the immunity in a non-adapted host. Using custom microarrays with 442 transcripts previously discovered in the cDNA libraries of *Pst*, Huang et al. (2011) identified several candidate effectors. Garnica et al. (2013) identified more than 400 HESPs of which above 60% were expressed during infection. By integrating genomic and transcriptomic analysis Cantu et al., (2013) re-sequenced four *Pst* isolates with differential virulence profile, identifying five candidate effectors associated with haustoria. More recently, (Liu et al., 2016) identified a candidate effector on *Pst* called PEC6 selected from transcripts expressed in haustoria which seems to suppress PTI by interacting with an adenosine kinase.

For the other economically relevant members of the *Puccinia* order (*Pgt* and *Pt*), the effector discovery has been focused also on the prediction from the full secretome and comparative analysis of the whole genome. Song et al. (2011), used a proteomic approach to analyze haustoria-enriched proteins in *Pt*, identifying six proteins with features of secreted effectors. These proteins were called *small secreted proteins* (SSPs), or *candidate secreted effector protein* (CSEPs). Kiran et al., (2016) using two pathogen isolates of *Pt* predicted 416 and 384 CSEPs for each isolate. CSEPs were selected based on the presence of a signal peptide, 4-8% of cysteine residues and a size range between 20-200 amino acids. One of the most extensive secretome sets, predicted on fungi correspond to *Pgt* (Choi et al., 2010; Duplessis et al., 2011a). Based on entire genome sequence and considering proteins with less than 300 amino acids, Duplessis et al., (2011a,b) predicted that the genome of *P. graminis* f. sp. *tritici* has 1,106 classified SSPs distributed across 164 families. It is estimated that over 200 of them can be potential effectors (Upadhyaya et al., 2014). Transcriptomes of germinated urediospores and haustoria in five *Pgt* Australian isolates were used by Upadhyaya et al., (2015) to identify 25 HESPs that displayed nucleotide polymorphisms, which could explain the virulence over several resistance genes.

Avr genes or effectors play an essential role in plant-pathogen interactions and the establishment of a successful pathogen infection whereby their identification has received much interest. However, only reduced number of rust fungi effectors has been identified, and no effectors had been characterized yet in cereal rusts. In the last years, several strategies have been used for the

identification of fungal effectors in cereal rust. These strategies had included classic approaches such as map-based cloning, screening of cDNA libraries, analysis of candidate effector proteins expressed during infection in haustoria screening of HR-inducing pathogen genes, etc. (Stergiopoulos & de Wit, 2009; Saunders et al., 2012). Unfortunately, the progress in the cloning and functional characterization of effectors on *Puccinales* and other biotrophs have been hindered by technical difficulties associated with the lack of better functional genetics approaches, and the fact that effector set is highly redundant and dispensable (Zambino et al., 2000; Lawrence et al., 2010; Grant et al., 2013; Chaudhari et al., 2014). Promising methods for effector discovery such as effector presence-absence polymorphism (Gilroy et al., 2011), genomic analysis of *de novo* mutations (Upadhyaya et al., 2015), association mapping (Plissonneau et al., 2017), gamma radiation (Poudel et al., 2017), and EMS mutants (Figueroa et al., 2016) are now possible thanks to the extensive use of *next generation sequencing technologies* (NGS).

This chapter presents the application of a forward genetics approach combining EMS-induced mutagenesis with whole-genome sequencing, to identify a the correspondant avirulence gene recognized by the *Sr35* gene (henceforth, *AvrSr35*). The analysis of the *AvrSr35* alleles present in a panel of *Sr35*-virulent and *Sr35*-avirulent isolates explains the effectiveness of the *Sr35* gene against *Ug99* race group, and demonstrate that the insertion of a transposon resulted in the origin of *Sr35*-virulent isolates. Furthermore, detailed microscopic analyses suggest that *AvrSr35* is a pre-haustorially expressed avirulent protein.

3.2 Objectives

- To evaluate the progression of *Pgt* infection in resistant (*Sr35*+) and susceptible (*Sr35*-) wheat genotypes using confocal laser scanning microscopy (CLSM).
- To identify the corresponding *Avr* gene (*AvrSr35*) for the *Sr35* gene using EMS-mutagenesis, forward genetics, whole genome sequencing and bioinformatic approaches.
- To assess the genetic diversity and evolution of *AvrSr35*.

3.3 Materials and methods

3.3.1 Plant bacterial and pathogenic materials

Hexaploid spring wheat cultivar *Morocco* (PI 431591, *Sr35*-), a susceptible check used by CIMMYT for cereal rust (Ali et al., 1994), was utilized for urediniospore increasing and as susceptible genotype in the CLSM experiments. Total RNAs used for RT-PCR and RNA-seq library preparation were obtained from hexaploid wheat Fielder infected with *Pgt*. Diploid wheat *Triticum monococcum* G2919 (= PI428170, *Sr35*+) was used to perform the screening of mutant urediniospores. Hexaploid resistant wheat genotype U6169 (KS05HW14*4//Mq(2) 5* G2919-k/Lakin, +*Sr35*) was used as resistant genotype for microscopy. Hexaploid wheat *Morocco-Lr19* with resistance against leaf rust was used to eliminate any possible contamination with *Puccinia triticina* (*Pt*) during increasing *Pgt* urediniospores. The *Pgt* race RKQQC (American Nomenclature system) isolate 99KS76A-1 (*Sr* virulent/ avirulent/ formula: 5,6,7b,8a,9a,9b,9d,9g,21,36,McN/9e,10,11,17,24,30,31, 35, 38,Tmp) (Rouse, et al., 2011a) was used to generate the EMS (ethyl methanesulfonate) mutant urediniospores, and in the inoculation of susceptible and resistant host genotypes. *Escherichia coli* DH5 α (Life Technologies, Carlsbad, CA) was used for transformation.

3.3.2 *Pgt* inoculation

Pgt inoculation was carried out as was described in the previous chapters. Wheat seedlings were germinated and grown in plastic pots or aluminum pans using Metro-Mix 360 soil (Sun-Gro Horticulture, Vancouver, Canada) in a growth chamber. Seedlings were growth at 22°C, photoperiod of 16 hours, 40-50% relative humidity, and 1000 lux light level until they reached two-leaf stage for inoculation (12 days old). *Pgt* urediniospores activated by immersion in a water bath at 42°C for 6 min, were resuspended in Soltrol[®] 170 isoparaffin solvent (Philips 66, Bartlesville, OK) Urediniospore suspension (1% w/v) was used to inoculate seedlings by air spraying using an atomizer and air compressor (Craftsman). Urediniospores were collected by vacuum 14-16 days post inoculation; fresh urediniospores were used directly for EMS mutagenesis and DNA isolation, or they were dried out in silica gel for three days before to be stored a -80°C.

3.3.3 EMS mutagenesis of *Pgt*

Seedlings for urediniospore multiplication were grown in aluminum pans with Metro-Mix 360 (Sun-Gro Horticulture, Vancouver, Canada) using 3 ounces per gallon of Cycocel cell elongation inhibitor (Olympic Horticultural Products, Mainland, PA). A single fresh pustule (uredinia) of *Pgt* race RKQQC was multiplied using the seedlings of *Morocco-Lr19* to eliminate any possible contamination with *Pt*. RKQQC urediniospores were then increased from a single pustule by re-infection on susceptible wheat cultivar *Morocco*. Inoculation was performed according to the procedure described in section 3.2.2. Urediniospores were collected by vacuum after 14-16 days, sieved from plant debris and weighted on a scale.

EMS mutagenesis of urediniospores was performed based on a modified protocol from Gates & Loegering, (1991). Four sets of 0.24 g urediniospores were suspended in an equal number of glass flask (250 ml) containing 100 ml of ethyl methanesulfonate (EMS) (Sigma, St Louis, MO) solutions (0.1 M, 0.05 M, 0.001 M and 0.005 M) and 0.01% Tween 20 (Sigma, St Louis, MO). EMS-urediniospore suspensions were agitated (80 rpm) for 2 hours in an orbital shaker at room temperature. EMS-urediniospores solutions were then pooled and filtered using a bottle-top vacuum filter system (Corning, Corning, NY). Previously a polycarbonate membrane filter 0.22 µm (Millipore, Billerica, MA) was placed on the bottom of receiver bottle to collect the urediniospores. Mutagenized urediniospores were washed by filtering 1 L of ddH₂O on the bottle-top of vacuum filter system. The polycarbonate membrane filter containing the urediniospores was taken using tweezers and placed in glass petri dish. Urediniosperes were then dried overnight at room temperature. Approximately one thousand seedlings (12 days old) from *Triticum monococcum* G2919 (*Sr35+*) were inoculated with mutant urediniospores under the conditions described above (Section 3.2.2).

The presence of *Sr35*-virulent pustules (hereafter, *Sr35*-virulent mutant strains) was evaluated 15 days after infection. *Sr35*-virulent pustules were confirmed and increased by re-infecting *Triticum monococcum* G2919 seedlings as a follows: independent mutant pustules were sprayed over 12 days-old seedlings growth in square pots (4³/₈ inches) and covered with breathable cellophane bags to avoid cross contamination. Mutant urediniospores were multiplied

independently using *Morroco* genotype seedlings. Confirmation of two *Sr35*-virulent mutant strains was carried out under controlled conditions at the Cereal Disease Laboratory, St. Paul, MN using a series panel of differential hosts (Roelfs & Martens, 1988) and six expanded panels of differential resistance genes, including the *Sr35* gene.

3.3.4 DNA isolation from *Pgt* urediniospores

Pgt DNA was isolated from *Sr35*-virulent mutant strains and the wild-type RKQQC race. Fresh-collected urediniospores (0.5 g) were ground by at least 5 min using a mortar, pestle and liquid nitrogen. Fungal DNA was isolated using the Omni Prep fungi DNA extraction kit (G-BioSciences, St. Louis, MO) with the following modifications: the Molecular Grinding Resine™ was not added to the Genomic Lysis Buffer, 2 ml of the Genomic Lysis Buffer was added to ground urediniospores and the incubation time was extended by 2 hours at 60°C with occasional inversion. Before the first hour of incubation ten µl of RNase A 100 mg/ml (Quiagen, Hilden, Germany) was added, followed by ten µl Proteinase K solution (Omni Prep for fungi DNA extraction) before the second hour of incubation. The concentration of the DNAs was checked using a Qubit 2.0 fluorometer (Life Technologies, Carlsbad, CA), the integrity of the DNA was determined by agarose gel electrophoresis 0.8 % and by the Agilent 2200 TapeStation (Agilent, Palo Alto, CA).

3.3.5 RNA isolation

Total RNA was isolated according to Rutter et al. (2017). Seedlings (12 days old) from hexaploid wheat cultivar Fielder were inoculated with urediniospores of *Pgt* race RKQQC as described in section 3.2.2. Leaf tissues (three biological repeats of the main leaf) were collected at 0, 24, 48, and 96 hours after the light treatment (hours after infection) in 1.5 ml microcentrifuge tubes containing two 4.5 mm steel beads. Tubes were frozen immediately in liquid nitrogen and placed in a -80°C freezer. For total RNA isolation, leaf tissues were frozen in liquid nitrogen and ground three times using a TissueLyser II (Quiagen, Hilden, Germany) at 25 Hz, for 30 sec. Ground tissues were used for RNA extraction using Trizol reagent (Invitrogen, Carlsbad, CA, USA) following manufacturer's instructions. RNA pellets were resuspended in 50

µl of RNase-free water. RNAs were quantified using Nanodrop-1000 (Agilent; Palo Alto, CA, USA) and RNAs integrity was evaluated using the 2100 Bioanalyzer (Agilent, Palo Alto, CA).

3.3.6 NGS libraries preparation and sequencing

To identify a candidate gene for *AvrSr35*, the genome of the RKQQC race was sequenced using three NGS sequencing platforms: MiSeq (Illumina), 454 (Roche) and SMRT (PacBio). DNA libraries preparation involving Illumina Miseq and Roche 454 technologies were carried out at the Kansas State University Integrated Genomics Facility (IGF). Libraries involving Illumina Hiseq were prepared at the University of Kansas Medical Center Genome Sequencing Facility. The PacBio libraries were prepared at the UC Davis Genome Center. Re-sequencing of the genomes of all *Sr35*-virulent EMS mutants was carried out using only Illumina platform (MiSeq and HiSeq2500).

Illumina libraries were prepared from one µg of genomic DNA, which was fragmented with the Covaris S220 Focused – Ultrasonicator (Covaris, Woburn, MA) using the manufacturers recommended settings to obtain DNA fragment of ~500 bp. The NEBNext DNA Library Prep Master Mix Set for Illumina (New England Biolabs, Ipswich, MA) and Illumina TruSeq adapters (Illumina Inc, San Diego, CA) were used for DNA sequencing library preparation following the New England Biolabs protocol. DNA library was subjected to 500-900 bp size selection using the Pippin Prep system (Sage Science, Beverly, MA). The size-selected DNA library was analyzed using the 2100 Bioanalyzer (Agilent Technologies, Palo Alto, CA) and quantified with Qubit 2.0 fluorometer (Life Technologies, Carlsbad, CA). Two sequencing runs were performed on the MiSeq personal sequencing system (Illumina Inc, San Diego, CA) using 600 cycles (2X 300 bp run) of the MiSeq reagent v3 kit (Illumina Inc, San Diego, CA) according to manufacturer's instructions. For Hiseq2500 the pair end libraries were 100 bp long (2 x 100 bp run). For the 454 life Science Roche DNA Library was prepared from 500 ng of genomic DNA with the GS FLX Titanium Rapid Library Preparation kit (Roche Diagnostics). The sample was sequenced with one 454 life Science Roche run using the Titanium chemistry following standard Roche protocols. Finally, fungal genomic DNA was used to produce 3-10 kb libraries size and was sequenced on one SMRT cell of PacBio RS II using P6C4 PacBio chemistry.

RNA isolated from the RKQQC-infected leaf tissue of Fielder genotype (Section 3.3.5) was used for the production a *de novo* RNA-Seq data assembly, which helps in the gene prediction and assembly annotation of RKQQC genome. One μg of total RNA was used for RNA sequencing (RNA-Seq) library construction using the TruSeq RNA Sample Preparation Kit v2 (Illumina). All RNA-seq libraries were prepared with the Biomek FXP Laboratory Automation Workstation (Beckman Coulter, Brea, CA). The RNA-seq libraries obtained were analyzed with a 2100 Bioanalyzer (Agilent Technologies, Palo Alto, CA) and quantified with a Qubit 2.0 fluorometer (Life Technologies, Carlsbad, CA). Indexed RNA-seq libraries were normalized to 10 nM and then pooled in equal volumes, six libraries per pool. Each pool was sequenced with one lane of HiSeq 2500 (2x100 bp) at the University of Kansas Medical Center Genome Sequencing Facility.

3.3.7 Bioinformatic analysis

3.3.7.1 Assembly of the RKQQC reference genome

Bioinformatic analysis was performed by Dr. Eduard Akhunov and Dr. Shichen Wang. Illumina sequence data were processed using FASTX-Toolkit (http://hannonlab.cshl.edu/fastx_toolkit/) to remove adaptors, low-quality bases (*Qphred* <20) (score 20 corresponds to a 99% probability of a correctly identified base) and low-quality reads (less than 70% of bases having quality ≥ 20). The Roche 454 data were adaptor and quality-trimmed using the program *Lucy* with the default settings (sourceforge.net/projects/lucy). Illumina paired-end reads were assembled using DISCOVAR *de novo* assembler with the default parameters (Weisenfeld et al., 2014). To extend the contig size, the data generated for the 454 and PacBio platforms were added using the program SSPACE (Boetzer & Pirovano, 2014), with “Minimum alignment length” = 100 and “Minimum identity of the alignment = 70”. Contigs longer than 1000 bp were retained. Plant contaminating sequence assemblies were excluded by performing BLASTN search in the NCBI’s non-redundant sequence database, and the contigs with the best hits to fungal sequences (e-value less than $1e^{-10}$ and alignment length more than or equal to 100 bp) were retained. The genome assembly and annotation are available at (<http://129.130.90.211/rustgenomics/Download>).

3.3.7.2 Annotation of RKQQC genome assembly

Quality-filtered reads generated by 2 x 100 bp paired-end sequencing on HiSeq2500 were assembled with the program Trinity (Grabherr et al., 2011) using the following parameters: “--genome_guided_max_intron 50000 --SS_lib_type FR -jaccard_clip”. Gene models were predicted by mapping the assemble transcripts to the *Pgt* RKQQC reference genome assembly using the PASA pipeline (Haas et al., 2011). The coding regions of genes were predicted using the TransDecoder tool of the PASA pipeline. The BUSCO program (Simao et al., 2015) was utilized to estimate the completeness of genome assembly. BUSCO uses a set of 1,441 phylogenetically conserved genes to assess the proportions of completely and partially sequenced genes in a genome or transcriptome.

3.3.7.3 Mutation discovery on RKQQC EMS mutants and identification of candidates for the *AvrSr35* gene

The Burrows-Wheeler Alignment tool (BWA-MEM) (Li & Durbin, 2009) was used to align reads generated from the 15 *Pgt* EMS mutant strains and the wild-type RKQQC to the reference genome assembly of the RKQQC race, using the default settings of the aligner. Before variant calling, the reads in BAM files were locally re-aligned using the GATK (McKenna et al., 2010) followed by marking and removal of duplicated reads using the Picard program (<https://broadinstitute.github.io/picard/>). The variant calling was performed using the GATK’s Unified Genotyper (McKenna et al., 2010) with the default settings. The raw variant calls were filtered to remove sites that had more than two allelic states or were monomorphic among the 15 mutant strains. Only the mutations CG > TA were selected because the transitions C-to-T and G-to-A are more frequently found under EMS treatment (Henry et al., 2014). Additional filtering was applied to read coverage data obtained for both wild-type and mutated allelic variants. Only the alleles with coverage of at least two reads were called, and alleles with a minimum coverage of 5 reads were used to call mutant alleles. To reduce the erroneous mutant calling due to the misalignment of duplicated paralogs or possible cross-contamination among the mutant *Pgt* strains during their increase in greenhouse or isolation, the mutant sites that were detected in more than three different EMS *Pgt* mutant strains were excluded. In addition, the Fisher’s exact test was applied to compare the depth of read coverage of mutant and wild-type alleles at each

site in the wild-type and mutant strains. The sites showing the statistically significant difference at $P\text{-value} \leq 10^{-4}$ were retained. Since the EMS produce random single point mutations, candidate *Avr* genes were expected to have knock-out mutations at different positions of the coding sequence in each independent mutant, the candidate genes with the maximum number of “gain of stop codons” mutations were considered.

3.3.8 PCR-based cloning of the *AvrSr35*

Once total RNAs quantity and quality were assessed, 1 μg of pooled total RNA (24, 48 and 96 hours after infection) isolated from seedlings of Fielder cultivar inoculated with *Pgt* race RKQQC (Section 3.3.5), was treated with 1 μl of DNase I amplification grade (1 U/ μl) (Invitrogen Inc, Carlsbad, CA) in a final volume of 10 μl according to manufacturer’s instructions. cDNA was obtained using ~ 0.8 μg of DNase treated RNA, which were reverse transcribed with 1 mM of Oligo (dT)₂₀, 0.5 mM dNTP mix and 1 μL Superscript III reverse transcriptase (200 U/ μl) (Invitrogen, Carlsbad, CA) in a final volume of 20 μL following the manufacturer’s instructions. RT-PCR for *AvrSr35* cloning was performed using 0.2 μM of primer s2351_1374F and primer s2351_3920R, 1X Q5 PCR buffer (New England Biolabs, Ipswich, MA) containing 2.5 mM MgCl_2 , 0.2 mM dNTP’s, 0.2 μl Q5[®] high fidelity DNA polymerase (5 U/ μl) (New England Biolabs, Ipswich, MA) and 2 μl of cDNA. PCR was denatured at 94°C for 5 min followed by 10 cycles at 94°C for 15 sec, 58°C for 30 sec and 72°C for 2 min and followed by 35 cycles of 94°C for 15 sec, 54°C for 30 sec and 72°C for 2 min and a final extension of 72°C for 7 min. Additional primers were used (Table 3.1) to confirm the expression of *AvrSr35* transcript using the same conditions. All PCR products were run on 1.8 % agarose gels (w/v) prepared in 1X TAE (40 mM Tris pH 7.6, 20 mM Acetic Acid, and 1 mM EDTA pH 8.0) buffer and stained with SYBR[®] Safe (Thermo Fisher Scientific, Waltham, MA). Electrophoresis was carried out at 4-8 V/cm and nucleic acid bands were visualized and documented under UV light (GeneFlash gel documentation system, Syngene, Frederick, USA). PCR product was cloned into. pGEMT-easy cloning kit (Promega, Madison, WI) according to the manufacturer’s instructions, to create the plasmid pGEMT-cDNA-*AvrSr35* which was used as DNA template for subsequent plasmid vector constructions (Chapter 4).

3.3.9 Confirmation by Sanger sequencing of predicted mutations on *Sr35*- virulent *Pgt* EMS-mutant strains

DNAs from 15 *Sr35*-virulent EMS mutant strains were used to amplify by PCR the *AvrSr35* gene and confirm the mutations predicted using NGS platforms and bioinformatic analysis. PCRs were carried out using 50 ng of mutant *Pgt* DNA, 10 µl Phusion® High-Fidelity PCR Master Mix (New England Biolabs, Ipswich, MA) and the primer combination s2351_1374F and s2351_3920R. PCR reactions were denatured at 98°C for 5 min followed by 10 cycles at 98°C for 15 sec, 64°C for 30 sec and 72°C for 2 min and followed by 35 cycles of 98°C for 15 sec, 60°C for 30 sec and 72°C for 2 min and a final extension of 72°C for 7 min.

Table 3.1. Primers used for the cloning and the diversity analysis of the *AvrSr35* candidate.

Name	Sequence	Use
s2351_1433F	ATGTCACATCACTTTGGATTACGTAA	Cloning /expression of <i>AvrSr35</i> from cDNA
s2351_3766R	TCACAATTTGCCTTCATGAACAT	Cloning /expression of <i>AvrSr35</i> from cDNA
s2351_2055R	TTTTGTTGTATGTGACCGGTCTTG	Cloning /expression of <i>AvrSr35</i> from cDNA
s2351_2027F	AAGATCCTAAAAGAGATTGAAGAACAAG	Cloning /expression of <i>AvrSr35</i> from cDNA
s2351_1374F	ACTAAAGATATTTATTTTCATTCCAACCT	Amplification of <i>AvrSr35</i> over <i>Pgt</i> DNA
s2351_3920R	TGGATTGAATATAATGGAATTTTGC	Amplification of <i>AvrSr35</i> over <i>Pgt</i> DNA

PCR products were sequenced by Sanger method (Rosenblum et al., 1997) using *BigDye* Terminator Cycle Sequencing Ready Reaction Kit (Applied Biosystems, Foster City, CA). PCR products were ExoSAP treated: 5 µl of the PCR products were mixed with 1 µl exonuclease (New England Biolabs, Ipswich, MA) and 2 µl shrimp alkaline phosphatase (New England Biolabs, Ipswich, MA) the mixture was incubated for 15 min at 37°C followed by heat inactivation at 80°C 15 min, then 30 µl of ddH₂O was added to dilute the ExoSAP-PCR product. Sequencing reactions were set up with 5X Sequencing Buffer (Applied Biosystems, Foster City, CA), 2 µl of 1.6 µmol of sequencing primer, 3 µl of ExoSAP-PCR product, 0.5 µl of The BigDye® Terminator v3.1 reaction mix (Applied Biosystems, Foster City, CA), and 0.5 µl of 50% DMSO, samples were set up until 10 µl with ddH₂O. Samples were denatured at 96°C for 5 min followed by 40 cycles at 96°C for 10 sec, 50°C for 30 sec and 72°C for 2 min. Sequencing reactions were cleaned up using sodium acetate/ethanol precipitation. Precipitates were resuspended in 20 µl Hi-Di™ Formamide (Applied Biosystems, Foster City, CA), and sequenced

in a capillary ABI 3110xl Genetic Analyzer (Applied Biosystems, Foster City, CA). Sequences were analyzed using Sequencher v 3.1 DNA sequence analysis software, (Gene Codes Corporation, Ann Arbor, MI).

3.3.10 Diversity analysis of *AvrSr35*

A genetic diversity study was conducted to determine the association between the presence of the *AvrSr35* allele with the avirulence against *Sr35*. This study involved the re-sequencing and analysis of the *AvrSr35* allele on *Pgt* field isolates virulent and avirulent for the *Sr35* gene. DNAs from 27 *Pgt* isolates were obtained from Cereal Disease Lab (Saint Paul, Minnesota) including well know *Pgt*-races and four members of *Ug99* group (Table 3.2). Conditions for PCR and sequencing were described above (Section 3.3.9). Allelic sequences were aligned using program MUSCLE with the default settings (Edgar, 2004). The composite likelihood substitution model implemented in program MEGA 6.06 (Tamura et al., 2013) was used to infer a phylogenetic tree. *AvrSr35* phylogenetic tree testing was performed utilizing the bootstrap method with 1,000 replicates and the visualization and annotation was made using the web-based tool Interactive Tree Of Life (<http://itol.embl.de>)(Letunic & Bork, 2016). The sequence of a highly divergent second non-functional allele of the *AvrSr35* gene identified in the RKQQC isolate 99KS76A-1 was used to root the tree.

3.3.11 Confocal laser scanning microscopy (CLSM)

In this study, modified protocols from Rohringer (1977), Figueroa et al., (2013) (Panwar et al., 2013b) and Ayliffe et al. (2011) were used to visualize the development of fungal infection structures and the presence of death cells on the host after *Pgt* infection. The major differences in the previous protocols involved the procedure to reduce their excess of fluorochromes after staining.

Observations were carried out in seedlings (12 days old) of the susceptible genotype *Morocco* (*Sr35*-) and the resistant genotype U6169 (*Sr35*+) inoculated with the *Sr35*-avirulent *Pgt* race RKQQC (Section 3.3.2). Likewise, the development of fungal infection structures was monitored in the susceptible genotype *Morocco* (*Sr35*-) infected with selected *Sr35*-virulent mutant strains.

Infected leaves were collected at 24, 48 and 72 hours after infection, then the two infected leaves per each time point were fixed and cleared with 95% ethanol by incubating at room temperature for five days in a 15 ml tube. The following washing and staining steps were performed using a rocket platform shaker. Fixed and cleared leaf samples were washed twice for 15 min each with 50% ethanol followed by incubation with NaOH 0.5 M 15 min. Specimens were then washed three times with ddH₂O and incubated in 50 mM Tris-HCl buffer, pH 5.8 for 30 min.

Table 3.2. *Pgt* isolates used for *AvrSr35* allele diversity analysis.

<i>Pgt</i> isolate	Location	Year	Race ^a	Virulence on <i>Sr35</i> gene ^b	Infection type ¹
75WA165-2A	Washington, USA	1975	QCCSM	Virulent	3,3 ⁺
59KS19	Kansas, USA	1959	MCCFC	Virulent	2,2 ⁺
76WA1358C	Washington, USA	1976	SMLLM	Virulent	3
09CA115-2	California, USA	2009	BCCBC	Virulent	3,2 ⁺
75WA1652	Washington, USA	1975	QCCSM	Virulent	3
01SD80A	South Dakota, USA	2001	QCCJB	Virulent	3
09ID073-2	Idaho, USA	2009	SCCSC	Virulent	3,2 ⁺
76WA1397B	Washington, USA	1976	QFBDC	Virulent	3
74WA1331B	Washington, USA	1974	BFBJC	Virulent	3
69MN399	Minnesota, USA	1969	QTHJC	Virulent	3,2 ⁺
06ND76C	North Dakota, USA	2006	QFCSC	Virulent	2 ⁺
76WA1204C	Washington, USA	1976	SBCSC	Virulent	3
74MN1049	Minnesota, USA	1974	TPMKC	Avirulent	0
04KEN156/04	Kenya	2004	TTKSK*	Avirulent	0,;
84KEN654B	Kenya	1984	R_TTF	Avirulent	0,;
01MN84A-1-2	Minnesota, USA	1984	TTTTF	Avirulent	
99KS76A_1	Kansas, USA	1999	RKQQC	Avirulent	0
77ND82A	North Dakota, USA	1977	RCRSC	Avirulent	0,;
72CA1A	California, USA	1972	TPLK	Avirulent	0
75_36_700_3	Minnesota, USA	1975	SCMLC	Avirulent	2
69SD657C	South Dakota, USA	1969	RHTS	Avirulent	0
61PA80A	Pennsylvania, USA	1961	RKLQ	Avirulent	0,;
06KEN19-V-3	Kenya	2006	TTKST*	Avirulent	0,;
Uv59.4	South Africa	2007	TTKSP*	Avirulent	0,;
07KEN24-4	Kenya	2007	TTTSK*	Avirulent	0,;
Uv55.24	South Africa	2009	TTKSF*	Avirulent	0,;
00MN99c	Minnesota, USA	2000	RCRSC	Avirulent	0,;

a) Race based on North American nomenclature (Jin et al., 2008). **b)** isolates were tested for virulence on the wheat line 4071 carrying the *Sr35* gene. Isolates were considered virulent if they showed scores from 2 to 4; isolates were classified as avirulent if they had scores 0 or 0; (Stakman 1962). *Races of the *Ug99* group.

Samples were stained for 5 min using 2 ml 0.1% Uvitex 2B (Polysciences Inc, Warrington, PA) in a 15 ml tube followed by washing three times with ddH₂O. Samples were treated with 0.1% (w/v) Acridine Orange (Sigma, St Louis, MO) for 5 min to stain the plant cell walls. Dyes excess was removed by adding 5 ml of 25% (v/v) glycerol followed by overnight incubation. Leaf samples were gently placed on a microscope slide using fine tweezers and some drops of 25% (v/v) glycerol was added. Ten fungal units were evaluated at each time point.

Fluorescence microscopy was carried out using an LSM 780 Confocal Laser Scanning Microscope (Zeiss, Oberkochen, Germany) at 40X magnification. Uvitex 2B and Acridine Orange were detected by excitation at 405 nm and scanning with filters at 411-485 and 550-560 nm respectively. Data image processing was carried out using Zeiss ZEN v8.1 (Zeiss, Oberkochen, Germany).

Cellular death on the wheat host during *Pgt* infection on *Morocco* (*Sr35*-) and the genotype U6169 (*Sr35*+) was evaluated modifying the protocol described by Ayliffe et al. (2011). The two first infected leaves of a seedling per each time point were fixed and cleared with 95% ethanol by incubating at room temperature for five days in a 15 ml tube. The following washing and staining steps were performed using a rocket platform shaker. Fixed and cleared samples were washed twice for 15 min each with 50% ethanol followed by incubation with NaOH 0.5 M 15 min. Specimens were washed three times with ddH₂O and place in 50 mM Tris-HCl buffer, pH 7.5 for 30 min. Fungal structures were stained by adding 1 ml of 50 mM Tris HCl buffer, pH 7.5 containing 20 µg/ml WGA-FITC (Sigma, St Louis, MO) and incubated for 15 min, then samples were washed three times with 50 mM Tris-HCl buffer, pH 7.5. Collapse cells nuclei were stained using propidium iodide 10 µg/ml (Life Technologies, Carlsbad, CA), followed by washing three times with ddH₂O. Leaf samples were gently placed on a microscope slide using fine tweezers and some drops of 25% (v/v) glycerol was added. Ten fungal units were evaluated at each time point. Fluorescence microscopy was carried out using an LSM 780 Confocal Laser Scanning Microscope (Zeiss, Oberkochen, Germany) at 40X magnification. WGA-FITC and propidium iodine were detected by excitation at 488 and 561nm and scanning with filters at 493-584 and 584-718 nm respectively. Data image processing was carried out using Zeiss ZEN v8.1 (Zeiss, Oberkochen, Germany).

3.4 Results

3.4.1 Histological characterization of early time course infection of *Pgt* on susceptible and resistant *Sr35* genotypes

The progression of *Pgt* infection to establish a compatible interaction with the wheat host was analyzed to understand the nature of the *Sr35*-resistance mechanism. *Pgt* development was evaluated using Confocal Laser Scanning Microscopy (CLSM) in combination with fluorochromes comparing the infection of the *Sr35*-avirulent race RKQQC in wheat genotypes lacking or carrying the *Sr35* gene. A series of developmental processes that occur in the first 36 hours after inoculation are required for the *Pgt* infection from the urediniospore germination until the formation of the haustoria and infection hyphae (Zhang et al., 2008). Histological examination using fluorochromes and microscopy is one of the most informative techniques to study in detail the development in biotroph fungi such as cereal rusts. Fluorochromes such as Uvitex 2B and its former less stable variant calcofluor, which binds specifically to chitin the main component of fungal mycelium, have been used for several years to investigate differentiation, fungal structure, morphology, infection development and other cellular processes (Koch & Pimslar, 1987).

The fluorochrome Uvitex 2B in combination with Orange Acridine was used to visualize both fungal infection structures (sub-stomatal vesicles, haustoria mother cells, infection hypha and haustoria) and the host cells. The combination of WGA-FITC and Propidium Iodide staining helped to identify the presence of cell death accompanying the hypersensitive response. At 24 hours after infection, there was an evident development of infection structures including appressorium, substomatal vesicle, infection hyphae and haustorial mother cell (characterized by a brighter blue fluorescence tip) in both the susceptible and resistant genotypes. However, clear haustoria were identified only inside mesophyll cells of the susceptible cultivar *Morocco* (*Sr35*-) (Figure 3.1A). At later time points, there was an increase in the number of haustorial mother cells, and the development of intercellular infection hyphae toward the establishment of fungal colonies on the susceptible *Morocco* genotype (Figure 3.1B and 3.1C). By contrast, the fungal growth was impaired 24 hours after infection on resistant genotypes U6169 (*Sr35*+), which never develop any haustorium during the first 72 hours (Figure 3.1D, E and F).

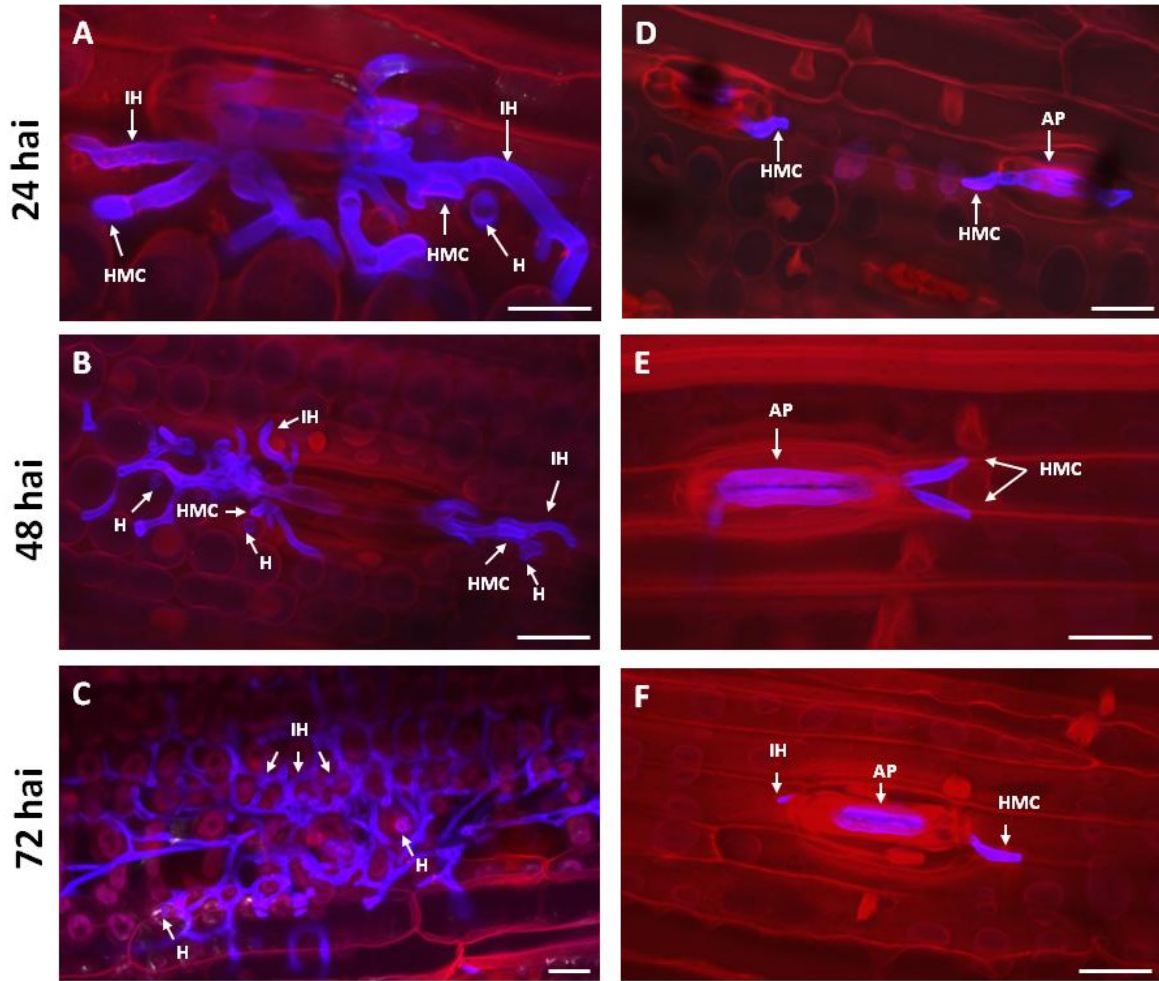


Figure 3.1. Confocal microscopy at the early stages of *Pgt* infection to detect fungal infection structures. Urediniospores of the *Sr35*-avirulent race RKQQC was used to infect seedlings of susceptible cultivar (*Sr35*-) *Morroco* and the resistant genotypes (*Sr35*+) U6169. Left side: 24 hai, 48 hai, and 72 hai rows refer to 24, 48 and 72 hours after infection. **A**, **B** and **C** *Morroco* infected with RKQQC. **D**, **E** and **F** U6169 infected with RKQQC. Infected leaves were stained with Uvitex 2B (fungal structures in blue) and orange acridine (host cells in red). Relevant fungal structures: **IH** = infection hyphae, **HMC** = Haustorial mother cell, **H** = haustorium.

To investigate the presence of cell death as mechanism of resistance, we stained infected leaves of wheat genotypes lacking or carrying the *Sr35* gene with the fluorochromes WGA-FITC (specific for chitin) and Propidium Iodide (specific to detect death cells) to avoid the overlapping on wavelength detection (Sasaki, 1987).

The results obtained using the WGA-FITC and Propidium Iodide staining were consistent with the observations made with Uvitex 2B and Orange Acridine. Also, WGA-FITC staining helped

to identify collapsed cells (death cells) on the host mesophyll tissue 48 hours after infection only on the resistant genotype U6169 (*Sr35+*) (Figure 3.2B and 3.2D) compared with susceptible cultivar *Morroco* (Figure 3.2A and 3.2C). Death cells were characterized by the nuclear staining product of Propidium Iodide (Sasaki et al., 1987), and the accumulation of an intense fluorescence signal and irregular shape (Ayliffe et al., 2011). Propidium iodide binds to DNA after the pass through plasma membrane of dead cells and can be used to differentiate them from live cells with intact membranes (Crowley et al., 2016). Collapsed cells on the wheat host were frequently found in close proximity with haustorial mother cells and were spread to adjacent mesophyll cells (Figure 3.2B and 3.2D).

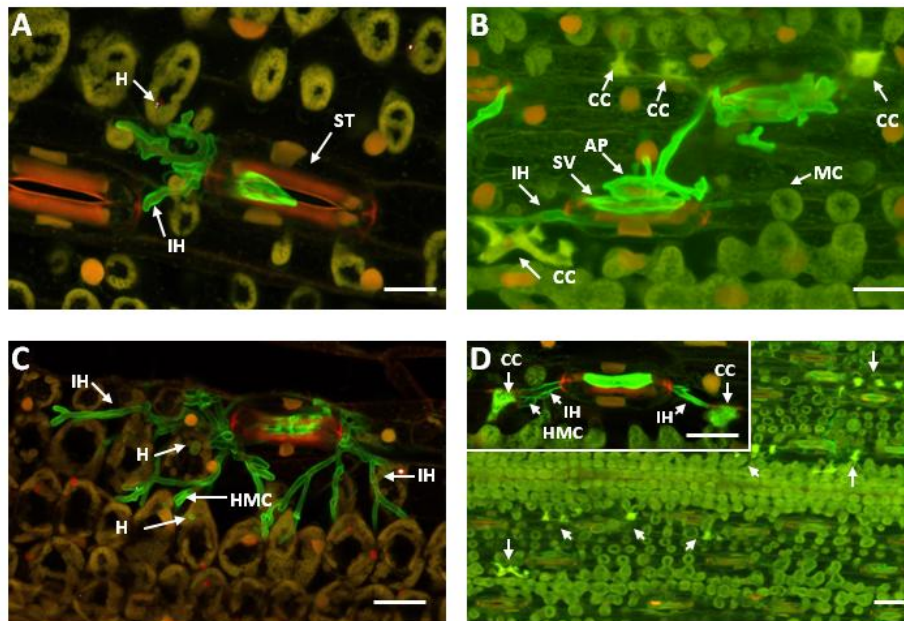


Figure 3.2. Confocal microscopy at early stages of *Pgt* infection to detect cell death on the wheat host. Urediniospores of the *Sr35*-avirulent race RKQQC was used to infect seedlings of susceptible (*Sr35*-) cultivar *Morroco* and the resistant genotypes (*Sr35+*). U6169. **A.** *Morroco* 24 hours after infection **B.** U6169 48 hours after infection **C.** *Morroco* 48 hours after infection **D.** U6169 48 hours after infection at lower magnification. Infected leaves were stained with WGA-FITC and Propidium Iodide. Relevant fungal and host structures: **IH** = infection hypha, **HMC** haustorial mother cell, **H** = haustorium, **AP** = appressorium, **CC** = collapsed cell, **ST** = stomata **MC** = mesophyll cell. Arrows in **D** (lower magnification) point to fluorescent collapsed cells.

3.4.2 Chemical mutagenesis of *Pgt* race RKQQC

In this study, the alkylating agent EMS was used to induce random point mutations in the genome of the *Sr35*-avirulent *Pgt* race RKQQC. Mutant urediniospores were screened to identify mutant variants with virulence for *Sr35*. The screening of EMS mutant urediniospores on the *Triticum monococcum* G2919 (*Sr35*+), identified 15 mutant strains that acquire virulence against the *Sr35* gene (Figure 3.3). Two additional rounds of infections of the *Pgt* mutant strains using the G2919 genotype confirmed the virulence against the *Sr35*.

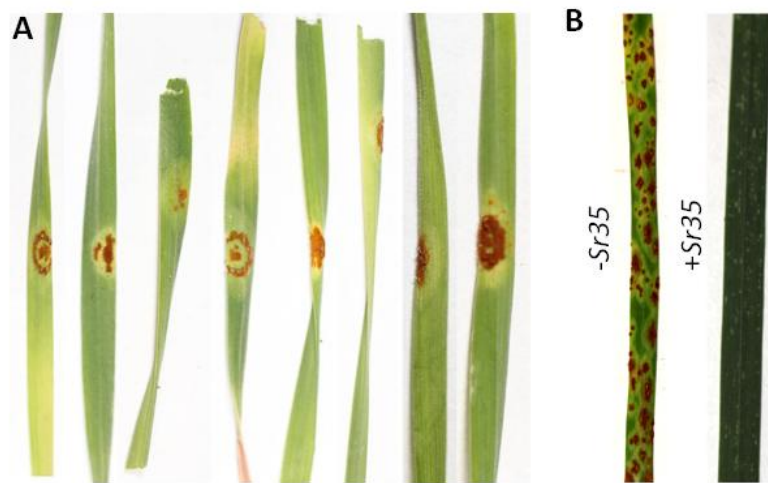


Figure 3.3. Phenotypic response at seedling stage of wheat infected with *Pgt*. **A.** Seedling stage response of diploid wheat accession G2919 (*Sr35*+) to infection with eight EMS mutant strains of the *Pgt*-race RKQQC. **B.** Seedling stage response of the resistant (*Sr35*+) and susceptible (*Sr35*-) wheat lines Marquis *Sr35* and Marquis, respectively, to infection with the wild-type *Pgt*-race RKQQC. The plant evaluation and imaging were performed 14 days after infection.

In order to determine if the mutant strains with virulence for the *Sr35* gene were the product of mutations in one or more avirulent genes and to exclude the possibility of cross *Pgt* race contamination, the virulence profile of two mutant strains was evaluated. The mutant strains identified as M1 and M7 were evaluated for their virulence profile by using wheat host differentials at USDA Cereal Disease Laboratory (Saint Paul, Minnesota). Virulence profile at seedling stage of the mutant strain M1 and M7 was similar to the virulence profile of wild-type RKQQC, except for a specific virulence against the *Sr35* gene (Appendix C, Table S2, Salcedo et al., 2017). This result proved that those mutant strains were true mutants with virulence to *Sr35* and not contamination with other races with virulence to *Sr35*. Also, these results suggest

that the avirulence for the *Sr35* gene in RKQQC race is based in the recognition of a single *Avr* gene.

Since the *Avr* genes encode for a protein with presumed virulence function (van der Hoorn & Kamoun, 2008; Hogenhout et al., 2009), the virulence capacity of the *Sr35*-virulent mutant strains M1, M4, and M7 compare the wild-type RKQQC race was evaluated. This evaluation was carried out analyzing the progression of infection during the first 72 hours using CLSM (Figure 3.4). These microscopic analyses did not show a substantial difference in the development of fungal infection structures in the mutant strains compared to the wild-type RKQQC, indicating that in the mutant strains the *Avr* gene knocked-out and recognized by *Sr35* is not involved in virulence or the RKQQC effector set redundancy is filling this virulence function (Rutter et al., 2017).

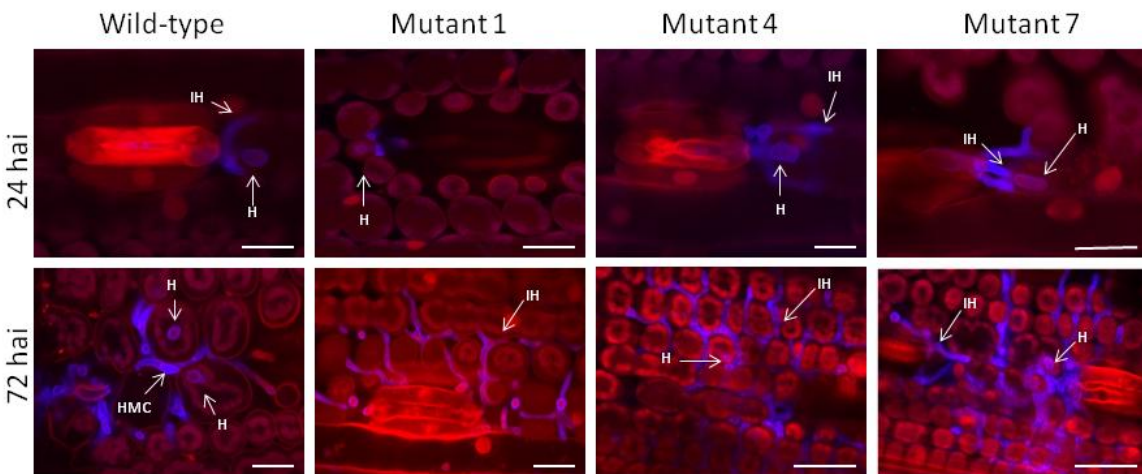


Figure 3.4. Laser-scanning confocal microscopy of *Pgt Sr35*-virulent mutant strains growth in leaves of susceptible wheat cultivar *Morocco (Sr35-)*. 24hai: 24 hours after infection and 72hai 72 hours after infection, wild-type: *Pgt* race RKQQC. Relevant fungal structures : **IH**= infection hypha, **HMC**= haustoria mother cell, **H**= haustorium. Plant tissues were stained with Uvitex 2B (fungal structures in blue) and orange acridine (host cells in red). Bars represent 50μm.

3.4.3 Bioinformatic analysis for the identification of the *AvrSr35* candidate

3.4.3.1 Assembling of RKQQC race genome

The advances in the new generation sequencing (NGS) had allowed the sequencing the entire genomes at relatively low cost (Metzker, 2010). These technologies have made possible the

assembly of high-quality reference genomes and the possibility of obtaining pan-genomes that involve multiple pathogen isolates with diverse virulent spectrum. These data allows comparative analysis of the genomic diversity to identify effector repertoire and investigate effector evolution (Gibriel et al., 2016; Figueroa et al., 2016). The identification of a candidate for *AvrSr35* gene requires the development of genomic resources, including an adequate reference genome for comparative bioinformatic analysis of the *Sr35*-virulent mutant strains. To accomplish this requisite, the genome of the wild-type RKQQC race (isolate 99KS76A-1) was sequenced and annotated using data produced by short and long reads of three NGS platform technologies (Salcedo et al., 2017) (NCBI database PRJNA313186 and <http://wheatgenomics.plantpath.ksu.edu/rustgenomics>). A summary of the statistics of the genome assembly is showed in the table 3.3. The RKQQC reference genome annotation was made using the RKQQC-infected leaf transcriptome assembly obtained from RNAseq experiments (295,186 contigs) and by combining gene models reported for the genome of *Pgt* strain 75-36-700-3 (Duplessis et al., 2011a), and gene models of five Australian *Pgt* isolates (Upadhyaya et al., 2015).

Table 3.3. Summary of the assembling metrics and completeness of the genome of *Pgt* wild-type RKQQC isolate 99KS76A-1.

RKQQC genome assembly metrics	
Number of scaffolds and contigs	168,313
N50	6,884 bp
N20	19,161 bp
Number of predicted genes	27328
Completeness of the transcriptomic assembly and annotation (Based on BUSCO, Simao et al., 2015)	
Complete genes	1153 (80%)
Partial genes	140 (10%)
Missing genes	145 (10%)

The completeness of both genome and transcriptome assembly for RKQQC was estimated to evaluate if they are representative of a fungal genome. Assembly completeness of RKQQC reference genome was quantified using the conserved gene set of Benchmarking Universal Single-Copy Orthologs (BUSCO) database, which is composed of 1438 fungal gene models (Simao et al., 2015) (Table 3.3). Combining both genomic and transcriptomic data, BUSCO

identified 93% of conserved genes in the assembly. The percentage completeness obtained for RKQQC genome reference were comparable with the prediction of genome assembly completeness using BUSCO for the 75–36-700–3 race (93%), the first assembly for a *Pgt* genome reported (Duplessis et al., 2011a; Simao et al., 2015).

3.4.3.2 Mutation discovery on *Pgt* mutants and identification of candidate gene for *AvrSr35*

Functional mutations in annotated coding sequences associated with a potential *Avr* gene were identified in every *Sr35*-virulent mutant strain. Genome-wide random mutations product of EMS treatment were detected using the GATK pipeline (McKenna et al., 2010). In average, 88.5 million quality-filtered paired-end reads per *Pgt* EMS-mutant were obtained, and nearly 80% of reads from each of the 15 *Pgt* EMS-mutants were mapped to the reference genome of the wild-type RKQQC (Salcedo et al., 2017). The detected variants were filtered to retain only CG>TA transitions, the most common types of mutations expected after EMS treatment (Henry et al., 2014), resulting in the discovery of 30,429 mutant sites. Bioinformatic analysis identified 158 gene models with nonsense mutations present in at least one of the *Sr35*-virulent mutant strain. The top candidate gene model located in the scaffold 2351 (NCBI accession number MF474174) (Appendix B) between positions 1,332 and 3,936 had “gain of stop codon” mutations in 12 mutant strain. The following candidate on the list, present in the scaffold 2217 had a “gain of stop codon” mutation in only three out of 15 *Pgt* -mutants. Strong effect mutations that resulted in intronic splice site disruption and non-synonymous codon change were also predicted in the candidate gene located in the scaffold 2351 (Table 3.4).

3.4.4 Sequence analysis of *AvrSr35* gene on *Sr35*-virulent mutant strains

Sanger sequencing of the genomic region containing coding sequence of the *AvrSr35* allele in 15 *Pgt Sr35*-virulent mutant strains validated the presence of single point mutations associated with EMS and predicted by SNP calling (Table 3.4) (Appendix B). Sanger sequencing also identified a mutation previously not detected using the NGS platforms. That was the case for the G>A variation in position 2206 of scaffold 2351 on the mutant M1. The same mutation was detected

in the M6 mutant, but since the mutation profiles are different between the two strains, we concluded that cross-contamination between those mutant strains was unlikely.

All point mutations confirmed after the *AvrSr35* allele re-sequencing, displayed strong effects on coding sequence according to the analysis of SnpEff program (Cingolani et al., 2012). In 12 out of 15 mutant strains (M2, M4, M5, M7, M8, M9, M10, M11, M12, M13, M15) nonsense mutations producing truncated AvrSr35 proteins were identified. Two mutants (M1 and M6) had non-synonymous mutations where the amino acid valine was substituted by isoleucine (V128I), and one mutant (M3) carried a splice site mutation (Table 3.4) (Appendix C). Since 1) all fifteen strain mutant strains carried strong effect mutations in the coding sequence of the gene identified on scaffold 2351 (NCBI MF474174), 2) the next *Avr* gene candidate on the list had nonsense mutations in only three mutant strains and 3) comparative virulence profile between mutants strains and wild-type RKQQC (Appendix D, Table S2, Salcedo et al., 2017) suggests the knockout of a single gene; the coding sequence located on scaffold 2351 was considered as the best candidate for *AvrSr35* gene.

Table 3.4. Predicted single point mutations of the *AvrSr35* gene on 15 *Sr35*-virulent RKQQC mutant strains. Positions on Scaffold 2351(NCBI MF474174) and gene model are indicated, as well as the point mutation (underlined)

Mutant name	Position in the Scaffold 2351/Gene model	Effect*
RKQQC_M1	2206/774	<u>G</u> TT to <u>A</u> TT (Val by Ile ^{**})
RKQQC_M2	3096/1664	T <u>G</u> G to T <u>G</u> A (Stop codon)
RKQQC_M3	2941/1509	<u>G</u> T to <u>A</u> T (splice site mutation)
RKQQC_M4	3287/1855	<u>C</u> AG to <u>T</u> AG (Stop codon)
RKQQC_M5	2009/577 [†]	<u>C</u> AG to <u>T</u> AG (Stop codon)
RKQQC_M6	2206/774	<u>G</u> TT to <u>A</u> TT (Val to Ile)
RKQQC_M7	2909/1477	T <u>G</u> G to T <u>G</u> A (Stop codon)
RKQQC_M8	3287/1855	<u>C</u> AG to <u>T</u> AG (Stop codon)
RKQQC_M9	3287/1855	<u>C</u> AG to <u>T</u> AG (Stop codon)
RKQQC_M10	3641/2209	<u>C</u> AA to <u>T</u> AA (Stop codon)
RKQQC_M11	1843/411	<u>C</u> AG to <u>T</u> AG (Stop codon)
RKQQC_M12	2460/1028	<u>C</u> AA to <u>T</u> AA (Stop codon)
RKQQC_M13	3161/1729	<u>C</u> AA to <u>T</u> AA (Stop codon)
RKQQC_M14	3096/1664	T <u>G</u> G to T <u>A</u> G (Stop codon)
RKQQC_M15	2546/1114	T <u>G</u> G to T <u>A</u> G (Stop codon)

*Mutations confirmed by Sanger sequencing **Mutation detected by Sanger sequencing

3.4.5 Diversity analyses of *Sr35*-virulent and *Sr35*-avirulent field isolates of *Pgt*

The *AvrSr35* gene locus was amplified and re-sequenced from a diverse set *Sr35*-virulent, and *Sr35*-avirulent *Pgt* field isolates. This re-sequencing confirmed that the gene present on the scaffold 2351 is the *AvrSr35*, showed the genetic changes that produced the virulence against the *Sr35* gene in these *Pgt* set.

Genomic DNA of 27 *Sr35*-virulent and *Sr35*-avirulent *Pgt* field isolates collected at different locations and years were provided by Dr. Lez Zsabo (Cereal Disease Lab, St Paul Minnesota) (Table 3.2). PCR primers were designed to amplify a PCR product from the 5' region to the 3' region of the gene model predicted for the best *AvrSr35* candidate. PCR products were sequenced directly or subcloned in TA plasmid vectors and then sequenced separately if length polymorphisms were identified (Section 3.3.9). An evident PCR-length polymorphism was detected between the virulent and avirulent isolates, where two allelic variants of 2,547 bp and 2,955 bp were detected (Figure 3.5). DNAs from virulent isolates amplified the larger molecular size allelic variant whereas the DNAs from avirulent isolates amplified either the shorter allelic variant or both allelic variants, the last isolates were considered PCR-length heterozygous for the functional and non-functional alleles of the *AvrSr35* candidate.

The hypothetical relationship among the genomic sequence of the *AvrSr35* alleles found in the set of *Sr35*-virulent and *Sr35*-avirulent *Pgt* field isolates, were modeled in a phylogenetic tree or dendrogram using an divergent *AvrSr35* allele as an outgroup to rooting the tree (Figure 3.6B). This divergent allele *AvrSr35* is a non-functional allele identified on the isolate 99KS76A-1, it contains a nonsense mutation in the position 1,320 of the gene model and differs in 27 amino acids compare to the functional allele present in the same isolate.

The *AvrSr35* haplotypes were clustered into two clades called clade A (avirulent) and clade V (virulent) (Figure 3.6B). The clade A included only the haplotypes present in the *Sr35*-avirulent isolates set, which contains the four members of the *Ug99* race group evaluated. The clade V included the haplotypes that were found in the *Sr35*-virulent isolates, but also included some haplotypes identified in five *Sr35*-avirulent isolates (77ND82A, 72CA1A, 7A, 69SD657C, 74MN1049, 7a(CDL_75_36_700_3)) that were heterozygous at the *AvrSr35* gene locus. These

results imply that the avirulence to the *Sr35* gene is caused by the haplotypes present on the clade A. The fragment polymorphism found in the all the haplotypes present on clade V was product of the insertion into the exon 6 of a 404 bp-long miniature inverted transposable element (MITE) (Figure 3.6A, Figure 3.7). and the virulence

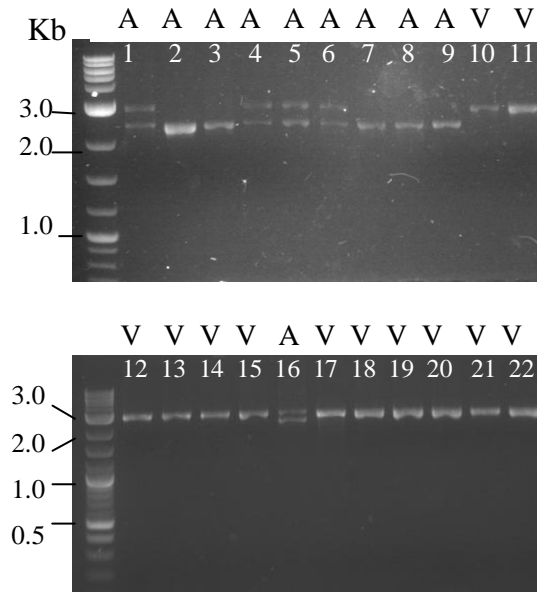


Figure 3.5. Ethidium Bromide-stained agarose gel (1.8%) showing PCR-product length polymorphism for the *AvrSr35* gene among several *Pgt* isolates. (A) *Sr35*-avirulent, (V) *Sr35*-virulent. PCR primers s2351_1374F and s2351_3920R (Table 3.1) were designed to amplify the entire coding region of the *AvrSr35* gene. All virulent isolates carried only the long allelic variant (2,955bp), whereas all avirulent isolates showed the presence of the short allelic variant (2,547 bp) with some isolates carrying both the short and long allelic variants. The presence of the two allelic variants in some of the avirulent isolates, suggest that they are heterozygous at the *AvrSr35* locus. The presence of only the long PCR product in all virulent isolates is consistent with the hypothesis that those virulent isolates carry a non-functional variant of the *AvrSr35* gene with a DNA insertion. *Sr35*-avirulent Isolates: **1:** 7ND82A, **2:** 04KEN156/04 (TTKSK AKA *Ug99*), **3:** 99KS76A-1 (RKQQC), **4:** 69SD657C, **5:** 72CA1A, **6:** 74MN1049, **7:** 84KEN654B, **8:** 61PA80A, **9:** 00MN99c. *Sr35*-virulent Isolates: **10:** 59KS19, **11:** 69MN399, **12:** 09CA115-2, **13:** 06ND76C, **14:** 75WA1652, **15:** 75WA1652A, **16:** 7a(CDL_75_36_700_3), **17:** 01SD80A, **18:** 09ID073-2, **19:** 76WA1397B, **20:** 76WA1204C, **21:** 76WA1358C, **22:** 74WA1331B.

MITEs belong to class II transposon characterized by the absence of RNA intermediate; they are non-autonomous TEs lacking of essential genes for transposition (Santana & Queiroz, 2015). MITEs have been considered as short (<800 bp) imperfect derivatives of autonomous TEs, and like them, they usually have terminal inverted repeats (TIRs) (≥ 10 bp), flanked by target site duplications (TSDs) (2~10 bp) (Chen et al., 2014a; Guo et al., 2017).

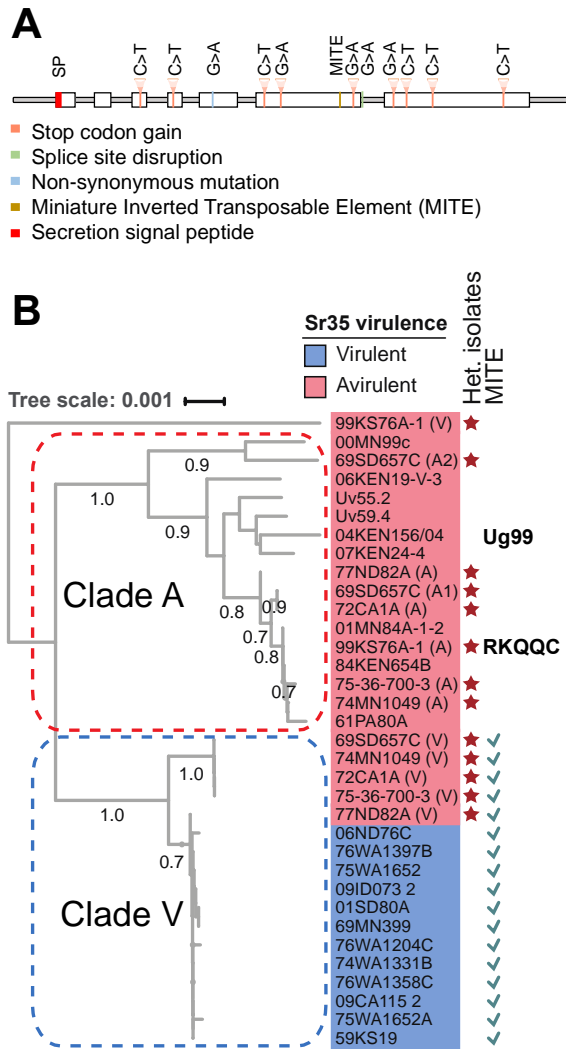


Figure 3.6. *AvrSr35* gene model and gene based phylogenetic relationship among *Sr35*-virulent and avirulent isolates. (Figure 2, Salcedo et al., 2017). **A.** Gene model and summary of *Pgt* RKQQC EMS-induced mutations positions in the candidate *AvrSr35* gene, and the insertion site of the miniature inverted transposable element MITE (position 1408) in the 6th exon. **B.** Phylogenetic tree of the candidate *AvrSr35* gene built using sequences obtained from 27 *Sr35*-virulent and *Sr35*-avirulent *Pgt* isolates. The sequences corresponding to the *Pgt* races RKQQC (99KS76A-1) and TTKSK (*Ug99*) are indicated. Sequences were aligned using program MUSCLE (Edgar, 2004), and the phylogenetic tree was constructed using the Neighbor-Joining method applying the maximum composite likelihood substitution model implemented in program MEGA 6.06 (Tamura et al., 2013) (bootstrap =1,000 replicates, threshold 0.7) bootstrap values are shown on the tree nodes. Phylogenetic tree was generated using Interactive Tree Of Life (<http://itol.embl.de>) (Letunic & Bork, 2016). The colored tree tips correspond to sequences originating from the *Sr35*-avirulent (red) and *Sr35*-virulent (blue) isolates. The *AvrSr35* candidate gene sequences were clustered into two large groups (A and V). The latter group includes haplotypes harboring the MITE insertion (marked by ticks). The sequences originating from the *Pgt* isolates heterozygous for PCR length in the *AvrSr35* gene candidate are marked with stars.

In this case, the MITE that was inserted into exon six corresponds to *Tc1/Mariner*-like transposable type, which is one of the most abundant TE family genomes fungi and their activity had been associated with biotic and abiotic stresses (Wicker et al., 2007). The presence of this MITE resulted in a premature termination codon (TAA) and truncation of the *AvrSr35* gene product to a peptide of 311 amino acids explaining the lack of recognition by the *Sr35* and virulence in the homozygous haplotypes present in the clade V. A nucleotide polymorphism (T/C) was identified in the position 1,582 of the MITE in some haplotypes of the V clade. These polymorphic haplotypes correspond to some of the *Sr35*-avirulent isolates heterozygous at the *AvrSr35* gene locus (Figure 3.6B).

→→→→→→→→→→→→→→→→→→→→→

```

TACAGCTAAACCGAAAAAGCTTGCGGGCTGTCTGAGTCGGAATATCCAAAAAAAAAAAAAAAAAACTGCAA
TTGGAATGTTAGGAAGAATACAGACAAGAATACAGGCTGCCGTATACCTGCCAGCAGCACCGGTGGGACCTGACC
GGCCCCCAGGGGATGCCTCAGCAGCAGCCATCAGCGGTAAGGGAAGGCCGTTGGAGTGAACCTTGCATCAGG
ATTCCGATGGTGTTACTCTCATCACCTGAAAATGAGAGAACAAAAGATAGCAAATTCAACCCAACATGATGCAT
CCATACATGAACCTGTATTCTTCCAAAACCTCCAGCTGTAGTCGGTAGATTTTTTTATTTTTTTATTTTTCTGACTT
CGGAGCCCGCAAGCTTCTCGTTATAGCTGTA

```

←←←←←←←←←←←←←←←←←←←←←

Figure 3.7. Sequence of the miniature inverted transposable element (MITE) inserted into the exon six of the *AvrSr35* gene on the group V of haplotypes (1408 bp from the start codon). MITE target site duplication (TA) is shown in green; the inverted terminal repeats are shown in red and the direction annotated using arrows.

The allele found in the isolate 04KEN156/04 which corresponds to TTKSK (*Ug99*) differs in six amino acid substitutions compare with the functional RKQQC allele. Amino acid substitutions were found also in other members of *Ug99*-race group with four substitutions for the race TTKSF, five substitutions for the race TTKSP and nine substitutions for the races TTKST and TTTSK. Other *Pgt* isolates displayed an identical amino acid sequence compare to RKQQC (TTTT and TPMKC) or several amino acid substitutions: CDL_75-36_700_3 (*Sr35*-avirulent allele 2) and MCCFC (*Sr35*-virulent) (25 identical substitutions).

3.4.6 PCR-based cloning of the *AvrSr35* candidate

The transcriptional activity of the *AvrSr35* candidate was evaluated by RT-PCR, and the PCR product was subcloned for further analysis and as template for the creation of vectors for functional characterization (Chapter 4). cDNA produced from pooled total RNA isolated from

leaves of susceptible genotype Fielder infected with RKQQC race was used as template to amplify the 5' and 3' UTR regions and the CDS of the *AvrSr35* candidate gene. Internal primers were used to confirm the presence of the *AvrSr35* transcript (Figure 3.8).

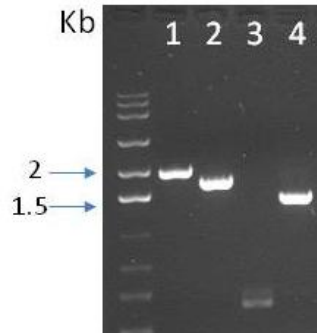


Figure 3.8. Ethidium Bromide-stained agarose gel (1.8%) showing the RT-PCR to amplify the *AvrSr35* gene. The cDNA was obtained from pooled RNA from leaf tissue of susceptible genotype Fielder. Seedlings of Fielder genotype were infected with RKQQC race (*Sr35*-avirulent) and collected at 24, 48 and 96 hours after infection **1**. Primer combination s235_1374F-s235_13920R amplified the 5' and 3' untranslated regions (UTR) and the open reading frame (ORF). **2**. Primer combination s235_1433F-s235_3766R amplified only the ORF. Internal primer combinations: **3**. s235_1374F-s235_2055R and **4**. s2351_2027F-s2351_3766R were used to confirm the expression of the *AvrSr35* gene.

3.4.7 Sequence analysis and characterization of *AvrSr35* candidate

The comparative analysis of the scaffold 2351 and the cDNA sequence revealed that the *AvrSr35* candidate gene is composed of 1773 nucleotides (NCBI MF474174) divided into seven exons (Figure 3.6) that encode a protein of 578 amino acids-long. The AVRSR35 deduced protein has three cysteine residues and a calculated Mw of 66.39 kDa.

Blastx similarity search on NCBI database of the *AvrSr35* deduce protein, found a similarity of 95% (e-value $2e^{-108}$) and 30% of coverage with the hypothetical protein 08475 of the race SCCL strain 75–36- 700–3 (Duplessis, 2011a) (Figure 3.9), this low coverage was explained because the ORF of the hypothetical protein 08475 was not fully annotated. Besides this sequence similarity on the NCBI, The *AvrSr35* deduced protein did not show any significant similarities with known proteins or domains after the search on secondary databases (Interpro, UniPro).

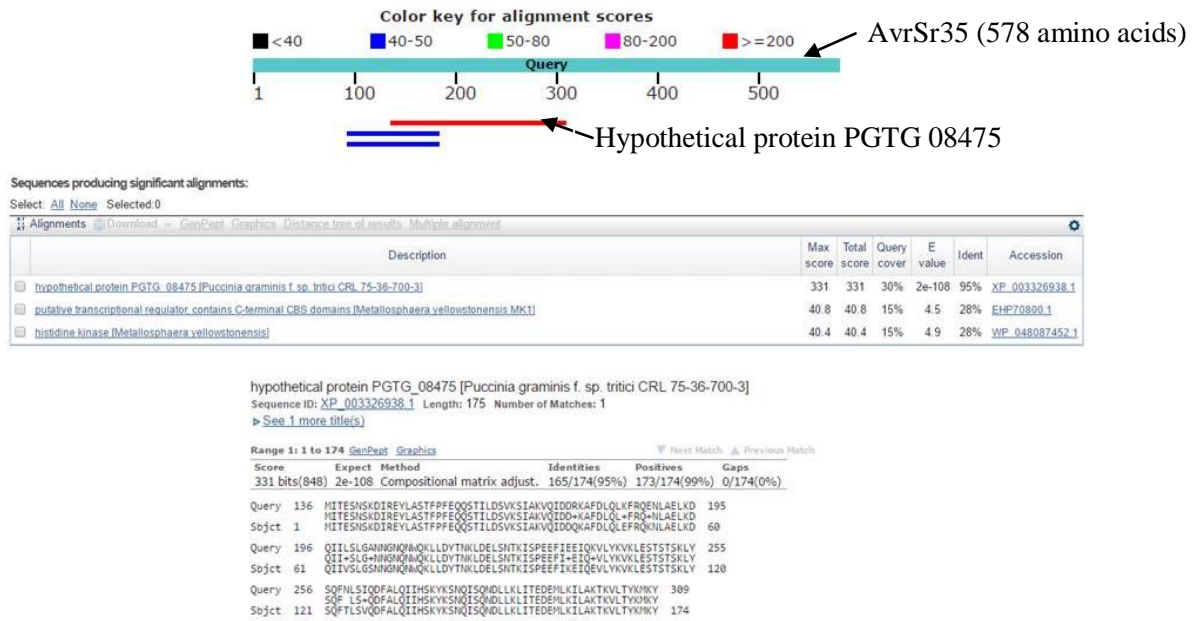


Figure 3.9. Search of similarity on NCBI database (Blastx) for *AvrSr35*. A significant hit was obtained with the partial sequence of the hypothetical protein 08475 reported for the *Pgt* race SCCL strain 75–36- 700–3.

An N-terminal signal peptide cleavage site between amino acids 25 and 26 was predicted using SignalP software (Emanuelsson et al., 2007) (Figure 3.10). Transit or signal peptides are associated with secretory proteins typically cleavage by peptidases that removed the transit peptide during translocations across the membranes (Coleman et al., 1985). The presence of signal peptide for secretion has been a criterion to define a candidate fungal effectors (Sonah et al., 2016).

The prediction of the secondary structure of the *AvrSr35* protein suggests that most of the protein is composed of alpha helix and loops with low representation of beta-sheets (Figure 3.11), and it could not be modeled based on any crystal structure present in databases.

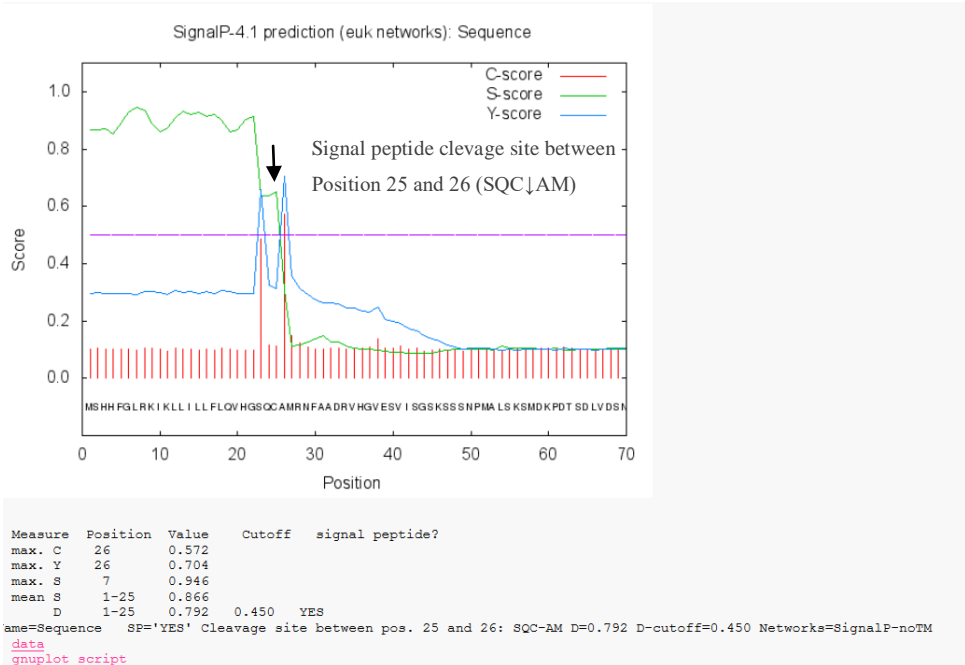


Figure 3.10. Prediction of the secretion signal peptide (SP) for the *AvrSr35* using SignalP software (Emanuelsson et al., 2007). The SP cleavage site (arrow) was detected between amino acids 25 and 26. The output of SignalP shows the values of raw cleavage site score (C-score), signal peptide score (S-score) and combined cleavage site score (Y-score). The D-score, a weighted average of the mean S-score and the maximum Y-score, is used to identify SPs. Aminoacid residues surrounding the cleavage site are showed.

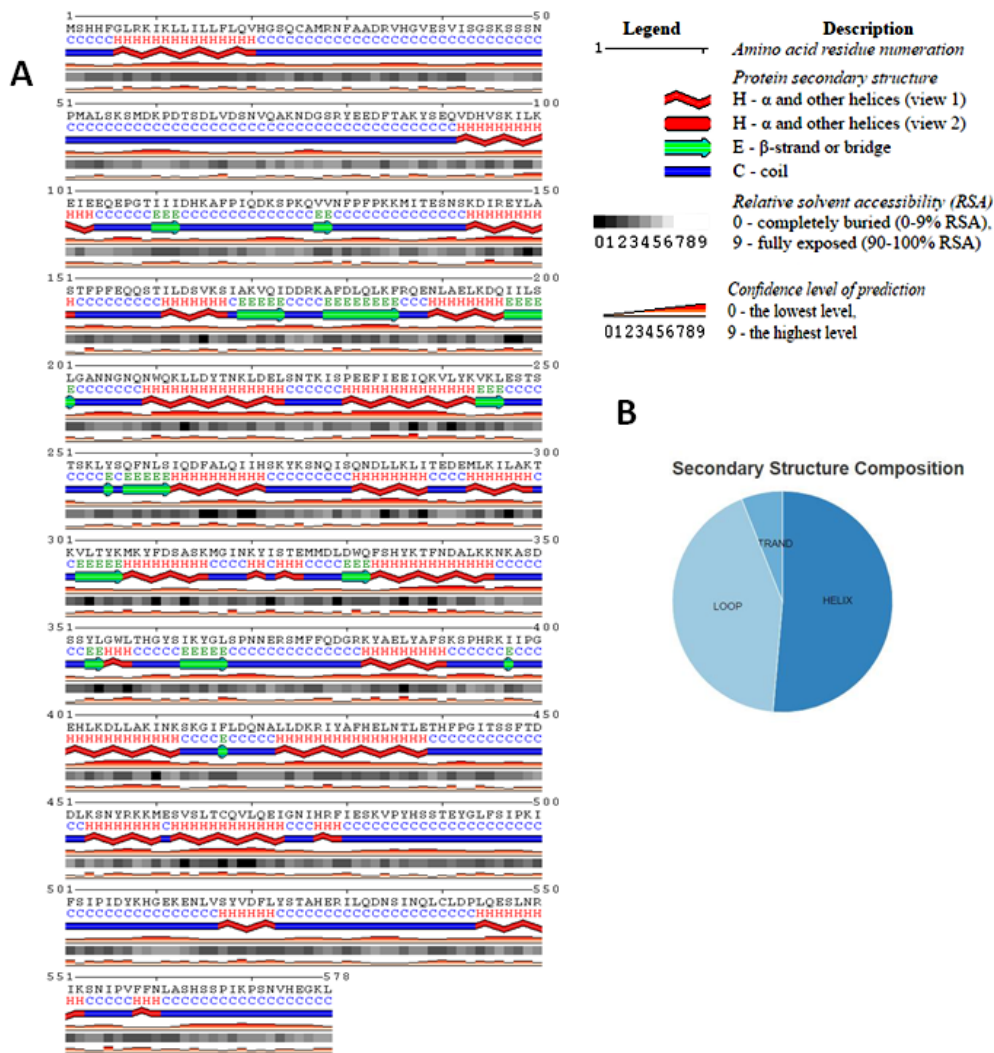


Figure 3.11. Secondary structure prediction based on amino acid sequence of the candidate gene *AvrSr35*. **A** SABLE protein predictor (<http://sable.cchmc.org/>). **B**. Pie chart showing the contribution of each protein secondary structure (www.predictprotein.org).

3.5 Discussion

In the last decade, the advances in genomic sciences have made possible the sequencing of the genome of non-model organisms such as *Pgt*, revealing that those parasitic symbionts possess a plethora of hundreds of candidate effectors (Raffaele & Kamoun, 2012). The identification of effectors provides a better understanding of the establishment of a successful compatible interaction and ultimately the biotrophism. However, because of the lack of similarity, extreme diversity, redundancy and few functional genetic approaches to study them, the discovery of fungal effectors have been delayed compared with their bacterial and oomycetes counterparts.

In this research, a combination of multiple approaches, which included chemical mutagenesis, an efficient selective forward genetic screening with the *Sr35* gene, and the assembly of pathogen reference genome and transcriptome during infection, resulted in the identification of a candidate for *Sr35*-avirulence gene. The forward genetic approach was supported by assessing the diversity of the *Avr* candidate on natural *Sr35*-virulent and *Sr35*-avirulent isolates, providing significant insights into effectors' evolution towards loss of recognition.

3.5.1 Developing of *Pgt* EMS-mutants with virulence for the *Sr35* gene

Geneticists have used forward genetics for decades to study gene function in different organisms. This strategy relies on the successful mutagenesis, either spontaneous or induced, of the organism of interest to study candidate genes. Mutagenesis of pathogens had been applied in agriculture for several research purposes including the production of pathogens with specific features to basic genetic studies (Simons, 1979; Luig, 1978). The artificial production or natural occurrence of *Pgt* with deficiencies in avirulence function is a valuable resource to understand stem rust resistance and clone *Avr* genes (Figuroa et al., 2016). In this study, urediniospores of an isolate from the North American *Pgt* race RKQQC, which is avirulent to the stem rust resistance gene *Sr35*, was used as the source for mutagenesis for the chemical agent EMS.

Alkylating agents like EMS are effective mutagens because they cause a mispairing on complementary nucleotides introducing mutations after DNA replication. Most of these mutations correspond to transitions G/C to A/T (Sega, 1984; Greene et al., 2003). The EMS mutations can be used not only to search for loss- or gain-of-function mutants but also to understand the role of specific amino acid residues in the protein function (Kim et al., 2006). In the production of RKQQC *Pgt* mutants, all urediniospores obtained after applying four concentrations of EMS (0.1 M, 0.05 M, 0.001 M and 0.005 M) were pooled making complicated an estimate of the individual effect of each EMS concentration. A visual inspection of the urediniospores viability under the dissecting microscope showed viability near to 60% when the urediniospores were plated in 2% agar and incubated for 24 hours at 30°C, the mortality rate was estimated based on germ tube to growth failure. Singh et al., (2013) previously reported that

viability of 50% is reached at EMS concentrations of 0.01-0.015 M for RKQQC, which was close to the median range (0.1-0.005 M) used in this study.

The expected outcome was that the virulence against *Sr35* of *Pgt* RKQQC-mutant strains would be associated with mutations in a single candidate gene for *AvrSr35*. The virulence ability *Pgt* mutated spores were screened on seedlings of a wheat genotype carrying the *Sr35*, finding 15 virulent mutant strains. The assumption behind this strategy was that the RKQQC isolated is expressing the avirulent gene product that is being recognized by *Sr35*, and potentially it is shared with the hypervirulent race TTKSK (*Ug99*).

Several factors contributed to the successful production of the avirulent RKQQC mutants. First, any possible source of contamination with other *Pgt* races was reduced, since the inoculation experiments in Eduard Akhunov's lab have been concentrated only on RKQQC and TPMKC *Pgt* races. The purity of the *Pgt* isolates was evaluated before the mutagenesis procedure using the genotype Morocco *Lr19* which eliminate a possible carryover of *Pt* urediniospores. The *Sr35* gene has a strong selection over the RKQQC since the infection type is near to immunity (IT= 0, ;), which make it a conclusive system for the screening for virulent mutants. Finally, the heterozygous genotype of the race RKQQC at the *AvrSr35* gene locus detected by the presence of a predicted recessive allele facilitated the discovery of the *AvrSr35* gene. In most of the regions of the world where stem rust is a problem, most of the clones display high levels of heterozygosity in the heterokaryon (Roelfs, 1988). Thus in heterozygous *Pgt* races for a given *Avr* gene, a single recessive mutation that produces a loss of function of the *Avr* gene should show an immediately phenotypic shift to virulence in the otherwise resistant host. By contrast, in homozygous races, both copies of the *Avr* gene need to be mutated in the heterokaryon to observe an effect on phenotype assuming that those mutations will not impose a fitness cost on pathogen (Statler, 1979; Figueroa et al., 2016). These constraints were observed in previous experiments that involved urediniospore mutagenesis where several cycles of recurrent mutations were required to produce virulent mutants (Teo & Baker, 1975; Luig, 1978).

Two RKQQC mutants (M1 and M7) were selected for further virulence analysis using a set of wheat lines containing different resistant genes (differentials). The differential test was carried

out by Dr. Matthew Rouse on Cereal Disease Lab (St. Paul, Minnesota). This test found that the *Pgt* mutants display the same virulence profile compared with the wild-type RKQQC except for an additional virulence to *Sr35* confirming that the mutants are not the product of other *Sr35*-virulent race contamination and also that the shift in virulence to *Sr35* was the result of a mutation in a single *Avr* gene. The fact that all mutants were virulent in two rounds of single uredinium infection over the genotype G2919 carrying *Sr35*, and the lack of noticeable morphological or developmental differences under the microscope of mutants M1, M4 and M7 compared with the wild type RKQQC suggested that they are not temporary virulent variants or the mutations produce by EMS probably did not impose a fitness cost. These data together with RNAseq-time course comparative analysis of this group of mutant strains with the RKQQC wild-type (Salcedo et al., 2017), suggests that *AvrSr35* is not involved in virulence function or a functional redundancy of other effectors compensates the absence of *AvrSr35*. The contribution to virulence of a candidate effector can be evaluated using deletion mutants (Schweizer et al., 2018), but since there is no an established protocol for cereal rust transformation, the loss-of-function EMS mutant strains can be used to estimated such contribution. However, additional experiments and further analysis of the remaining mutant strains are required to identify differences in the pathogenicity, uredinium size, volume of uredinia and infection development.

Independent *Pgt* mutant strains with virulence for *Sr35* gene generated after the mutagenesis of urediniospores of RKQQC race with EMS, displayed transition mutations C/T (7 mutants) and G/A (6 mutants) which explain the lack of recognition by *Sr35*. The transition G to A or C to T resulted in premature stop codons that created deduced truncate proteins in 12 mutant strains. A mutant allele present in the mutant M3 changed the GT by AT on 5' site of the predicted splice site for the exon 6. These mutated dinucleotides are fundamental for the recognition of the spliceosome, and their mutations result in detrimental outcomes such as exon skipping, activation of cryptic splice site or intron retention (Ward & Cooper, 2010).

Two mutants M1 and M6 had a non-synonymous mutation in the same position of candidate gene present in the scaffold 2351. This mutation substituted the amino acid valine by isoleucine on the position 128 of the *AvrSr35* protein. Both valine and isoleucine are hydrophobic and aliphatic amino acids that rarely are involved in catalysis, but they can be involved in substrate

recognition. Valine and isoleucine only differ in a methyl group, and it is expected that this change represent only a small deformation of the protein structure (Berg et al., 2012). However, certain hydrophobic environments can be optimized for biological interactions of either V or I (Godoy et al., 2005). Hence, this kind of substitutions can affect the evolutionary and structural optimization of the *AvrSr35* interactions. Changes in a single amino acid in *Avr* proteins have been associated with the gain of virulence in several pathogens including *Avr2* of *Fusarium oxysporum* f. sp. *lycopersici* (Houterman et al., 2009), lack of interaction on protein-protein assays in the *Avr-Pita* of *Magnaportha Orizae* (Jia et al., 2000) or affecting the specificity of recognition by the *R* gene and the strength of the HR response (Wang et al., 2007a; Blondeau et al., 2015).

3.5.2 Diversity analysis of *AvrSr35* locus

PCR amplicons for the *AvrSr35* gene locus were generated from fungal DNA in a set of *Sr35*-virulent and *Sr35*-avirulent *Pgt* field isolates collected at different locations and years. The re-sequencing of independent field isolates with different avirulence phenotypes would provides information about the nature of molecular events that lead to the changes in virulence towards *Sr35* gene. A Phylogenetic analysis based on the entire genomic sequence of the *Avrsr35* locus grouped the *AvrSr35* alleles in two clades called A and V. The clade A contains haplotypes associate with *Sr35*-avirulent isolates including the *Ug99* race group, whereas the clade V included all *Sr35*-virulent isolates and some *Sr35*-avirulent isolates with the *AvrSr35* locus in a heterozygous state. This finding suggests that the *AvrSr35* haplotypes of clade A, including some members of the *Ug99* race group, are functional alleles that cause avirulence when they are recognized for *Sr35*. Moreover, the polymorphism detected by PCR due to the insertion of a 404 bp long MITE element in exon six on haplotypes of clade V, produced non-functional alleles with a premature stop codon, this was confirmed on homozygous haplotypes for the *avrSr35* allele in all *Pgt* isolates from the V group. This insertion was responsible for the origin of virulence to the *Sr35* in those isolates.

The initial strategy to identify *AvrSr35* contemplated the use of presence-absence variation (PAV) on candidate effectors by comparing the genome of *Pgt Sr35*-virulent and *Sr35*-

avirulent. This preliminary effort was based on the fact that the pathogen races display a high degree of synteny, but a significant variation in the number and similarity of effector sets (Spanu & Kämper, 2010; Yoshida et al., 2009; Gilroy et al., 2011). Candidate effectors present on avirulent races and absent on virulent races are then screened for their ability to induce ETI (Catanzariti et al., 2006). This strategy did not show any result using EtHAn system for ETI screening on wheat carrying *Sr35* gene mainly because the PAV strategy did not analyzed candidate *Avr* genes showing MITEs polymorphism that derivates in the pseudogenization and the gain of virulence.

The *Avr* gene or effector diversification is the result of genomic modifications that range from simple nucleotide substitution to complex chromosomal structural variation that can affect the gene content (Raffaele & Kamoun, 2012; Dong et al., 2015). Transposable elements such as MITEs play roles in the increase of genetic variability, genomic organization, and the adaptation to the environment in filamentous fungi. Several studies demonstrate that their activity affects structure and expression of *Avr* genes (Daboussi & Capy, 2003; Santana & Queiroz, 2015), allowing to the pathogens to adapt to host sources of resistance (Grandaubert et al., 2014). In recent years, it has been demonstrated that numerous pathogen genomes have a dual architecture designed as ‘two-speed genome’ model, where genomic regions associated with effectors are enriched with TEs and repetitive sequences. These regions are considered hot spots of rapid adaptive evolution contrasting with other regions of the genome associated with basic metabolism (Dong et al., 2015). The genome of *Pgt* is larger than other fungi due to the expansion of repetitive sequences which constitute the 44% of the total genome. However, unlike other fungal genomes, the TEs found in the *Pgt* are randomly distributed with no apparent association to a particular class of genes (Szabo et al., 2014).

Analysis of filamentous fungi genomes shows that pathogenesis related genes, as well as *Avr* genes, are not randomly distributed on the genome. They are frequently immersed in genomic regions with high genomic flexibility such as telomeres heterochromatin, or they are surrounded by dispersing transposable elements (TE) and repetitive derived transposon-rich regions. These regions facilitate genomic changes in effectors such as duplication, mutation, and recombination which can promote effector gene mutation (Spanu et al., 2010; Spanu & Kämper, 2010; Ali et

al., 2014). MITEs and other TEs are activated and silenced by epigenetic switches that increasing both the size and diversity of the genome. (Spanu & Kämper, 2010; Raffaele & Kamoun, 2012; Gijzen et al., 2014; Dong et al., 2016; Fedoroff, 2000). An example of gain of virulence product of a TE over a coding sequence of an *Avr* gene was found in the *Avr1* gene of *F. oxysporum* by Inami et al., (2012). The coding sequence of *Avr1* gene was truncated by a copy of the autonomous transposon *Hornet 1*. Another example was provided by Ali et al., (2014) on the *Avr UhAvr1* from *Ustilago hordei* (causal agent of barley smut). In this case, the shift to virulence arose from a transposable element of 5.5 Kb which got inserted in the promoter sequence of *UhAvr1*, modifying its expression and most likely the recognition by the cognate *R* gene. Recently the insertion of retrotransposon called *Pto* similar to *Tc1/mariner* in the promoter region of the avirulent gene *PWT3* was identified as the cause of the emergence of the wheat blast (Inoue et al., 2017). Previously, a member of the same transposon was identified as the responsible for the loss of recognition of the *Avr-Pita* gene (Kang et al., 2001). These examples highlight the dispensability and redundancy of effectors which can be lost and recovered on pathogen populations or lineages, making more difficult its detection (Gijzen et al., 2014; Rutter et al., 2017).

Comparative sequence analysis showed polymorphism on the deduced amino acid sequence among the haplotypes identified in the *AvrSr35* locus. The haplotype found in RKQQC differs in several substitutions with all members *Ug99* race group evaluated and others *Pgt* races. Despite this divergence in amino acid sequences, recent studies in fungal effector show convergence in structural similarity. This similarity in structure would lead effectors to reach structural stability by a conserved folding but enough plasticity to target new host proteins (Franceschetti et al., 2017).

3.5.3 Microscopy analysis of *Pgt* time course of infection

The use of Confocal Laser Scanning Microscopy (CLSM) to monitoring the development of infection structures during wheat-*Pgt* interactions has proved to be valuable to understand the *Sr35*-mechanism of resistance. CLSM provides informative and detailed 2D and 3D images of the infection structures that are reconstructed from stacked serial images using analysis software.

These images are possible because this type of microscopy allows the slicing of thin optical sections with high resolution without the necessity of mechanical perturbation of the specimen. (Inoué, 2006; Kitin et al., 2000).

The images obtained from the confocal microscope depend of multiple factors that need to be adjusted and optimized for each tissue and experimental objectives (Kitin et al., 2000). Several protocols and protocol variants have been described in the last years to fix and stain leaves infected with wheat rust fungi (Rohringer, 1977; Jacobs et al., 1996; Zhang & Dickinson, 2001; Moldenhauer et al., 2006; Ayliffe et al., 2011; Figueroa et al., 2013; Panwar et al., 2013b; Dugyala et al., 2015). The protocols developed in this study mixed strategies described in previous publications and some modifications that made possible differentiate both the fungal structures from plant tissue and dead cells from intact cells.

We used a variation of the protocols developed by Rohringer, (1977) Panwar et al., (2013b) and Figueroa et al., (2013) to compare the progression of the infection of RKQQC in hexaploid wheat genotypes lacking or carrying the *Sr35* gene. The infected leaves were cleared and fixed for three days on ethanol at 95%, which shortens the time for clearing and fixing in some days compare with the protocol described by Figueroa et al., (2013), but still time-consuming compared to other protocols where the clearing and fixing process takes hours (Dugyala et al., 2015). This could make the protocol used in this study unsuitable for high throughput experiments. Dugyala et al., (2015) concluded that the critical factors to obtain effective staining implied a minimum time incubation of 15 minutes with Tris HCl buffer and staining with Uvitex 2B 0.3 % pre-heated during 5 min at 65 °C. By contrast, the protocol used in this study, applied a smaller concentration of Uvitex2B (0.1%) in combination with Acridine Orange (0.1%) incubated at room temperature (~25 °C), but a more extended incubation for staining (5 min) compare with Figueroa et al., (2013) who used a shorter incubation time (2 min).

In this study, we combined Uvitex 2B with the fluorescent dye Acridine Orange, avoiding the overlapping of emission signal between fungus and plant tissues. Acridine Orange has mainly utilized to stain nucleic acids of dead cells. However, cells walls and subcellular structures stained with Acridine Orange emit red fluorescence, a phenomena known as *metachromatic*

fluorescence (Stockert & Blazquez-Castro, 2017), that can be used to differentiate the plant cells from fungal mycelium. We also washed overnight the specimen with glycerol 25% (v/v) to remove the excess of fluorochrome improving the images quality.

The analysis of CLSM images on leaves of wheat genotypes carrying *Sr35* did not show the formation of any haustorium during the first 72 hours after inoculation with the *Sr35*-avirulent race RKQQC. Also, the staining with WGA-FITC and propidium iodide showed that the *Sr35* resistance involves single cell necrosis visualized as strong fluorescence of few host mesophyll cells in near contact with haustorial mother cells. Resistance in plants has a wide dynamic range of quantitative and qualitative variation, ranging from extreme resistance (micro HR) to systemic HR (Künstler et al., 2016). HR is considered a hybrid physiological phenomenon between apoptosis and necrosis (Mukhtar et al., 2016). Histological studies of the host-pathogen interaction between plants and rust fungi suggest that two distinctive resistance mechanisms occur: prehaustorial and post-haustorial resistance. The pre-haustorial resistance is elicited at the first hours after infection earlier stages of development resulting in the interruption of infection structures before the expected time for haustoria formation. Post-haustorial resistance implies that the fungal development is arrested after the formation of haustorium (Niks & Dekens, 1991; Wang et al., 2015b). The time course analysis of infection led to the conclusion that the rust resistance provided by *Sr35* is pre-haustorial. This resistance is characterized by rapid single cell death (micro HR) and the impairment of the haustorium a structure essential for the establishment of a compatible interaction with the host. This reaction was expected since in the resistance provided by *Sr35* involves a near immune response (IT 0, ; or immune, hypersensitive flecks), implying the growth of RKQQC is stopped at early stages of development.

Pre-haustorial resistance was shown for the resistance gene *Rpg1* in barley, which triggers an immune response as early as urediniospore landing on plant tissues (Nirmala et al., 2011). Other examples of pre-haustorial resistance are provided by the *Sr36* gene which confers near immunity against the races 151-QSH, 56-MBC, MCCFC, and RCCDM (Rowell, 1981; Wang, et al., 2015b). Race-specific resistance to different isolates of *Pt* was also identified by Serfling et al., (2016) in the *Triticum monococcum* accession PI272560 where haustorial mother cells are rarely produced after infection.

Pre-haustorial resistance has usually been associated with the non-host resistance, where the haustorial mother cell can be produced, but the formation of haustoria is blocked by cell wall appositions called papillae (Niks & Dekens, 1991). The main component of the papillae is the polymer (1,3)- β -glucan (Voigt, 2014), which can be accumulated within 24 hours after infection in plants carrying the *Sr36* and *Sr5* gene (Wang et al., 2015b). We did not observe callose accumulation under the microscope, but a simple experiment can be done to measure the direct accumulation of the polysaccharide compound of (1,3)- β -glucan (Yin & Hulbert, 2010) or reactive oxygen species associated with callose deposition (Thordal-Christensen et al., 1997). Typically during non-host resistance, haustoria are not formed because of the blocking of callose deposition, and it is speculated that effectors may not enter into the host cells activating immune responses related to PTI (Bettgenhaeuser et al., 2014). However, since in this study, there is evidence that the interaction of *AvrSr35* with *Sr35* gene products is occurring inside the host cell (Chapter 4), it is possible that *AvrSr35* protein is secreted in structures like sub-stomal vesicle or haustorial mother cells and translocated to the host cells by a cellular mechanism yet to be determined.

3.6 Conclusions and perspectives

1. In this chapter, it is reported the identification of the first wheat rust *Avr* gene for cereal rusts. This study utilized a forward genetic approach that combined chemical mutagenesis of *Pgt* urediniospores and whole genome next-generation sequencing and *Avr* allele diversity analysis to overcome the limitations posed by the lack of tools for functional validation and the complexity of effectors set in this biotrophic pathogen.
2. Comparative analysis of the time course infection of *Pgt* using Confocal Laser Scanning Microscopy (CLSM) and fluorophores concluded that the *Sr35* display a pre-haustorial resistance associated to a rapid single cell death.
3. The *AvrSr35* found in the *Sr35*-avirulent race RKQQC led to the identification of the allele present in the race TTKSK (*Ug99*) and other members of the *Ug99* race group, constituting

an advance in the understanding of the host-pathogen interaction in this problematic race group.

4. The size *AvrSr35* (578 amino acids) was larger than previously characterized fungal effector (<300 amino acids), and also has low cysteine content and it is secreted without haustoria formation (pre-haustorial), suggesting those attributes should not be used as main criteria for fungal effector identification.
5. The origin of *Sr35*-virulent isolates was the result of a transposable element-related mutation, similar to previous reports (Inami et al., 2012; Ali et al., 2014; Inoue et al., 2017). The search for polymorphism in genes for secreted proteins associated with the presence of transposable elements could be helpful to identify more candidate *Avr* genes.
6. The success of breeding for resistance relies on our capacity to predict the future population genetic structure of pathogen population (McIntosh et al., 1995). The identification of *AvrSr35* will provide screening tools for monitoring pathogen virulence and diversity which can give clues about the emergence of new virulent races.
7. Several variants (haplotypes) of *AvrSr35* were identified in the diversity *Pgt* panel. This polymorphism can be determining the recognition properties of immune receptors providing insights into the *Avr-R* gene co-evolution.
8. Algorithms used for ranking proteins according to the likelihood to be effector had based multiple properties based in the information about effectors discovered in the last years (< 300 amino acids, high cysteine content, N- terminal signal protein, similarity to haustorial proteins, etc.) (Saunders et al., 2012). The discovery of *AvrSr35* will help to improve effector predictive algorithms including the recently developed *EffectorP* which uses a machine learning algorithm with non-strict rules to predict effectors (Sperschneider et al., 2016b).
9. The identification *AvrSr35* will help to assess resistant germplasms with gene pyramids by evaluating specific recognitions of the resistant gene components contributing with the

optimal deploy of *Sr* gene combinations on the field (Vleeshouwers & Oliver, 2014). Moreover, the spatiotemporal deployment of *R* genes can be decided based on surveys of the allelic diversity of effectors in pathogen's populations helping breeders to evaluate the potential of a given *R* gene (Vleeshouwers et al., 2011). Also, the studies deciphering the molecular basis for race specificity in cereals may contribute to the production of durable rust resistant germplasm (Horvath et al., 2003).

Chapter 4 - Functional characterization of the *AvrSr35* gene

4.1 Introduction

The analysis of the function and expression of effectors is essential for the understanding of the genetic changes that allow *Pgt* strains to defeat the resistance provided by the *Sr* genes, the nature of host-parasite interactions and the pathogenicity and colonization processes (Zambino et al., 2000; Hogenhout et al., 2009). Evidence found in Oomycetes and fungal systems, suggest that at specific stages of infection there are sequential waves of coordinated expression of different sets of effectors (Hacquard et al., 2012; Cantu et al., 2013; Soyer et al., 2014; Gervais et al., 2016). Wang et al., (2011) observed two waves of effectors with antagonistic effects in the oomycete *Phytophthora sojae*. Functional analysis experiments showed that the first wave involved cell death-suppression effectors, whereas the second wave includes cell death-inducing effectors. Some effectors are expressed before haustoria formation and were considered as *immediate-early effectors*, which would function as countermeasures against the host immune system. Immediate-early effectors are suggested to block the ETI as preparation for early effectors whose function is the suppression of PTI. In that way, different set of effectors may target different branches of host defense, and the detailed molecular aspects of this early interaction need to be understood in different pathosystems (Wang et al., 2015a).

Molecular pathologists have developed several tools and resources for genomics and functional analysis of pathogens (Cairns et al., 2016). However, the progress in the functional characterization of effectors on *Puccinales* and other biotrophs have been hindered by technical difficulties associated with the lack functional genetics approaches to study them, and the fact that effector set is highly redundant and dispensable (Zambino et al., 2000; Lawrence et al., 2010; Grant et al., 2013; Chaudhari et al., 2014). Despite the reports for successful transformation of flax rust (*Melampsora lini*) (Lawrence et al., 2010) and *Uromyces fabae* (Djulich et al., 2011), the genetic transformation for rust fungi is especially difficult due to the lack of proper reporter markers that can be applied when the fungi starts its life cycle on the host (Webb & Fellers, 2006) and the inability of the fungus to sporulate *in vitro* (Djulich et al., 2011). This especially true for *Pgt* for which no transformation system has been developed neither gene-knockout strategies broadly used in other fungi had been applied (Figuroa et al., 2016). Rust

fungi can grow with difficulty on artificial media developing abnormal ploidy and losing the capacity to infect its host plant (Leonard & Szabo, 2005).

Other possibilities for functional analysis are more time-consuming and contemplate the production of transgenic plants by particle bombardment transformation to express *Avr* candidates followed by crossing with *Sr* resistant line to test HR induction. (Leister et al., 1996; Jia et al., 2000). *Avr* candidate gene activity is detected when a loss of reporter protein, usually β -glucuronidase, is masked by cell death after *Avr* recognition. However, the wheat transformation is a very inefficient process and high throughput analysis of a large number of genes currently is not feasible (Yin & Hulbert, 2010).

An alternative approach in effector functional analysis in cereal rusts is the use of plant-expressed silencing constructs or Host Induce Gene Silencing (HIGS). Under this strategy, plants are transformed with an RNAi construct against the tested effector, the pathogen uptakes the double-stranded RNA (dsRNA) or small interfering RNA (siRNA) silencing the effector, and then the phenotype is evaluated (Yin et al., 2015). Lawrence et al., (2010) used this strategy to silence the avirulence gene *AvrL567* using as host flax lines carrying the corresponding *R* gene (*L6*) confirming the avirulence function of this effector. HIGS has been used to target the *Avr10* in powdery mildew fungus, *Blumeria graminis*, affecting the development of the fungus during infection (Nowara et al., 2010), and in the functional analysis of ribonuclease like effectors in the same fungus (Pliego et al., 2013). In the case of cereal rust, the HIGS system has gained popularity in the last years. Yin et al., (2011, 2015) introduced sequences of cereal rusts *Pgt*, *Pt* and *Ps* lowering the expression of the target genes in the pathogen during rust infection and reducing the fungal development. Panwar et al., (2013) used wheat leaf infiltration with *A. tumefaciens* to deliver a siRNA for *Pt* reducing the expression of pathogenicity genes and affecting the development and sporulation of the pathogen. However, these technologies have not been used extensively in cereals, and the off-target effects on fungi need to be assessed to avoid false positive phenotypes (Panwar et al., 2013).

The expression of candidate effectors on homologous or heterologous host systems provides clues about effector function. The induction of HR by the effectors in presence of R proteins is

considered as strong evidence in favor of interaction (Dodds et al., 2004). The susceptibility of *N. benthamiana* to a wide variety of pathogens and easy transformation by agroinfiltration make it an ideal and high throughput heterologous system for plant immunity studies (Houterman et al., 2009; Ma et al., 2012b). *N. benthamiana* can be infiltrated by *A. tumefaciens* cell suspension carrying binary vectors allowing for the transient expression of target proteins in plant cells. After approximately 24 to 48 hours of incubation, the infiltrated sections can be assessed visually and sampled for microscopy or biochemical analyses (Goodin et al., 2008). This approach has been used broadly to confirm candidate *Avr* genes based in their capacity to trigger cell death when they are transiently co-expressed with the corresponding resistance gene (Dodds et al., 2004; Bourras et al., 2015).

Another approach relies on delivering candidate effectors as fused proteins with the N-terminal secretion-translocation signals from the well-characterized *P. syringae* effectors *AvrRpm1* (Rentel et al., 2008) or *AvrRps4* (Sohn et al., 2007), candidate effector proteins are delivered using the bacterial type III secretion system (TTSS) into the plant cells. This system has been applied successfully for the identification of *Avr* proteins from oomycete pathogen *Hyaloperonospora parasitica* using the TTSS of *P. syringae* pv. Tomato (*Pst*) strain DC3000. To overcome problems associated with the stability and masking effects of the genetic background of *Pst* DC3000, Thomas et al., (2009) modified the non-pathogenic *P. fluorescens* Pf0-1 with TTSS genomic region to create a system for effector delivery called Effector to Host Analyzer (EtHAn). The utility of the EtHAn system for studying effectors on cereals was demonstrated by Yin & Hulbert, (2010) who delivered the *Avr* protein *AvrRpt2* on wheat seedlings. Complementary approaches such as cellular localization, protein-protein interaction (yeast two-hybrid assay, co-immunoprecipitation, or bi-molecular fluorescence complexes) are considered best ways to investigate and validate biotrophic pathogens from the functional point of view (Chaudhari et al., 2014).

The effector delivery mechanisms in fungi and oomycetes are less understood than bacterial pathogens (Yin & Hulbert, 2010). An significant advance was made by Rafiqi et al., (2010) who accumulated evidence that shows that the entry flax rust effectors *AvrL567* and *AvrM* is conditioned by specific regions in N-terminal uptake domain. Functional analysis of additional

rust effectors is required to determine if they use a common pathway to be translocated on plant cells (Duplessis et al., 2011b). Also, the understanding of effector delivery system could be key for improving the bioinformatics methods for effector predictions (Sperschneider et al., 2016a).

In this chapter, we reported the functional characterization of the *AvrSr35* gene. We showed that *AvrSr35* is expressed at early stages of infection consistent with the pre-haustorial resistance mechanism predicted for the *Sr35* gene. By using several *in planta* assays, we demonstrated that *AvrSr35* triggers HR in presence of its complementary resistant gene *Sr35*. Subcellular localization experiments in tobacco leaves showed *AvrSr35* and *Sr35* gene products co-localize and likely accumulate in the endoplasmic reticulum (ER) and plasma membrane. Applying the methods of co-immunoprecipitation (co-IP) and bi-molecular fluorescence complementation (BiFC) we confirmed that the *AvrSr35* and *Sr35* proteins interact in plant cells.

4.2 Objectives

- Evaluate the changes in gene expression of the *AvrSr35* gene candidate during early stages of infection.
- Demonstrate the avirulence function of *AvrSr35* using *in planta* assays.
- Study the subcellular localization of both *AvrSr35* and *Sr35* proteins in tobacco.
- Investigate the interaction between *AvrSr35* and *Sr35* proteins using co-IP and BiFC.

4.3 Materials and methods

4.3.1 Plant material

Susceptible cultivar Marquis (*Sr35* -) and resistant cultivar Marquis-*Sr35* (Mq(2)/5*G2919) (*Sr35*+) were used for *in planta* assays of *AvrSr35* heterologous protein infiltration. Hexaploid wheat cultivar Fielder was used as host to measure the expression of candidate *AvrSr35* after the infection with the *Pgt* race RKQQC. Four to five weeks-old *N. benthamiana* leaves were used for agroinfiltration to validate *in planta* the *AvrSr35* avirulent activity and protein-protein interaction.

4.3.2 Bacterial strains

Escherichia coli DH5 α (Life Technologies, Carlsbad, CA) was used for transformation by electroporation and plasmid propagation. *Escherichia coli* BL21 (DE3) was used for heterologous protein expression. *Agrobacterium tumefaciens* strain C5851 was used for agroinfiltration on *N. benthamiana*.

4.3.3 Time course expression analysis of *AvrSr35*

Seedlings (12 days old) from wheat cultivar Fielder were inoculated by spraying a spore suspension *Pgt* race RKQQC (Section 3.3.2). Total RNAs were isolated from leaf tissue harvested at 0, 24, 48, and 96 hours after transfer the seedlings from the dew chamber to the growth chamber and their quality were determined according to the section 3.3.5. Specific primers for *AvrSr35* were designed with Beacon designerTM (PrimerBiosoft) where the reverse primer spanned the exons 2 and 3 boundaries. Once total RNAs quantity and quality were assessed, 1 μ g total RNA was treated with 1 μ l of DNase I amplification grade (1 U/ μ l) (Invitrogen Inc, Carlsbad, CA) in a final volume of 10 μ l according to manufacturer's instructions. cDNAs were obtained from each sample using ~0.8 μ g of DNase treated RNA, which were reverse transcribed with 1 mM of Oligo (dT)₂₀, 0.5 mM dNTP mix and 1 μ L Superscript III reverse transcriptase (200 U/ μ l) (Invitrogen, Carlsbad, CA) in a final volume of 20 μ L following the manufacturer's instructions. The qRT-PCRs were performed in a CFX96 TouchTM real-time PCR detection system (BioRad, Hercules, CA) using SYBR[®] Green to monitor dsDNA synthesis.

Reactions were prepared containing 5 μ L of 2X IQTM SYBR[®] Green Super Mix reagent (BioRad, Hercules, CA), 1 μ L of cDNA and 250 nM of the *AvrSr35* gene-specific primers s2351_156F and s2351_323R (Table 4.1) in a final volume of 10 μ l. The following thermal profile was used for all PCRs: 95°C for 3 min; 40 cycles of 95°C for 15 sec, 60°C for 30 sec and 72°C for 40 sec. At the end of this profile, the PCR samples were subjected to an automatic dissociation analysis to confirm the specificity of the amplicon. Two technical replications were performed for cDNA at each time point. Data were analyzed using the CFX ManagerTM software v.2.1 (BioRad, Hercules, CA). Primer amplification efficiency for every primer set was

calculated from the slopes of a calibration curve of serial dilutions of cDNA (Pfaffl, 2004), Ct values were used to calculate the relative change in gene expression relative to the tubulin gene (Scholtz & Visser, 2013), by using the Δ Ct method (Livak & Schmittgen, 2001). Expression values for each time point were based on three biological replicates and two independent technical replications.

4.3.4 Tobacco agroinfiltration

4.3.4.1 Binary vector construction for *N. benthamiana* agroinfiltration

A list of primers and vectors used for *in planta* experiments is shown in Table 4.1, 4.2 and figure 4.1. For tobacco infiltration vector constructions were made using the binary vectors pIPKb004 (Himmelbach et al., 2007), pSITE (Chakrabarty et al., 2007) and Gateway[®] technology (Life Technologies, Carlsbad, CA). Modified primers carrying the attB1 and attB2 recombination sites were designed to be present on both sides of target sequences amplified by PCR, facilitating the recombination reaction (Table 4.1). Primers s2351_1433F2_attb1 and s2351_3766R_attb2 were used to amplify the entire coding sequence or open reading frame (ORF) of the *AvrSr35* gene to create the binary vector pAvrSr35-ORF-TDNA. Primers s2351_1508F1_attb1 and s2351_3766R_attb2 were used to amplify the coding sequence of the mature protein of the *AvrSr35* gene without the deduced signal peptide (-SP) (AA27-578) to create the binary vector pAvrSr35- Δ SP-TDNA. The primers s2351_1508F1_attb1 and AvrSr35_Q72_attB2_rev were used to create the construct pAvrSr35(Q72*)- Δ SP which is truncated versions of the *AvrSr35* without signal peptide.

Table 4.1. Primer list used for binary vector construction.

Name	Sequence	Use
AvrSr35_Q72_attB2_rev	GGGGACCACTTTGTACAAGAAAGCTGGGTCTAAACATTTGAATCTACCAAATCAGATGTG	Creation of Avr-Q72 truncated mutant
s2351_1508F1_attb1	GGGGACAAGTTTGTACAAAAAAGCAGGCTATGGCCATGAGGAACTTTGCTGC	Construction of AvrSr35-SP-TDNA
s2351_1433F2_attb1	ACAAGTTTGTACAAAAAAGCAGGCTCTCCAACCACCATGGCCATGAGGAACTTTGCTGC	Construction of AvrSr35-ORF-TDNA
s2351_3766R_attb2	TCCGCCACCACCAACCACTTTGTACAAGAAAGCTGGGTACAATTTGCCTTCATGAACATT	Construction of AvrSr35-SP-TDNA
s2351_1508F2	ATGGCCATGAGGAACTTTGCTGC	Construction of the pET-SUMO-AvrSr35-SP
s2351_1508F2_attb1	GGG GACAAGTTTGTACAAAAAAGCAGGCTGCCATGAGGAACTTTGCTGC	Amplification of <i>AvrSr35</i> for EThAN
Flag_Sr35_rev	TCACTTATCGTCGTCATCCTTGTAATCCCATATATCGAGGATGGGACGGTTG	Binary vectors for CoIP experiments
AttB2_flag_rev	GGGGACCACTTTGTACAAGAAAGCTGGGTTCCTTATCGTCGTCATCCTTGTAATC	Binary vectors for CoIP experiments
HA_tag_s2351_for	ATGTACCCATACGATGTTCCAGATTACGCTGCCATGAGGAACTTTGCTGC	Binary vectors for CoIP experiments
AttB1_HA_tag_for	GGGGACAAGTTTGTACAAAAAAGCAGGCTACCATGTACCCATACGATGTTCCAGATTACG	Binary vectors for CoIP experiments
attB1_Sr35_for	GGGGACAAGTTTGTACAAAAAAGCAGGCTACCATGGAGATTGCCATGGGGGCTATC	Binary vectors for CoIP experiments
s2351_156F	GGCACTGTCTAAGTCCAT	Expression analysis <i>AvrSr35</i>
s2351_323R	GTTCCAGGCTCTTGTCT	Expression analysis <i>AvrSr35</i>
Tubulin_F	CAAGGAGGTGGACGAGCAGATG	Expression analysis <i>AvrSr35</i>
Tubulin_R	GACTTGACGTTGTTGGGGATCCA	Expression analysis <i>AvrSr35</i>
NbPP2A_F	GACCCTGATGTTGATGTTGCT/	Expression coinfiltration constructs
NbPP2A_R	GAGGGATTTGAAGAGAGATTTTC	Expression coinfiltration constructs
AVR_qPCR_for1	CCATGAGGAACTTTGCTGCA	Expression coinfiltration constructs
AVR_qPCR_rev1	GAATCTACCAAATCAGATGTGTCTGG	Expression coinfiltration constructs
Sr35_Rev1	CTCATTGAAGTAGCTGTCACCGAGCTC	Expression coinfiltration constructs
Sr35_For1	CTTTGGCAAGAGTCGTCCTTGCTAACC	Expression coinfiltration constructs

For cloning *AvrSr35* and *Sr35* sequences with the tag epitopes FLAG and HA, the primer combinations attB1_Sr35_for with primer Flag_Sr35_rev and the primer combinations HA_tag_s2351_for with primer s2351_3766R_attb2 were used to generate PCR products that were used as template to amplify a second round of PCR product. The second round of PCRs were carried out using the primers combination attB1_Sr35_for and AttB2_flag_rev and the primer combinations AttB1_HA_tag_for and s2351_3766R_attb2 to create the constructs pSr35-Flag-TDNA and pHA-AvrSr35-ΔSP-TDNA respectively. PCR reactions for Gateway[®] technology cloning was performed using 0.2 μM of forward and reverse primer 1X Q5 PCR buffer (New England Biolabs, Ipswich, MA) containing 2.5 mM MgCl₂ 0.2 mM dNTP's, 0.2 μl Q5[®] high-fidelity DNA polymerase (5U/ μl) (New England Biolabs, Ipswich, MA) and 1 ng of the template (pGEMT-AvrSr35 plasmid or *Sr35* CDS). PCR reaction was denatured at 94°C for 5 min followed by 35 cycles at 94°C for 15 sec, 58°C for 30 sec and 72°C for 2 min and a final extension of 72°C for 7 min. PCR products were cloned in pGEMT-easy (Promega, Madison, WI) according to the manufacturer's instructions. Plasmids were used to transfer the sequence into the pDONR-Zeo vector by Gateway[®] BP cloning (Life Technologies, Carlsbad, CA) and then transferred into destination vector pPKb004 by Gateway[®] LR cloning (Life Technologies, Carlsbad, CA) (Figure 4.1). Constructs sequence correctness was confirmed by Sanger sequencing (Section 3.3.9).

The postdoctoral research associate Dr. William Rutter provided nine constructs used in this research (Table 4.2. Figure 4.1). Those constructs were used for HR test on tobacco plants, and include the construct pSr35-TDNA which carried the CDS of *Sr35*; the construct pSr35(K206L)-TDNA with a mutation in the P-loop motif of the NBS domain of *Sr35* gene associated with loss-of-function of the gene (Marone et al., 2013), and the construct pSr35v1120-TDNA which carried three natural occurring mutations in the LRR domain of *Sr35* (Saintenac et al., 2013). Dr. Rutter provided the constructs pSr35(K206L)-GFP and pAvrSr35-ΔSP-mRFP used for sub-cellular localization of *AvrSr35* and *Sr35*. Finally, Dr. Rutter shared bimolecular fluorescent complementation (BiFC) assay data generated by using the constructs pSr35(K206L)-cYFP, pSr35(K206L)_{M1120}-cYFP, pSr35(K206L+Q464*)-cYFP and pnYFP-AvrSr35-ΔSP. Dr. Jorge Dubcosky provided the construct pGWBS Sr35gDNA-auto with the auto-activate mutant form of *Sr35* used as control in HR test on tobacco plants.

Table 4.2. Summary of vectors used *in planta* assay experiments.

Construct Name	Experiment	Vector backbone	Antibiotic	Insert description	Produced by
pGEMT-cDNA-AvrSr35	Cloning of RT-PCR product	pGEM-T(TA cloning)	Ampicillin	AvrSr35 (AA1-578)	Andres Salcedo
pAvrSr35-ORF-TDNA	Tobacco HR assay	pIPKb004 (Gateway destination vector)	Streptomycin	CaMV 35S - AvrSr35 (AA1-578)	Andres Salcedo
pAvrSr35-ΔSP-TDNA	Tobacco HR assay	pIPKb004 (Gateway destination vector)	Streptomycin	CaMV 35S - AvrSr35 (AA27-578)	Andres Salcedo
pAvrSr35(Q72*)-ΔSP	Tobacco HR assay	pIPKb004 (Gateway destination vector)	Streptomycin	CaMV 35S - AvrSr35(AA27-71)	Andres Salcedo
pSr35-TDNA	Tobacco HR assay	pIPKb004 (Gateway destination vector)	Streptomycin	CaMV 35S - Sr35 (AA1-919)	William Rutter
pSr35(K206L)-TDNA	Tobacco HR assay	pIPKb004 (Gateway destination vector)	Streptomycin	CaMV 35S - Sr35 (AA1-919); p.K206L Sr35(AA1-919);	William Rutter
pSr35v1120-TDNA	Tobacco HR assay	pIPKb004 (Gateway destination vector)	Streptomycin	p.R854H+W856R+T858S	William Rutter
pSr35(K206L)-GFP	Sub-cellular localization	pSITE-4NA (Gateway Destination vector)	Kanamycin	Fusion of Sr35(AA1-919) to the C-terminal of GFP CDS	William Rutter
pAvrSr35-ΔSP-mRFP	Sub-cellular localization	pSITE-4NA (Gateway Destination vector)	Kanamycin	Fusion of AvrSr35(AA27-578) to the C-terminal of mRFP CDS	William Rutter
pSr35(K206L)-cYFP	BiFC	pIPKb004 (Gateway destination vector)	Streptomycin	Fusion of CaMV 35S - Sr35(AA1-919); p.K206L to the C-terminal domain of eYFP (AA155-239)	William Rutter
pnYFP-AvrSr35-ΔSP	BiFC	pIPKb004 (Gateway destination vector)	Streptomycin	CaMV 35S - AvrSr35(AA27-578) N-terminal fusion with eYFP (AA1-154)	William Rutter
pSr35(K206L) _{M1120} -cYFP	BiFC	pIPKb004 (Gateway destination vector)	Streptomycin	CaMV 35S - Sr35(AA1-919);p.K206L +R854H+W856R+T858S to the C-terminal domain of eYFP (AA155-239)	William Rutter
pSr35(K206L+Q464*)-cYFP	BiFC	pIPKb004 (Gateway destination vector)	Streptomycin	CaMV 35S - Sr35(AA1-919); p.K206L+Q464* to the C-terminal domain of eYFP (AA155-239)	William Rutter
pET-SUMO-AvrSr35-ΔSP	Protein expression	pET-SUMO (TA cloning)	Kanamycin	AvrSr35 (AA27-578)	Andres Salcedo
pSr35-Flag-TDNA	CoIP	pIPKb004 (Gateway destination vector)	Streptomycin	CaMV 35S - Sr35 (AA1-919)-Flag	Andres Salcedo
pHA-AvrSr35-ΔSP-TDNA	CoIP	pIPKb004 (Gateway destination vector)	Streptomycin	CaMV 35S – HA-AvrSr35 (AA27-578)	Andres Salcedo

HR: hypersensitive response, BiFC: Bifluorescence complementation and CoIP: Coimmunoprecipitation.

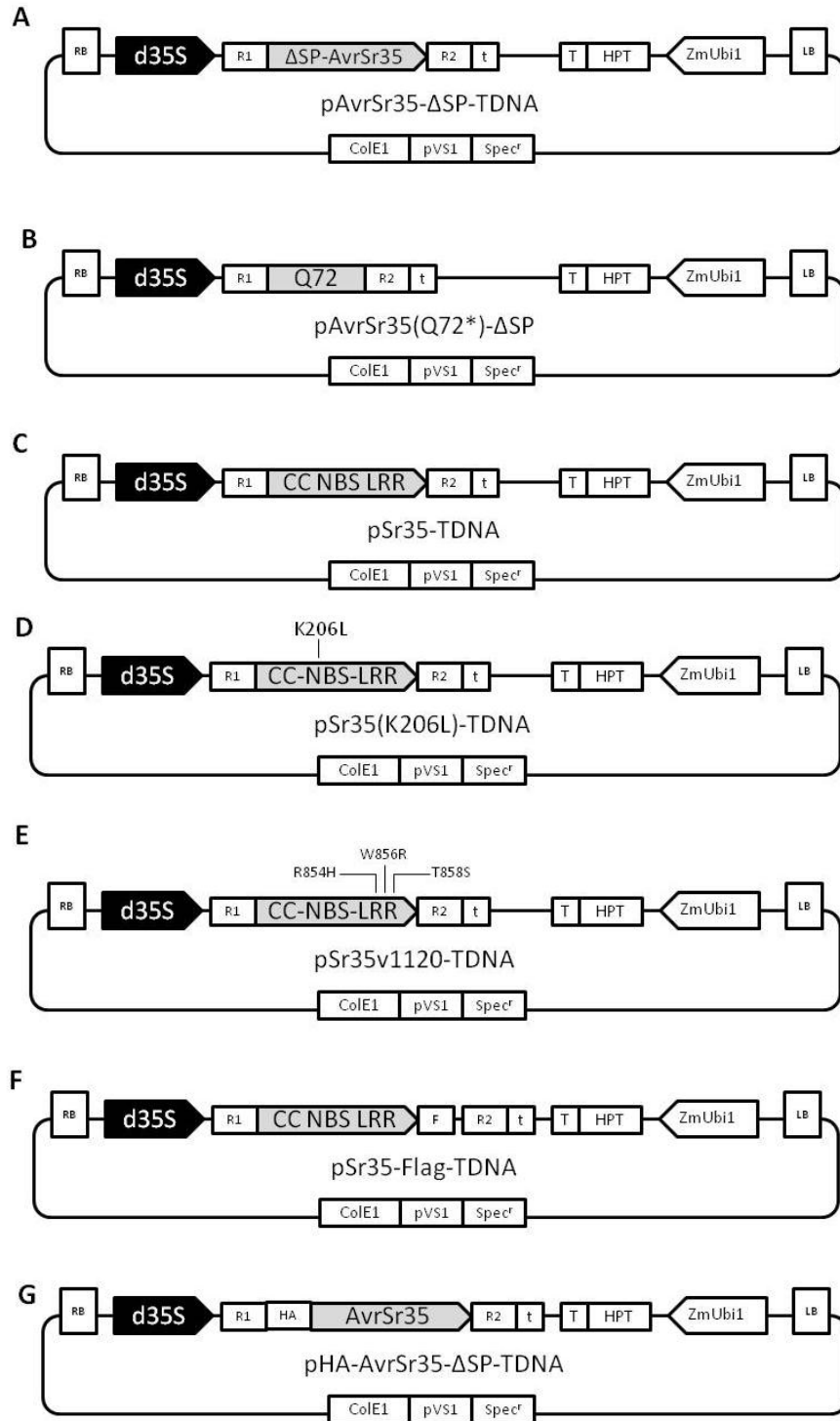


Figure 4.1. Binary vectors used in *N. benthamiana* agroinfiltration. All constructs were produced using Gateway[®] technology and the backbone of the binary vector pIPkb004 (Gene bank EU161570) (Himmelbach et al., 2007). Components of vector **SP** Signal peptide, **RB** (right border), **LB** (left border), **d35S** (double 35S promoter), **R1** and **R2** (attR2 recombination attachment site sequences), **t** (*A. tumefaciens* nos terminator), **T** (the CaMV 35S termination

signal), **ColE1** (origin of replication for *E. coli*), **pVS1** (origin of replication for *A. tumefaciens*), **Spec^r** (streptomycin/ spectinomycin bacterial resistance), **Hpt^r** (hygromycin phosphotransferase), **ZmUbi1** (the ubiquitin 1 maize promoter), **F** FLAG-tag epitope (DYKDDDDK), **HA** Human influenza hemagglutinin tag epitope (YPYDVPDYA).

4.3.4.2 *Agrobacterium* transformation

Agrobacterium chemical competent cells were prepared by inoculating a single colony of *Agrobacterium tumefaciens* strain C58C1 into 25 ml of LB media. LB culture was grown at 28°C (250 rpm) overnight, and 2 ml of this overnight culture was transferred to 100 ml of LB media. Bacterial culture was grown at 28°C (250 rpm) for 4 hours and then centrifuged at 4,000 x g for 5 min at 4°C. The supernatant was removed, and cells were resuspended in 4 ml of ice-cold 20 mM CaCl₂. Aliquots (150 µL) were stored in microfuge tubes, frozen instantly with liquid nitrogen and stored at -80°C.

Agrobacterium transformation was performed by mixing 0.1-1 µg of binary vector DNA with competent cells (thawed on ice for 30 min) followed by incubating on ice for 5 min. The mixture was flash frozen in liquid nitrogen and thawed at 37°C in a water bath for 5 min. Cells were transferred to a 15 ml tubes with 1 ml of LB media and shaken at 250 rpm at 28°C for 3-4 hours. Cells were collected by centrifugation 2 min at 5,000 rpm, resuspended in 200 µl of LB media and plated on LB plates containing rifampicin (10 µg/ml) and spectinomycin (50 µg/ml). Plates were incubated at 30°C for two days.

4.3.4.3 *Agrobacterium* mediated transient assay in *N. benthamiana*

Transient expression of gene constructs was carried out in 4–5 weeks-old *N. benthamiana* plants. *N. benthamiana* plants were grown at a 22/20°C day/night temperature cycle and 16-h light/8-h-dark cycle in a growth chamber. Five ml of LB supplemented with rifampicin (10 µg/ml) and spectinomycin (50 µg/ml) was inoculated with a single colony of *A. tumefaciens* C5851 harboring a binary vector (Table 4.2, Figure 4.1) and growth overnight at 28°C. One ml of the overnight starter culture was inoculated into 25 ml of LB media supplemented with rifampicin (10 µg/ml), spectinomycin (50 µg/ml) and 20 µM of acetosyringone (Sigma, St Louis, MO). The cell cultures were grown overnight until they reached an OD₆₀₀ = 0.6 - 2. Cells were harvested by

centrifugation (5,000 x g, 15 min) and the pellets were gently resuspended in the infiltration solution (MgCl₂ 10 mM, MES-KOH 0.5 M pH 5.6 sterile). Acetosyringone was added to the infiltration solution to a final concentration of 100 µM immediately before OD adjusting. Bacterial cultures were adjusted until a final OD₆₀₀ = 0.25 and incubated at room temperature for 3 hours. Bacterial cultures containing different binary vectors were mixed in equal proportions immediately before to infiltration. Infiltrations were performed on the abaxial side of the second and third leaves using a 1 ml needleless syringe. Co-infiltrated plants were kept at room temperature (25°C), and leaves were scored between 36 and 72 hours post-infiltration at the first visible symptom of hypersensitive response (HR). *In planta* expression of each construct was assayed by extracting total RNA from leaf sections infiltrated with individual *Agrobacterium* culture as was described in section 3.3.5. RNA samples were treated with 1 µl of DNase I amplification grade (1 U/µl) (Invitrogen Inc, Carlsbad, CA) in a final volume of 10 µl according to manufacturer's instructions. cDNA was obtained from each sample using ~0.8 µg of DNase treated RNA, which were reverse transcribed with 1 mM of Oligo (dT)₂₀, 0.5 mM dNTP mix and 1 µL Superscript III reverse transcriptase (200 U/µl) (Invitrogen, Carlsbad, CA) in a final volume of 20 µL following the manufacturer's instructions. The presence of constructs transcripts was tested using gene-specific primers for *Sr35*, *AvrSr35* and the housekeeping gene Protein phosphatase 2A (NbPP2A, Genebank TC21939) (Liu et al., 2012) (Table 4.1).

4.3.4.4 Hypersensitive response evaluation using 3'3-DAB uptake method

Co-infiltrated leaves of *N. benthamiana* were assayed for the presence of reactive oxygen species using the 3'3 diaminobenzidine (3'3-DAB) uptake method previously described by Thordal-Christensen et al. (1997). Briefly, co-infiltrated leaves were harvested 20 hours after infiltration, before visible signs of HR were visible. Leaves were incubated for 9 hours in a 3'3-DAB (Sigma, St Louis, MO) (1 mg/mL, pH 3.8) solution, and subsequently cleared by boiling in 96% ethanol for 10 min. Leaves were washed with ddH₂O and preserved with 70% ethanol, and then pictures were taken.

4.3.5 Infiltration of AvrSr35 heterologous protein on wheat

4.3.5.1 Construction of recombinant expression vectors

The coding sequence of mature protein of the *AvrSr35* without the predicted signal peptide (SP) was amplified using primers: forward s2351-1508F2 and s2351-3766R added at 0.4 μ M, 10 μ l of the 2X Phusion[®] High-Fidelity PCR Master Mix (New England Biolabs, Ipswich, MA) and 1 ng of the plasmid pGEMT-AvrSr35 as template (Section 3.3.8). PCR was denatured at 98°C for 5 min followed by 30 cycles at 98°C for 15 sec, 60°C for 30 sec, 72°C for 2 min, and a final extension at 72°C for 7 min. A-overhangs were added by transferring 2 μ l of PCR product which was added to a reaction mixture containing 2.5 mM of MgCl₂, 0.2 mM dATP, 1 μ l of 10X PCR buffer and 5 U of recombinant taq polymerase (Thermo Fisher Scientific, Waltham, MA). The mixture was then incubated at 70°C for 15 min. AvrSr35- Δ SP protein was expressed using Champion[™] pET SUMO Protein Expression System kit (Invitrogen, Carlsbad, CA) according to the manufacturer's instructions. Briefly, the PCR fragment with the A-overhangs was cloned into pET SUMO vector to make the pET-SUMO-AvrSr35- Δ SP (Table 4.2), which was transformed into *E. coli* BL21 (DE3) chemically competent cells. The presence and orientation of the insert was confirmed by PCR, the correctness of the construct was confirmed by Sanger sequencing (Section 3.3.8).

4.3.5.2 Expression, detection, purification and cleavage of (–SP) AvrSr35 recombinant protein

A single colony of *E. coli* BL21 (DE3) with the pET-SUMO-AvrSr35- Δ SP construct was grown overnight in 5 ml of LB media pre-culture supplemented with 1% of glucose and 50 μ g/ml of kanamycin. The overnight culture (2.5 ml) was used to inoculate 500 ml of LB media supplemented with 1% of glucose and 50 μ g/ml of kanamycin. The culture was grown at 37°C, 250 rpm until it reached OD₆₀₀ = 0.5. The expression of the heterologous protein was induced by adding isopropyl-b-D thiogalactopyranoside (IPTG) (Invitrogen, Carlsbad, CA) to a final concentration of 0.5 mM. The culture was incubated overnight at 25°C, with agitation (250 rpm). Samples of the uninduced and IPTG-induced bacterial cultures were taken to analyze the soluble and insoluble protein fraction.

Cells were harvested by centrifugation at 10,000 x g for 15 min at 4°C. Cell pellet was suspended in 50 ml of lysis buffer: 50 mM sodium phosphate buffer pH 6.8, 300 mM NaCl, 10 mM imidazole, 10 mM phenylmethylsulfonyl fluoride and 0.05 mg of lysozyme (Thermo Fisher Scientific, Waltham, MA). The suspension was incubated for two hours in a cold room (~4 – 6°C) using a rocket platform shaker, and then it was subjected to three cycles of freezing and thawing using liquid nitrogen and a water bath set at 42°C. Cell lysate was harvested by centrifugation at 10,000 x g for 20 min at 4°C. The upper phase was transferred to a 50 ml tube and kept on ice.

The AvrSr35-ΔSP recombinant protein was purified using HisPur Ni-NTA spin columns (Thermo Fisher Scientific, Waltham, MA). The columns were first equilibrated using two resin-bed volumes of equilibration buffer (50 mM sodium phosphate buffer pH 6.8, 300 mM NaCl, 10 mM imidazole), followed by centrifugation at 700 x g for 2 min at 4°C. Cell lysate was added to the column and centrifuged at 700 x g for 2 min at 4°C. The Ni-NTA resin was washed with 8 resin-bed volumes of wash buffer (50 mM sodium phosphate buffer pH 6.8, 300 mM NaCl, 20 mM imidazole) followed by centrifugation at 700 x g for 2 min at 4°C. The AvrSr35-ΔSP recombinant protein was collected from the column by five successive elutions using a bed volume of elution buffer (50 mM sodium phosphate buffer pH 6.8, 300 mM NaCl, 150 mM imidazole) followed by centrifugation at 700 x g for 2 min at 4°C. Protein concentration was determined using the Bradford method (Bradford, 1976) using the Biorad protein assay dye (Bio-Rad, Hercules, CA) and serial dilutions of bovine serum albumin (BSA) as standard. Protein expression was analyzed in a 10% SDS PAGE. Approximately 5 mg of purified AvrSr35-ΔSP recombinant protein were cleaved with 100 units of SUMO protease (Thermo Fisher Scientific, Waltham, MA) and 1X SUMO protease buffer by incubating the mixture for 16 hours at 4°C. Cleaved protein was analyzed in a 10% SDS-PAGE to confirm the N-terminal cleavage. SDS-PAGE was stained by immersing the gel in a solution of Coomassie blue dye G-250, 10% of acetic acid (Sigma, St Louis, MO) and heating in a microwave for 1 minute 30 sec. The gels were de-stained in 10% solution of acetic acid overnight.

Cleaved AvrSr35-ΔSP protein was dialyzed using a Slide-A-Lyzer™ Dialysis kit (Thermo Fisher Scientific, Waltham, MA). The Slide-A-Lyzer cassette containing the cleaved protein was

dialyzed in 5 L of ddH₂O with stirring overnight in a cold room (~4 – 6°C). After dialysis, the protein was purified using HisPur Ni-NTA spin columns (Thermo Fisher Scientific, Waltham, MA). The columns were equilibrated with two resin bed volumes of ddH₂O, followed by centrifugation at 700 x g for 2 min at 4°C. The dialyzed protein was passed through the column by centrifugation at 700 x g for 2 min at 4°C. The flow-through containing AvrSr35-ΔSP protein was collected, frozen in liquid nitrogen and lyophilized for at least 24 hours using a Labconco FreeZone[®] 6 Liter Benchtop Freeze Dry Systems (Labconco Corporation, Kansas City, MO) under vacuum (0.08 mBar) and a condenser temperature set at -50°C for at least 24 hours. Lyophilized protein was dissolved in 1 ml of ice-cold PBS 1X (Phosphate Buffer Saline). The final protein concentration was determined by the Bradford method (Bradford, 1976) using the Bio-Rad protein assay dye (BioRad, Hercules, CA) and serial dilutions of bovine serum albumin (BSA) as standard. Primary leaf (12 days old) of resistant genotype Marquis-Sr35 (*Sr35+*) and susceptible genotype Marquis (*Sr35-*) were infiltrated with a needleless syringe from the abaxial side of the leaf. Infiltration was made with AvrSr35-ΔSP protein at different concentrations ranging from 0.001 to 0.5 mg/mL in 1X PBS. Bovine serum albumin (BSA) was used as control at the same range of concentrations. Infiltrated seedlings were kept at 22°C, photoperiod of 16 hours, 40-50% relative humidity. Infiltrated wheat leaves were evaluated for HR 24-48 hours after infiltration.

4.3.6 Subcellular localization in *N. benthamiana* leaves

Fluorescent fusion constructs for subcellular localization were produced by cloning the coding sequence to the pSITE Gateway[®] destination vectors (Chakrabarty et al., 2007). The coding sequence of *AvrSr35* gene without signal peptide (AA27-578) was cloned in the binary vector pSITE-4NA and fused to the monomeric red fluorescent protein (RFP). The CDS of *Sr35* was cloned into pSITE-2NB vector fused to the enhanced green fluorescent protein (GFP). Constructs sequence correctness was confirmed by Sanger sequencing (Section 3.3.9). Constructs were transformed into *Agrobacterium* strain C58C1, and co-infiltrated into the *N. benthamiana* leaves as described above (Section 4.3.4.3). Leaf sections were cut and soaked in perfluorodecalin (PFD) (Sigma, St Louis, MO) to increase confocal image resolution and depth. Cell plasmolysis was induced by adding a 0.8 M mannitol solution (Sigma, St Louis, MO).

Fluorescence microscopy on leaf sections was carried out using an LSM 780 Confocal Laser Scanning Microscope (Zeiss, Oberkochen, Germany) at 40X magnification. The GFP and RFP were detected using 488 nm and 561 nm excitation laser, respectively, and fluorescence scanning with 490-535 and 588-615 nm filters respectively. Data image processing was carried out using Zeiss ZEN v8.1 (Zeiss, Oberkochen, Germany).

4.3.7 Bimolecular fluorescent complementation (BiFC) assay in *N. benthamiana* leaves

The interaction between the *AvrSr35* and *Sr35* gene products was tested *in planta* by the Bimolecular fluorescent complementation (BiFC) assay. BiFC was performed using three mutant versions of the *Sr35* gene in the constructs pSr35(K206L)-cYFP, pSr35(K206L)_{M1120}-cYFP and pSr35(K206L+Q464*)-cYFP combined with the *AvrSr35* gene without signal peptide in the construct pnYFP-AvrSr35- Δ SP. *AvrSr35* and *Sr35* mutant sequences were fused with the N-terminal (1–174 AA) or the C-terminal (175–239 AA) portions of the yellow fluorescent protein (nYFP or cYFP, respectively). Fusion sequences were produced by fusion PCR. This technique fuses two primary PCR products (in this case target gene and a portion of YFP) using a set of nested primers (Hobert, 2002). Constructs were transformed into *Agrobacterium* strain C58C1 and co-infiltrated into the *N. benthamiana* leaves as described above (Section 4.3.4.3). The interaction between the gene constructs was inferred based on the appearance of YFP-specific fluorescence signal on leaf sections using an LSM 780 Confocal Laser Scanning Microscope (Zeiss, Oberkochen, Germany) at 40X magnification. YFP was detected using 488 nm excitation laser and fluorescence scanning with 490-535nm filters. Image processing was carried out using Zeiss ZEN v8.1 (Zeiss, Oberkochen, Germany).

4.3.8 Co-immunoprecipitation assay

The plasmids pSr35-Flag-TDNA and pHA-AvrSr35- Δ SP-TDNA with the FLAG epitope on C-terminal and with the HA epitope on the N-terminal region, respectively, were individually transformed into *Agrobacterium tumefaciens* strain C5851. *Agrobacterium* strains cultures containing each binary construct were grown to OD₆₀₀ = 1 and mixed in equal proportions immediately before to the infiltrations. All *N. benthamiana* infiltrations were performed on 4-5

week old plants as described by Ma et al. (2012b). The controls were non-infiltrated tobacco and single-construct infiltrations with each construct. Protein complex co-immunoprecipitations were performed according to Steinbrenner et al. (2014) using μ MACSTM anti-human influenza hemagglutinin (HA) and DYKDDDDK (FLAG) microbeads (Miltenyl Biotec, Germany). Immunoprecipitation input and output samples were separated on the 10% SDS-PAGE gels until the dye front reached the bottom of the gel. Then the proteins were transferred to the PVDF membranes for one hour at 100V in Western blot buffer (25 mM Tris pH 8.3, 192 mM Glycine and 20% Methanol). After the transfer, the membranes were washed once with TBS (10 mM Tris-HCl pH 8.0, 150 mM NaCl). The membranes were then blocked using 5% BSA (Sigma, St Louis, MO) in TBST (10 mM Tris-HCl pH 8.0, 150 mM NaCl, 0.05% Tween 20) and incubated overnight at 4°C using a rocket platform shaker. Membranes were incubated for one hour at room temperature with specific antibodies anti-FLAG antibody, or anti-HA antibody diluted 1:6,000 (Roche Applied Science) in 5% BSA dissolved TBST followed by four washes using TBST (10 min each). Membranes were incubated in TBST buffer in a fridge (4-6°C) for one week. Proteins were detected using Super Signal West Femto Chemiluminescent Substrate (Thermo Fisher Scientific, Waltham, MA), following the manufacturer's instructions. Images were acquired using an Odyssey Fc Imaging System (LI-COR Biosciences, Lincoln, NE) and analyzed using Image StudioTM Lite v 3.1 (LI-COR Biosciences Lincoln, NE).

4.4 Results

4.4.1 Time course gene expression of *AvrSr35* during the infection

The changes in the expression of the *AvrSr35* were measured on leaves of Fielder cultivar infected with the *Pgt* race RKQQC. Leaf tissues were collected at 0, 24, 48, and 96 hours after infection (HAI). A primer set for gene expression was designed using Beacon designerTM (PrimerBiosoft), where the reverse primer was designed for spanning exon 2-3 boundaries avoiding genomic DNA nonspecific amplification. The primer efficiency for the reference gene (tubulin) and target gene were comparable being calculated as 105% and 106%, respectively. Primers specificity was evaluated *in silico* using BlastX against NCBI database, the RKQQC genome assembly and *in vitro* by melting curves of the qRT-PCR product. The analysis of the *AvrSr35* gene showed a progressive increase of transcript levels expression to nearly 18 times at

96 HAI compared to the amount of the transcript detected in the infected tissues right after transferring plants to the growth chamber (Figure 4.2).

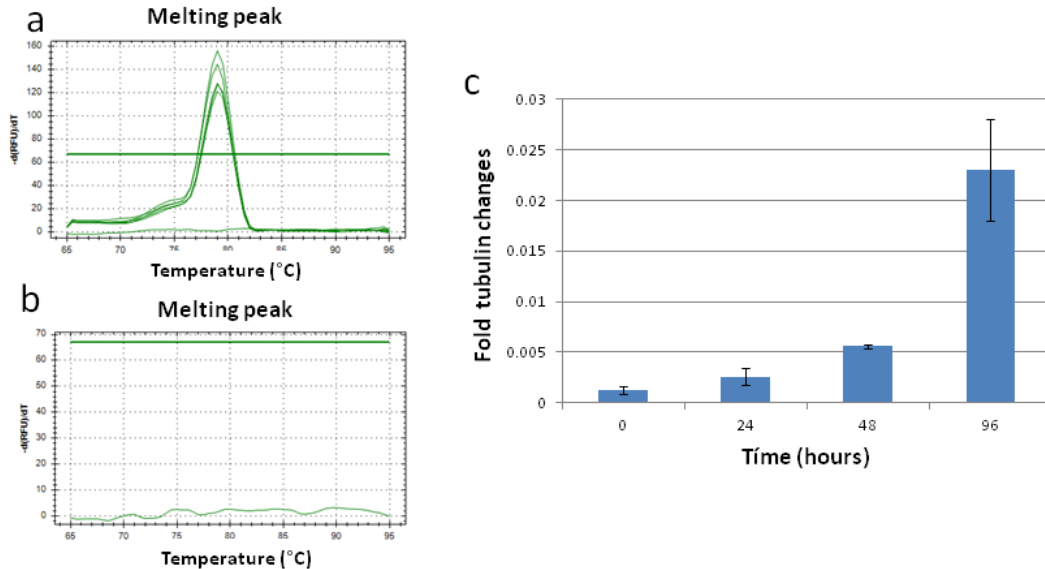


Figure 4.2. Relative expression of the *AvrSr35* gene during time course of infection with *Pgt* race RKQQC. Dissociation analysis to determine the specificity of primer set used for qRT-PCR **a.** cDNA **b.** *Pgt*-RKQQC genomic DNA **c.** Transcript levels of the *AvrSr35* gene during infection of RKQQC on leaves of susceptible cultivar Fielder. Leaf samples started to be collected after the transfer from the dew chamber to growth chamber. Transcript levels are expressed relative to the tubulin gene internal control (Scholtz & Visser, 2013) using the $2^{-\Delta Ct}$ method (Livak & Schmittgen, 2001). Bars represent the standard errors of the mean based on three biological and two technical replicates.

4.4.2 Agroinfiltration of *N. benthamiana* leaves

The heterologous system based in transient expression on leaves of *N. benthamiana* was used to evaluate the *Sr35*-dependent HR activation in presence of the *AvrSr35*. Preliminary experiments and optimization of the system were conducted by the postdoctoral research associate William Rutter. Initially, the constructs containing the entire ORF of the *AvrSr35* gene, which encode for a protein with a deduced signal peptide (pAvrSr35-ORF-TDNA), and the version without signal peptide (pAvrSr35- Δ SP-TDNA) were co-agroinfiltrated independently with the construct that carries the CDS for *Sr35* (pSr35-TDNA). The co-agroinfiltration of both *AvrSr35* constructs with *Sr35* induced visible HR after 48 hours, which was comparable with the cell death observed in the control infiltration with of the auto-activated *Sr35* form. Within the considered timeframe, no

obvious cell death was observed in the leaves infiltrated with the single constructs carrying the *AvrSr35* or *Sr35* genes (Figure 4.3).

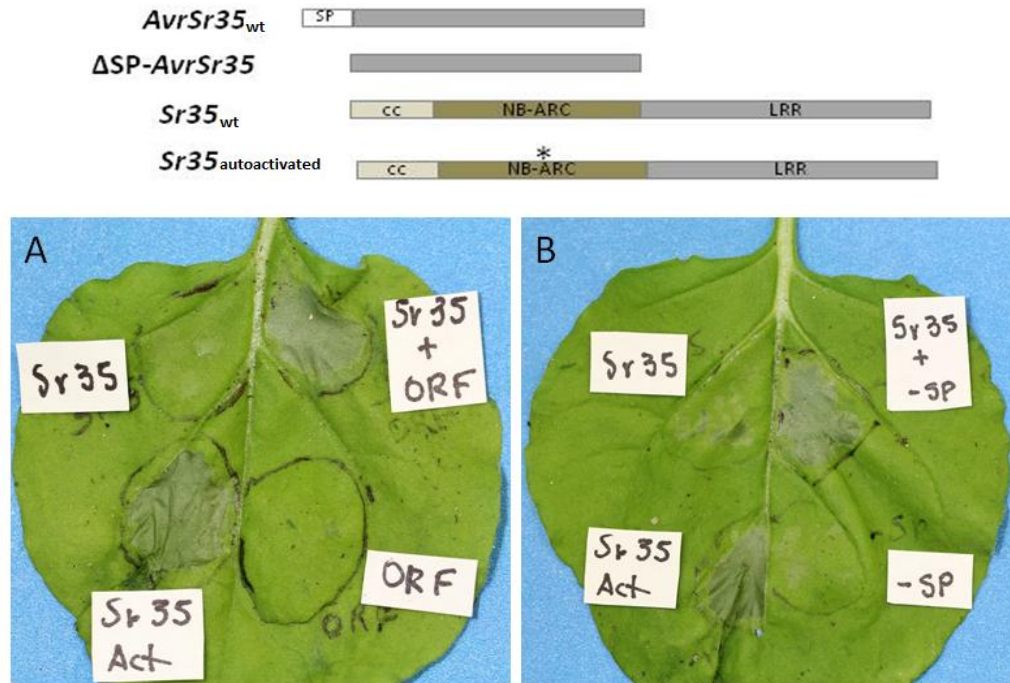


Figure 4.3. *AvrSr35* with and without deduced signal peptide (SP) induces HR in the presence of *Sr35* in *N. benthamiana* leaves. Pictures were taken 48 hours after agroinfiltration **Top:** Schematic representation of sequences cloned into the binary vectors used for agroinfiltration. Agroinfiltration of *AvrSr35* with (A) and (B) without signal peptide. *Sr35*_{wild type} (*Sr35*), *AvrSr35*_{wild type} (ORF), Δ SP *AvrSr35* (-SP), *Sr35*_{autoactivated} (*Sr35* Act).

To confirm the specific ability of *AvrSr35* to trigger *Sr35*-mediated HR, both the wild-type and mutated versions of *AvrSr35* and *Sr35* were agroinfiltrated into the *N. benthamiana* leaves (Figure 4.4). The combination of *AvrSr35* (construct pAvrSr35- Δ SP-TDNA) with *Sr35* (construct pSr35-TDNA) triggered HR after 48 hours of infiltration. However, HR was not detected when the *Sr35* gene constructs with the mutations in the P-loop (construct pSr35(K206L)-TDNA) or LRR domain (construct pSr35v1120-TDNA) were paired with the wild-type *AvrSr35* (construct pAvrSr35- Δ SP-TDNA). The former mutant version of the *Sr35* harbored an amino acid change (K206L) in the P-loop motif of the NB-ARC domain, which is critical for nucleotide binding and triggering of HR (Tamelung et al., 2006). The mutations in the LRR domain were first detected in the loss-of-function EMS mutant *sr35*¹¹²⁰ in *T. monococcum* accession G2919. The *sr35*¹¹²⁰ lost resistance to both the TTKSK (*Ug99*) and RKQQC compared

to the wild-type (Saintenac et al., 2013). Likewise, the combination of the wild-type *Sr35* construct with the truncated version of the *avrSr35* gene (Q72*) found in the *Pgt*-EMS mutant strain M11(Chapter 3) did not induce *Sr35*-dependent cell death.

HR has been associated with the accumulation of reactive oxygen species (ROS) that work as messenger of defense response, strengthening plant cell walls and as protective agent eliminating the pathogens (Thordal-Christensen et al., 1997; Lamb and Dixon, 1997; Dat et al., 2000). In this study, co-agroinfiltrated leaves of *N. benthamiana* were exposed to DAB (3,3-diaminobenzidine) for *in situ* detection of ROS. The accumulation of ROS was detected clearly after 20-24 hours of infiltration only in the combination of wild type *AvrSr35* and *Sr35*.

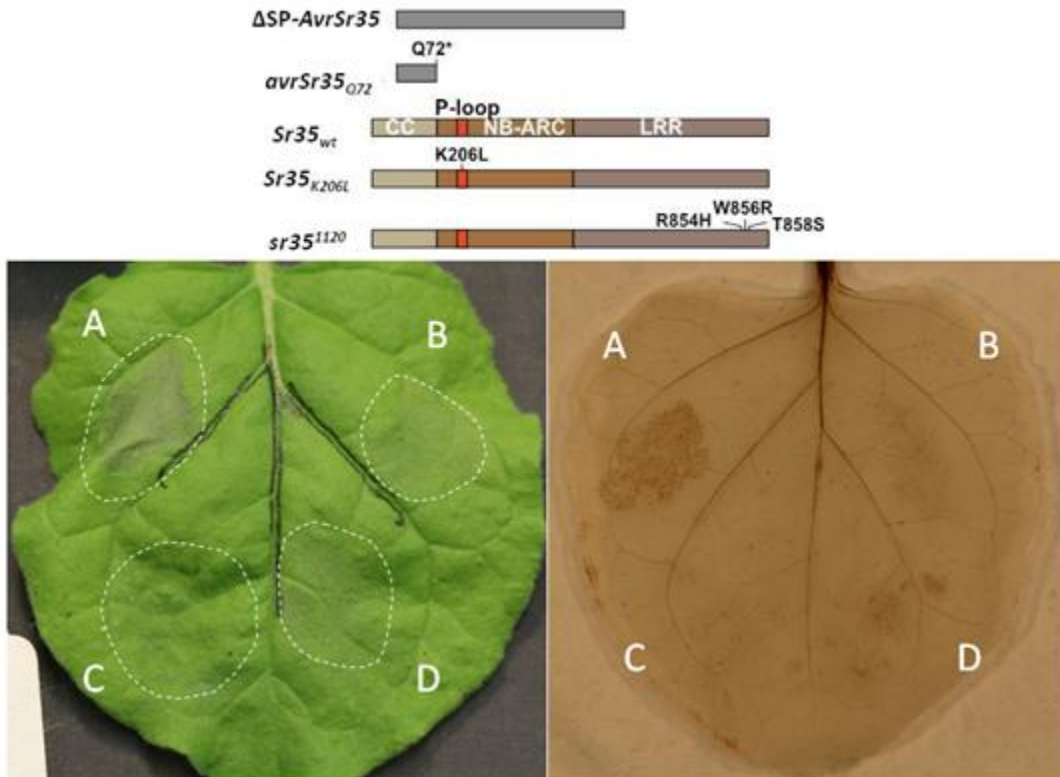


Figure 4.4. *AvrSr35* induces specific HR in the presence of *Sr35*. **Top:** schematic representation of sequences cloned into binary vectors and used for agroinfiltration. **Left:** *N. benthamiana* leaf 48 hours after co-agroinfiltration. **Right:** *N. benthamiana* leaf after DAB treatment showing a visible brown spot result of active oxygen species accumulation. Tobacco leaves were co-infiltrated with *Agrobacterium* cultures expressing wild-type and mutant or truncated versions of *AvrSr35* and *Sr35*. Combinations: **A.** (Δ SP-*AvrSr35* and *Sr35*_{wt}) **B.** (*AvrSr35*_{wt} and *sr35*^{I120}) **C.** (*AvrSr35*_{wt} and *Sr35*_{K206L}) **D.** (*avrSr35*_{Q72*} and *Sr35*_{wt}) Dotted lines show the boundaries infiltrated leaf area infiltration for each combination.

To exclude the possibility that the absence of HR in the agroinfiltrations was due to low transient expression of the constructs, the transcriptional activities of the infiltrated constructs were measured by RT-PCR. This evaluation showed the genes were still active after 48 hours of agroinfiltration (Figure 4.5), supporting the results obtained by the agroinfiltration of *N benthamiana* leaves.

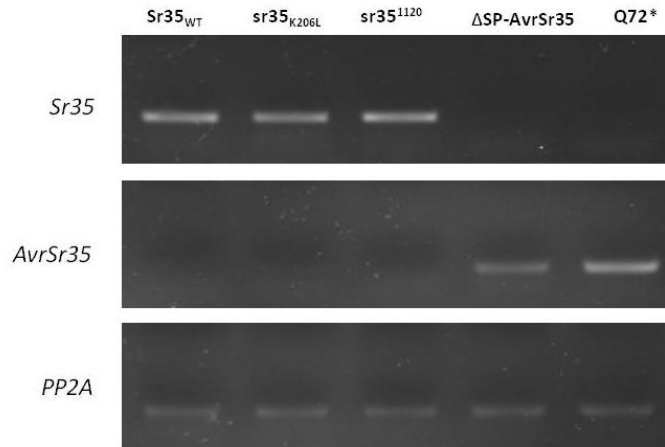


Figure 4.5. Evaluation of the *Sr35* and *AvrSr35* expression on tobacco leaves after agroinfiltration. RT-PCR was used to evaluate the cDNAs synthesized from RNA isolated from leaves 48 hours after agroinfiltration. Expression of *Sr35*, *AvrSr35* and reference gene *PP2A* was measured in the leaves agroinfiltrated with in the binary vector constructs carrying wild-type and mutated variants of the *Sr35* and *AvrSr35* genes **Top:** sequences cloned in binary vectors for agroinfiltration. **Left:** target genes (*Sr35*, *AvrSr35*) and reference gene (*PP2A*)(Liu et al., 2012).

4.4.3 AvrSr35 heterologous protein infiltration on wheat leaves

To evaluate the ability of *AvrSr35* to induce HR in wheat lines carrying the *Sr35*, the Δ SP-AVRSR35 heterologous protein was produced using the ChampionTM pET SUMO Protein Expression System Kit (Invitrogen, Carlsbad, CA). The best conditions to produce the recombinant protein in *E. coli* BL21 (DE3) harboring pET-SUMO-AvrSr35- Δ SP were: incubation 25°C, 250 rpm overnight after the induction with IPTG 0.5 mM (Figure 4.6). Δ SP-AvrSr35 protein was identified in both the soluble and insoluble portions of the protein crude extract. Under these conditions, using 1L culture of the bacterial strain expressing SUMO- Δ SP-AvrS35 we obtained approximately 10 μ g of protein. The optimal conditions and timing for cleavage of SUMO- Δ SP-AvrSr35 protein to generate the native protein Δ SP-AvrSr35 were 20 U of SUMO protease per mg of protein followed by incubation at 6-4°C for 16 hours (Figure 4.7).

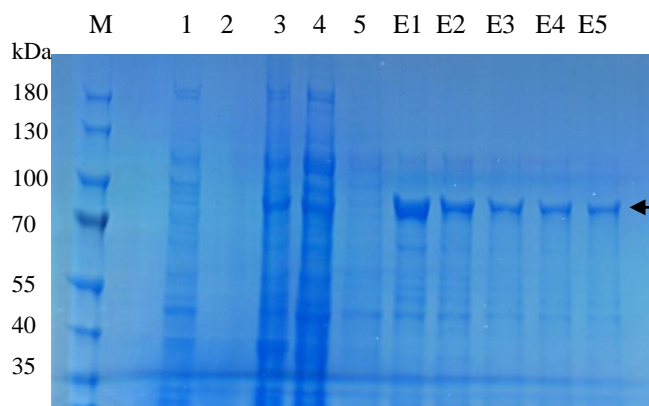


Figure 4.6. Expression and purification of the fusion protein SUMO- Δ SP-AvrSr35. The bacterial culture was induced by 0.5 mM of IPTG and incubated overnight at 25°C. Recombinant protein was obtained on five successive elutions. Samples were run in SDS-PAGE (10%) and stained with coomassie blue **M**: molecular weight marker, **1**. Insoluble portion uninduced, **2**. Soluble portion uninduced, **3**. insoluble portion induced, **4**. Soluble portion induced, **5**. flow-through wash, **E1** to **E5** show five successive elutions of purified recombinant protein. Expected size of recombinant protein = 74 kDa (showed by an arrow).

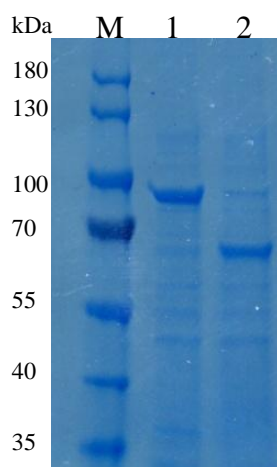


Figure 4.7. Cleavage of the SUMO portion of fusion recombinant protein SUMO- Δ SP-AvrSr35. **1**. Recombinant protein SUMO- Δ SP-AvrSr35 (before SUMO protease) expected size of the recombinant protein: 74 kDa. **2**. Δ SP-AvrSr35 obtained after SUMO protease incubation (16 hours at 6-4°C), expected sized of protein 63.5 kDa. Samples were run in SDS-PAGE (10%) and stained and with coomassie blue.

The hexaploid wheat cultivars Marquis (*Sr35*⁻) and Marquis *Sr35* (*Sr35*⁺) were used to infiltrate leaves with the Δ SP-AvrSr35 protein. Our preliminary experiments demonstrated that Marquis cultivar was less prone to mechanical damage during protein infiltration compared with other wheat genotypes, thereby reducing the confounding effect of this factor on the HR scoring. Also,

Marquis cultivar was valuable in this experiment since it is susceptible to several *Pgt* races (Ellis et al., 2014), reducing any effect of the genetic background in the results observed.

By testing several dilutions of AvrSr35 protein on Marquis (*Sr35*-) and Marquis *Sr35* (*Sr35*+) genotypes we found that >0.5 mg/ml of protein suspension in PBS 1X can induce necrosis in both genotypes. However, when the concentration was reduced to a range between 0.1 and 0.3 mg/ml, only the *Pgt* resistant genotype Marquis-*Sr35* showed symptoms of HR or necrosis (Table 4.3, Figure 4.8). At concentrations lower than 0.1 mg/ml, the infiltration with the AvrSr35 protein did not show visible HR effects on both genotypes. A Fisher showed significant association ($p=0.0391$, $n=17$) between HR and the presence of the *Sr35* gene when the AvrSr35 protein was infiltrated (Table 4.3).

Table 4.3. Evaluation of HR 24 hours after the infiltration with the heterologous protein Δ SP-AvrSr35 into leaves of resistant Marquis-*Sr35* (*Sr35*+) and susceptible Marquis (*Sr35*-) wheat cultivars. Different concentrations of the heterologous protein Δ SP-AvrSr35 and the control with bovine serum albumin (BSA) were infiltrated into the main leaf of 12 days-old wheat seedlings. 1-4 refer to the number of leaves tested for each protein dilution. (+) HR, (-) non-HR.

Treatments	Concentration (mg/ml)	Genotypes							
		Marquis (<i>Sr35</i> +)				Marquis (<i>Sr35</i> -)			
		1	2	3	4	1	2	3	4
Δ SP-AvrSr35	0.5	(+)				(+)			
	0.3	(+)				(-)			
	0.2	(+)	(+)	(-)		(-)	(-)	(-)	
	0.1	(+)	(+)	(+)	(-)	(-)	(-)	(-)	(-)
	0.05	(-)	(-)	(-)	(-)	(-)	(-)	(-)	(-)
	0.005	(-)	(-)	(-)	(-)	(-)	(-)	(-)	(-)
Control (BSA)	0.5	(-)	(-)	(-)	(-)	(-)	(-)	(-)	(-)
	0.3	(-)	(-)	(-)	(-)	(-)	(-)	(-)	(-)
	0.2	(-)	(-)	(-)	(-)	(-)	(-)	(-)	(-)
	0.1	(-)	(-)	(-)	(-)	(-)	(-)	(-)	(-)
	0.05	(-)	(-)	(-)	(-)	(-)	(-)	(-)	(-)
	0.005	(-)	(-)	(-)	(-)	(-)	(-)	(-)	(-)

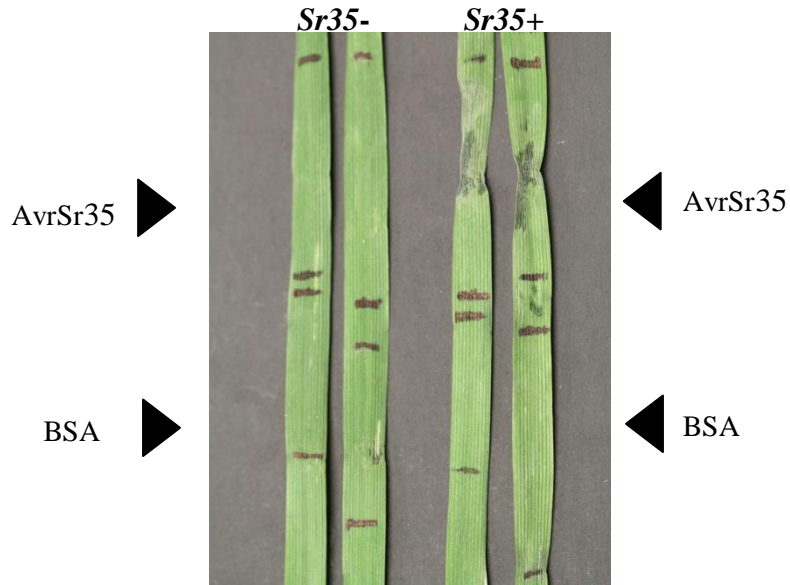


Figure 4.8. Infiltration of Δ SP-AvrSr35 protein into leaves of Marquis-*Sr35*(*Sr35*+) and Marquis (*Sr35*-) cultivars. The abaxial side of the leaf was infiltrated with 0.2 mg/ml of Δ SP-AvrSr35 protein. BSA: Bovine Serum Albumin (BSA) (0.2 mg/ml) was used as negative control. Picture was taken 24 hours after infiltration. Lines define boundaries of the soaked area after infiltration.

4.4.4 Subcellular localization of *AvrSr35* and *Sr35*

A series of experiments led by the Dr. William Rutter were carried out to examine the subcellular localization of candidate *AvrSr35* and *Sr35* (Salcedo et al., 2017). A fluorescence fusion constructs were produced by cloning the coding sequences into the binary vector pSITE-4NA (Chakrabarty et al., 2007). The *A. tumefaciens* C5851 harboring the mature *AvrSr35* candidate sequence (construct pAvrSr35- Δ SP-mRFP) fused to mRFP (monomeric red fluoresce protein) was infiltrated in 4-5 weeks *N. benthamiana* leaves, and their localization was examined by confocal laser scanning microscopy (CLSM). The red fluorescence (mRFP signal of *AvrSr35:mRFP* construct) was mainly accumulated in perinuclear space in a reticulated pattern consistent with the endoplasmic reticulum (ER) suggesting that when *AvrSr35* is expressed in *N. benthamiana* leaves is likely associated with ER (Figure 4.9A, C). The localization of *Sr35* relative to *AvrSr35* was evaluated by co-infiltrating constructs with the coding sequence of *Sr35* and *AvrSr35* fused with the green (eGFP) and the red fluorescent proteins (mRFP) respectively.

The distribution of the fluorescent signal in the tobacco cells expressing both protein fusions showed that the *AvrSr35* and *Sr35* localize in the same subcellular compartment (Fig. 4.9B-D).

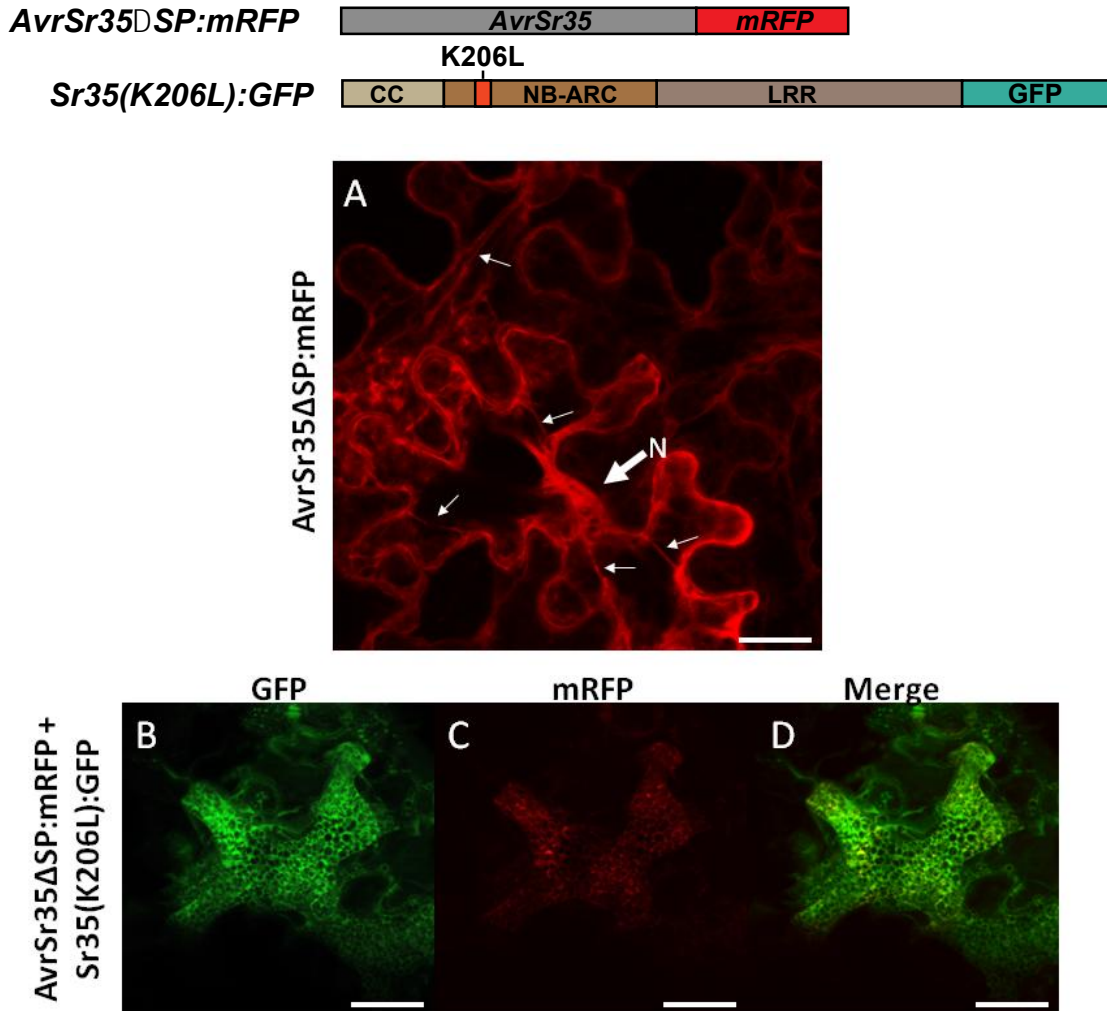


Figure 4.9. Subcellular localization of the *Sr35* and *AvrSr35* gene products. Images of *N. benthamiana* cell leaf cells 48 hours after infiltration with *AvrSr35* Δ SP:mRFP and *Sr35*(K206L):GFP constructs. **Top:** schematic representation of sequences cloned into binary vector constructs and used for agroinfiltration. **(A)** The ER strands (small arrows), perinuclear region (large arrow). From **B** to **D** Co-expression of the *AvrSr35* Δ SP:mRFP and *Sr35*(K206L):GFP constructs shows co-localization of fluorescence signals from both mRFP and GFP on ER. Scale bar: 10 μ m.

4.4.5 Bimolecular fluorescent complementation (BiFC) assay

Bimolecular fluorescent complementation (BiFC) assays led by Dr. William Rutter were conducted to validate *Sr35*-*AvrSr35* protein interaction (Salcedo et al., 2017). BiFC detects

potential interaction based on the appearance of fluorescent signal after reconstitution of the fragments of a functional fluorescent protein. Fluorescent protein is reconstituted when fragments are fused to the proteins of interest and co-expressed (Kerppola, 2008). The interaction between the *AvrSr35* and *Sr35* genes was evaluated agroinfiltrating on *N. benthamiana* leaves with constructs carrying *AvrSr35* and *Sr35* fused with portions of the yellow fluorescent protein (nYFP or cYFP, respectively). The *Sr35* was fused with the nYFP N-terminal (1–174 AA) (construct: pnYFP-*AvrSr35*- Δ SP) and the *AvrSr35* was fused with the cYFP C-terminal (175–239 AA) (construct: p*Sr35*(K206L)-cYFP). The p*Sr35*(K206L)-cYFP construct carries substitution (K206L) on the P-loop motif, that inhibits downstream signaling for HR, but does not interfere with target binding. The interaction between the gene products was inferred based on the appearance and intensity of the YFP-specific fluorescence signal. The N- and C-terminal parts of the yellow fluorescent protein (YFP) fused with the *AvrSr35* and *Sr35*, respectively. Microscopic observations of agroinfiltrated *N. benthamiana* leaves showed fluorescence signal accumulation (Figure 4.10A), suggesting that the *AvrSr35* and *Sr35* proteins are capable of interacting in plant cells.

To evaluate the role of the LRR domain of the *Sr35* protein in the interaction with *AvrSr35* protein, and also, to evaluate the possibility of false positives signals due to the self-assembly of the YFP fragments two additional experiments were carried out. In these experiments the *AvrSr35* construct nYFP:*AvrSr35* Δ SP was co-infiltrated with 1) p*Sr35*(K206L)_{M1120}-cYFP construct, which carries a *Sr35* loss of function allele (*sr35*¹¹²⁰) with mutations on LRR domain (Saintenac et al., 2013), and 2) with the construct p*Sr35*(K206L+Q464*)-cYFP that has the deletion of the LRR domain. These experiments showed a notable reduction in the intensity of the fluorescence signal (Figure 4.10B, C).

4.4.6 Co-immunoprecipitation of *AvrSr35* and *Sr35* on tobacco leaves

A protein co-immunoprecipitation (Co-IP) assay was carried out to provide additional validation for the interaction between *AvrSr35* and *Sr35*. This technique takes advantage of the protein epitopes that are fused with the N-terminus or C-terminus of the protein of interest. Commercial

monoclonal antibodies against epitope tags can be used to purify tagged proteins from a cell lysate to characterize protein-protein interactions (Brizzard, 2008).

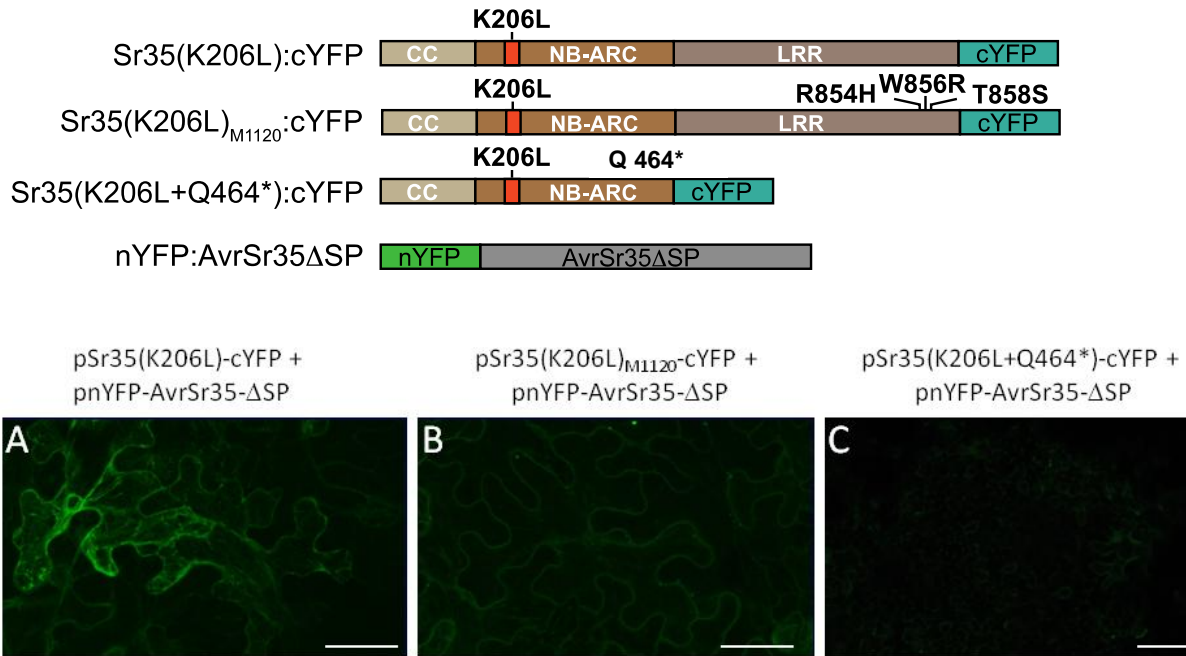


Figure 4.10. Bimolecular fluorescent complementation (BiFC) assay confirming interaction between Sr35 and AvrSr35 proteins. Confocal laser microscopy of tobacco leaves co-infiltrated with the nYFP:AvrSr35ΔSP construct combined with the Sr35(K206L):cYFP (A), Sr35(K206L)_{M1120}:cYFP (B), and Sr35(K206L+ Q464*):cYFP constructs (C). Scale bar: 50 μm.

The epitopes FLAG and HA were used to tag the Sr35 and AvrSr35 on N- and C- terminal respectively and were co-infiltrated on tobacco leaves. The interaction between Sr35 and AvrSr35 proteins was confirmed since the fusion Sr35–FLAG was detected in the protein complex co-immunoprecipitated with anti-HA, after being co-infiltrated with both Sr35–FLAG and HA–AvrSr35. Reciprocally, the interaction was also confirmed by detection of HA–AvrSr35 co-immunoprecipitated with anti-FLAG antibody. Negative controls (buffer infiltrated tobacco) did not show bands of comparable size after with the co-immunoprecipitation. Positive controls using single Sr35–FLAG or HA–AvrSr35 infiltrations detected the corresponding epitope using the respective antibody (Figure 4.11).

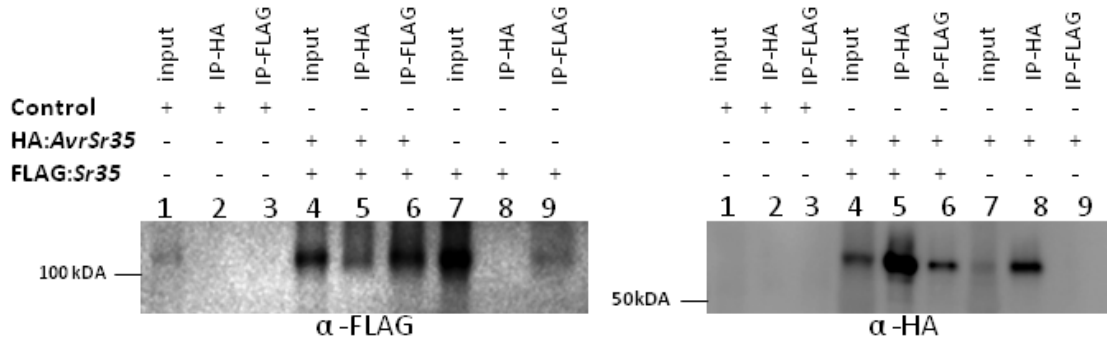


Figure 4.11. Co-immunoprecipitation assays confirming interaction between Sr35 and AvrSr35 proteins. Co-expressed Sr35-FLAG and HA-AvrSr35 in tobacco leaves were immunoprecipitated with anti-FLAG or anti-HA microbeads. Western blots were performed with anti-FLAG or anti-HA antibodies. Non-infiltrated tobacco leaf (lanes 1-3) and tobacco leaves infiltrated with single constructs (lanes 7-9) were used as negative and positive controls, respectively.

4.5 Discussion

4.5.4 Relative expression *AvrSr35* during time course infection

To characterize the expression profile of the *AvrSr35* gene, a time course qRT-PCR analysis was carried out at early stages of infection using the *Pgt* race RKQQC in susceptible wheat cultivar Fielder (*Sr35* -). The expression of *AvrSr35* was detected as early as 0 hours after transferring the seedlings from dew chamber to the growth chamber. At this time, *Pgt* had developed the germ tube and appressorium; the development of these fungal structures coincides with stomata opening stimulated by the light inside the growth chamber creating conditions for infection and establishment (Zhang et al., 2008). The *AvrSr35* transcript abundance continued rising during the first 96 hours of infection, most likely due to fungal mycelia growth.

Transcription profiles of several candidate effectors in *Puccinales* had showed differences in their expression during pathogen infection and establishment suggesting that they could be suppressing plant defense response at different stages (Cantu et al., 2013; Ramachandran et al., 2016). Since *AvrSr35* is expressed before haustoria formation, it fits in the criterion that describes immediate-early effectors type (Wang et al., 2015a). The expression of this type of effectors is detected at the very early stages of infection between urediniospore germination and the formation of the first haustoria (Bolton et al., 2008). This early expression of *AvrSr35* is

consistent with an early detection by plant immune system and a pre-haustorial response accompanied by the death of individual cells and arresting of fungal development observed under the microscope. These results provide explanation for the HR symptoms observed on the leaves of accessions carrying the *Sr35* resistance gene when they are inoculated with the *Sr35*-avirulent race RKQQC.

4.5.6 AvrSr35 induces HR in presence of Sr35

In this research, a series of experiments were conducted *in planta* using agroinfiltration to evaluate if *AvrSr35* is triggering HR in the presence of *Sr35*, confirming the identity of *AvrSr35* as avirulent gene. Agroinfiltration into *N. benthamiana* leaves has become a popular and simple method for the analysis of effector function by transient co-expression of proteins (Wang et al., 2011; Chen et al., 2013). T-DNA constructs encoding the entire (with signal peptide) and mature (without 25-aminoacids of signal peptide signal) versions of *AvrSr35*, driven by the 35S promoter of cauliflower mosaic virus, were independently co-expressed with *Sr35* in the heterologous system *N. benthamiana*. Transient co-expression of these two versions of the *AvrSr35* triggered *Sr35*-dependent HR. These results were indicative of the ability of *Sr35* to detect *AvrSr35* inside the host cells. No differences in the rate of HR development or its severity were observed between the two versions of *AvrSr35* suggesting that the presence or absence of signal peptide does not have a detrimental effect on the HR induction.

To determine the specificity of HR reaction, the mature version *AvrSr35* was co-expressed independently in the tobacco leaves with two mutant versions of the *Sr35* gene. One mutant has loss-of-function mutations in the LRR region (*sr35*¹¹²⁰), and another has mutations in the P-loop motif (K206L) of the NBS domain. It was expected that the LRR mutations would alter the direct recognition of the effector by the *R* gene or the effector's target (van der Hoorn & Kamoun, 2008), whereas the P-loop mutations affect the *Sr35*'s ability to trigger HR due to the interruption of the downstream HR signal pathway. In both co-expressed combinations with the *Sr35* mutants, no HR was observed after 48 hours of infiltration. The same result was found when a truncated version of *avrSr35* (Q72) was co-infiltrated with the wild-type *Sr35*.

The specificity of the *Sr35*-dependent HR was further confirmed by detecting the localized accumulation of the reactive oxygen species (ROS) in the leaves co-infiltrated with the wild-type versions of the *Sr35* and *AvrSr35* after the DAB treatment. Accumulation of ROS on plant host is indicative of HR and resistance-related oxidative burst response against invading organism (Thordal-Christensen et al., 1997; Dmochowska-Boguta et al., 2013). The ability of wild-type *AvrSr35* to trigger HR in presence of wild-type *Sr35* and the lack of HR response in combinations that included mutated or truncated versions *AvrSr35* and *Sr35* genes, suggest that this HR observed in the tobacco leaves is specifically triggered and implying that the candidate *AvrSr35* is the avirulent gene recognized by the *Sr35* resistance gene.

The avirulent function of *AvrSr35* was also evaluated using protein infiltration in a homologous system (wheat). Previously, protein infiltration has been used successfully used to validate candidate effector *Avr1b* of *Phytophthora sojae* on soybean plants (Shan et al., 2004), proteins that activate the stem rust resistance protein RPG1 on wheat (Nirmala et al., 2011), and the host response to the toxin *Tox3* of the necrotrophic fungus *Stagonospora nodorum* on wheat (Winterberg et al., 2014). The Δ SP-*AvrSr35* protein caused a specific HR only when it was infiltrated into leaves of resistant cultivar Marquis *Sr35* (*Sr35*+) in concentrations between 0.1-0.3 mg/ml. Interestingly, when the concentration of the Δ SP-*AvrSr35* protein was increased to 0.5 mg/ml, both susceptible and resistant genotype displayed HR. By contrast, HR was not observed when BSA control protein was infiltrated at any concentration in both cultivars. The direct association between the Δ SP-*AvrSr35* protein infiltration and *Sr35*-dependent HR induction confirmed in wheat the avirulent function of *AvrSr35*. The necrosis observed in both cultivars when Δ SP-*AvrSr35* protein was infiltrated at 0.5 mg/ml, can be the product of a non-specific immune reaction dependent on the protein concentration. It is still not clear how the infiltrated Δ SP-*AvrSr35* protein was translocated from the apoplastic space to inside the host cells, or alternatively if the *AvrSr35* target is located on the plasma membrane and triggering HR after the recognition of the *Sr35* gene.

4.5.7 AvrSr35 and Sr35 proteins co-localizes in the same sub-cellular compartment and interacts

An important aspect of effector biology research is to characterize the subcellular localization of the *Avr* gene products. The effector's subcellular localization helps to determine its mode of action, protein interactors and understand the function of the effector in the cellular environment (Alfano, 2009; Caillaud et al., 2012, Liu et al., 2016; Sperschneider et al., 2016a). The overexpression of fluorescently-tagged proteins in *N. benthamiana* combined with the use of confocal microscopy is a common strategy for evaluating both the subcellular localization and the protein interactions (Schornack et al., 2010; Petre et al., 2015). This strategy is often chosen because the natural protein levels of effectors, *R* genes, and their interactors are usually low (Boevink et al., 2014). Subcellular localization analyses in the *N. benthamiana* leaves showed that overexpression of AvrSr35 and Sr35-fusion proteins accumulated fluorescent signals in the plasma membranes and the endoplasmic reticulum (ER), suggesting that both proteins co-localized in these cellular compartments, and also suggesting that interaction between the gene products can occur.

To confirm the interaction between the AvrSr35 and Sr35 proteins, we opted to use the BiFC assays instead of other commonly used methods based on the yeast two-hybrid assays. The main shortcoming of the latter assays is that the protein interactions are prone to false positives, the test is conducted in a non-native cellular environment and require follow-up *in planta* validation (Petschnigg et al., 2012). The BiFC assay allows for visualizing protein-protein interactions in living plants helping to understand the function of interacting proteins (Hu et al., 2002; Hu & Kerppola, 2003). The BiFC method is based on the observation that the N- and C-terminal sub-fragments of GFP and its derivatives, such as YFP, do not reconstitute as fluorophore spontaneously. However, if the N and C non-functional terminal fragments are fused to different interacting proteins, the tight contact between the YFP fragments reconstitutes fluorescence *de novo*. BiFC assay has become a routine method for studying interacting proteins with several advantages including the absence of background signal, specificity, and stability (Bhat et al., 2006).

The success of the BiFC assays often depends on to which protein terminus the parts of the YFP protein are fused. In our study, we determined that the N- and C-terminal parts of the yellow fluorescent protein (YFP) fused with the N-terminal of AvrSr35 (construct nYFP:AvrSr35 Δ SP) and C-terminal of Sr35 (construct pSr35(K206L)-TDNA:cYFP), respectively, can produce consistent fluorescence signal that was accumulated on the plasma membranes and ER.

To exclude the possibility of false positive signals due to self-assembly of YFP protein fusions expressed from the highly active cauliflower mosaic virus 35S promoter, we conducted control experiments including mutant variants of the Sr35 protein. The BiFC assays using AvrSr35 (nYFP: AvrSr35 Δ SP) combined with Sr35 without the LRR domain Sr35(K206L+Q464*:cYFP) displayed a reduced fluorescence signal indicating that the observed fluorescence signal is not a false-positive. To test the biological significance of the interaction between AvrSr35 and Sr35 proteins, we conducted the BiFC experiment using a loss-of-function mutant version of *Sr35* (sr35¹¹²⁰) that carried mutations in the LRR domain (Saintenac et al., 2013). This *Sr35* mutant was detected in the M1120 mutant of *T. monococcum*, and made the plant susceptible to RKQQC and *Ug99* race group. We observed a substantial decrease in the intensity of fluorescence in the plant cells co-expressing the nYFP:AvrSr35 Δ SP with Sr35(K206L)_{M1120}-cYFP or Sr35(K206L+Q464*:cYFP) constructs. This result suggests that the loss of resistance in the M1120 mutant line is likely associated with the inability of mutant Sr35 protein to effectively interact with AvrSr35 protein (Saintenac et al., 2013), and corroborates the critical role of LRR domain in the *Sr35*-*AvrSr35* interaction.

BiFC determines close protein-protein proximity but is not absolute and conclusive proof of protein-protein interaction (Bhat et al., 2006). Alternative methods have been used to validate protein-protein interaction; those methods include pull-down assay protein, complex purification using gel filtration, and protein complex immunoprecipitation (Co-IP) (Bracha-Drori et al., 2004). Co-IP experiments were carried out to independently validate the physical interaction between AvrSr35 and Sr35 suggested by subcellular localization and BiFC experiments. One of the advantages provided by the Co-IP assays is that the small size (10–15 amino acids) of the antibody-recognition epitopes (HA and FLAG) fused with the target proteins reduces interference with protein-protein interaction (Boevink et al., 2014). In our study, reciprocal Co-

IP experiments demonstrated that AvrSr35 and Sr35 proteins interact. Further studies will be required to discern if this interaction is direct or indirect. If the interaction between AvrSr35 and Sr35 proteins is indirect the Co-IP using *N. benthamiana* combine with mass spectrophotometry could provide important information about orthologous genes of the protein interactors (i.e., effectors's targets)(Petre et al., 2015).

Our cellular localization experiments indicate that AvrSr35 and Sr35 proteins can be associated with the plasma membranes and ER (Salcedo et al., 2017). The ER comprises the most extensive endomembrane system in eukaryotes being the main source of secretory membrane trafficking and is one of the most frequent compartments targeted by effectors (Wang et al., 2005). During early stages of the fungal infection process, there is a global rearrangement of the cytoskeleton that involves a polarization of cellular components (ER, Golgi apparatus, nucleus, etc.) towards the developing haustoria. This process is accompanied by the induction of secretory pathways to direct defense compounds towards the pathogen attack site, and the accumulation of membrane-bound vesicles at the site of host-pathogen interaction. While this polarization facilitates effector delivery from the fungal side, it also maximizes the delivery of antimicrobial proteins, peroxisomal and papillae compounds that eventually impair hyphal growth. Furthermore, cellular component polarization requires cytoskeletal reorganization that depends on external signaling including the recognition and internalization of PAMPs, and it appears that endocytic trafficking plays a role in the perception of and cellular responses to fungal attack (Hückelhoven, 2007; Frey & Robatzek, 2009; Ma & Shang, 2009; Caillaud et al., 2012).

Diverse *R* genes associated with cellular membranes have been demonstrated experimentally, including *R* genes associated to ER such as the *Arabidopsis* *R* gene *RPPI-WSA* and *RPW8* (Weaver et al., 2006; Wang et al., 2007b; Takemoto et al., 2012). This membrane localization/association might play an important role in the Avr protein recognition. Consistent with this hypothesis, several pathogen effectors from bacterial pathosystem have also shown to be associated with the host membranes. This association is possible by the N-terminal acylation of the proteins (the covalent attachment of fatty acids at certain motifs providing attachment to membranes, particularly myristoylation and palmitoylation) (Takemoto et al., 2012; Popa et al., 2016). The membrane localization plays important roles in protein dimerization or

oligomerization for downstream signaling either after or before effector recognition event. Also, the membrane localization would help in R protein stabilization, and facilitate the effector recognition by targeting both the *R* gene and the target's effector in the same location avoiding interference with closely related R proteins (Takemoto et al., 2012). Therefore, it is possible that the association of Sr35 and AvrSr35 with plasma membranes and ER is critical for pathogen recognition.

The determination of the effector physiological role is crucial to understand its pathogenic function (White et al., 2000), typically effectors have been associated with the suppression of host plant immunity (Pais et al., 2013). However, the comparative microscopic analyses of susceptible wheat lines infected with the wild-type and three mutant *Pgt* strains carrying non-functional alleles of *AvrSr35* showed no substantial differences in the progression of infection at the first 72 HAI. Likewise, the transcriptome profiling of a compatible wheat line infected with the wild-type and mutant *Pgt* strains showed no differences in the host gene expression suggesting that *AvrSr35* is likely not critical for *Pgt* virulence (Salcedo et al., 2017). One of the possible explanations is the functional redundancy of effectors secreted by the fungal pathogens. These results are consistent with our earlier findings based on the analyses of the gene co-expression networks build using transcriptomes of leaf tissues infected with different *Pgt* isolates including the RKQQC race (Rutter et al., 2017). In these networks, the same host genes were connected with the distinct sets of effectors in each *Pgt* isolate suggesting that pathogens can utilize different effectors to target the same host pathways or functional redundancy to establish a compatible interaction with the host (Rutter et al., 2017).

Another fundamental question of effector biology is the mechanism exploited by the fungal effectors to translocate to the host cells (Ellis et al., 2006; Petre & Kamoun, 2014). The current models for both oomycetes and fungi suggest that effectors carry an N-terminal translocation signal that is necessary to enter the host cells (Whisson et al., 2007; Rafiqi et al., 2010). In pathogenic fungi oomycetes, some effectors carried a conserved N-terminal amino acid sequence called RxLR motif, which is responsible for cell translocation via receptor-mediated endocytosis (Whisson et al., 2007; Kale & Tyler, 2011). This motif consists of the sequence 'RxLRx5-21ddEER' (where R=Arg, x=any aminoacid residue, L=Leu, E=glutamate and d = frequently

aspartate), related to a protein transport motif of virulence proteins secreted by pathogen *Plasmodium falciparum* (Ellis et al., 2006). Other translocation motifs included tripeptide RGD (arginine-glycine-aspartate) motif found in *toxA* of *Pyrenophora tritici-repentis* and *Stagonospora nodorum* (Manning & Ciuffetti, 2005), LFLAK motif present in the Crinkler (CRN) family of oomycetes (Schornack et al., 2010), and CHxC (cysteine, histidine, any, cysteine) motif (Kemen et al., 2011). Several potential translocation motifs were inferred based on homology search: [L/I]xAR (Godfrey et al., 2010), YxSL[R/K] (Saunders et al., 2012), [R/K]VY[L/I]R (Ridout et al., 2006), and [Y/F/W]xC (Dodds et al., 2009). However, these motifs have not been experimentally validated for their ability to translocate through the host membrane (Kale & Tyler, 2011). Our preliminary analyses failed to identify previously characterized translocation motifs in the AvrSr35 protein sequence. However, our experiments with the infiltration of AvrSr35 protein into the wheat leaves suggest that it has the capacity to translocate into the host cell and induce HR. Further functional and bioinformatical analyses of the *AvrSr35* gene will provide the possibility to broaden our understanding of the effector translocation mechanisms in the Puccinales order and other biotrophs.

4.6 Conclusions and Perspectives

1. Our study reports the functional validation of the first *Avr/R* gene pair in cereal rusts; interaction between this pair of proteins triggers specific resistance response accompanied by cell death.
2. Based on cellular co-localization, BiFC and co-immunoprecipitation experiments, it was concluded that AvrSr35 and Sr35 interact, and likely are associated with the plasma membrane and endoplasmic reticulum.
3. Both microscopic analyses and expression profiling did not conclude a virulence function for the *AvrSr35* gene. It is likely that other effectors compensate the loss-of-function of the *AvrSr35* gene in *Pgt* mutants with partially or entirely overlapping functionality.

4. Discovery of the *AvrSr35* gene opens doors to identifying the potential protein(s) that interact with this effector. Effectors' targets facilitate compatible interaction and can be used for developing biotechnology-based approaches to control fungal diseases. For example, effector targets can be mutated or modified using genome editing approaches making them unrecognizable by the effector (Gawehns et al., 2013). Also, the effectors' targets can be transformed using biotechnological approaches into "decoys" to expand the recognition specificity to confer more durable resistance (Kim et al., 2016). Compared with the traditional deployment of *R* genes, this approach can be straightforward and less complex compared with other strategies such as gene pyramiding.

5. The cloning of *AvrSr35* could help to shed some light on the fungal effector uptake mechanisms. This area of research which is still under development, but has promised to answer fundamental questions about plant pathogenesis and help to develop approaches to control cereal rust using biotechnological methods (Petre & Kamoun, 2014; Lo Presti et al., 2015).

Chapter 5 - Final conclusions

Plant pathogens like cereal rust, demonstrate a considerable evolutionary potential and representing excellent models to study co-evolution, rapid adaptation, and population dynamics of two biological systems (McDonald & Linde, 2002). The mutually antagonistic relationships between host and pathogen described by an arms race model (Van Valen, 1973) are driven by strong selection acting on both *R* gene variants that allows host to recognize pathogen proteins and *Avr* gene variants that help pathogen to defeat the host' immune system. Contrary to natural ecosystems, the strength of selection in the agro-ecosystems dominated by monocultures is higher facilitating the rapid adaptation of pathogen (Stukenbrock & McDonald, 2008).

Therefore, to maintain the steady growth of wheat production, the timely development of wheat varieties with new resistance genes effective against newly emerged pathogens is required. However, the classical resistance trait breeding that is based on the discovery and introduction of new *R* genes into cultivars, although well established, is a very time-consuming process. Moreover, the majority of newly deployed *R* genes are rendered ineffective within several years after deployment. Thus, to alleviate the threats to future food production posed by cereal rusts, there is an urgent need for new translational strategies to develop resistant traits in wheat and other crops. To be effective and durable, these strategies should be based on a comprehensive understanding of the components of the fungal pathogen – host pathosystem that are involved in the immune response.

The rapid technological advances in “omics” approaches allowed us to start unravelling the molecular determinants of resistance to wheat stem rust. The identification of avirulence factors in rusts is complicated because the complex life cycle of obligate biotrophic pathogens makes them unamenable to experimental manipulation. In this study, we filled the gap in the availability of functional genomics tools for the identification of avirulence factors in biotrophic fungal pathogens by combining whole genome next-generation sequencing with the analyses of natural and chemically-induced DNA sequence diversity. This approach has a potential to become a powerful tool for studying host-pathogen interactions in other cereal rust fungi.

The identified *AvrSr35* gene allowed us to understand the origin of *Sr35*-virulent isolates of *Pgt* resulting from the loss-of-function mutation due to the insertion of a transposable element. It is likely that the proliferation of transposable elements in the large genomes of wheat rusts is one of the important factors contributing to the erosion of wheat *R* genes conferring resistance to rusts. Likewise, one of the probable scenarios for the evolution of *Ug99* race group was the accumulation of mutations in the avirulence effectors recognized by the wheat stem rust resistance genes (Visser et al., 2009; Park et al., 2011).

When additional *Avr* genes will be identified, they will provide a valuable tool for molecular surveillance and early detection of new virulent races, which can inform the deployment of resistance genes to prevent large epidemics. Using the *Avr* gene diversity data, we can start investigating the mechanisms, and temporal and spatial dynamic of new virulence origin, and learn how to predict the virulence of new isolates based on genome sequence analysis. The population scale *Avr* gene diversity data combined with the characterized virulence on known *Sr* genes will also provide a valuable resource that can help us to predict the possibility of rust outbreaks. The *Avr* genes identified can be also used to confirm the expression of a functional *R* proteins in transgenic cassettes. As more resistance genes and the corresponding *Avr* genes will be identified, this information can be used to select resistance genes targeted by different effectors to increase the durability of the deployed gene pyramids. Finally, the identification of *Avr* and *R* genes will provide a unique opportunity to discover the effector's host targets that are largely unknown for cereal rusts. These targets will provide entry point for inferring one of the host's susceptibility pathways and associated with it other fungal effectors (if any), thereby advancing our understanding of host-pathogen interaction pathways at more mechanistic level.

The co-evolutionary models of host-pathogen interaction suggest that the fitness cost associated with the virulence is in part responsible for the maintenance of genetic variation (Simms & Triplett, 1994). These models suggest that virulence acquired by the loss of avirulence function should have a substantial fitness cost resulting in the reduced fitness of the virulent pathogen compared to that of the avirulent pathogen in the absence of *R* gene (Simms, 1996). However, the experimental evaluation of this hypothesis has been limited by the small number of *R/Avr* gene pairs characterized. The Data available suggest that the actual fitness cost is relatively low

due to some compensatory mechanisms that reduce the efficiency of natural selection against virulence genes (Montarry et al., 2010). Consistently, there were no obvious differences in the virulence between the RKQQC EMS mutants and wild-type strain analyzed in the CDL and Akhunov's lab using the panel differentials. Also, the microscopy analysis did not reveal differences in the development of the wild-type strain compared to the EMS mutants (Salcedo et al., 2017). Both lines of evidence suggest that there is a very low fitness cost associated with the loss of *AvrSr35* function. One of the possible explanations for the lack of visible fitness cost associated with the loss of *AvrSr35* function could be the existence of other fungal effectors capable of compensating for this mutation. The support for this hypothesis comes from our independent study that showed that the divergent sets of effectors from different fungal *Pgt* isolates can target the same host pathways (Rutter et al., 2017). However, more detailed analyses of *Pgt* EMS mutants might be required to understand fitness cost associated with *AvrSr35*. If such cost exists, it can be assessed comparing physiological and developmental phenotypes such as the time of urediniospore emergence (latent period) and the size of the uredinia (spore density). Another possibility, which I consider less likely is that *AvrSr35* is not involved directly in virulent function, being a "conventional" protein of pathogen's metabolism; the avirulence function would be a secondary consequence of the evolution of the host mechanism (*R* genes) to detect the pathogen. Effectors are extraordinary examples of constant biological innovation that include amazing proteins key to understand and influence discoveries in plant immunity, plant biology and pathogen evolution (Win et al., 2012); effector study will continue impacting the advancing of biological sciences.

References

- Afzal, A., Riaz, A., Mirza, Javed, I., Shah, K. (2016). Status of wheat breeding at global level for combating *Ug99* –a review *Pakistan Journal of Phytopathology*, 27(2), 210–217. Retrieved from <http://pjp.pakps.com/index.php/PJP/article/view/180>
- Agrios, G. N. (2005). *Plant Pathology* (5th ed.). Burlington USA: Academic Press.
- Ahmed, A. A., Pedersen, C., & Thordal-Christensen, H. (2016). The barley powdery mildew effector candidates CSEP0081 and CSEP0254 promote fungal infection success. *PLoS ONE*, 11(6), 1–12. <http://doi.org/10.1371/journal.pone.0157586>
- Aime, M. C. (2006). Toward resolving family-level relationships in rust fungi (Uredinales). *Mycoscience*, 47(3), 112–122. <http://doi.org/10.1007/s10267-006-0281-0>
- Albersheim, P., & Prouty, A. J. (1975). Carbohydrates, Proteins, Cell Surfaces, and the Biochemistry of Pathogenesis. *Annual Review of Phytopathology*, 26, 31–52.
- Alexopoulos, C. ., Mins, C. ., & Blackwell, M. (1996). *Introduction to Mycology* (Fourth Ed). John Wiley & Sons, Inc.
- Alfano, J. R. (2009). Roadmap for future research on plant pathogen effectors: Micro-Review. *Molecular Plant Pathology*, 10(6), 805–813. <http://doi.org/10.1111/j.1364-3703.2009.00588.x>
- Ali, S., Laurie, J. D., Linning, R., Cervantes-Chávez, J. A., Gaudet, D., & Bakkeren, G. (2014). An Immunity-Triggering Effector from the Barley Smut Fungus *Ustilago hordei* Resides in an Ustilaginaceae-Specific Cluster Bearing Signs of Transposable Element-Assisted Evolution. *PLoS Pathogens*, 10(7). <http://doi.org/10.1371/journal.ppat.1004223>
- Andaya, C. B., Ronald, P. C. (2003). A catalytically impaired mutant of the rice *Xa21* receptor kinase confers partial resistance to *Xanthomonas oryzae* pv *oryzae*. *Physiological and Molecular Plant Pathology*, 62(4), 203–208. [http://doi.org/10.1016/S0885-5765\(03\)00060-](http://doi.org/10.1016/S0885-5765(03)00060-)
- Anderson, J. P., Gleason, C. A., Foley, R. C., Thrall, P. H., Burdon, J. B., & Singh, K. B. (2010). Plants versus pathogens: An evolutionary arms race. *Functional Plant Biology*, 37(6), 499–512. <http://doi.org/10.1071/FP09304>
- Anderson, C., Khan, M. A., Catanzariti, A.-M., Jack, C. A., Nemri, A., Lawrence, G. J., ... Song, K. (2016). Genome analysis and avirulence gene cloning using a high-density RADseq linkage map of the flax rust fungus, *Melampsora lini*. *BMC Genomics*, 17(1), 667. <http://doi.org/10.1186/s12864-016-3011-9>

- Anikster, Y. (1984). The Formae Speciales. In A. P. Bushnell, W.R., Roelfs (Ed.), *The Cereal Rusts Volume I origins specificity structure and physiology* (pp. 124–137). Orlando, FL: Academic Press.
- Anikster, Y., Wahl, L. (1979). Coevolution of the rust fungi on gramine and liliaceae and their host. *Annual Review of Phytopathology*, *17*, 367–403.
- Ayella, A. K., Trick, H. N., & Wang, W. (2007). Enhancing lignan biosynthesis by over-expressing pinoresinol lariciresinol reductase in transgenic wheat. *Molecular Nutrition and Food Research*, *51*(12), 1518–1526. <http://doi.org/10.1002/mnfr.200700233>
- Ayliffe, M. A., Frost, D. V., Finnegan, E. J., Lawrence, G. J., Anderson, P. A., & Ellis, J. G. (1999). Analysis of alternative transcripts of the flax *L6* rust resistance gene. *Plant Journal*, *17*(3), 287–292. <http://doi.org/10.1046/j.1365-313X.1999.00377.x>
- Ayliffe, M., Devilla, R., Mago, R., White, R., Talbot, M., Pryor, A., & Leung, H. (2011). Nonhost resistance of rice to rust pathogens. *Molecular Plant-Microbe Interactions : MPMI*, *24*(10), 1143–55. <http://doi.org/10.1094/MPMI-04-11-0100>
- Bajgain, P., Rouse, M. N., Bulli, P., Bhavani, S., Gordon, T., Wanyera, R., ... Pumphrey, M. O. (2015). Association mapping of North American spring wheat breeding germplasm reveals loci conferring resistance to *Ug99* and other African stem rust races. *BMC Plant Biology*, *15*(2015), 249. <http://doi.org/10.1186/s12870-015-0628-9>
- Bauer, R., Begerow, D., Sampaio, J. P., Weiß, M., & Oberwinkler, F. (2006). The simple-septate basidiomycetes: A synopsis. *Mycological Progress*, *5*(1), 41–66. <http://doi.org/10.1007/s11557-006-0502-0>
- Bhat, R. A., Lahaye, T., & Panstruga, R. (2006). The visible touch: in planta visualization of protein-protein interactions by fluorophore-based methods. *Plant Methods*, *2*, 12. <http://doi.org/10.1186/1746-4811-2-12>
- Belkhadir, Y., Subramaniam, R., Dangl, J. L. (2004). Plant disease resistance protein signaling: NBS-LRR proteins and their partners. *Current Opinion in Plant Biology*, *7*(4), 391–399. <http://doi.org/10.1016/j.pbi.2004.05.009>
- Bent, A. F., & Mackey, D. (2007). Elicitors, effectors, and *R* genes: the new paradigm and a lifetime supply of questions. *Annual Review of Phytopathology*, *45*, 399–436. <http://doi.org/10.1146/annurev.phyto.45.062806.094427>
- Berg, Jeremy, Tymoczko J., Stryer, L. (2012). Protein Composition and Structure Biochemistry (7th Edition). W.H. Freeman and Company.
- Bettgenhaeuser, J., Gilbert, B., Ayliffe, M., & Moscou, M. J. (2014). Nonhost resistance to rust pathogens a continuation of continua. *Frontiers in Plant Science*, *5*(December), 1–15. <http://doi.org/10.3389/fpls.2014.00664>

- Bhardwaj, S. C., Prashar, M., P., & P. (2014). *Ug99-Future Challenges*. In C. Goyal, Aakash. Manoharachary (Ed.), *Future Challenges in Crop Protection Against Fungal Pathogens* (pp. 231–248). New York, NY: Springer.
- Biffen, R. H. (1905). Mendel laws of inheritance and wheat breeding. *Journal of Agricultural Science and Technology*, *1*, 4–48.
- Black, D. L. (2003). Mechanisms of Alternative Pre-Messenger RNA Splicing. *Annual Review of Biochemistry*, *72*(1), 291–336. <http://doi.org/10.1146/annurev.biochem.72.121801.161720>
- Blondeau, K., Blaise, F., Graille, M., Kale, S. D., Linglin, J., Ollivier, B., ... Fudal, I. (2015). Crystal structure of the effector *AvrLm4-7* of *Leptosphaeria maculans* reveals insights into its translocation into plant cells and recognition by resistance proteins. *Plant Journal*, *83*(4), 610–624. <http://doi.org/10.1111/tpj.12913>
- Boetzer, M., & Pirovano, W. (2014). SSPACE-LongRead: scaffolding bacterial draft genomes using long read sequence information. *BMC Bioinformatics*, *15*(1), 211. <http://doi.org/10.1186/1471-2105-15-211>
- Boevink, P., McLellan, H., Bukharova, T., Engelhardt, S., & Birch, P. (2014). *n Vivo Protein-Protein Interaction Studies with BiFC: Conditions, Cautions, and Caveats*. In P. Birch, J. T. Jones, & J. I. B. Bos (Eds.), *Plant-Pathogen Interactions: Methods and Protocols* (pp. 81–90). Totowa, NJ: Humana Press.
- Bohnert, H. U., Fudal, I., Dioh, W., Tharreau, D., Notteghem, JL., Marc-Henri, L. (2004). A Putative Polyketide Synthase/Peptide Synthetase from *Magnaporthe grisea* Signals Pathogen Attack to Resistant Rice. *The Plant Cell Online*, *16*(9), 2499–2513. <http://doi.org/10.1105/tpc.104.022715>
- Boller, T., & Felix, G. (2009). A Renaissance of Elicitors: Perception of Microbe-Associated Molecular Patterns and Danger Signals by Pattern-Recognition Receptors. *Annu. Rev. Plant Biol.*, *60*, 379–406. <http://doi.org/10.1146/annurev.arplant.57.032905.105346>
- Bolton, M. D., Kolmer, J., & Garvin, D. (2008). Wheat leaf rust caused by *Puccinia triticina*. *Molecular Plant Pathology*, *9*(5), 563–575. <http://doi.org/10.1111/J.1364-3703.2008.00487.X>
- Borhan, M. H., Holub, E. B., Beynon, J. L., Rozwadowski, K., & Rimmer, S. R. (2004). The Arabidopsis TIR-NB-LRR gene *RAC1* confers resistance to *Albugo candida* (white rust) and is dependent on *EDS1* but not *PAD4*. *Molecular Plant-Microbe Interaction*, *17*(7), 711–719. <http://doi.org/10.1094/MPMI.2004.17.7.711>
- Bouktila, D., Khalfallah, Y., Habachi-Houimli, Y., Mezghani-Khemakhem, M., Makni, M., & Makni, H. (2014). Large-scale analysis of NBS domain-encoding resistance gene analogs in Triticeae. *Genetics and Molecular Biology*, *37*(3), 598–610. <http://doi.org/10.1590/S1415-47572014000400017>

- Bourras, S., McNally, K. E., Ben-David, R., Parlange, F., Roffler, S., Praz, C. R., ... Keller, B. (2015). Multiple avirulence loci and allele-specific effector recognition control the *Pm3* race-specific resistance of wheat to powdery mildew. *The Plant Cell*, 27(10), 2991–3012. <http://doi.org/10.1105/tpc.15.00171>
- Bozkurt, T. O., Schornack, S., Banfield, M. J., & Kamoun, S. (2012). Oomycetes, effectors, and all that jazz. *Current Opinion in Plant Biology*, 15(4), 483–492. <http://doi.org/10.1016/j.pbi.2012.03.008>
- Bowden, R., Shoyer, J., Roozeboom, K., Claasen, M., Evans, P., Gordon, B., & Heer, B., Janssen, K., Long, J., Martin, J., Schlegel, A., Sears, R., Witt, M. (2001). Performance of wheat variety blends in Kansas. Kansas State University. University Agric. Extension.
- Bracha-Drori, K., Shichrur, K., Katz, A., Oliva, M., Angelovici, R., Yalovsky, S., & Ohad, N. (2004). Detection of protein-protein interactions in plants using bimolecular fluorescence complementation. *Plant Journal*, 40(3), 419–427. <http://doi.org/10.1111/j.1365-313X.2004.02206.x>
- Bradford, M. M. (1976). Rapid and sensitive method for the quantitation of microgram quantities of protein utilizing the principle of protein-dye binding. *Annals of Biochemistry*, 72, 248–254.
- Brandwagt, B. F., Mesbah, L. a, Takken, F. L., Laurent, P. L., Kneppers, T. J., Hille, J., Nijkamp, H. J. (2000). A longevity assurance gene homolog of tomato mediates resistance to *Alternaria alternata* f. sp. *lycopersici* toxins and fumonisin B1. *Proceedings of the National Academy of Sciences of the United States of America*, 97(9), 4961–4966. <http://doi.org/10.1073/pnas.97.9.4961>
- Brandwagt, B. F., Kneppers, T. J. a, Nijkamp, H. J. J., & Hille, J. (2002). Overexpression of the tomato Asc-1 gene mediates high insensitivity to AAL toxins and fumonisin B1 in tomato hairy roots and confers resistance to *Alternaria alternata* f. sp. *lycopersici* in *Nicotiana umbratica* plants. *Molecular Plant-Microbe Interactions*, 15(1), 35–42. <http://doi.org/10.1094/MPMI.2002.15.1.35>
- Brizzard, B. (2008). Epitope tagging. *BioTechniques*, 44(5), 693–695. <http://doi.org/10.2144/000112841>
- Brown, J. K. M., & Rant, J. C. (2013). Fitness costs and trade-offs of disease resistance and their consequences for breeding arable crops. *Plant Pathology*, 62(S1), 83–95. <http://doi.org/10.1111/ppa.12163>
- Brueggeman, R., Rostoks, N., Kudrna, D., Kilian, A., Han, F., Chen, J., ... Kleinhofs, A. (2002). The barley stem rust-resistance gene *Rpg1* is a novel disease-resistance gene with homology to receptor kinases. *Proc Natl Acad Sci U S A*, 99(14), 9328–9333. <http://doi.org/10.1073/pnas.142284999>

- Brueggeman, R., Druka, A., Nirmala, J., Cavileer, T., Drader, T., Rostoks, N., ... Kleinhofs, A. (2008). The stem rust resistance gene *Rpg5* encodes a protein with nucleotide-binding-site, leucine-rich, and protein kinase domains. *Proc Natl Acad Sci U S A*, *105*(39), 14970–14975. <http://doi.org/0807270105> [pii]r10.1073/pnas.0807270105
- Brunner, S., Hurni, S., Herren, G., Kalinina, O., von Burg, S., Zeller, S. L., ... Keller, B. (2011). Transgenic *Pm3b* wheat lines show resistance to powdery mildew in the field. *Plant Biotechnology Journal*, *9*(8), 897–910. <http://doi.org/10.1111/j.1467-7652.2011.00603.x>
- Burdon, J. J., Barrett, L. G., Rebetzke, G., & Thrall, P. H. (2014). Guiding deployment of resistance in cereals using evolutionary principles. *Evolutionary Applications*, *7*(6), 609–624. <http://doi.org/10.1111/eva.12175>
- Büschges, R., Hollricher, K., Panstruga, R., Simons, G., Wolter, M., Frijters, A., van Daelen, R., van der Lee, T., Diergaarde, P., Groenendijk, J., Töpsch, S., Vos, P., Salamini, F., Schulze-Lefert, P. (1997). The barley Mlo gene: a novel control element of plant pathogen resistance. *Cell*, *88*(5), 695–705.
- Bushnell, W. R., & Rowell, J. B. (1981). Suppressors of defense reactions - a model for roles in specificity. *Phytopathology*, *71*(10), 1012-1014
- Caillaud, M. C., Piquerez, S. J. M., Fabro, G., Steinbrenner, J., Ishaque, N., Beynon, J., & Jones, J. D. G. (2012). Subcellular localization of the Hpa RxLR effector repertoire identifies a tonoplast-associated protein HaRxL17 that confers enhanced plant susceptibility. *Plant Journal*, *69*(2), 252–265. <http://doi.org/10.1111/j.1365-313X.2011.04787.x>
- Cairns, T. C., Studholme, D. J., Talbot, N. J., & Haynes, K. (2016). New and Improved Techniques for the Study of Pathogenic Fungi. *Trends in Microbiology*, *24*(1), 35–50. <http://doi.org/10.1016/j.tim.2015.09.008>
- Cantu, D., Segovia, V., MacLean, D., Bayles, R., Chen, X., Kamoun, S., ... Uauy, C. (2013). Genome analyses of the wheat yellow (stripe) rust pathogen *Puccinia striiformis* f. sp. *tritici* reveal polymorphic and haustorial expressed secreted proteins as candidate effectors. *BMC Genomics*, *14*, 270. <http://doi.org/10.1186/1471-2164-14-270> [pii]
- Catanzariti, A.-M., Dodds, P. N., Lawrence, G. J., Ayliffe, M. A., & Ellis, J. G. (2006). Haustorially expressed secreted proteins from flax rust are highly enriched for avirulence elicitors. *The Plant Cell*, *18*(1), 243–56. <http://doi.org/10.1105/tpc.105.035980>
- Cesari, S., Bernoux, M., Moncuquet, P., Kroj, T., & Dodds, P. N. (2014). A novel conserved mechanism for plant NLR protein pairs: the “integrated decoy” hypothesis. *Frontiers in Plant Science*, *5*(November), 606. <http://doi.org/10.3389/fpls.2014.00606>
- Cesari, S., Thilliez, G., Ribot, C., Chalvon, V., Michel, C., Jauneau, A., ... Kroj, T. (2013). The rice resistance protein pair RGA4/RGA5 recognizes the *Magnaporthe oryzae* effectors

- AVR-Pia and AVR1-CO39 by direct binding. *The Plant Cell*, 25(4), 1463–1481. <http://doi.org/10.1105/tpc.112.107201>
- Chakrabarty, R., Banerjee, R., Chung, S.-M., Farman, M., Citovsky, V., Hogenhout, S. a, ... Goodin, M. (2007). PSITE vectors for stable integration or transient expression of autofluorescent protein fusions in plants: probing *Nicotiana benthamiana*-virus interactions. *Molecular Plant-Microbe Interactions: MPMI*, 20(7), 740–750. <http://doi.org/10.1094/MPMI-20-7-0740>
- Chandra-Shekara, A. C., Navarre, D., Kachroo, A., Kang, H. G., Klessig, D., Kachroo, P. (2004). Signaling requirements and role of salicylic acid in HRT- and rrt-mediated resistance to turnip crinkle virus in *Arabidopsis*. *Plant Journal*, 40(5), 647–659. <http://doi.org/10.1111/j.1365-313X.2004.02241.x>
- Chaudhari, P., Ahmed, B., Joly, D. L., & Germain, H. (2014). Effector biology during biotrophic invasion of plant cells. *Virulence*, 5(7), 1–7. <http://doi.org/10.4161/viru.29652>
- Chen, W. P., Chen, P. D., Liu, D. J., Kynast, R., Friebe, B., Velazhahan, R., ... Gill, B. S. (1999). Development of wheat scab symptoms is delayed in transgenic wheat plants that constitutively express a rice thaumatin-like protein gene. *Theoretical and Applied Genetics*, 99(5), 755–760. <http://doi.org/10.1007/s001220051294>
- Chen, Y., Liu, Z., & Halterman, D. A. (2012). Molecular determinants of resistance activation and suppression by *Phytophthora infestans* effector IPI-O. *PLoS Pathogens*, 8(3). <http://doi.org/10.1371/journal.ppat.1002595>
- Chen, S., Songkumarn, P., Venu, R. C., Gowda, M., Bellizzi, M., Hu, J., ... Wang, G.-L. (2013). Identification and characterization of in planta-expressed secreted effector proteins from *Magnaporthe oryzae* that induce cell death in rice. *Molecular Plant-Microbe Interactions: MPMI*, 26(2), 191–202. <http://doi.org/10.1094/MPMI-05-12-0117-R>
- Chen, J., Hu, Q., Zhang, Y., Lu, C., & Kuang, H. (2014a). P-MITE: A database for plant miniature inverted-repeat transposable elements. *Nucleic Acids Research*, 42(D1), 1176–1181. <http://doi.org/10.1093/nar/gkt1000>
- Chen, W., Wellings, C., Chen, X., Kang, Z., & Liu, T. (2014b). Pathogen profile Wheat stripe (yellow) rust caused by *Puccinia striiformis* f. sp. tritici. *Molecular Plant Pathology*, 15, 433–446. <http://doi.org/10.1111/mpp.12116>
- Chen, S., Rouse, M. N., Zhang, W., Jin, Y., Akhunov, E., Wei, Y., & Dubcovsky, J. (2015). Fine mapping and characterization of *Sr21*, a temperature-sensitive diploid wheat resistance gene effective against the *Puccinia graminis* f. sp. tritici Ug99 race group. *Theoretical and Applied Genetics*, 128(4), 645–656. <http://doi.org/10.1007/s00122-015-2460-x>
- Chester, K. S. (1946). The nature and prevention of the cereal rusts as exemplified in the leaf rust of wheat (Chronica B). New York, NY: The Cronica Botanica, Waltham.

- Choi, J., Park, J., Kim, D., Jung, K., Kang, S., & Lee, Y.-H. (2010). Fungal secretome database: integrated platform for annotation of fungal secretomes. *BMC Genomics*, *11*, 105. <http://doi.org/10.1186/1471-2164-11-105>
- Christelle, Danielle Ekom, T., Benchekroun, M. N., Mahabal Udupa, S., Iraqi, D., & Ennaji, M. M. (2015). Wheat Genetic Transformation as Efficient Tools to Fight against Fungal Diseases. *Journal of Agricultural Science and Technology A*, *5*(3), 153–161. <http://doi.org/10.17265/2161-6256/2015.03.001>
- Cingolani, P., Platts, A., Wang, L. L., Coon, M., Nguyen, T., Wang, L., ... Ruden, D. M. (2012). A program for annotating and predicting the effects of single nucleotide polymorphisms, SnpEff. *Fly*, *6*(2), 80–92. <http://doi.org/10.4161/fly.19695>
- Cloutier, S., McCallum, B. D., Loutre, C., Banks, T. W., Wicker, T., Feuillet, C., ... Jordan, M. C. (2007). Leaf rust resistance gene *Lr1*, isolated from bread wheat (*Triticum aestivum* L.) is a member of the large psr567 gene family. *Plant Molecular Biology*, *65*, 93–106. <http://doi.org/10.1007/s11103-007-9201-8>
- Coleman, J., Inukai, M., & Inouye, M. (1985). Dual functions of the signal peptide in protein transfer across the membrane. *Cell*, *43*(1), 351–360. [http://doi.org/10.1016/0092-8674\(85\)90040-6](http://doi.org/10.1016/0092-8674(85)90040-6)
- Collier, S. M., & Moffett, P. (2009). NB-LRRs work a “bait and switch” on pathogens. *Trends in Plant Science*, *14*(10), 521–9. <http://doi.org/10.1016/j.tplants.2009.08.001>
- Collins, N. C., Webb, C. a, Seah, S., Ellis, J. G., Hulbert, S. H., & Pryor, a. (1998). The isolation and mapping of disease resistance gene analogs in maize. *Molecular Plant-Microbe Interactions : MPMI*, *11*(10), 968–978. <http://doi.org/10.1094/MPMI.1998.11.10.968>
- Cook, D. E., Mesarich, C. H., & Thomma, B. P. H. J. (2015). Understanding Plant Immunity as a Surveillance System to Detect Invasion. *Annual Review of Phytopathology*, *53*(1), 541–563. <http://doi.org/10.1146/annurev-phyto-080614-120114>
- Costanzo, S., & Jia, Y. (2009). Alternatively spliced transcripts of *Pi-ta* blast resistance gene in *Oryza sativa*. *Plant Science*, *177*(5), 468–478. <http://doi.org/10.1016/j.plantsci.2009.07.012>
- Cowger, C. (2007). Blended Wheat Varieties Show Their Strength. *Agricultural Research USDA*, *55*(5).
- Crute, I. R., & Pink, D. A. (1996). Genetics and Utilization of Pathogen Resistance in Plants. *The Plant Cell*, *8*(10), 1747–1755. <http://doi.org/10.1105/tpc.8.10.174>
- Cuomo, C. A., Bakkeren, G., Khalil, H. B., Panwar, V., Joly, D., Linning, R., ... Fellers, J. P. (2016). Comparative analysis highlights variable genome content of wheat rusts and divergence of the mating loci. *bioRxiv*, *0*, 60665. <http://doi.org/10.1101/060665>

- Daboussi, M.-J., & Capy, P. (2003). Transposable elements in filamentous fungi. *Annual Review of Microbiology*, *57*, 275–299. <http://doi.org/10.1146/annurev.micro.57.030502.091029>
- Dagvadorj, B., Ozketen, A. C., Andac, A., Duggan, C., Bozkurt, T. O., & Akkaya, M. S. (2017). A *Puccinia striiformis* f. sp. *tritici* secreted protein activates plant immunity at the cell surface. *Nature*, *7*(1), 1141. <http://doi.org/10.1038/s41598-017-01100-z>
- Dangl, J. L., Jones, J. D. G. (2001). Defence responses to infection. *Nature*, *411*, 826–833.
- de Wit, P. J. G. M. (1992). Molecular characterization of gene-for-gene systems in plant-fungus interactions and the application of avirulence genes in control of plant pathogens. *Annual Review of Phytopathology*, *30*, 391–418.
- de Wit, P. J., Hofman, A. E., Velthuis, G., & Kuc, J. (1985). Isolation and characterization of an elicitor of necrosis isolated from intercellular fluids of compatible interactions of *Cladosporium fulvum* and tomato. *Plant Phys.*, *77*, 642–647.
- de Wit, P. J. G. M., Mehrabi, R., Van Den Burg, H. A., Stergiopoulos, I. (2009). Fungal effector proteins: Past, present and future: Review. *Molecular Plant Pathology*, *10*(6), 735–747. <http://doi.org/10.1111/j.1364-3703.2009.00591.x>
- De Wolf, E., T. Murray, P. Pierce, L. Osborne, and A. T. (2011). Identification and Management of Stem Rust on Wheat and Barley. Retrieved from <http://smallgrains.wsu.edu/>
- Dean, R., Van Kan, J. A. L., Pretorius, Z. A., Hammond-Kosack, K. E., Di Pietro, A., Spanu, P. D., ... Foster, G. D. (2012). The Top 10 fungal pathogens in molecular plant pathology. *Molecular Plant Pathology*, *13*(4), 414–430. <http://doi.org/10.1111/j.1364-3703.2011.00783.x>
- Deslandes, L., Olivier, J., Peeters, N., Feng, D. X., Khounlotham, M., Boucher, C., ... Marco, Y. (2003). Physical interaction between RRS1-R, a protein conferring resistance to bacterial wilt, and PopP2, a type III effector targeted to the plant nucleus. *Proceedings of the National Academy of Sciences of the United States of America*, *100*(13), 8024–9. <http://doi.org/10.1073/pnas.1230660100>
- Dinesh-Kumar, S. P., & Baker, B. J. (2000). Alternatively spliced N resistance gene transcripts: their possible role in tobacco mosaic virus resistance. *Proceedings of the National Academy of Sciences of the United States of America*, *97*, 1908–1913. <http://doi.org/10.1073/pnas.020367497>
- Djamei, A., & Kahmann, R. (2012). *Ustilago maydis*: Dissecting the Molecular Interface between Pathogen and Plant. *PLoS Pathogens*, *8*(11), 11–14. <http://doi.org/10.1371/journal.ppat.1002955>

- Djulich, A., Schmid, A., Lenz, H., Sharma, P., Koch, C., Wirsel, S. G. R., & Voegelé, R. T. (2011). Transient transformation of the obligate biotrophic rust fungus *Uromyces fabae* using biolistics. *Fungal Biology*, *115*(7), 633–642.
- Dmochowska-Boguta, M., Nadolska-Orczyk, A., & Orczyk, W. (2013). Roles of peroxidases and NADPH oxidases in the oxidative response of wheat (*Triticum aestivum*) to brown rust (*Puccinia triticina*) infection. *Plant Pathology*, *62*(5), 993–1002. <http://doi.org/10.1111/ppa.12009>
- Dodds, P. N., Lawrence, G. J., Catanzariti, A.-M., Teh, T., Wang, C.-I. A., Ayliffe, M. A., ... Ellis, J. G. (2006). Direct protein interaction underlies gene-for-gene specificity and coevolution of the flax resistance genes and flax rust avirulence genes. *Proceedings of the National Academy of Sciences of the United States of America*, *103*(23), 8888–8893. <http://doi.org/10.1073/pnas.0602577103>
- Dodds, P. N., Rafiqi, M., Gan, P. H. P., Hardham, A. R., Jones, D. A., & Ellis, J. G. (2009). Effectors of biotrophic fungi and oomycetes: Pathogenicity factors and triggers of host resistance. *New Phytologist*, *183*(4), 993–1000. <http://doi.org/10.1111/j.1469-8137.2009.02922.x>
- Dodds, P. N., Lawrence, G. J., Catanzariti, A.-M., Ayliffe, M. A., & Ellis, J. G. (2004). The *Melampsora lini AvrL567* avirulence genes are expressed in haustoria and their products are recognized inside plant cells. *The Plant Cell*, *16*(3), 755–68. <http://doi.org/10.1105/tpc.020040>
- Dodds, P. N., & Rathjen, J. P. (2010). Plant immunity: towards an integrated view of plant-pathogen interactions. *Nature Reviews. Genetics*, *11*(8), 539–48. <http://doi.org/10.1038/nrg2812>
- Dong, S., Raffaele, S., Kamoun, S. (2015). The two-speed genomes of filamentous pathogens: Waltz with plants. *Current Opinion in Genetics and Development*, *35*, 57–65. <http://doi.org/10.1016/j.gde.2015.09.001>
- Dong, Y., Li, Y., Qi, Z., Zheng, X., & Zhang, Z. (2016). Genome plasticity in filamentous plant pathogens contributes to the emergence of novel effectors and their cellular processes in the host. *Current Genetics*, *62*(1), 47–51. <http://doi.org/10.1007/s00294-015-0509-7>
- Dubin, H. J., & Brennan, J. P. (2009). Combating Stem and Leaf Rust of Wheat Historical Perspective, Impacts, and Lessons Learned Discussion Paper 00910. International Food Policy Research Institute.
- Dugyalá, S., Borowicz, P., & Acevedo, M. (2015). Rapid protocol for visualization of rust fungi structures using fluorochrome Uvitex 2B. *Plant Methods*, *11*(1), 54. <http://doi.org/10.1186/s13007-015-0096-0>

- Dunckel, S. M., Olson, E. L., Rouse, M. N., Bowden, R. L., & Poland, J. A. (2015). Genetic mapping of race-specific stem rust resistance in the synthetic hexaploid W7984 X opata M85 mapping population. *Crop Science*, 55(6), 2580–2588. <http://doi.org/10.2135/cropsci2014.11.0755>
- Duplessis, S. (2011a). Obligate biotrophy features unraveled by the genomic analysis of rust fungi. *Proceedings of the National Academy of Sciences of the United States of America*, 108(22), 1–23.
- Duplessis, Sébastien Joly, David L. Dodds, P. N. (2011b). Rust Effectors. In *Effectors in Plant–Microbe Interactions* (p. 155–193.). Wiley-Blackwell.
- Eckardt, N. A. (2007). Positive and Negative Feedback Coordinate Regulation of Disease Resistance Gene Expression. *The Plant Cell Online*, 19(9), 2700–2702. <http://doi.org/10.1105/tpc.107.056226>
- Edgar, R. C. (2004). MUSCLE: Multiple sequence alignment with high accuracy and high throughput. *Nucleic Acids Research*, 32(5), 1792–1797. <http://doi.org/10.1093/nar/gkh340>
- Eitas, T. Dangl, J. (2010). NB-LRR proteins: Pairs, pieces, perception, partners and Pathways. *Current Opinion in Plant Biology*, 1(13), 472–477.
- Ellis, J. G., Lagudah, E. S., Spielmeier, W., & Dodds, P. N. (2014). The past, present and future of breeding rust resistant wheat. *Front Plant Sci*, 5: 641.
- Ellis, J., Dodds, P., & Pryor, T. (2000). Structure, function and evolution of plant disease resistance genes. *Current Opinion in Plant Biology*, 3(4), 278–84.
- Ellis, J. G. (2016). Integrated decoys and effector traps: how to catch a plant pathogen. *BMC Biology*, 14(1), 13. <http://doi.org/10.1186/s12915-016-0235-8>
- Ellis, J. G., Rafiqi, M., Gan, P., Chakrabarti, A., & Dodds, P. N. (2009). Recent progress in discovery and functional analysis of effector proteins of fungal and oomycete plant pathogens. *Current Opinion in Plant Biology*, 12(4), 399–405. <http://doi.org/10.1016/j.pbi.2009.05.004>
- Emanuelsson, O., Brunak, S., von Heijne, G., & Nielsen, H. (2007). Locating proteins in the cell using TargetP, SignalP and related tools. *Nature Protocols*, 2(4), 953–971. <http://doi.org/10.1038/nprot.2007.131>
- FAO. (2014). Strengthening capacities and promoting collaboration to prevent wheat rust epidemics. Wheat Rust Diseases Global Programme 2014-2017 (Vol. 1). Rome. <http://doi.org/10.1017/CBO9781107415324.004>
- Faraji, J. (2011). Wheat cultivar blends: A step forward to sustainable agriculture. *African Journal of Agricultural Research*, 6(33), 6780–6789. <http://doi.org/10.5897/ajarx11.047>

- Faris, J. D., Zhang, Z., Lu, H., Lu, S., Reddy, L., Cloutier, S., ... Friesen, T. L. (2010). A unique wheat disease resistance-like gene governs effector-triggered susceptibility to necrotrophic pathogens. *Proceedings of the National Academy of Sciences of the United States of America*, *107*(30), 13544–9. <http://doi.org/10.1073/pnas.1004090107>
- Fedoroff, N. V. (2000). Transposable Elements and Genome Evolution. *Science*, *338*(November), 95–99.
- Ferrier-Cana, E., Macadré, C., Sévignac, M., David, P., Langin, T., & Geffroy, V. (2005). Distinct post-transcriptional modifications result into seven alternative transcripts of the CC-NBS-LRR gene JA1tr of *Phaseolus vulgaris*. *Theoretical and Applied Genetics*, *110*(5), 895–905. <http://doi.org/10.1007/s00122-004-1908-1>
- Feuillet, C., Travella, S., Stein, N., Albar, L., Nublát, A., & Keller, B. (2003). Map-based isolation of the leaf rust disease resistance gene *Lr10* from the hexaploid wheat (*Triticum aestivum* L.) genome. *Proceedings of the National Academy of Sciences*, *100*(25), 15253–15258. <http://doi.org/10.1073/pnas.2435133100>
- Feuillet, C., Langridge, P., & Waugh, R. (2008). Cereal breeding takes a walk on the wild side. *Trends in Genetics*, *24*(1), 24–32. <http://doi.org/10.1016/j.tig.2007.11.001>
- Figuroa, M., Alderman, S., Garvin, D. F., & Pfender, W. F. (2013). Infection of *Brachypodium distachyon* by Formae Speciales of *Puccinia graminis*: Early Infection Events and Host-Pathogen Incompatibility. *PLoS ONE*, *8*(2), 1–9.
- Figuroa, M., Upadhyaya, N. M., Sperschneider, J., Park, R. F., Szabo, L. J., Steffenson, B., ... Dodds, P. N. (2016). Changing the Game: Using Integrative Genomics to Probe Virulence Mechanisms of the Stem Rust Pathogen *Puccinia graminis* f. sp. *tritici*. *Frontiers in Plant Science*, *7*(February), 1–10. <http://doi.org/10.3389/fpls.2016.00205>
- Flor H.H. (1942). "Inheritance of pathogenicity in *Melampsora lini*. *Phytopathology*.(32): 653–669.
- Flor, H.H. (1947). Inheritance of reaction to rust in flax. *Journal of Agriculture. Research* (74): 241–262.
- Flor, H. H. (1971). Current status of the gene-for-gene concept. *Annual reviews of phytopathology* (9) 275–296. <http://doi.org/10.1146/annurev.py.09.090171.001423>
- Franceschetti, M., Maqbool, A., Jimenez-Dalmaroni, J., Pennigton, H., Kamoun, S., & Banfield, M. J. (2017). Effectors of filamentous plant pathogens: commonalities amid diversity. *Microbiology and Molecular Biology reviews*, *81*(2), 1–17.
- Frey, N. F. d., & Robatzek, S. (2009). Trafficking vesicles: pro or contra pathogens? *Current Opinion in Plant Biology*, *12*(4), 437–443. <http://doi.org/10.1016/j.pbi.2009.06.002>

- Fu, D., Uauy, C., Distelfeld, A., Blechl, A., Epstein, L., Chen, X., ... Dubcovsky, J. (2009). A Kinase-START Gene Confers Temperature-Dependent Resistance to Wheat Stripe Rust. *Science*, 323(5919), 1357–1360.
- Fudal, I., Ross, S., Gout, L., Blaise, F., Kuhn, M. L., Eckert, M. R., ... Rouxel, T. (2007). Heterochromatin-like regions as ecological niches for avirulence genes in the *Leptosphaeria maculans* genome: map-based cloning of *AvrLm6*. *Molecular Plant-Microbe Interactions : MPMI*, 20(4), 459–470. <http://doi.org/10.1094/MPMI-20-4-0459>
- Garnica, D. P., Upadhyaya, N. M., Dodds, P. N., & Rathjen, J. P. (2013). Strategies for Wheat Stripe Rust Pathogenicity Identified by Transcriptome Sequencing. *PLoS ONE*, 8(6). <http://doi.org/10.1371/journal.pone.0067150>
- Gates, J. E., & Loegering, W. Q. (1991). Mutation to wider virulence in *Puccinia graminis* f. sp. tritici: Evidence for the existence of loci which allow the fungus to overcome several host stem rust resistance genes simultaneously. *Applied and Environmental Microbiology*, 57(8), 2332–2336.
- Gawehns, F., Cornelissen, B. J. C., & Takken, F. L. W. (2013). The potential of effector-target genes in breeding for plant innate immunity. *Microbial Biotechnology*, 6(3), 223–229. <http://doi.org/10.1111/1751-7915.12023>
- Germán, S., Barcellos, A., Chaves, M., Kohli, M., Campos, P., & De Viedma, L. (2007). The situation of common wheat rusts in the Southern Cone of America and perspectives for control. *Australian Journal of Agricultural Research*, 58(6), 620–630. <http://doi.org/10.1071/AR06149>
- Gervais, J., Plissonneau, C., Linglin, J., Meyer, M., Labadie, K., Cruaud, C., ... Rouxel, T. (2016). Different waves of effector genes with contrasted genomic location are expressed by *Leptosphaeria maculans* during cotyledon and stem colonization of oilseed rape. *Molecular Plant Pathology*, 1–14. <http://doi.org/10.1111/ejh.12389>
- Gibriel, H. A. Y., Thomma, B. P. H. J., & Seidl, M. F. (2016). The age of effectors: genome-based discovery and applications. *Phytopathology*, (778), 1–31. <http://doi.org/10.1094/PHYTO-02-16-0110-FI>
- Gijzen, M., Ishmael, C., & Shrestha, S. D. (2014). Epigenetic control of effectors in plant pathogens. *Frontiers in Plant Science*, 5(November), 638.
- Gilroy, E. M., Breen, S., Whisson, S. C., Squires, J., Hein, I., Kaczmarek, M., ... Birch, P. R. J. (2011). Presence/absence, differential expression and sequence polymorphisms between *PiAVR2* and *PiAVR2*-like in *Phytophthora infestans* determine virulence on R2 plants. *The New Phytologist*, 191(3), 763–76. <http://doi.org/10.1111/j.1469-8137.2011.03736.x>
- Giraldo, M. C., Dagdas, Y. F., Gupta, Y. K., Mentlak, T. a, Yi, M., Martinez-Rocha, A. L., ... Valent, B. (2013). Two distinct secretion systems facilitate tissue invasion by the rice blast

- fungus *Magnaporthe oryzae*. *Nature Communications*, 4(May), 1996. <http://doi.org/10.1038/ncomms2996>
- Giraldo, M. C., & Valent, B. (2013). Filamentous plant pathogen effectors in action. *Nature Reviews. Microbiology*, 11(11), 800–814. <http://doi.org/10.1038/nrmicro3119>
- Godfrey, D., Böhlenius, H., Pedersen, C., Zhang, Z., Emmersen, J., & Thordal-Christensen, H. (2010). Powdery mildew fungal effector candidates share N-terminal Y/F/WxC-motif. *BMC Genomics*, 11(1), 317. <http://doi.org/10.1186/1471-2164-11-317>
- Godoy-Ruiz, R., Perez-Jimenez, R., Ibarra-Molero, B., & Sanchez-Ruiz, J. M. (2005). A stability pattern of protein hydrophobic mutations that reflects evolutionary structural optimization. *Biophysical Journal*, 89(5), 3320–31. <http://doi.org/10.1529/biophysj.105.067025>
- Goodin MM, Zaitlin D, Naidoo RA, L. S. (2008). *Nicotiana benthamiana* : Its history and future as a model for plant-pathogen. *PubMed*, 21(8), 18616398. <http://doi.org/10.1094/MPMI>
- Grabherr, M. G., Haas, B. J., Yassour, M., Levin, J. Z., Thompson, D. A., Amit, I., ... Regev, A. (2011). Full-length transcriptome assembly from RNA-Seq data without a reference genome. *Nature Biotechnology*, 29(7), 644–52. <http://doi.org/10.1038/nbt.1883>
- Grandaubert, J., Lowe, R. G. T., Soyer, J. L., Schoch, C. L., Van de Wouw, A. P., Fudal, I., ... Rouxel, T. (2014). Transposable element-assisted evolution and adaptation to host plant within the *Leptosphaeria maculans*-*Leptosphaeria biglobosa* species complex of fungal pathogens. *BMC Genomics*, 15(891), 1–27. <http://doi.org/10.1186/1471-2164-15-891>
- Grant, M. R., Kazan, K., & Manners, J. M. (2013). Exploiting pathogens' tricks of the trade for engineering of plant disease resistance: Challenges and opportunities. *Microbial Biotechnology*, 6(3), 212–222. <http://doi.org/10.1111/1751-7915.12017>
- Graveley, B. (2001). Alternative splicing: increasing diversity in the proteomic world. *Trends in Genetics*, 17(2), 100–107. [http://doi.org/10.1016/S0168-9525\(00\)02176-4](http://doi.org/10.1016/S0168-9525(00)02176-4)
- Greene, E. A., Codomo, C. A., Taylor, N. E., Henikoff, J. G., Till, B. J., Reynolds, S. H., ... Henikoff, S. (2003). Spectrum of chemically induced mutations from a large-scale reverse-genetic screen in Arabidopsis. *Genetics*, 164(2), 731–740.
- Groth, J.V. Roelfs, A. P. (1987). The concept and measurement of phenotypic diversity in *Puccinia graminis* on wheat. *Phytopathology*, 77, 1395–1399.
- Gu, K., Yang, B., Tian, D., Wu, L., Wang, D., Sreekala, C., ... Yin, Z. (2005). R gene expression induced by a type-III effector triggers disease resistance in rice. *Nature*, 435(7045), 1122–1125. <http://doi.org/10.1038/nature03630>

- Gu, L., Si, W., Zhao, L., Yang, S., & Zhang, X. (2015). Dynamic evolution of NBS_LRR genes in bread wheat and its progenitors. *Molecular Genetics and Genomics*, 290(2), 727–738. <http://doi.org/10.1007/s00438-014-0948-8>
- Guo, C., Spinelli, M., Ye, C., Li, Q. Q., & Liang, C. (2017). Genome-Wide Comparative Analysis of Miniature Inverted Repeat Transposable Elements in 19 *Arabidopsis thaliana* Ecotype Accessions. *Scientific Reports*, 7(1), 1–12. <http://doi.org/10.1038/s41598-017-02855-1>
- Gupta, S., Chakraborti, D., Basu, D., Das, S. (2010). In search of Decoy/Guardee to R Genes. *Plant Signaling & Behavior*, 5(9), 1081–1087. <http://doi.org/10.4161/psb.5.9.12234>
- Gururani, M. A., Venkatesh, J., Upadhyaya, C. P., Nookaraju, A., Pandey, S. K., Park, S. W. (2012). Plant disease resistance genes: Current status and future directions. *Physiological and Molecular Plant Pathology*, 78, 51–65. <http://doi.org/10.1016/j.pmpp.2012.01.002>
- Haas, B. J., Zeng, Q., Pearson, M. D., Cuomo, C. A., & Wortman, J. R. (2011). Approaches to Fungal Genome Annotation. *Mycology*, 2(3), 118–141.
- Hann, D., & Boller, T. (2011). Microbial Effectors and Their Role in Plant Defense Suppression. In *Effectors in Plant–Microbe Interactions*. Wiley-Blackwell.
- Hacquard, S., Joly, D. L., Lin, Y.-C., Tisserant, E., Feau, N., Delaruelle, C., ... Duplessis, S. (2012). A comprehensive analysis of genes encoding small secreted proteins identifies candidate effectors in *Melampsora larici-populina* (poplar leaf rust). *Molecular Plant–Microbe Interactions*, 25(3), 279–93. <http://doi.org/10.1094/MPMI-09-11-0238>
- Haile, J. K., Nachit, M. M., Hammer, K. ., Badebo, A., & Röder, M. S. (2012). QTL mapping of resistance to race Ug99 of *Puccinia graminis* f. sp. *tritici* in durum wheat (*Triticum durum* Desf.). *Molecular Breeding*, 30(3), 1479–1493. <http://doi.org/10.1007/s11032-012-9734-7>
- Haile, J., & Röder, M. (2013). Status of genetic research for resistance to Ug99 race of *Puccinia graminis* f. sp. *tritici*: A review of current research and implications. ... *Journal of Agricultural Research*, 8(50), 6670–6680. <http://doi.org/10.5897/AJAR2013.7257>
- Halpin, C. (2005). Gene stacking in transgenic plants - The challenge for 21st century plant biotechnology. *Plant Biotechnology Journal*, 3(2), 141–155. <http://doi.org/10.1111/j.1467-7652.2004.00113.x>
- Halterman, Dennis., wei, Fusheng., Wise, R. (2003). Powdery Mildew-Induced Mla mRNAs Are Alternatively Spliced and Contain Multiple Upstream Open Reading Frames. *Plant Physiology*, 131(2), 558–567. <http://doi.org/10.1104/pp.014407>
- Hammond-Kosack, K. E., & Jones, J. D. G. (1997). Plant Disease Resistance Genes. *Annual Review of Plant Physiology and Plant Molecular Biology*, 48(1), 575–607. <http://doi.org/10.1146/annurev.arplant.48.1.575>

- Heath, M. C. (1991). The role of gene-for-gene interactions in the determination of host species specificity. *Phytopathology*, *81*, 127–130.
- Henry, I. M., Nagalakshmi, U., Lieberman, M. C., Ngo, K. J., Krasileva, K. V, Vasquez-Gross, H., ... Comai, L. (2014). Efficient Genome-Wide Detection and Cataloging of EMS-Induced Mutations Using Exome Capture and Next-Generation Sequencing. *The Plant Cell*, *26*(4), 1382–1397. <http://doi.org/10.1105/tpc.113.121590>
- Himmelbach, A., Zierold, U., Hensel, G., Riechen, J., Douchkov, D., Schweizer, P., & Kumlehn, J. (2007). A set of modular binary vectors for transformation of cereals. *Plant Physiology*, *145*(December), 1192–1200. <http://doi.org/10.1104/pp.107.111575>
- Hobert, O. (2002). PCR fusion-based approach to create reporter gene constructs for expression analysis in transgenic *C. elegans*. *BioTechniques*, *32*(4), 728–730.
- Hogenboom, N. G. (1993). Economic Importance of Breeding for Disease Resistance. In T. Jacobs & J. E. Parlevliet (Eds.), *Durability of Disease Resistance* (pp. 5–9). Dordrecht: Springer Netherlands.
- Hogenhout, S. a, Van der Hoorn, R. a L., Terauchi, R., & Kamoun, S. (2009). Emerging concepts in effector biology of plant-associated organisms. *Molecular Plant-Microbe Interactions : MPMI*, *22*(2), 115–122. <http://doi.org/10.1094/MPMI-22-2-0115>
- Holub, E. B., Brose, E., Tör, M., Clay, C., Crute, I. R., Beynon, J. L., ... Beynon, J. L. (1995). Phenotypic and genotypic variation in the interaction between *Arabidopsis thaliana* and *Albugo candida*. *Molecular Plant-Microbe Interactions*, *8*(6), 916–928. <http://doi.org/10.1094/MPMI-8-0916>
- Horvath, H., Rostoks, N., Brueggeman, R., Steffenson, B., von Wettstein, D., & Kleinhofs, A. (2003). Genetically engineered stem rust resistance in barley using the *Rpg1* gene. *Proc Natl Acad Sci U S A*, *100*(1), 364–369. <http://doi.org/10.1073/pnas.0136911100>
- Houterman, P. M., Ma, L., Van Ooijen, G., De Vroomen, M. J., Cornelissen, B. J. C., Takken, F. L. W., Rep, M. (2009). The effector protein Avr2 of the xylem-colonizing fungus *Fusarium oxysporum* activates the tomato resistance protein I-2 intracellularly. *Plant Journal*, *58*(6), 970–978. <http://doi.org/10.1111/j.1365-313X.2009.03838.x>
- Hu, C. D., Chinenov, Y., & Kerppola, T. K. (2002). Visualization of interactions among bZIP and Rel family proteins in living cells using bimolecular fluorescence complementation. *Molecular Cell*, *9*(4), 789–798. [http://doi.org/10.1016/S1097-2765\(02\)00496-3](http://doi.org/10.1016/S1097-2765(02)00496-3)
- Hu, C.-D., & Kerppola, T. (2003). Simultaneous visualization of multiple protein interactions in living cells using multicolor fluorescence complementation analysis. *Nature Biotechnology*, *21*(5), 539–545. <http://doi.org/10.1038/nbt816>

- Huang, L., Brooks, S. a, Li, W., Fellers, J. P., Trick, H. N., & Gill, B. S. (2003). Map-based cloning of leaf rust resistance gene *Lr21* from the large and polyploid genome of bread wheat. *Genetics*, *164*(2), 655–64.
- Huang, X., Chen, X., Coram, T., Wang, M., & Kang, Z. (2011). Gene expression profiling of *Puccinia striiformis* f. sp. *tritici* during development reveals a highly dynamic transcriptome. *Journal of Genetics and Genomics*, *38*(8), 357–371. <http://doi.org/10.1016/j.jgg.2011.07.004>
- Inami, K., Yoshioka-Akiyama, C., Morita, Y., Yamasaki, M., Teraoka, T., & Arie, T. (2012). A genetic mechanism for emergence of races in *Fusarium oxysporum* f. sp. *lycopersici*: Inactivation of avirulence gene *AVR1* by transposon insertion. *PLoS ONE*, *7*(8), 1–10. <http://doi.org/10.1371/journal.pone.0044101>
- Inoué, S. (2006). Foundations of Confocal Scanned Imaging in Light Microscopy. In J. Pawley (Ed.), *Handbook of Biological Confocal Mycroscopy* (Third, p. 985). New York, NY: Springer US.
- Inoue, A. Y., Vy, T. T. P., Yoshida, K., & Asano, H. (2017). Evolution of the wheat blast fungus through functional losses in a host specificity determinant, *Science* *583*, 80–83. <http://doi.org/10.1126/science.aam9654>
- Ishida, Y., Hiei, Y., & Komari, T. (2015). High Efficiency Wheat Transformation Mediated by *Agrobacterium tumefaciens*. In Y. Ogihara, S. Takumi, & H. Handa (Eds.), *Advances in Wheat Genetics: From Genome to Field* (pp. 167–173). Tokyo: Springer Japan.
- Jacobs, A. S., Pretorius, Z. A., Kloppers, F. J., & Cox, T. S. (1996). Mechanisms associated with wheat leaf rust resistance derived from *Triticum monococcum*. *Phytopathology*, *86*, 588–595.
- Jain, S. K., Prashar, M., Bhardwaj, S. C., Singh, S. B., & Sharma, Y. P. (2009). Emergence of Virulence to *Sr25* of *Puccinia graminis* f. sp. *tritici* on Wheat in India. *Plant Disease*, *93*(8), 840.
- Janakiraman, V., Steinau, M., McCoy, S. B., & Trick, H. N. (2002). Recent Advances in Wheat Transformation. *In Vitro Cellular & Developmental Biology - Plant*, *38*(5), 404–414. <http://doi.org/10.1079/IVP2002320>
- Jia, Y., McAdams, S., Bryan, G., Hershey, H., Valent, B., & 15. (2000). Direct interaction of resistance gene and avirulence gene products confers rice blast resistance. *Embo*, *19*(15), 4004–4014.
- Jiang, G. H., Xia, Z. H., Zhou, Y. L., Wan, J., Li, D. Y., Chen, R. S., ... Zhu, L. H. (2006). Testifying the rice bacterial blight resistance gene *xa5* by genetic complementation and further analyzing *xa5* (*Xa5*) in comparison with its homolog *TFIIAγ1*. *Molecular Genetics and Genomics*, *275*(4), 354–366. <http://doi.org/10.1007/s00438-005-0091-7>

- Jin, Y., Singh, R. P., Ward, R. W., Wanyera, R., Kinyua, M., Njau, P., ... Yahyaoui, a. (2007). Characterization of Seedling Infection Types and Adult Plant Infection Responses of Monogenic *Sr* Gene Lines to Race TTKS of *Puccinia graminis* f. sp. *tritici*. *Plant Disease*, 91(9), 1096–1099. <http://doi.org/10.1094/pdis-91-9-1096>
- Jin, Y., Szabo, L. J., Pretorius, Z. a., Singh, R. P., Ward, R., & Fetch, T. (2008). Detection of virulence to resistance gene *Sr24* within race TTKS of *Puccinia graminis* f. sp. *tritici*. *Plant Disease*, 92(6), 923–926. <http://doi.org/10.1094/PDIS-92-6-0923>
- Johal, G.S., Briggs, S. P. (1992). Reductase activity encoded by the *Hm1* disease resistance gene in maize. *Science*, 258, 985–987.
- Jones, J. D. G., & Dangl, J. L. (2006). The plant immune system. *Nature*, 444(7117), 323–9. <http://doi.org/10.1038/nature05286>
- Jonge, R. De, Esse, H. P. Van, Kombrink, A., Shinya, T., Desaki, Y., Bours, R., ... Thomma, B. P. H. J. (2010). Conserved Fungal LysM Effector *Ecp6* Prevents Chitin-Triggered Immunity in Plants. *Science*, 329, 953–955. <http://doi.org/10.1126/science.1190859>
- Joosten, M. H. A. J., Cozijnsen, T. J., & de Wit, P. J. G. M. (1994). Host resistance to a fungal tomato pathogen lost by a single base-pair change in avirulence gene. *Nature*, 367, 384–385.
- Joosten, M. H. A. J., & de Wit, P. J. G. M. (1999). The tomato *Cladosporium fulvum* interaction: a versatile experient system to study plant aphthogen interaction. *Annual Review of Phytopathology*, 37(14), 335–367.
- Kale, S. D., & Tyler, B. M. (2011). Entry of oomycete and fungal effectors into plant and animal host cells. *Cellular Microbiology*, 13(12), 1839–1848. <http://doi.org/10.1111/j.1462-5822.2011.01659.x>
- Kalyana, M., Simpson, C. G., Syed, N. H., Lewandowska, D., Marquez, Y., Kusenda, B., ... Brown, J. W. S. (2012). Alternative splicing and nonsense-mediated decay modulate expression of important regulatory genes in *Arabidopsis*. *Nucleic Acids Research*, 40(6), 2454–2469. <http://doi.org/10.1093/nar/gkr932>
- Kang, S., Lebrun, M. H., Farrall, L., & Valent, B. (2001). Gain of virulence caused by insertion of a Pot3 transposon in a *Magnaporthe grisea* avirulence gene. *Molecular Plant-Microbe Interactions*, 14(5), 671–4. <http://doi.org/10.1094/MPMI.2001.14.5.671>
- Kamoun, S. (2007). Groovy times: filamentous pathogen effectors revealed. *Current Opinion in Plant Biology*, 10(4), 358–365. <http://doi.org/10.1016/j.pbi.2007.04.017>
- Kay, S., Bonas, U. (2009). How *Xanthomonas* type III effectors manipulate the host plant. *Current Opinion in Microbiology*, 12(1), 37–43. <http://doi.org/10.1016/j.mib.2008.12.006>

- Keane, P. J. (2012). Horizontal or Generalized Resistance to Pathogens. In C. J. Cumagun (Ed.), *Plant pathology*. InTech. <http://doi.org/10.5772/30763>
- Keller, B., Feuillet, C., & Messmer, M. (2000). Genetics of disease resistance. In A. J. Slusarenko, R. S. S. Fraser, van L. C. (Eds.), *Mechanisms of Resistance to Plant Diseases* Springer.
- Kemen, E., Gardiner, A., Schultz-Larsen, T., Kemen, A. C., Balmuth, A. L., Robert-Seilaniantz, A., ... Jones, J. D. G. (2011). Gene gain and loss during evolution of obligate parasitism in the white rust pathogen of *Arabidopsis thaliana*. *PLoS Biology*, 9(7). <http://doi.org/10.1371/journal.pbio.1001094>
- Kemen, E., Kemen, A., Ehlers, A., Voegele, R., & Mendgen, K. (2013). A novel structural effector from rust fungi is capable of fibril formation. *Plant Journal*, 75(5), 767–780. <http://doi.org/10.1111/tpj.12237>
- Kemen, E., Kemen, A. C., Rafiqi, M., Hempel, U., Mendgen, K., Hahn, M., & Voegele, R. T. (2005). Identification of a Protein from Rust Fungi Transferred from Haustoria into Infected Plant Cells. *Molecular Plant-Microbe Interactions*, 18(11), 1130–1139. <http://doi.org/10.1094/MPMI-18-1130>
- Khan, M. H., Bukhari, A., Dar, Z. A., & Rizvi, S. M. (2013). Status and strategies in breeding for rust resistance in wheat. *Agricultural Sciences*, 4(6), 292–301. <http://doi.org/10.4236/as.2013.46042>
- Khush, G. (2001). Green revolution : the way forward. *Nature Reviews. Genetics*, (2) 815–822
- Kim, S. H., Kwon, S. Il, Saha, D., Anyanwu, N. C., & Gassmann, W. (2009). Resistance to the *Pseudomonas syringae* effector HopA1 is governed by the TIR-NBS-LRR protein RPS6 and is enhanced by mutations in SRFR1. *Plant Physiology*, 150(4), 1723–32. <http://doi.org/10.1104/pp.109.139238>
- Kim, S. H., Qi, D., & Helm, M. (2016). Using decoys to expand the recognition specificity of a plant disease resistance protein. *Science*, 351(6274), 684–687. <http://doi.org/doi:10.1126/science.aad3436>
- Kim, Y., Schumaker, K. S., & Zhu, J.-K. (2006). EMS Mutagenesis of *Arabidopsis*. In J. Salinas & J. J. Sanchez-Serrano (Eds.), *Arabidopsis Protocols* (pp. 101–103). Totowa, NJ: Humana Press.
- Kinyoro, J., Wanyera, R., Kilonzo, S. (2013). Evaluation of Fungicides for Controlling Stem Rust Race *Ug99* on Bread Wheat. *Journal of Agricultural Science and Technology*, 3, 404–409.
- Kiran, K., Rawal, H. C., Dubey, H., Jaswal, R., Devanna, B. ., Gupta, D. K., ... Sharma, T. R. (2016). Draft genome of the wheat rust pathogen (*Puccinia triticina*) unravels genome-wide

- structural variations during evolution. *Genome Biology and Evolution*, 8(9), evw197. <http://doi.org/10.1093/gbe/evw197>
- Kirk, P.M., Cannon, P.F., Minter, D.W., Stalpers, J. A. (2008). *Dictionary of the Fungi* (10th ed.). Wallingford, UK: CABI.
- Kitin, P., Funada, R., Sano, Y., & Ohtani, J. (2000). Analysis by confocal microscopy of the structure of cambium in the hardwood *Kalopanax pictus*. *Annals of Botany*, 86(6), 1109–1117. <http://doi.org/10.1006/anbo.2000.1281>
- Kislev, M. E. (1982). Stem rust of wheat 3300 years old found in Israel. *Science*, 216, 993–994.
- Knott, D. (1988). Using polygenic resistance to breed for stem rust resistance in wheat. In S. Simmonds, N.W., Rajaram (Ed.), *Breeding Strategies for Resistance to the Rusts of Wheat* (pp. 39–47). Mexico, D.F.: CIMMYT.
- Koch, H. H., & Pimsler, M. (1987). Evaluation of Uvitex 2B: a nonspecific fluorescent stain for detecting and identifying fungi and algae in tissue. *Lab. Med*, 18(9), 603–606.
- Kolmer, J., Chen, X., & Jin, Y. (2009a). Diseases Which Challenge Global Wheat Production—the Wheat Rusts. In B. F. Carver (Ed.), *Wheat Science and Trade* (pp. 89–124). Ames, Iowa: Wiley-Blackwell. [http://doi.org/10.1016/S0376-7361\(09\)70018-4](http://doi.org/10.1016/S0376-7361(09)70018-4)
- Kolmer, J. A., Dyck, P. L., Roelfs, A. P. (1991). An appraisal of stem rust resistance in North American hard red spring wheats and the probability of multiple mutations to virulence in populations of cereal rust fungi. *Phytopathology*. 81(3), 237-239
- Kolmer, J. (2013). Leaf rust of wheat: Pathogen biology, variation and host resistance. *Forests*, 4(1), 70–84. <http://doi.org/10.3390/f4010070>
- Kolmer, James., Ordonez, Maria., & Groth, J. (2009b). The Rust Fungi. In *Encyclopedia of Life Sciences*. Chichester: John Wiley & Sons, Ltd.
- Kota, R., Spielmeier, W., McIntosh, R. A., & Lagudah, E. S. (2006). Fine genetic mapping fails to dissociate durable stem rust resistance gene *Sr2* from pseudo-black chaff in common wheat (*Triticum aestivum* L.). *Theoretical and Applied Genetics*, 112(3), 492–499. <http://doi.org/10.1007/s00122-005-0151-8>
- Krattinger, S. G., Lagudah, E. S., Spielmeier, W., Singh, R. P., Huerta-espino, J., Mcfadden, H., ... Keller, B. (2009). A Putative ABC Transporter Confers Durable Resistance to Multiple Fungal Pathogens in Wheat. *Science*, 323(6), 1360–1363.
- Kumar, J., Pratap, A. (2014). Alien Gene Transfer: Challenges and Opportunities. Volume 1: Innovations, Methods and Risk Assessment. In J. Pratap, A Kumar (Ed.), *Alien Gene Transfer in Crop Plants* (pp. 289–307). New York.

- Künstler, A., Bacsó, R., Gullner, G., Hafez, Y. M., & Király, L. (2016). Staying alive - is cell death dispensable for plant disease resistance during the hypersensitive response? *Physiological and Molecular Plant Pathology*, 93(January), 75–84. <http://doi.org/10.1016/j.pmpp.2016.01.003>
- Hamada, H., Linghu, Q., Nagira, Y., Miki, R., Taoka, N., & Imai, R. (2017). An in planta biolistic method for stable wheat transformation. *Scientific Reports*, 7(1), 2–9. <http://doi.org/10.1038/s41598-017-11936-0>
- Hogenboom, N. G. (1993). Economic Importance of Breeding for Disease Resistance. In T. Jacobs & J. E. Parlevliet (Eds.), *Durability of Disease Resistance* (pp. 5–9). Dordrecht: Springer Netherlands.
- Lamb, C., & Dixon, R. A. (1997). The oxidative burst in plant disease resistance. *Annu Rev Plant Physiol and Plant Mol Biol*, 48. <http://doi.org/10.1146/annurev.arplant.48.1.251>
- Lawrence, G. J., Finnegan, E. J., Ayliffe, M. A., & Ellis, J. G. (1995). The *L6* gene for flax rust resistance is related to the *Arabidopsis* bacterial resistance gene *RPS2* and the tobacco viral resistance gene *N*. *The Plant Cell*, 7(8), 1195–1206. <http://doi.org/10.1105/tpc.7.8.1195>
- Lawrence, G. J., Dodds, P. N., & Ellis, J. G. (2010). Transformation of the flax rust fungus, *Melampsora lini*: Selection via silencing of an avirulence gene. *Plant Journal*, 61(2), 364–369. <http://doi.org/10.1111/j.1365-313X.2009.04052.x>
- Leister, R. T., Ausubel, F. M., & Katagiri, F. (1996). Molecular recognition of pathogen attack occurs inside of plant cells in plant disease resistance specified by the *Arabidopsis* genes *RPS2* and *RPM1*. *Proceedings of the National Academy of Sciences of the United States of America*, 93(December), 15497–15502.
- Leornad, K.J., Szabo, L. S. (2005). Pathogen profile Stem rust of small grains and grasses caused by *Puccinia graminis*. *Molecular Pathology*, 6(2), 99–111. <http://doi.org/10.1111/J.1364-3703.2004.00273.X>
- Letunic, I., & Bork, P. (2016). Interactive Tree Of Life (iTOL): An online tool for phylogenetic tree display and annotation. *Bioinformatics*, 23(1), 127–128. <http://doi.org/10.1093/bioinformatics/bt1529>
- Levy, M., Edelbaum, O., Sela, I. (2004). Tobacco Mosaic Virus Regulates the Expression of Its Own Resistance Gene *N1*. *Plant Physiology*, 135, 2392–2397.
- Li, H., & Durbin, R. (2009). Fast and accurate short read alignment with Burrows-Wheeler transform. *Bioinformatics (Oxford, England)*, 25(14), 1754–60.
- Li, Y., Tessaro, M. J., Li, X., & Zhang, Y. (2010). Regulation of the Expression of Plant Resistance Gene *SNC1* by a Protein with a Conserved *BAT2* Domain. *Plant Physiology*, 153(3), 1425–1434. <http://doi.org/10.1104/pp.110.156240>

- Li, J., Ye, X., An, B., Du, L., & Xu, H. (2012). Genetic transformation of wheat: Current status and future prospects. *Plant Biotechnology Reports*, 6(3), 183–193. <http://doi.org/10.1007/s11816-011-0213-0>
- Li, Z. K., Arif, M., Zhong, D. B., Fu, B. Y., Xu, J. L., Domingo-Rey, J., ... Khush, G. S. (2006). Complex genetic networks underlying the defensive system of rice (*Oryza sativa* L.) to *Xanthomonas oryzae* pv. *oryzae*. *Proceedings of the National Academy of Sciences of the United States of America*, 103(21), 7994–9. <http://doi.org/10.1073/pnas.0507492103>
- Lindgren, P. B. (1997). The role of hrp genes during plant bacterial interactions. *Annual Review of Phytopathology*, 35(40), 129–152. <http://doi.org/10.1146/annurev.phyto.35.1.129>
- Liu, C., Pedersen, C., Schultz-Larsen, T., Aguilar, G. B., Madriz-Ordeñana, K., Hovmøller, M. S., & Thordal-Christensen, H. (2016). The stripe rust fungal effector PEC6 suppresses pattern-triggered immunity in a host species-independent manner and interacts with adenosine kinases. *New Phytologist*. <http://doi.org/10.1111/nph.14034>
- Liu, J., Liu, X., Dai, L., Wang, G. (2007). Recent progress in elucidating the structure, function and evolution of disease resistance genes in plants. *Journal of Genetics and Genomics*, 34(9), 765–776. [http://doi.org/10.1016/S1673-8527\(07\)60087-3](http://doi.org/10.1016/S1673-8527(07)60087-3)
- Liu, D., Shi, L., Han, C., Yu, J., Li, D., & Zhang, Y. (2012). Validation of Reference Genes for Gene Expression Studies in Virus-Infected *Nicotiana benthamiana* Using Quantitative Real-Time PCR. *PLoS ONE*, 7(9). <http://doi.org/10.1371/journal.pone.0046451>
- Liu, W., Frick, M., Huel, R., Nykiforuk, C. L., Wang, X., Gaudet, D. A., ... Laroche, A. (2014). The Stripe Rust Resistance Gene *Yr10* Encodes an Evolutionary-Conserved and Unique CC-NBS-LRR Sequence in Wheat. *Molecular Plant*, 7(12), 1740–1755. <http://doi.org/10.1093/mp/ssu112>
- Liu, J.-J., Sturrock, R. N., Snieszko, R. a., Williams, H., Benton, R., & Zamany, A. (2015). Transcriptome analysis of the white pine blister rust pathogen *Cronartium ribicola*: de novo assembly, expression profiling, and identification of candidate effectors. *BMC Genomics*, 16(1), 678. <http://doi.org/10.1186/s12864-015-1861-1>
- Liu, Z., Zhang, Z., Faris, J. D. ., Oliver, R. P., Syme, R., McDonald, M. C., ... Friesen, T. L. (2012). The cysteine rich necrotrophic effector *SnTox1* produced by *Stagonospora nodorum* triggers susceptibility of wheat lines harboring Snn1. *PLoS Pathogens*, 8(1). <http://doi.org/10.1371/journal.ppat.1002467>
- Livak, K. J., & Schmittgen, T. D. (2001). Analysis of relative gene expression data using real-time quantitative PCR and. *Methods*, 25, 402–408. <http://doi.org/10.1006/meth.2001.1262>
- Lo Presti, L., Lanver, D., Schweizer, G., Tanaka, S., Liang, L., Tollot, M., ... Kahmann, R. (2015). Fungal Effectors and Plant Susceptibility. *Annual Review of Plant Biology*, 66, 513–545. <http://doi.org/10.1146/annurev-arplant-043014-114623>

- Lo Presti, L., Zechmann, B., Kumlehn, J., Liang, L., Lanver, D., Tanaka, S., ... Kahmann, R. (2016). An assay for entry of secreted fungal effectors into plant cells. *New Phytologist*, 213, 956–964. <http://doi.org/10.1111/nph.14188>
- Loehrer, M., Vogel, A., Huettel, B., Reinhardt, R., Benes, V., Duplessis, S., ... Schaffrath, U. (2014). On the current status of *Phakopsora pachyrhizi* genome sequencing. *Frontiers in Plant Science*, 5, 377. <http://doi.org/10.3389/fpls.2014.00377>
- Loutre, C., Wicker, T., Travella, S., Galli, P., Scofield, S., Fahima, T., ... Keller, B. (2009). Two different CC-NBS-LRR genes are required for *Lr10*-mediated leaf rust resistance in tetraploid and hexaploid wheat. *Plant Journal*, 60(6), 1043–1054. <http://doi.org/10.1111/j.1365-313X.2009.04024.x>
- Lowe, I., Cantu, D., & Dubcovsky, J. (2011). Durable resistance to the wheat rusts: Integrating systems biology and traditional phenotype-based research methods to guide the deployment of resistance genes. *Euphytica*, 179(1), 69–79. <http://doi.org/10.1007/s10681-010-0311-z>
- Luig, N. H. (1978). Close association of two factors for avirulence in *Puccinia graminis tritici*. *Phytopathology*, 68(i), 936–937. <http://doi.org/10.1094/Phyto-68-936>
- Ma, L., van den Burg, H.A., Cornelissen, B.J.C., Takken, F. L. W. (2012a). Molecular basis of effector recognition by plant NB-LRR proteins. In G. Sessa (Ed.), *Molecular Plant Immunity* (pp. 23–36). John Wiley & Sons, Inc.
- Ma, L., Lukasik, E., Gawehns, F., & Takken, F. L. W. (2012b). The Use of Agroinfiltration for Transient Expression of Plant Resistance and Fungal Effector Proteins in *Nicotiana benthamiana* Leaves. In M. D. Bolton & B. P. H. J. Thomma (Eds.), *Plant Fungal Pathogens: Methods and Protocols* (pp. 61–74). Totowa, NJ: Humana Press.
- Macqueen, A., & Bergelson, J. (2016). Modulation of R-gene expression across environments. *Journal of Experimental Botany*, 67(7), 2093–2105. <http://doi.org/10.1093/jxb/erv530>
- Makandar, R., Essig, J. S., Schapaugh, M. a, Trick, H. N., & Shah, J. (2006). Genetically engineered resistance to Fusarium head blight in wheat by expression of *Arabidopsis* NPR1. *Molecular Plant-Microbe Interactions*, 19(2), 123–129.
- Manning, V. A., & Ciuffetti, L. M. (2005). Localization of Ptr ToxA Produced by *Pyrenophora tritici-repentis* Reveals Protein Import into Wheat Mesophyll Cells. *The Plant Cell*, 17, 3203–3212. <http://doi.org/10.1105/tpc.105.035063>
- Manoharachary, C., & Kunwar, I. (2014). Host–Pathogen Interaction, Plant Diseases, Disease Management Strategies, and Future Challenges. In A. Goyal & C. Manoharachary (Eds.), *Future Challenges in Crop Protection Against Fungal Pathogens* (pp. 185–230). New York, NY: Springer US.

- Marcroft, S. J., Van de Wouw, A. P., Salisbury, P. A., Potter, T. D., & Howlett, B. J. (2012). Effect of rotation of canola (*Brassica napus*) cultivars with different complements of blackleg resistance genes on disease severity. *Plant Pathology*, *61*(5), 934–944. <http://doi.org/10.1111/j.1365-3059.2011.02580.x>
- Marone, D., Russo, M. A., Laidò, G., De Leonardis, A. M., Mastrangelo, A. M. (2013). Plant nucleotide binding site-leucine-rich repeat (NBS-LRR) genes: Active guardians in host defense responses. *International Journal of Molecular Sciences*, *14*(4), 7302–7326. <http://doi.org/10.3390/ijms14047302>
- McDonald, B. A., & Linde, C. (2002). Pathogen Population Genetics, evolutionary Potential and Durable Resistance. *Annual Review of Phytopathology*, *40*(1), 349–379. <http://doi.org/10.1146/annurev.phyto.40.120501.101443>
- McHale, L., Tan, X., Koehl, P., & Michelmore, R. W. (2006). Plant NBS-LRR proteins: adaptable guards. *Genome Biology*, *7*(4), 212. <http://doi.org/10.1186/gb-2006-7-4-212>
- McIntosh, R. A., Wellings, C.R., Park, R. F. (1995). *Wheat Rusts: an atlas of resistance genes*. Melbourne, Australia: CSIRO.
- McIntosh, R. (1988). The Role of Specific Genes in Breeding for Durable Stem Rust Resistance in Wheat and Triticale. In S. Simmonds, N.W., Rajaram (Ed.), *Breeding strategies for resistance to rust of wheat* (pp. 1–9). Mexico, D.F.: CIMMYT.
- McKenna, A., Hanna, M., Banks, E., Sivachenko, A., Cibulskis, K., Kernytsky, A., ... DePristo, M. a. (2010). The Genome Analysis Toolkit: a MapReduce framework for analyzing next-generation DNA sequencing data. *Genome Research*, *20*(9), 1297–303. <http://doi.org/10.1101/gr.107524.110>
- Mackey, D., Holt, B. F., Wiig, A., & Dangl, J. L. (2002). RIN4 interacts with *Pseudomonas syringae* type III effector molecules and is required for RPM1-mediated resistance in *Arabidopsis*. *Cell*, *108*, 743–754. [http://doi.org/10.1016/S0092-8674\(02\)00661-X](http://doi.org/10.1016/S0092-8674(02)00661-X)
- Mackey, D., Belkhadir, Y., Alonso, J. M., Ecker, J. R., & Dangl, J. L. (2003). *Arabidopsis* RIN4 is a target of the type III virulence effector AvrRpt2 and modulates RPS2-mediated resistance. *Cell*, *112*(3), 379–389. [http://doi.org/10.1016/S0092-8674\(03\)00040-0](http://doi.org/10.1016/S0092-8674(03)00040-0)
- Mago, R., Zhang, P., Vautrin, S., Šimková, H., Bansal, U., Luo, M.-C., ... Dodds, P. N. (2015). The wheat *Sr50* gene reveals rich diversity at a cereal disease resistance locus. *Nature Plants*, *1*, 15186. Retrieved from <http://dx.doi.org/10.1038/nplants.2015.186>
- Mengiste, T. (2012). Plant Immunity to Necrotrophs. *Annual Review of Phytopathology*, *50*(1), 267–294. <http://doi.org/10.1146/annurev-phyto-081211-172955>
- Mesarich, C. H., Griffiths, S. A., van der Burgt, A., Okmen, B., Beenen, H. G., Etalo, D. W., ... de Wit, P. J. G. M. (2014). Transcriptome Sequencing Uncovers the *Avr5* Avirulence Gene

- of the Tomato Leaf Mold Pathogen *Cladosporium fulvum*. *Molecular Plant-Microbe Interactions* : *MPMI*, 27(8), 846–57. <http://doi.org/10.1094/MPMI-02-14-0050-R>
- Metzker, M. L. (2010). Sequencing technologies - the next generation. *Nature Reviews. Genetics*, 11(1), 31–46. <http://doi.org/10.1038/nrg2626>
- Michelmore, R. W., Meyers, B. C., & Young. (1998). Cluster of resistance genes in plants evolve by divergent selection and a birth-and-death process. *Genome Research*, 8, 1113–1130. [http://doi.org/10.1016/S1369-5266\(00\)00081-9](http://doi.org/10.1016/S1369-5266(00)00081-9)
- Mikaberidze, A., McDonald, B.A., Bonhoeffer, S. (2015). Developing smarter host mixtures to control plant disease. *Plant Pathology*, 64, 996–1004. <http://doi.org/10.1111/ppa.12321>
- Mogga, V., Delventhal, R., Weidenbach, D., Langer, S., Bertram, P. M., Andresen, K., ... Schaffrath, U. (2016). *Magnaporthe oryzae* effectors MoHEG13 and MoHEG16 interfere with host infection and MoHEG13 counteracts cell death caused by *Magnaporthe*-NLPs in tobacco. *Plant Cell Reports*, 35(5), 1169–1185. <http://doi.org/10.1007/s00299-016-1943-9>
- Moldenhauer, J., Moerschbacher, B. M., & Van Der Westhuizen, A. J. (2006). Histological investigation of stripe rust (*Puccinia striiformis* f.sp. *tritici*) development in resistant and susceptible wheat cultivars. *Plant Pathology*, 55(4), 469–474. <http://doi.org/10.1111/j.1365-3059.2006.01385.x>
- Montarry, J., Hamelin, F. M., Glais, I., Corbière, R., & Andrivon, D. (2010). Fitness costs associated with unnecessary virulence factors and life history traits : evolutionary insights from the potato late blight pathogen *Phytophthora infestans*. *BMC Evolutionary Biology*, 10(283).
- Moore, J. W., Herrera-Foessel, S., Lan, C., Schnippenkoetter, W., Ayliffe, M., Huerta-Espino, J., ... Lagudah, E. (2015). A recently evolved hexose transporter variant confers resistance to multiple pathogens in wheat. *Nature Genetics*, 47(12), 1494–1498. <http://doi.org/10.1038/ng.3439>
- Mucyn, T. S., Clemente, A., Andriotis, V. M. E., Balmuth, A. L., Oldroyd, G. E. D., Staskawicz, B. J., Rathjen, J. P. (2006). The tomato NBARC-LRR protein Prf interacts with Pto kinase in vivo to regulate specific plant immunity. *The Plant Cell*, 18(10), 2792–806. <http://doi.org/10.1105/tpc.106.044016>
- Mukhtar, M. S., McCormack, M. E., Argueso, C. T., & Pajerowska-Mukhtar, K. M. (2016). Pathogen Tactics to Manipulate Plant Cell Death. *Current Biology*, 26(13), R608–R619. <http://doi.org/10.1016/j.cub.2016.02.051>
- Mundt, C. (2002). Use of Multiline Cultivars and Cultivar mixtures for Disease Management. *Annual Review of Phytopathology*, 40(1), 381–410.

- Murray, T., Milus, G., McMullen, M., Carson, M., Chen, X., Jin, Y., & Marshall, D. (2010). Recovery Plan for Stem Rust of Wheat caused by *Puccinia graminis* f. sp. *tritici* Ug99 (race TTKSK) and its derivatives. USDA *The American Phytopathological Society*.
- Na, R., & Gijzen, M. (2016). Escaping Host Immunity: New Tricks for Plant Pathogens. *PLoS Pathogens*, *12*(7), 1–6. <http://doi.org/10.1371/journal.ppat.1005631>
- Nagori, A. (2009). Genetically modified varieties of wheat that are resistant to stem or leaf rust. *Basic Biotechnology*, *5*, 91–95.
- Nandety, R. S., Caplan, J. L., Cavanaugh, K., Perroud, B., Wroblewski, T., Michelmore, R. W., & Meyers, B. C. (2013). The role of TIR-NBS and TIR-X proteins in plant basal defense responses. *Plant Physiology*, *162*(3), 1459–72. <http://doi.org/10.1104/pp.113.219162>
- Narusaka, M., Shirasu, K., Noutoshi, Y., Kubo, Y., Shiraiishi, T., Iwabuchi, M., Narusaka, Y. (2009). RRS1 and RPS4 provide a dual Resistance-gene system against fungal and bacterial pathogens. *Plant Journal*, *60*(2), 218–226. <http://doi.org/10.1111/j.1365-313X.2009.03949.x>
- Nemri, A., Saunders, D. G. O., Anderson, C., Upadhyaya, N. M., Win, J., Lawrence, G. J., ... Dodds, P. N. (2014). The genome sequence and effector complement of the flax rust pathogen *Melampsora lini*. *Frontiers in Plant Science*, *5*(March), 98. <http://doi.org/10.3389/fpls.2014.00098>
- Niks, R. ., & Dekens, R. G. (1991). Prehaustorial and posthaustorial resistance to wheat Leaf rust in diploid wheat seedlings. *Phytopathology*, *81*, :847–51.
- Nilsen, T. W., & Graveley, B. R. (2010). Expansion of the eukaryotic proteome by alternative splicing. *Nature*, *463*(7280), 457–463. <http://doi.org/10.1038/nature08909>.
- Nirmala, J., Drader, T., Lawrence, P. K., Yin, C., Hulbert, S., & Steber, C. M. (2011). Concerted action of two avirulent spore effectors activates Reaction to *Puccinia graminis* 1 (Rpg1) - mediated cereal stem rust resistance. *Pnas*, *108*, 14676–14681.
- Niu, Z., Klindworth, D. L., Friesen, T. L., Chao, S., Jin, Y., Cai, X., & Xu, S. S. (2011). Targeted introgression of a wheat stem rust resistance gene by DNA marker-assisted chromosome engineering. *Genetics*, *187*(4), 1011–21. <http://doi.org/10.1534/genetics.110.123588>
- Nowara, D., Gay, A., Lacomme, C., Shaw, J., Ridout, C., Douchkov, D., ... Schweizer, P. (2010). HIGS: Host-Induced Gene Silencing in the Obligate Biotrophic Fungal Pathogen *Blumeria graminis*. *The Plant Cell*, *22*(9), 3130–3141.
- O’Connell, R. J., & Panstruga, R. (2006). Tete a tete inside a plant cell: Establishing compatibility between plants and biotrophic fungi and oomycetes. *New Phytologist*, *171*(4), 699–718. <http://doi.org/10.1111/j.1469-8137.2006.01829.x>

- Oerke, E.C. (2006). Crop losses to pests. *The Journal of Agricultural Science*, 144(1), 31. <http://doi.org/10.1017/S0021859605005708>
- Okubara, P. A., Blechl, A. E., McCormick, S. P., Alexander, N. J., Dill-Macky, R., & Hohn, T. M. (2002). Engineering deoxynivalenol metabolism in wheat through the expression of a fungal trichothecene acetyltransferase gene. *TAG. Theoretical and Applied Genetics*, 106(1), 74–83. <http://doi.org/10.1007/s00122-002-1066-2>
- Oliver, R. P. (2014). A reassessment of the risk of rust fungi developing resistance to fungicides. *Pest Management Science*, 70(11), 1641–1645. <http://doi.org/10.1002/ps.3767>
- Olivera, P. D., Jin, Y., Rouse, M., Badebo, A., Fetch, T., Singh, R. P., & Yahyaoui, A. H. (2012). Races of *Puccinia graminis* f. sp. *tritici* with Combined Virulence to *Sr13* and *Sr9e* in a Field Stem Rust Screening Nursery in Ethiopia. *Plant Disease*, 96(5), 623–628. <http://doi.org/10.1094/PDIS-09-11-0793>
- Olivera, P., Newcomb, M., Szabo, L. J., Rouse, M., Johnson, J., Gale, S., ... Jin, Y. (2015). Phenotypic and genotypic characterization of race TKTTF of *Puccinia graminis* f. sp. *tritici* that caused a wheat stem rust epidemic in southern Ethiopia in 2013-14. *Phytopathology*, 105(7), 917–928. <http://doi.org/10.1094/PHYTO-11-14-0302-FI>
- Olivera Firpo, P. D., Newcomb, M., Flath, K., Sommerfeldt, N., Szabo, L. J., Carter, M., Luster, D. G. and Jin, Y. (2017). Characterization of *Puccinia graminis* f. sp. *tritici* isolates derived from an unusual wheat stem rust outbreak in Germany in 2013. *Plant Pathology*.
- Orbach, M. J., Farrall, L., Sweigard, J. A., Chumley, F. G., & Valent, B. (2000). A Telomeric Avirulence Gene Determines Efficacy for the Rice Blast Resistance Gene Pi-ta, 12(November), 2019–2032.
- Pais, M., Win, J., Yoshida, K., Etherington, G. J., Cano, L. M., Raffaele, S., ... Go Saunders, D. (2013). From pathogen genomes to host plant processes: the power of plant parasitic oomycetes. *Genome Biology*, 14(6), 211. <http://doi.org/10.1186/gb-2013-14-6-211>
- Panwar, V., McCallum, B., & Bakkeren, G. (2013). Endogenous silencing of *Puccinia triticina* pathogenicity genes through in planta-expressed sequences leads to the suppression of rust diseases on wheat. *Plant Journal*, 73(3), 521–532. <http://doi.org/10.1111/tpj.12047>
- Panwar, V., McCallum, B., & Bakkeren, G. (2013b). Host-induced gene silencing of wheat leaf rust fungus *Puccinia triticina* pathogenicity genes mediated by the Barley stripe mosaic virus. *Plant Molecular Biology*, 81(6), 595–608. <http://doi.org/10.1007/s11103-013-0022-7>
- Periyannan, S., Moore, J., Ayliffe, M., Bansal, U., Wang, X., Huang, L., ... Lagudah, E. (2013). The gene *Sr33* and Ortholog of Barley *Mla* Genes, Encodes Resistance to Wheat Stem Ruts Race *Ug99*. *Science*, 341(6147), 786–788.

- Park, R. F. (2007). Stem rust of wheat in Australia. *Australian Journal of Agricultural Research*, 58, 558–566.
- Park, R., Fetch, T., Hodson, D., Jin, Y., Nazari, K., Prashar, M., & Pretorius, Z. (2011). International surveillance of wheat rust pathogens: Progress and challenges. *Euphytica*, 179(1), 109–117. <http://doi.org/10.1007/s10681-011-0375-4>
- Parker, J. E., Coleman, M. J., Szabò, V., Frost, L. N., Schmidt, R., van der Biezen, E. A., ... Jones, J. D. G. (1997). The *Arabidopsis* downy mildew resistance gene *RPP5* shares similarity to the toll and interleukin-1 receptors with N and L6. *The Plant Cell*, 9(6), 879–894. <http://doi.org/10.1105/tpc.9.6.879>
- Parlange, F., Daverdin, G., Fudal, I., Kuhn, M. L., Balesdent, M. H., Blaise, F., ... Rouxel, T. (2009). *Leptosphaeria maculans* avirulence gene *AvrLm4-7* confers a dual recognition specificity by the Rlm4 and Rlm7 resistance genes of oilseed rape, and circumvents Rlm4-mediated recognition through a single amino acid change. *Molecular Microbiology*, 71(4), 851–863. <http://doi.org/10.1111/j.1365-2958.2008.06547.x>
- Parlevliet, J. E. (1978). Race-specific aspects of polygenic resistance of barley to leaf rust,. *Eur. J. Plant Pathol.*, 84, 121–126.
- Parlevliet, J. (2002). Durability of resistance against fungal, bacterial and viral pathogens; present situation. *Euphytica*, 124, 147–156. <http://doi.org/10.1023/A:1015601731446>
- Parniske, M., Hammond-Kosack, K. E., Golstein, C., Thomas, C. M., Jones, D. A., Harrison, K., ... Jones, J. D. G. (1997). Novel disease resistance specificities result from sequence exchange between tandemly repeated genes at the Cf-4/9 locus of tomato. *Cell*, 91(6), 821–832. [http://doi.org/10.1016/S0092-8674\(00\)80470-5](http://doi.org/10.1016/S0092-8674(00)80470-5)
- Petschnigg, J., Wong, V., Snider, J., & Stagljar, I. (2012). Investigation of Membrane Protein Interactions Using the Split-Ubiquitin Membrane Yeast Two-Hybrid System. In B. Suter & E. E. Wanker (Eds.), *Two Hybrid Technologies: Methods and Protocols* (pp. 225–244). Totowa, NJ: Humana Press.
- Perchepped, L., Dogimont, C., Pitrat, M. (2005). Strain-specific and recessive QTLs involved in the control of partial resistance to *Fusarium oxysporum* f. sp. melonis race 1.2 in a recombinant inbred line population of melon. *Theoretical and Applied Genetics*, 111(1), 65–74. <http://doi.org/10.1007/s00122-005-1991-y>
- Person, C. (1959). Gene-for gene relationships in host: parasite systems. *Canadian Journal of Botany*, 37(5), 1101–1130.
- Petre, B., Saunders, D. G., Sklenar, J., Lorrain, C., Win, J., Duplessis, S., & Kamoun, S. (2015). Candidate Effector Proteins of the Rust Pathogen *Melampsora Larici-Populina* Target Diverse Plant Cell Compartments. *Molecular Plant-Microbe Interactions: MPMI*, 28(6), 689–700. <http://doi.org/10.1094/MPMI-01-15-0003-R>

- Petre, B., Joly, D. L., & Duplessis, S. (2014). Effector proteins of rust fungi. *Frontiers in Plant Science*, 5, 416. <http://doi.org/10.3389/fpls.2014.00416>
- Petre, B., & Kamoun, S. (2014). How Do Filamentous Pathogens Deliver Effector Proteins into Plant Cells? *PLoS Biology*, 12(2). <http://doi.org/10.1371/journal.pbio.1001801>
- Pfaffl, M. (2004). Quantification Strategies in real-time PCR. In S. A. Bustin (Ed.), *The Real-Time PCR Encyclopedia A–Z of Quantitative PCR* (pp. 87–120). La Jolla, CA: International University Line.
- Pliego, C., Nowara, D., Bonciani, G., Gheorghe, D. M., Xu, R., Surana, P., ... Spanu, P. D. (2013). Host-Induced Gene Silencing in Barley Powdery Mildew Reveals a Class of Ribonuclease-Like Effectors. *Molecular Plant-Microbe Interactions*, 26(6), 633–642. <http://doi.org/10.1094/MPMI-01-13-0005-R>
- Plissonneau, C., Benevenuto, J., Mohd-Assaad, N., Fouché, S., Hartmann, F. E., & Croll, D. (2017). Using Population and Comparative Genomics to Understand the Genetic Basis of Effector-Driven Fungal Pathogen Evolution. *Frontiers in Plant Science*, 8(February), 1–15. <http://doi.org/10.3389/fpls.2017.00119>
- Plett, J. M., Kemppainen, M., Kale, S. D., Kohler, A., Legué, V., Brun, A., ... Martin, F. (2011). A secreted effector protein of laccaria bicolor is required for symbiosis development. *Current Biology*, 21(14), 1197–1203. <http://doi.org/10.1016/j.cub.2011.05.033>
- Poland, J. A., Balint-Kurti, P. J., Wisser, R. J., Pratt, R. C., & Nelson, R. J. (2009). Shades of gray: the world of quantitative disease resistance. *Trends in Plant Science*, 14(1), 21–29. <http://doi.org/10.1016/j.tplants.2008.10.006>
- Poudel, R., Solanki, S., Shrestha, S., Richards, J., & Brueggeman, R. (2017). Rise to the bait: Towards identifying the *Puccinia graminis* effector Avr4/5 “baited in” by the Rpg5 protein kinase integrated decoy domain. In *29th Fungal Genetics Conference Rust workshop*.
- Popa, C. M., Tabuchi, M., & Valls, M. (2016). Modification of Bacterial Effector Proteins Inside Eukaryotic Host Cells. *Frontiers in Cellular and Infection Microbiology*, 6(July), 1–13. <http://doi.org/10.3389/fcimb.2016.00073>
- Pretorius, Z. A., Szabo, L. J., Boshoff, W. H. P., Herselman, L., & Visser, B. (2012). First Report of a New TTKSF Race of Wheat Stem Rust (*Puccinia graminis* f. sp. *tritici*) in South Africa and Zimbabwe. *Plant Disease*, 96(4), 590.
- Pretorius, Z., Singh, R., Wagoire, W., Payne, T. (2000). Detection of Virulence to Wheat Stem Rust Resistance Gene *Sr31* in *Puccinia graminis* f. sp. *tritici* in Uganda. *Plant Disease*, 84, 203.
- Pritchard, L., & Birch, P. R. J. (2014). The zigzag model of plant-microbe interactions: is it time to move on? *Molecular Plant Pathology*, 15, 865–870. <http://doi.org/10.1111/mpp.12210>

- Pumphrey, M. (2012). Stocking the Breeder's Toolbox: An update on the status of resistance to stem rust in wheat. In R. McIntosh (Ed.), *Proceedings Borlaug Global Rust Initiative 2012 Technical Workshop* (pp. 23–29). Beijing, China.
- Purnhauser, L., Tar, M., Bona, L., & Lang, L. (2006). The occurrence of *Sr31* and *Sr36* stem rust resistance genes in wheat cultivars registered in Hungary in the past 25 years, 2006–2008.
- Raffaele, S., & Kamoun, S. (2012). Genome evolution in filamentous plant pathogens: why bigger can be better. *Nature Reviews Microbiology*, *10*(6), 417–430. <http://doi.org/10.1038/nrmicro2790>
- Rafiqi, M., Gan, P. H. P., Ravensdale, M., Lawrence, G. J., Ellis, J. G., Jones, D. a, ... Dodds, P. N. (2010). Internalization of flax rust avirulence proteins into flax and tobacco cells can occur in the absence of the pathogen. *The Plant Cell*, *22*(6), 2017–2032. <http://doi.org/10.1105/tpc.109.072983>
- Rahmatov, M., Rouse, M. N., Steffenson, B. J., Andersson, S. C., Wanyera, R., Pretorius, Z. A., ... Johansson, E. (2016b). Sources of Stem Rust Resistance in Wheat-Alien Introgression Lines. *Plant Disease*, *100*(6), 1101–1109. <http://doi.org/10.1094/PDIS-12-15-1448-RE>
- Ramachandran, S., Yin, C., Kud, J., Tanaka, K., Mahoney, A., Xiao, F., & Hulbert, S. H. (2016). Effectors from wheat rust fungi suppress multiple plant defense responses. *Phytopathology*, *107*(1), 75–83.
- Reddy, P. P. (2013). Variety Mixtures/Cultivar Mixtures/Multilines. In *Recent advances in crop protection* (pp. 201–221). New Delhi: Springer India.
- Rentel, M. C., Leonelli, L., Dahlbeck, D., Zhao, B., & Staskawicz, B. J. (2008). Recognition of the *Hyaloperonospora parasitica* effector ATR13 triggers resistance against oomycete, bacterial, and viral pathogens. *Proceedings of the National Academy of Sciences of the United States of America*, *105*(3), 1091–6. <http://doi.org/10.1073/pnas.0711215105>
- Ribeiro Do Vale, F. X., Parlevliet, J. E., & Zambolim, L. (2001). Concepts in plant disease resistance. *Fitopatologia Brasileira*, *26*(3), 577–589. <http://doi.org/10.1590/S0100-41582001000300001>
- Ridout, C. J. Skamnioti, P., Porritt, O., Sacristan, S., Jones, J.D.G., Brown, J. (2006). Multiple Avirulence Paralogues in Cereal Powdery Mildew Fungi May Contribute to Parasite Fitness and Defeat of Plant Resistance. *The Plant Cell Online*, *18*(9), 2402–2414. <http://doi.org/10.1105/tpc.106.043307>
- Risk, J. M., Selter, L. L., Krattinger, S. G., Viccars, L. A., Richardson, T. M., Buesing, G., ... Keller, B. (2012). Functional variability of the *Lr34* durable resistance gene in transgenic wheat. *Plant Biotechnology Journal*, *10*(4), 477–487. <http://doi.org/10.1111/j.1467-7652.2012.00683.x>Makandar

- Roelfs, A. P., Singh, R. P. Saari. E. E. (1992). Rust diseases of wheat: Concepts and methods of disease management. Mexico, D.F.CIMMYT.
- Roelfs, A.P., Martens, W. (1988). An international system of nomenclature for *Puccinia graminis* f. sp. *tritici* *Phytopathology*, 78, 526–533.
- Rohringer, R. (1977). Calcofluor: An Optical Brightener for Fluorescence Microscopy of Fungal Plant Parasites in Leaves. *Phytopathology*, 67, 808
- Römer, P., Hahn, S., Jordan, T., Strauss, T., Bonas, U., Lahaye, T. (2007). Plant pathogen recognition mediated by promoter activation of the pepper *Bs3* resistance gene. *Science*, 318(5850), 645–648.
- Rosegrant, M.W., Agcaoili- Sombilla, M., Perez, N. (1995). Global food projections to 2020: implications for investment. Food, Agriculture and the Environment Discussion, Paper 5. Washington: International Food Policy Research Institute.
- Rosenblum, B. B., Lee, L. G., Spurgeon, S. L., Khan, S. H., Menchen, S. M., Heiner, C. R., & Chen, S. M. (1997). New dye-labeled terminators for improved DNA sequencing patterns. *Nucleic Acids Research*, 25(22), 4500–4504. <http://doi.org/10.1093/nar/25.22.4500>
- Rouse, M. N., & Jin, Y. (2011). Stem Rust Resistance in A-Genome Diploid Relatives of Wheat. *Plant Disease*, 95(8), 941–944. <http://doi.org/10.1094/PDIS-04-10-0260>
- Rouse, M. N., Wanyera, R., Njau, P., & Jin, Y. (2011a). Sources of Resistance to Stem Rust Race *Ug99* in Spring Wheat Germplasm. *Plant Disease*, 95(1), 762–766. <http://doi.org/10.1094/PDIS-12-10-0940>
- Rouse, M. N., Olson, E. L., Gill, B. S., Pumphrey, M. O., & Jin, Y. (2011b). Stem rust resistance in *Aegilops Tauschii* germplasm. *Crop Science*, 51(5), 2074–2078. <http://doi.org/10.2135/cropsci2010.12.0719>
- Rowell, J. B. (1981). Relation of postpenetration events in Idaed 59 wheat seedlings to low receptivity to infection by *Puccinia graminis* f. sp. *tritici*. *Phytopathology*, 71, 732–736.
- Rutherford, K., Parkhill, J., Crook, J., Horsnell, T., Rice, P., Rajandream, M. A., & Barrell, B. (2000). Artemis: sequence visualization and annotation. *Bioinformatics*, 16(10), 944–945. <http://doi.org/10.1093/bioinformatics/16.10.944>
- Rutter, W. B., Salcedo, A., Akhunova, A., He, F., Wang, S., Liang, H., ... Akhunov, E. (2017). Divergent and convergent modes of interaction between wheat and *Puccinia graminis* f. sp. *tritici* isolates revealed by the comparative gene co-expression network and genome analyses. *BMC Genomics*, 18(1), 291. <http://doi.org/10.1186/s12864-017-3678-6>

- Saari, E. E., and Prescott, J. M. (1985). World distribution in relation to economic losses. In “The Cereal Rusts, Vol. II: Diseases, Distribution, Epidemiology, and Control”(A. P. Roelfs and W. R. Bushnell, eds.). Academic Press, Orlando.
- Saintenac, C., Zhang, W., Salcedo, A., Rouse, M., Trick, H., Akhunov, E., & Dubcovsky, J. (2013). Identification of Wheat Gene *Sr35* that Confers Resistance to *Ug99* Stem Rust Race Group. *Science*, *341*, 783–786.
- Salcedo, A., Rutter, W., Wang, S., Akhunova, A., Bolus, S., Chao, S., ... Akhunov, E. (2017). Variation in the *AvrSr35* gene determines *Sr35* resistance against wheat stem rust race Ug99. *Science*, *358*(6370), 1604–1606. <http://doi.org/10.1126/science.aao7294>
- Sánchez-Vallet, A., Saleem-Batcha, R., Kombrink, A., Hansen, G., Valkenburg, D. J., Thomma, B. P. H. J., & Mesters, J. R. (2013). Fungal effector Ecp6 outcompetes host immune receptor for chitin binding through intrachain LysM dimerization. *eLife*, *2013*(2), 1–16. <http://doi.org/10.7554/eLife.00790>
- Santana, M., & Queiroz, M. V. (2015). Transposable Elements in Fungi : A Genomic Approach. *Scientific Journal of Genetics and Gene Therapy*, *1*, 12–16.
- Sanseverino, W., & Ercolano, M. R. (2012). In silico approach to predict candidate R proteins and to define their domain architecture. *BMC Research Notes*, *5*(1), 1. <http://doi.org/10.1186/1756-0500-5-678>
- Sarris, P. F., Cevik, V., Dagdas, G., Jones, J. D. G., & Krasileva, K. V. (2016). Comparative analysis of plant immune receptor architectures uncovers host proteins likely targeted by pathogens. *BMC Biology*, *14*(1), 8. <http://doi.org/10.1186/s12915-016-0228-7>
- Saunders, D. G. O., Win, J., Cano, L. M., Szabo, L. J., Kamoun, S., & Raffaele, S. (2012). Using hierarchical clustering of secreted protein families to classify and rank candidate effectors of rust fungi. *PloS One*, *7*(1), e29847. <http://doi.org/10.1371/journal.pone.0029847>
- Schmidt, S. M., Lukaszewicz, J., Farrer, R., van Dam, P., Bertoldo, C., & Rep, M. (2016). Comparative genomics of *Fusarium oxysporum* f. sp. melonis reveals the secreted protein recognized by the Fom-2 resistance gene in melon. *New Phytologist*, *209*, 307–318
- Scholtz, J. J., & Visser, B. (2013). Reference gene selection for qPCR gene expression analysis of rust-infected wheat. *Physiological and Molecular Plant Pathology*, *81*, 22–25. <http://doi.org/10.1016/j.pmpp.2012.10.006>
- Schornack, S., van Damme, M., Bozkurt, T. O., Cano, L. M., Smoker, M., Thines, M., ... Huitema, E. (2010). Ancient class of translocated oomycete effectors targets the host nucleus. *Proceedings of the National Academy of Sciences of the United States of America*, *107*(40), 17421–17426. <http://doi.org/10.1073/pnas.1008491107>

- Schumann, G. L., and Leonard, K. J. (2000). Stem rust of wheat (black rust). The Plant Health Instructor. DOI: 10.1094/PHI-I-2000-0721-01. Accessed 2/26/2017
- Schweizer, G., Münch, K., Mannhaupt, G., Schirawski, J., Kahmann, R., & Dutheil, J. Y. (2018). Positively Selected Effector Genes and Their Contribution to Virulence in the Smut Fungus *Sporisorium reilianum*. *Genome Biology and Evolution*, 10(2), 629–645.
- Sega, G. A. (1984). A review of the genetic effects of ethyl methanesulfonate. *Mutation Research*, 134, 113–142.
- Sela, H., Spiridon, L. N., Petrescu, A. J., Akerman, M., Mandel-Gutfreund, Y., Nevo, E., ... Fahima, T. (2012). Ancient diversity of splicing motifs and protein surfaces in the wild emmer wheat (*Triticum dicoccoides*) LR10 coiled coil (CC) and leucine-rich repeat (LRR) domains. *Molecular Plant Pathology*, 13(3), 276–287.
- Selin, C., de Kievit, T. R., Belmonte, M. F., & Fernando, W. G. D. (2016). Elucidating the role of effectors in plant-fungal interactions: Progress and challenges. *Frontiers in Microbiology*, 7, 1–21. <http://doi.org/10.3389/fmicb.2016.00600>
- Serfling, A., Templer, S. E., Winter, P., & Ordon, F. (2016). Microscopic and Molecular Characterization of the Prehaustorial Resistance against Wheat Leaf Rust (*Puccinia triticina*) in Einkorn (*Triticum monococcum*). *Frontiers in Plant Science*, 7(November), 1–18. <http://doi.org/10.3389/fpls.2016.01668>
- Shabab, M., Shindo, T., Gu, C., Kaschani, F., Pansuriya, T., Chintha, R., ... van der Hoorn, R. A. L. (2008). Fungal Effector Protein AVR2 Targets Diversifying Defense-Related Cys Proteases of Tomato. *Plant Cell*, 20(4), 1169–1183. <http://doi.org/10.1105/tpc.107.056325>
- Shan, W., Cao, M., Leung, D., & Tyler, B. M. (2004). The Avr1b locus of *Phytophthora sojae* encodes an elicitor and a regulator required for avirulence on soybean plants carrying resistance gene *Rps1b*. *Molecular Plant-Microbe Interactions: MPMI*, 17(4), 394–403. <http://doi.org/10.1094/MPMI.2004.17.4.394>
- Sharma, R. K., Singh, P. K., Vinod, Joshi, A. K., Bhardwaj, S. C., Bains, N. S., & Singh, S. (2013). Protecting South Asian Wheat Production from Stem Rust (*Ug99*) Epidemic. *Journal of Phytopathology*, 161(5), 299–307. <http://doi.org/10.1111/jph.12070>
- Shirano, Y., Kachroo, P., Shah, J., Klessig, D. F. (2002). A gain-of-function mutation in an *Arabidopsis* Toll Interleukin-1 Receptor-Nucleotide Binding Site-Leucine-Rich Repeat type R gene triggers defense responses and results in enhanced disease resistance. *Plant Cell*, 14(12), 3149–3162. <http://doi.org/10.1105/tpc.005348>
- Shewry, P. R. (2009). Wheat. *Journal of Experimental Botany*, 60(6), 1537–1553. <http://doi.org/10.1093/jxb/erp058>

- Shyu, A.-B., Wilkinson, M. F., & van Hoof, A. (2008). Messenger RNA regulation: to translate or to degrade. *The EMBO Journal*, 27(3), 471–481.
- Simao, F. a., Waterhouse, R. M., Ioannidis, P., Kriventseva, E. V., & Zdobnov, E. M. (2015). BUSCO: assessing genome assembly and annotation completeness with single-copy orthologs. *Bioinformatics*, (June), 1–3. <http://doi.org/10.1093/bioinformatics/btv351>
- Simms, E. L. (1996). The Evolutionary Genetics of Plant-pathogen systems. *Bioscience*, 46(2), 136–145.
- Simms, Ellen., Triplett, J. (1994). Costs and Benefits of Plant Responses to Disease: Resistance and Tolerance, 48(6), 1973–1985.
- Simons, M. D. (1979). Modification of host-parasite interactions through artificial mutagenesis. *Annual Review of Phytopathology*, (17), 75–96.
- Sinapidou, E., Williams, K., Nott, L., Bahkt, S., Tör, M., Crute, I., ... Beynon, J. (2004). Two TIR:NB:LRR genes are required to specify resistance to *Peronospora parasitica* isolate Cala2 in *Arabidopsis*. *Plant Journal*, 38(6), 898–909. <http://doi.org/10.1111/j.1365-313X.2004.02099.x>
- Singh , G., Nirmala, J., Rouse, M. . (2013). EMS mutagenesis of avirulent *Puccinia graminis* f. sp. tritici urediniospores. In *BGRI 2013 Technical Workshop* (p. 112). New Delhi.
- Singh, R., Hodson D.P., Jin, Y. Huerta-Espino, J., Kinyua, M.G., Wanyera, R., Njau, P., Ward, R. W. (2006). Current status, likely migration and strategies to mitigate the threat to wheat production from race Ug99 (TTKS) of stem rust pathogen. *CAB Reviews: Perspectives in Agriculture, Veterinary Science, Nutrition and Natural Resources*, 1(54), 1–13. <http://doi.org/10.1079/PAVSNNR20061054>
- Singh, R.P., Hodson, D.P. , Huerta-Espino, J. Jin, Y., Njau, P., Wanyera, R., & Herrera-Foessel, S.A., Bhavani, S., Singh, D., Singh, P. K. (2008a). Global status of Ug 99 spread and efforts to mitigate the threat. In S. A. M. Singh, G.P., Prabhu, K. V. (Ed.), *Proceeding of International Conference on Wheat Stem Rust Ug99- A Threat to Food Security* (pp. 1–8). New Delhi: Indian Agricultural Research Institute.
- Singh, R. P., Hodson, D. P., Huerta-Espino, J., Jin, Y., Njau, P., Wanyera, R., Herrera-Foessel, Sybil A., Ward, R. W. (2008b). Will Stem Rust Destroy the World’s Wheat Crop? *Advances in Agronomy*, 98(8), 271–309. [http://doi.org/10.1016/S0065-2113\(08\)00205-8](http://doi.org/10.1016/S0065-2113(08)00205-8)
- Singh, R. P., Hodson, D. P., Jin, Y., Lagudah, E. S., Ayliffe, M. A., Bhavani, S., ... Hovmöller, M. S. (2015). Emergence and spread of new races of wheat stem rust fungus: continued threat to food security and prospects of genetic control. *Phytopathology*, 105(7), 872–884. <http://doi.org/10.1094/PHYTO-01-15-0030-FI>

- Singh, R. P., Hodson, D. P., Huerta-Espino, J., Jin, Y., Bhavani, S., Njau, P., ... Govindan, V. (2011). The Emergence of Ug99 Races of the Stem Rust Fungus is a Threat to World Wheat Production. *Annual Review of Phytopathology*, 49(April), 465–481. <http://doi.org/10.1146/annurev-phyto-072910-095423>
- Smedegaard-Petersen, V., & Stolen, O. (1981). Effect of Energy-Requiring Defense Reactions on Yield and Grain Quality in a Powdery Mildew-Resistant Barley Cultivar. *Phytopathology*, 71, 396–399.
- Soanes, D. M., Alam, I., Cornell, M., Wong, H. M., Hedeler, C., Paton, N. W., ... Talbot, N. J. (2008). Comparative genome analysis of filamentous fungi reveals gene family expansions associated with fungal pathogenesis. *PLoS ONE*, 3(6). <http://doi.org/10.1371/journal.pone.0002300>
- Soergel DAW, Lareau LF, Brenner SE. Regulation of Gene Expression by Coupling of Alternative Splicing and NMD. In: Madame Curie Bioscience Database [Internet]. Austin (TX): Landes Bioscience; 2000-2013. Available from:
- Sonah, H., Deshmukh, R. K., & Bélanger, R. R. (2016). Computational Prediction of Effector Proteins in Fungi: Opportunities and Challenges. *Frontiers in Plant Science*, 7(February), 1–14. <http://doi.org/10.3389/fpls.2016.00126>
- Sohn, K. H., Lei, R., Nemri, A., & Jones, J. D. G. (2007). The downy mildew effector proteins ATR1 and ATR13 promote disease susceptibility in *Arabidopsis thaliana*. *The Plant Cell*, 19(12), 4077–90. <http://doi.org/10.1105/tpc.107.054262>
- Song, X., Rampitsch, C., Soltani, B., Mauthe, W., Linning, R., Banks, T., ... Bakkeren, G. (2011). Proteome analysis of wheat leaf rust fungus, *Puccinia triticina*, infection structures enriched for haustoria. *PROTEOMICS*, 11(5), 944–963.
- Soyer, J. L., El Ghalid, M., Glaser, N., Ollivier, B., Linglin, J., Grandaubert, J., ... Fudal, I. (2014). Epigenetic Control of Effector Gene Expression in the Plant Pathogenic Fungus *Leptosphaeria maculans*. *PLoS Genetics*, 10(3).
- Spanu, P., & Kämper, J. (2010). Genomics of biotrophy in fungi and oomycetes-emerging patterns. *Current Opinion in Plant Biology*, 13(4), 409–414.
- Sperschneider, J., Catanzariti, A.-M., DeBoer, K., Petre, B., Gardiner, D., Singh, K., ... Taylor, J. (2016a). LOCALIZER: subcellular localization prediction of plant and effector proteins in the plant cell. *bioRxiv*. <http://doi.org/10.1101/092726>
- Sperschneider, J., Gardiner, D. M., Dodds, P. N., Tini, F., Covarelli, L., Singh, K. B., ... Taylor, J. M. (2016b). EffectorP: Predicting fungal effector proteins from secretomes using machine learning. *New Phytologist*, 210(2), 743–761. <http://doi.org/10.1111/nph.13794>

- St.Clair, D. A. (2010). Quantitative Disease Resistance and Quantitative Resistance Loci in Breeding. *Annual Review of Phytopathology*, 48(1), 247–268.
- Staal, J., Kaliff, M., Dewaele, E., Persson, M., & Dixelius, C. (2008). RLM3, a TIR domain encoding gene involved in broad-range immunity of Arabidopsis to necrotrophic fungal pathogens. *Plant Journal*, 55(2), 188–200.
- Stakman E.C, Stewart D.M, Loegering, W. . (1962). *Identification of physiologic races of Puccinia graminis var. tritici*. U.S Agriculture Research Service ARS E617.
- Staples, R. C. (2000). Research on the Rust Fungi During the Twentieth Century. *Annual Review of Phytopathology*, 38, 49–69. <http://doi.org/10.1177/000312240507000602>
- Statler, G. (1979). Inheritance of Pathogenicity of Culture 70-1, Race 1, of *Puccinia recondita tritici*. *Phytopathology*, 69, 661–663.
- Stergiopoulos, I., de Wit, P. J. G. M. (2009). Fungal effector proteins. *Annual Review of Phytopathology*, 47, 233–63. <http://doi.org/10.1146/annurev.phyto.112408.132637>
- Steinbrenner, J., Eldridge, M., Tomé, D. F. A., & Beynon, J. L. (2014). A Simple and Fast Protocol for the Protein Complex Immunoprecipitation (Co-IP) of Effector: Host Protein Complexes. In P. Birch, J. T. Jones, & J. I. B. Bos (Eds.), *Plant-Pathogen Interactions: Methods and Protocols* (pp. 195–211). Totowa, NJ: Humana Press.
- Steuernagel, B., Periyannan, S. K., Hernández-Pinzón, I., Witek, K., Rouse, M. N., Yu, G., ... Wulff, B. B. H. (2016). Rapid cloning of disease-resistance genes in plants using mutagenesis and sequence capture. *Nature Biotechnology*, 34(6), 652–657. <http://doi.org/10.1038/nbt.3543>
- Stewart, H. E., Bradshaw, J. E., & Pande, B. (2003). The effect of the presence of R-genes for resistance to late blight (*Phytophthora infestans*) of potato (*Solanum tuberosum*) on the underlying level of field resistance. *Plant Pathology*, 52(2), 193–198. <http://doi.org/10.1046/j.1365-3059.2003.00811.x>
- Strange, R. (2003). *Introduction to Plant Pathology*. (J. W. and & Sons., Ed.). New York.
- Stockert, C., & Blazquez-Castro, A. (2017). *Flourescence Mycroscopy in Life Sciences*. Sharjah, UAE: Betham Science.
- Stotz, H. U., Mitrouisia, G. K., de Wit, P. J. G. M., Fitt, B. D. L. (2014). Effector-triggered defence against apoplastic fungal pathogens. *Trends in Plant Science*, 19(8), 491–500. <http://doi.org/10.1016/j.tplants.2014.04.009>
- Stukenbrock, E. H., & McDonald, B. A. (2008). The Origins of Plant Pathogens in Agro-Ecosystems. *Annual Review of Phytopathology*, 46(1), 75–100.

- Surico, G. (2013). The concepts of plant pathogenicity, virulence/avirulence and effector proteins by a teacher of plant pathology. *Phytopathologia Mediterranea*, 52(3), 399–417. http://doi.org/10.14601/Phytopathol_Mediterr-12077
- Szabo, L. J., Cuomo, C. A., & Park, R. F. (2014). *Puccinia graminis*. In R. A. Dean, A. Lichens-Park, & C. Kole (Eds.), *Genomics of Plant-Associated Fungi: Monocot Pathogens* (pp. 177–196). Berlin, Heidelberg: Springer Berlin Heidelberg. http://doi.org/10.1007/978-3-662-44053-7_
- Takemoto, D., Rafiqi, M., Hurley, U., Lawrence, G. J., Bernoux, M., Hardham, A. R., ... Jones, D. a. (2012). N-terminal motifs in some plant disease resistance proteins function in membrane attachment and contribute to disease resistance. *Molecular Plant-Microbe Interactions : MPMI*, 25(3), 379–92. <http://doi.org/10.1094/MPMI-11-10-0272>
- Takken, F. L. W., & Govere, A. (2012). How to build a pathogen detector: Structural basis of NB-LRR function. *Current Opinion in Plant Biology*, 15(4), 375–384. <http://doi.org/10.1016/j.pbi.2012.05.001>
- Takken, F. L. W., Luderer, R., Gabriëls, S. H. E. J., Westerink, N., Lu, R., De Wit, P. J. G. M., & Joosten, M. H. A. J. (2000). A functional cloning strategy, based on a binary PVX-expression vector, to isolate HR-inducing cDNAs of plant pathogens. *Plant Journal*, 24(2), 275–283. <http://doi.org/10.1046/j.1365-313X.2000.00866.x>
- Tameling, W. I. L., Vossen, J. H., Albrecht, M., Lengauer, T., Berden, J. a, Haring, M. a, ... Takken, F. L. W. (2006). Mutations in the NB-ARC domain of I-2 that impair ATP hydrolysis cause autoactivation. *Plant Physiology*, 140(4), 1233–1245. <http://doi.org/10.1104/pp.105.073510>
- Tamura, K., Stecher, G., Peterson, D., Filipski, A., & Kumar, S. (2013). MEGA6: Molecular evolutionary genetics analysis version 6.0. *Molecular Biology and Evolution*, 30(12), 2725–2729. <http://doi.org/10.1093/molbev/mst197>
- Tang, F., Yang, S., Gao, M., & Zhu, H. (2013). Alternative splicing is required for RCT1-mediated disease resistance in *Medicago truncatula*. *Plant Molecular Biology*, 82(4–5), 367–374. <http://doi.org/10.1007/s11103-013-0068-6>
- Tang, C., Wang, X., Cheng, Y., Liu, M., Zhao, M., Wei, J. (2015). New insights in the battle between wheat and *Puccinia striiformis*. *Frontiers of Agriculture Science and Engineering*, 2(2), 101–114. <http://doi.org/10.15302/J-FASE-2015068>
- Teo, C., & Baker, E. P. (1975). Mutagenic effects of ethyl methanesulphonate on the oat stem rust pathogens (*Puccinia graminis* f. sp. *avenae*). *Proc. Linnean Soc. N. S. W.*, 99, 166–173. Retrieved from <http://biostor.org/reference/68639>

- Thrall, P. H., Barrett, L. G., Dodds, P. N., Burdon, J. J. (2015). Epidemiological and Evolutionary Outcomes in Gene-for-Gene and Matching Allele Models. *Frontiers in Plant Science*, 6(1084). <http://doi.org/10.3389/fpls.2015.01084>
- Thatcher, L. F., Williams, A. H., Garg, G., Buck, S.-A. G., & Singh, K. B. (2016). Transcriptome analysis of the fungal pathogen *Fusarium oxysporum* f. sp. medicaginis during colonisation of resistant and susceptible *Medicago truncatula* hosts identifies differential pathogenicity profiles and novel candidate effectors. *BMC Genomics*, 17(1), 860. <http://doi.org/10.1186/s12864-016-3192-2>
- Thomas, W. J., Thireault, C. a, Kimbrel, J. a, Chang, J. H. (2009). Recombineering and stable integration of the *Pseudomonas syringae* pv. syringae 61 hrp/hrc cluster into the genome of the soil bacterium *Pseudomonas fluorescens* Pf0-1. *The Plant Journal*, 60(5), 919–28. <http://doi.org/10.1111/j.1365-313X.2009.03998.x>
- Thomma, B. P. H. J., Nürnberger, T., & Joosten, M. H. A. J. (2011). Of PAMPs and effectors: the blurred PTI-ETI dichotomy. *The Plant Cell*, 23(1), 4–15.
- Thon, M. R., Nuckles, E. M., Vaillancourt, L. J. (2000). Restriction Enzyme-Mediated Integration Used to Produce Pathogenicity Mutants of *Colletotrichum graminicola*. *Molecular Plant-Microbe Interactions*, 13(12), 1356–1365.
- Thordal-Christensen, H. (2003). Fresh insights into processes of nonhost resistance. *Current Opinion in Plant Biology*, 6(4), 351–357. [http://doi.org/10.1016/S1369-5266\(03\)00063-3](http://doi.org/10.1016/S1369-5266(03)00063-3)
- Thordal-Christensen, H., Zhang, Z., Wei, Y., & Collinge, D. B. (1997). Subcellular localization of H₂O₂ in plants. H₂O₂ accumulation in papillae and hypersensitive response during the barley-powdery mildew interaction. *Plant Journal*. <http://doi.org/10.1046/j.1365-313X.1997.11061187.x>
- Thrall, P. H., Barrett, L. G., Dodds, P. N., & Burdon, J. J. (2015). Epidemiological and Evolutionary Outcomes in Gene-for-Gene and Matching Allele Models. *Frontiers in Plant Science*, 6, 1084
- Upadhyaya, N., Ellis, J.G., Dodds, P. (2014). A Bacterial Type III Secretion-Based Delivery System for Functional Assays of Fungal Effectors in Cereals. In J. I. . Birch, P., Jones, J.T., Bos (Ed.), *Plant Pathogen interactions Methods and protocols* (2nd ed., pp. 277–290). New York: Springer US.
- Upadhyaya, N. M., Garnica, D. P., Karaoglu, H., Sperschneider, J., Nemri, A., Xu, B., ... Dodds, P. N. (2015). Comparative genomics of Australian isolates of the wheat stem rust pathogen *Puccinia graminis* f. sp. *tritici* reveals extensive polymorphism in candidate effector genes. *Frontiers in Plant Science*, 5, 759. <http://doi.org/10.3389/fpls.2014.00759>
- van der Biezen, E. A., & Jones, J. D. G. (1998). Plant disease-resistance proteins and the gene-for-gene concept. *Trends in Plant Science*, 23, 454–456.

- van der Hoorn, R. A. L., & Kamoun, S. (2008). From Guard to Decoy: a new model for perception of plant pathogen effectors. *The Plant Cell*, 20(8), 2009–17. <http://doi.org/10.1105/tpc.108.060194>
- Van der Plank, J. E. (1963). *Plant Diseases: Epidemics and Control*. Academic Press.
- Van der Plank, J. E. (1968). *Disease Resistance in Plants*. Academic Press.
- Van der Plank, J. E. (1978). *Genetic and Molecular Basis of Plant Pathogenesis*. Berlin: Springer-Verlag.
- van Esse, H. P. (2012). Identification of HR-Inducing cDNAs from Plant Pathogens via a Gateway®-Compatible Binary Potato Virus X-Expression Vector. In M. D. Bolton & B. P. H. J. Thomma (Eds.), *Plant Fungal Pathogens: Methods and Protocols* (pp. 97–106). Totowa, NJ: Hu.
- van Kan, J. A., van den Ackerveken, G. F. J. M., & de Wit, P. J. G. M. (1991). Cloning and characterization of cDNA of avirulence gene *avr9* of the fungal pathogen *Cladosporium fulvum*, causal agent of tomato leaf mold. *Molecular Plant-Microbe Interactions*. <http://doi.org/10.1371/journal.pone.0053937>
- Van Valen, L. (1973). A new evolutionary law. *Evolutionary Theory*, (1), 1–30.
- Visser, B., Herselman, L., & Pretorius, Z. A. (2009). Genetic comparison of *Ug99* with selected South African races of *Puccinia graminis* f.sp. *tritici*. *Molecular Plant Pathology*, 10(2), 213–222. <http://doi.org/10.1111/j.1364-3703.2008.00525.x>
- Vleeshouwers, V. G. A. A., Raffaele, S., Vossen, J. H., Champouret, N., Oliva, R., Segretin, M. E., ... Kamoun, S. (2011). Understanding and Exploiting Late Blight Resistance in the Age of Effectors. *Annual Review of Phytopathology*, 49(1), 507–531. <http://doi.org/10.1146/annurev-phyto-072910-095326>
- Vleeshouwers, V. G. A. A., & Oliver, R. P. (2014). Effectors as Tools in Disease Resistance Breeding Against Biotrophic, Hemibiotrophic, and Necrotrophic Plant Pathogens. *Molecular Plant-Microbe Interactions*, 27(3), 196–206. <http://doi.org/10.1094/MPMI-10-13-0313-IA>
- Voegelé, R. T., Voegelé, R. T., & Mendgen, K. (2003). Rust haustoria: nutrient uptake and beyond. *New Phytologist*, 93–100. <http://doi.org/10.1046/j.1469-8137.2003.00761.x>
- Voigt, C. A. (2014). Callose-mediated resistance to pathogenic intruders in plant defense-related papillae. *Frontiers in Plant Science*, 5(April), 168. <http://doi.org/10.3389/fpls.2014.00168>
- Wang, C.-I. A. C.-I. a, Guncar, G., Forwood, J. K., Teh, T., Catanzariti, A.-M. A.-M., Lawrence, G. J., ... Kobe, B. (2007a). Crystal structures of flax rust avirulence proteins AvrL567-A

- and -D reveal details of the structural basis for flax disease resistance specificity. *The Plant Cell*, 19(9), 2898–912. <http://doi.org/10.1105/tpc.107.053611>
- Wang, W., Devoto, A., Turner, J. G., & Xiao, S. (2007b). Expression of the Membrane-Associated Resistance Protein RPW8 Enhances Basal Defense Against Biotrophic Pathogens. *Molecular Plant-Microbe Interactions*, 20(8), 966–976.
- Wang, D., Weaver, N. D., Kesarwani, M., & Dong, X. (2005). Induction of protein secretory pathway is required for systemic acquired resistance. *Science*, 308(5724), 1036–1040. <http://doi.org/10.1126/science.1108791>
- Wang, M., Wang, S., & Xia, G. (2015a). From genome to gene: A new epoch for wheat research? *Trends in Plant Science*, 20(6), 380–387.
- Wang, Q., Han, C., Ferreira, A. O., Yu, X., Ye, W., Tripathy, S., ... Wang, Y. (2011). Transcriptional programming and functional interactions within the *Phytophthora sojae* RXLR effector repertoire. *The Plant Cell*, 23(6), 2064–86.
- Wang, X., McCallum, B. D., Fetch, T., Bakkeren, G., & Saville, B. J. (2015b). Sr36 - and Sr5 - Mediated Resistance Response to *Puccinia graminis f. sp. tritici* is Associated with Callose Deposition in Wheat Guard Cells. *Phytopathology*, 105(6), 728–737.
- Wang, X., Richards, J., Gross, T., Druka, a, Kleinhofs, a, Steffenson, B., ... Brueggeman, R. (2013). The rpg4-mediated resistance to wheat stem rust (*Puccinia graminis*) in barley (*Hordeum vulgare*) requires Rpg5, a second NBS-LRR gene, and an actin depolymerization factor. *Molecular Plant-Microbe Interactions*, 26(4), 407–18.
- Wang, X., Jiang, N., Liu, J., Liu, W., & Wang, G.-L. (2014). The role of effectors and host immunity in plant-necrotrophic fungal interactions. *Virulence*, 5(7), 722–32. <http://doi.org/10.4161/viru.29798>
- Wanyera, R., Macharia, J.K., Kilonzo, S. M. (2010). Challenges of fungicide control on wheat rusts in Kenya. In O. Carisse (Ed.), *Fungicides* (p. 123–138.). InTech. DOI: 10.5772/13769. Available from: <https://www.intechopen.com/books/fungicides/challenges-of-fungicide-control-on-wheat-rusts-in-kenya>
- Wanyera, R., Macharia, J. K., Kilonzo, S. M., & Kamundia, J. W. (2009). Foliar Fungicides to Control Wheat Stem Rust, Race TTKS (*Ug99*), in Kenya. *Plant Disease*, 93(9), 929–932. <http://doi.org/10.1094/PDIS-93-9-0929>
- Ward, A. J., & Cooper, T. a. (2010). The Pathobiology of Splicing. *Journal of Pathology*, 220(2), 152–163. <http://doi.org/10.1002/path.2649>.
- Weaver, M., Swiderski, M. R., Li, Y., & Jones, J. D. G. (2006). The *Arabidopsis thaliana* TIR-NB-LRR R-protein, RPP1A; protein localization and constitutive activation of defence by

- truncated alleles in tobacco and Arabidopsis. *Plant Journal*, 47(6), 829–840. <http://doi.org/10.1111/j.1365-313X.2006.02834.x>
- Webb, C. A., Richter, T. E., Collins, N. C., Nicolas, M., Trick, H. N., Pryor, T., & Hulbert, S. H. (2002). Genetic and molecular characterization of the maize rp3 rust resistance locus. *Genetics*, 162(1), 381–394.
- Webb, C. A., & Fellers, J. P. (2006). Cereal rust fungi genomics and the pursuit of virulence and avirulence factors. *FEMS Microbiology Letters*, 264(1), 1–7. <http://doi.org/10.1111/j.1574-6968.2006.00400.x>
- Weiberg, A., Wang, M., Lin, F.-M., Zhao, H., Zhang, Z., Kaloshian, I., ... Peer, Y. Van de. (2013). Fungal small RNAs suppress plant immunity by hijacking host RNA interference pathways. *Science (New York, N.Y.)*, 342(6154), 118–23.
- Weisenfeld, N. I., Yin, S., Sharpe, T., Lau, B., Hegarty, R., Holmes, L., ... Jaffe, D. B. (2014). Comprehensive variation discovery in single human genomes. *Nature Genetics*, 46(12), 1350–5. <http://doi.org/10.1038/ng.3121>
- West, J. S., Townsend, J. A., Stevens, M., & Fitt, B. D. L. (2012). Comparative biology of different plant pathogens to estimate effects of climate change on crop diseases in Europe. *European Journal of Plant Pathology*, 133(1), 315–331. <http://doi.org/10.1007/s10658-011-9932-x>
- Whisson, S. C., Boevink, P. C., Moleleki, L., Avrova, A. O., Morales, J. G., Gilroy, E. M., ... Chapman, S. (2007). A translocation signal for delivery of oomycete effector proteins into host plant cells. *Nature*, 450, 115–118. <http://doi.org/10.1038/nature06203>
- White, Frank, Yang, Bing, Johnson, L. (2000). Prospects for understanding avirulence gene function. *Curr Opin Plant Biol.*, 3(4), 291–298.
- Win, J., Chaparro-Garcia, A., Belhaj, K., Saunders, D. G. O., Yoshida, K., Dong, S., ... Kamoun, S. (2012). Effector biology of plant-associated organisms: Concepts and perspectives. *Cold Spring Harbor Symposia on Quantitative Biology*, 77, 235–247.
- Winterberg, B., Du Fall, L. A., Song, X., Pascovici, D., Care, N., Molloy, M., ... Solomon, P. S. (2014). The necrotrophic effector protein SnTox3 re-programs metabolism and elicits a strong defence response in susceptible wheat leaves. *BMC Plant Biology*, 14(1), 215. <http://doi.org/10.1186/s12870-014-0215-5>
- Wirthmueller, L., Maqbool, A., & Banfield, M. J. (2013). On the front line: structural insights into plant-pathogen interactions. *Nature Reviews. Microbiology*, 11(11), 761–76. <http://doi.org/10.1038/nrmicro3118>

- Wolfe, M. S. (1988). The use of variety mixtures to control disease and stabilize yield. In S. Simmonds, N. W., and Rajaram (Ed.), *Breeding strategies for resistance to the rust of wheat* (pp. 91–100). Mexico D.F.
- Wolfe, & M. (2001). *Variety mixtures in theory and practice*. Dundee, Scotland.: Scottish Crop Res. Inst.
- Wu, J., Sakthikumar, S., Dong, C., Zhang, P., Cuomo, C. A., & Park, R. F. (2017). Comparative genomics integrated with association analysis identifies candidate effector genes corresponding to *Lr20* in phenotype-paired *Puccinia triticina* isolates from Australia. *Frontiers in Plant Science*, 8(February), 148. <http://doi.org/10.3389/FPLS.2017.00148>
- Wulff, B. B., Thomas, C. M., Smoker, M., Grant, M., & Jones, J. D. (2001). Domain swapping and gene shuffling identify sequences required for induction of an *Avr*-dependent hypersensitive response by the tomato Cf-4 and Cf-9 proteins. *The Plant Cell*, 13(2), 255–272. <http://doi.org/10.1105/tpc.13.2.255>
- Wulff, B. B. H., & Moscou, M. J. (2014). Strategies for transferring resistance into wheat: from wide crosses to GM cassettes. *Frontiers in Plant Science*, 5(December), 692. <http://doi.org/10.3389/fpls.2014.00692>
- Xia, C., Wang, M., Wan, A., Jiwan, D. A., See, D. R., & Chen, X. (2016). Association Analysis of SP-SNPs and Avirulence Genes in *Puccinia striiformis* f. sp. *tritici*, the Wheat Stripe Rust Pathogen, (January), 126–137.
- Xiao, S., Brown, S., Patrick, E., Brearley, C., Turner, J. G. (2003). Enhanced Transcription of the *Arabidopsis* Disease Resistance Genes RPW8 . 1 and RPW8 . 2 via a Salicylic Acid – Dependent Amplification Circuit is Required for Hypersensitive Cell Death. *The Plant Cell*, 15(January), 33–45. <http://doi.org/10.1105/tpc.006940.2001>
- Yang, S., Tang, F., & Zhu, H. (2014). Alternative splicing in plant immunity. *International Journal of Molecular Sciences*, 15(6), 10424–10445. <http://doi.org/10.3390/ijms150610424>
- Yi, H., & Richards, E. J. (2007). A cluster of disease resistance genes in *Arabidopsis* is coordinately regulated by transcriptional activation and RNA silencing. *The Plant Cell*, 19(9), 2929–2939. <http://doi.org/10.1105/tpc.107.051821>
- Yin, C., Chen, X., Wang, X., Han, Q., Kang, Z., & Hulbert, S. H. (2009). Generation and analysis of expression sequence tags from haustoria of the wheat stripe rust fungus *Puccinia striiformis* f. sp. *tritici*. *BMC Genomics*, 10, 626. <http://doi.org/10.1186/1471-2164-10-626>
- Yin, C., & Hulbert, S. (2010). Prospects for functional analysis of effectors from cereal rust fungi. *Euphytica*, 179(1), 57–67. <http://doi.org/10.1007/s10681-010-0285-x>

- Yin, C., Jurgenson, J. E., & Hulbert, S. H. (2011). Development of a host-induced RNAi system in the wheat stripe rust Fungus *Puccinia striiformis* f. sp. *tritici*. *Molecular Plant-Microbe Interactions*, *24*(5), 554–561. <http://doi.org/10.1094/MPMI-10-10-0229>
- Yin, C., Downey, S. I., Klages-Mundt, N. L., Ramachandran, S., Chen, X., Szabo, L. J., ... Hulbert, S. H. (2015). Identification of promising host-induced silencing targets among genes preferentially transcribed in haustoria of Puccinia. *BMC Genomics*, *16*(1), 579. <http://doi.org/10.1186/s12864-015-1791-y>
- Yoshida, K., Saitoh, H., Fujisawa, S., Kanzaki, H., Matsumura, H., Yoshida, K., ... Terauchi, R. (2009). Association genetics reveals three novel avirulence genes from the rice blast fungal pathogen *Magnaporthe oryzae*. *The Plant Cell*, *21*(5), 1573–91.
- Yoshimura, S., Yamanouchi, U., Katayose, Y., Toki, S., Wang, Z. X., Kono, I., ... Sasaki, T. (1998). Expression of *Xa1*, a bacterial blight-resistance gene in rice, is induced by bacterial inoculation. *Proceedings of the National Academy of Sciences of the United States of America*, *95*(4), 1663–1668. <http://doi.org/10.1073/pnas.95.4.1663>
- Yu, L. X., Barbier, H., Rouse, M. N., Singh, S., Singh, R. P., Bhavani, S., ... Sorrells, M. E. (2014). A consensus map for *Ug99* stem rust resistance loci in wheat. *Theoretical and Applied Genetics*, *127*(7), 1561–1581. <http://doi.org/10.1007/s00122-014-2326-7to>
- Yu, G. T., Zhang, Q., Klindworth, D. L., Friesen, T. L., Knox, R., Jin, Y., ... Xu, S. S. (2010). Molecular and cytogenetic characterization of wheat introgression lines carrying the stem rust resistance gene *Sr39*. *Crop Science*, *50*(4), 1393–1400.
- Zambino, P. J., Kubelik, a R., & Szabo, L. J. (2000). Gene Action and Linkage of Avirulence Genes to DNA Markers in the Rust Fungus *Puccinia graminis*. *Phytopathology*, *90*(8), 819–826. <http://doi.org/10.1094/PHYTO.2000.90.8.819>
- Zhang, W., Chen, S., Abate, Z., Nirmala, J., Rouse, M. N., & Dubcovsky, J. (2017). Identification and characterization of *Sr13*, a tetraploid wheat gene that confers resistance to the Ug99 stem rust race group. *Proceedings of the National Academy of Sciences*, *114*(45), E9483–E9492. <http://doi.org/10.1073/pnas.1706277114>
- Zhang, L., & Dickinson, M. (2001). Fluorescence from rust fungi: a simple and effective method to monitor the dynamics of fungal growth in planta. *Physiological and Molecular Plant Pathology*, *59*(3), 137–141. <http://doi.org/10.1006/pmpp.2001.0349>
- Zhang, L., Castell-Miller, C., Dahl, S., Steffenson, B., & Kleinhofs, A. (2008). Parallel expression profiling of barley-Stem rust interactions. *Functional and Integrative Genomics*, *8*(3), 187–198. <http://doi.org/10.1007/s10142-007-0069-0>
- Zhang, W., Olson, E., Saintenac, C., Rouse, M., Abate, Z., Jin, Y., ... Dubcovsky, J. (2010). Genetic Maps of Stem Rust Resistance Gene in Diploid and Hexaploid Wheat. *Crop Science*, *50*(6), 2464. <http://doi.org/10.2135/cropsci2010.04.0202>

- Zhang, X.-C., & Gassmann, W. (2007). Alternative Splicing and mRNA Levels of the Disease Resistance Gene RPS4 Are Induced during. *Plant Physiology*, *145*(December), 1577–1587. <http://doi.org/10.1104/pp.107.108720>
- Zhang, D., Bowden, R. L., Yu, J., Carver, B. F., & Bai, G. (2014a). Association analysis of stem rust resistance in U.S. winter wheat. *PLoS ONE*, *9*(7). <http://doi.org/10.1371/journal.pone.0103747>
- Zhang, S., & Xu, J. R. (2014b). Effectors and Effector Delivery in *Magnaporthe oryzae*. *PLoS Pathogens*, *10*(1), 1–4. <http://doi.org/10.1371/journal.ppat.1003826>
- Zhao, J., Wang, M., Chen, X., & Kang, Z. (2016). Role of Alternate Hosts in Epidemiology and Pathogen Variation of Cereal Rusts. *Annual Review of Phytopathology*, *54*(1), 207–228. <http://doi.org/10.1146/annurev-phyto-080615-095851>
- Zipfel, C., Kunze, G., Chinchilla, D., Caniard, A., Jones, J. D. G., Boller, T., & Felix, G. (2006). Perception of the Bacterial PAMP EF-Tu by the Receptor EFR Restricts *Agrobacterium*-Mediated Transformation. *Cell*, *125*(4), 749–760. <http://doi.org/10.1016/j.cell.2006.03.037>

Appendix A -

Main isoform analysis of variance

I=infected (RKQQC)

NI= non infected (Mock)

Analysis of variance

Variable	N	R ²	Adj R ²	CV
Expression	60	0.20	0.05	62.54

Analysis of variance table (Partial SS)

S.V.	SS	df	MS	F	p-value
Model.	1.23	9	0.14	1.36	0.2301
Time	1.23	9	0.14	1.36	0.2301
Error	5.02	50	0.10		
Total	6.25	59			

Isoform-2 analysis of variance

I=infected (RKQQC)

NI= non infected (Mock)

Analysis of variance

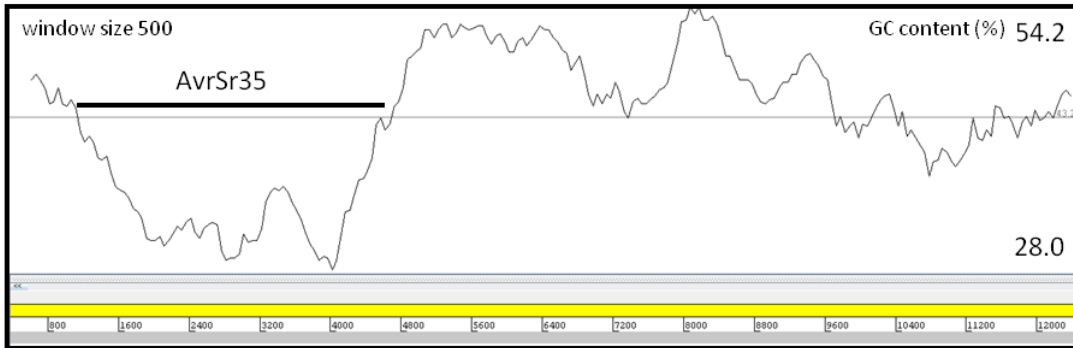
Variable	N	R ²	Adj R ²	CV
expression	60	0.17	0.02	72.61

Analysis of variance table (Partial SS)

S.V.	SS	df	MS	F	p-value
Model.	0.05	9	0.01	1.11	0.3749
Time	0.05	9	0.01	1.11	0.3749
Error	0.26	50	0.01		
Total	0.31	59			

Appendix B -

Annotation of GC content (%) of the scaffold 2351 containing the genomic sequence of the *AvrSr35* using Artemis software (Rutherford et al., 2000). The relative position of *AvrSr35* into the scaffold is showed (black bar).



Appendix C -

AvrSr35 sequence alignment for *Pgt* EMS mutant strains

WT	<i>TTCCAACCTATCAATCTTCACATCATCCCATCAACCAAC</i> ^{Start} <i>ATGTCACATCACTTTGGATTA</i>
M1
M3
M4
M6
M7
M8
M9
M10
M11
M12
M13
M14
M15
WT	<i>CGTAAAATAAACTACTGATTTTGCTCTTCCTTCAAGTTCATGGGAGTCAATGTGCCATG</i>
M1
M3
M4
M6
M7
M8
M9
M10
M11
M12
M13
M14
M15
WT	<i>AGGAACTTTGCTGCA</i> GGTGATTTGCACTGATATACCTACCATAATTAATTTGTACAGC
M1
M3
M4
M6
M7
M8
M9
M10
M11
M12
M13
M14
M15
WT	CTTCTGACTATGATTTATGTACCATGATTCATAACTATCTCCAG <u>ATAGAGTCCATGGGG</u>
M1
M3
M4

M6
M7
M8
M9
M10
M11
M12
M13
M14
M15

WT **TAGAATCAGTCATTTCCGGGTCCAAGAGCTCATCTAATCCCATGGCACTGTCTAAGTCCA**
M1
M3
M4
M6
M7
M8
M9
M10
M11
M12
M13
M14
M15

WT **TGGATAAACCAG**TGATTTGTTTGAATCCTTCTATATTTTGGCAATTTGGAAACTGAATT
M1
M3
M4
M6
M7
M8
M9
M10
M11
M12
M13
M14
M15

WT CAATTTGCATTACTAATACCTTCTATTGTAACTCCCTCTATTATTAAATATTTACAAG
M1
M3
M4
M6
M7
M8
M9
M10
M11
M12
M13
M14
M15

WT ACACATCTGATTTGGTAGATTCAAATGTTTCAGGCAAAAAATGATGGGAGCAGATATGAAG
M1
M3
M4
M6
M7
M8
M9
M10 Premature
M11 stop codon T
M12
M13
M14
M15

WT AAGTAATCTTATTTTCATCCAAATAAACTTTTACCTTATATTCCATGGACCACATGCACA
M1
M3
M4
M6
M7
M8
M9
M10
M11
M12
M13
M14
M15

WT AATTGGAAAATTTGGACTGAATTTGATTTATTTAAACATTATCTTCCACCAGATTTTACA
M1
M3
M4
M6
M7
M8
M9
M10
M11
M12
M13
M14
M15

WT GCTAAATATTCTGAGCAAGTAGATCATGTTTCTAAGATCCTAAAAGAGATTGAAGAACAA
M1
M3
M4
M6
M7
M8
M9
M10

M11
M12
M13
M14
M15

WT GGTGACCATTTTCAATTTCTCTTTCCATGTTGAAATTACTATAAAAGACCCTAAATCTGAT
M1
M3
M4
M6
M7
M8
M9
M10
M11
M12
M13
M14
M15

WT TTTCATGAATTATGTTGCTAATTTTCAGAGCCTGGAACTATAATTATTGATCATAAAAGCAT
M1
M3
M4
M6
M7
M8
M9
M10
M11
M12
M13
M14
M15

WT TCCCAATCCAAGACAAATCACCAAAACAGGTGGTTAATTTCCCTTTTCCAAAAAAGATGA
M1 A.
M3 Non
M4 synonymous
M6 valine to
M7 isoleucine A.
M8
M9
M10
M11
M12
M13
M14
M15

WT TTACAGAATCTAATTCAAAAGACATCAGAGAATATCTTGCAAGCACATTTCCCTTTTGAAC
M1
M3
M4
M6
M7

M8
M9
M10
M11
M12
M13
M14
M15

WT **AGCAATCAACTATATTAGACAGTGTGAAATCAA**GTACGTTTAAATTATAAAATCTAGTAG
M1
M3
M4
M6
M7
M8
M9
M10
M11
M12
M13
M14
M15

WT ACAGAAAGTACTTTAATGTGCTCCATTTGACTTTGATTTTGTCTTCTGAAAATCATTTTA
M1
M3
M4
M6
M7
M8
M9
M10
M11
M12
M13
M14
M15

WT TGCAGTTGCCAAAGTACAAATAGATGACCG**AAAGGCATTTGATCTTCAATTGAAATTCAG**
M1
M3
M4
M6
M7
M8
M9
M10
M11
M12 Premature **T**
M13 stop codon
M14
M15

WT **ACAGGAAAACCTGGCAGAACTCAAGGATCAAATTATACTTTCAC TGGGTGCAAATAATGG**
M1
M3
M4
M6
M7
M8
M9
M10
M11
M12
M13
M14
M15

WT **AAATCAAACCTGGCAAAGTTACTTGATTACACAAATAAGTTGGATGAA TTGAGCAACAC**
M1
M3
M4
M6
M7
M8
M9
M10
M11
M12
M13
M14
M15 Premature .A.
stop codon

WT **CAAAATTCCCCTGAAGAATTTATTGAGGAGATTCAAAGGTATTGTACAAGGTCAAATT**
M1
M3
M4
M6
M7
M8
M9
M10
M11
M12
M13
M14
M15

WT **GGAATCTACATCAACATCCAAGCTTTACAGTCAATTTAATCTATCAATTCAAGATTTTGC**
M1
M3
M4
M6
M7
M8
M9
M10

M11
M12
M13
M14
M15

WT **ACTTCAAATAATTCATTCAAAATACAAGTCAAATCAAATAAGTCAAATGATCTTTTGAA**

M1
M3
M4
M6
M7
M8
M9
M10
M11
M12
M13
M14
M15

WT **GTTGATCACAGAGGATGAGATGCTAAAAATTCTGGCAAAGACCAAGGTTCTCACCTACAA**

M1
M3
M4
M6
M7
M8
M9
M10
M11
M12
M13
M14
M15

WT **GATGAAATATTTTGATTTCAGCATCAAAAATGGGAATCAATAAATATATCAGTACTGAGAT**

M1
M3
M4
M6
M7
M8
M9
M10
M11
M12
M13
M14
M15

WT **GATGGACCTGGACTGGCAATTTTCACATTATAAGACTTTCAATGATG**GTGAGATACATTC

M1
M3 Splicing site A
M4
M6
M7 Prématuré A
stop codon

M8
M9
M10
M11
M12
M13
M14
M15

WT AATTGCAGAAAAATGATCAAAATTGAATAATTTAAAAATATTGATGAATTTGATCTTCCA
M1
M3
M4
M6
M7
M8
M9
M10
M11
M12
M13
M14
M15

WT ATTTTAAAAAATTTGTTGGTTCATAAAAAATTGAAATAG CTTGAAAAAATAAAGCA
M1
M3
M4
M6
M7
M8
M9
M10
M11
M12
M13
M14
M15

WT AGTGATTCAAGCTATCTTGGATGGCTAACCCATGGGTATTCTATCAAATACGGATTATCT
M1 K
M3
M4
M6
M7
M8
M9
M10
M11
M12
M13
M14 Premature ^A
M15 stop codon

WT CCTAATAATGAAAGGAGTATGTTTTTCCAAGATGGAAGAAAATATGCTGAATTGTATGCA

M1
M3
M4
M6
M7
M8
M9
M10
M11
M12
M13 Premature T
M14 stop codon
M15

WT **TTTTCTAAAAGTCCCCACAGGAAAATAATACCTGGGGAGCACCTCAAAGATCTGTTAGCT**
M1
M3
M4
M6
M7
M8
M9
M10
M11
M12
M13
M14
M15

WT **AAAATCAATAAATCCAAAGGTATTTTTCTGGATCAGAATGCCTTGCTAGATAAAAAGGATC**
M1
M3
M4 T
M6
M7 Premature
M8 stop codon T
M9 T
M10
M11
M12
M13
M14
M15

WT **TATGCATTTTCATGAGTTGAACACTCTTGAAACACATTTTCCAGGAATAACTTCATCTTTT**
M1
M3
M4
M6
M7
M8
M9
M10
M11
M12
M13
M14

M15

WT ACGGATGATTTGAAATCAAATTACCGCAAGAAGATGGAATCTGTTTCTCTCACATGCCAG

M1

M3

M4

M6

M7

M8

M9

M10

M11

M12

M13

M14

M15

WT GTTCTTCAAGAAATGGCAACATTCACCGGTTCAATGAATCTAAAGTCCCATATCACAGT

M1

M3

M4

M6

M7

M8

M9

M10

M11

M12

M13

M14

M15

WT TCCACAGAATATGGATTGTTTCTATCCCCAAGATATTTTCAATCCCAATCGATTATAAG

M1

M3

M4

M6

M7

M8

M9

M10

M11

M12

M13

M14

M15

WT CATGGAGAAAAGGAGAATTTGGTCTCCTATGTTGACTTTCTTTACTCCACTGCTCATGAA

M1

M3

M4

M6

M7

M8

M9

M10

```

M11 .....
M12 .....
M13 .....
M14 .....
M15 .....

WT AGAATTCTCCAGGATAATTCAATTAATCAACTTTGCCTTGACCCATTACAAGAATCCTTA
M1 .....
M3 .....
M4 .....
M6 .....
M7 .....
M8 .....
M9 .....
M10 .....      Prémature      T
M11 .....      stop codon
M12 .....
M13 .....
M14 .....
M15 .....

WT AACCGTATTAAAAGCAATATACCTGTTTTCTTCAACTTAGCTTCCCATAGTTCACCAATC
M1 .....
M3 .....
M4 .....
M6 .....
M7 .....
M8 .....
M9 .....
M10 .....
M11 .....
M12 .....
M13 .....
M14 .....
M15 .....

WT AAGCCATCCAATGTTTCATGAAGCAAATGstopTGATGTTTTTTTTTACTTCATAATTCAAAT
M1 .....
M3 .....
M4 .....
M6 .....
M7 .....
M8 .....
M9 .....
M10 .....
M11 .....
M12 .....
M13 .....
M14 .....
M15 .....

```

Figure S2 Alignment of *AvrSr35 Pgt* EMS-RKQQC mutant alleles. Conserved nucleotides are showed as dots. Changes in nucleotides are showed with its effect. Exonic sequences are showed underlined and in bold. Start and stop codons are indicated (red).

Appendix D -

Table S1. Screening data for EMS uredinospore mutants M#1 and M#7 using host differentials for stem rust.

Set	Diff #	Line	Gene	Exp. LIT	CDL RKQQ	EMS mutant	
					99KS76A	M#1	M#7
I	1	ISr5-Ra	5	0, 0;	3+	3+	3+
	2	CnS_T_mono_deriv	21	1, 2-	3+	3+	3+
	3	Vernstine	9e	;1+	2	2	2
	4	ISr7b-Ra	7b	2	3+	3+	3+
II	5	ISr11-Ra	11	;2-, 2+3-	2-	2-/3+	-
	6	ISr6-Ra	6	0;	3+	3+	3+
	7	ISr8a-Ra	8a	2	3+	3+	3+
	8	CnSr9g	9g	2-	3+	3+	3+
III	9	W2691SrTt-1	36	0, 0;, X (LIF)	3+	3+	3+ lif
	10	W2691Sr9b	9b	22+	3+	3+	3+
	11	BtSr30Wst	30	2	2	2-	2-
	12	Combination VII	17+13	0, ;1	2+	22+	2
IV	13	ISr9a-Ra	9a	2-, 23	3+	3+	3+
	14	ISr9d-Ra	9d	;2-	3+	3+	3+
	15	W2691Sr10	10	;1+	;1	0;	0;
	16	CnsSrTmp	Tmp	2-	;1	0;	0;
V	17	LcSr24Ag	24	2	2	22+	22+
	18	Sr31/6*LMPG	31	;1+	2-	2	22-
	19	Trident	38	0;	0;	0;	0;
	20	McNair 701	McN	;1	3+	3+	3+
VI	21	Line E	-		3+	3+	3+
	22	Acme	9g		3+	3+	3+
	23	Siouxland	24+31		2-	2	2
	24	Sisson	31+36		2-	2-	0 esc?
VII	25	SwSr22T.B.	22		2	2	2
	26	Agatha/9*LMPG	25		22+	22+	22+
	27	Eagle	26		2	2-	2-
	28	73,214,3-1/9*LMPG	27		0;1/3+	0;1/3+	0;1-/3+
VIII	29	Federation*4/Kavkaz	31		0;	0;	0;
	30	ER 5155	32		2	2	2-
	31	Tetra Canthatch/Ae. Squarrosa	33		2-	2-	2-
	32	Mq(2)5XG2919	35		0;	2-	2-
IV	33	W3563	37		0;/3+	0;	0;/3+
	34	RL6082	39		-	2-	2-
	35	RL6088	40		2-	2-	2-
	36	TAF 2	44		;2-	2-	;2-

X	37	DAS15	47	;	0;	0;
	38	Satu	Satu	0;	0;	0;
	39	TAM 107-1 Fed*3/Gabo*51BL.1RS-	1A.1R	12-	;2-	2-
	40	1-1	R	0;	0;	0;
XI	41	Iumillo	9g,12,+	0;	0;	0;
	42	Leeds	9e,13,+	0;	0;	0;
	43	ST464	13	2	2	2
	44		Sr7a	11+	1+3-	31+
XII	45	Steptoe	- Rpg1, rpg4,	0;13-z	1+3- lif	1+3 lif
	46	Q21861	Rpg5	0;	0;1	0;
	47	Morex	Rpg1	0;11+z	12-	11+ lif
	48	QSM20	rpg4/Tpg5	0;	0;1	0;1
		DV92	Sr35	0;	3+	3+

Expect low infection type (Exp LIT). Infection types (ITs) scale (0 to 4) are based in (Stakman et al.,1962).

IT="0" indicates immune reaction: no uredia or other visible symptoms.

IT= ';' indicates a nearly immune reaction: no uredia, but visible hypersensitive flecks.

IT= '1' indicates a very resistant reaction: small, round uredia were observed immediately surrounded by necrotic or chlorotic plant tissue.

IT= '3' indicates a moderately susceptible reaction: medium, elongated uredia observed often associated with limited chlorotic plant tissue.

When multiple infection types were observed on the same leaf, all infection types were recorded in order, starting with the most common IT. Signs '+' or '-' indicate larger or smaller size uredia within each infection type. 'z' variable size with larger uredinia towards the leaf base. 'LIF' indicates low infection frequency.

Appendix E -

Solutions and media

50X TAE electrophoresis buffer

Component	Per liter	
Tris Base	242 g	Sigma T1378
Glacial acetic acid	57.2 ml	Fisher S70048
0.5 M EDTA	100 ml	Sigma E4884

Adjust to 1 liter with deionized water

DNA Lysis buffer

Buffer A (1 L)

NaCl	100 ml	100 ml
Tris HCl 1 M	100 ml	
EDTA	100 ml	100 ml

pH to 7.2 and fill to 1000 ml

Prepare fresh Lysis Buffer (30 samples)

Components:

Buffer A	25 ml	
Sodium bisulfate	0.125 g	Sigma S9000
Sodium diethyldithio carbamate	0.038 g	Sigma D3506
Ascorbic Acid	0.25 g	Sigma A5960
Polyvinylpyrrolidone (PVP10)	0.5 g	Sigma

1X TE buffer

10 mM Tris-Cl, pH 7.5
1 mM EDTA

PBS 1X (Phosphate Buffer Saline)

Dissolve the following components in 800 ml distilled H₂O.

Amount	Final concentration
8 g of NaCl	137 mM NaCl
0.2 g of KCl	2.7 mM KCl
1.44 g of Na ₂ HPO ₄	10 mM Na ₂ HPO ₄
0.24 g of KH ₂ PO ₄	2 mM KH ₂ PO ₄

Adjust pH to 7.4 with HCl.

Adjust volume to 1 L with additional distilled H₂O.

Sterilize by autoclaving.